

**Constitutively Active Akt1 in B Cells Plays an
Important Role in MZ B Cell Fate Decision and
Impairs CSR**

Dissertation
zur Erlangung des Grades
Doktor der Naturwissenschaften

Am Fachbereich Biologie
der Johannes Gutenberg-Universität Mainz

vorgelegt von
Eva-Maria Cox
geb. am 25. März 1985 in Bad Soden, Deutschland

Mainz 2015

Table of Contents

1	Introduction	1
1.1	The Immune System.....	1
1.2	B Cell Development	1
1.2.1	Marginal Zone B Cells	3
1.2.2	Germinal Center	5
1.3	Class Switch Recombination	6
1.4	Activation-induced Cytidine Deaminase.....	7
1.5	The B Cell Antigen Receptor	8
1.6	Akt, the Protein Kinase B (PKB)	10
1.6.1	Akt in B Cells.....	13
1.7	Objectives	16
2	Material and Methods.....	17
2.1	Used Material	17
2.1.1	Chemicals and Reagents.....	17
2.1.2	Equipment	19
2.1.3	Disposable Materials	19
2.1.4	Buffer and Media	20
2.2	Molecular Biology.....	22
2.2.1	Preparation of Genomic DNA.....	22
2.2.2	RNA Isolation and Quantitative Real-Time PCR	22
2.2.3	Agarose Gel Electrophoresis.....	23
2.2.4	Quantification of DNA and RNA.....	23
2.2.5	Polymerase Chain Reaction (PCR)	23
2.3	Biochemistry.....	25
2.3.1	Protein Extract Preparations.....	25
2.3.2	Western Blot.....	25
2.4	Cell Biology.....	27
2.4.1	Single Cell Suspensions of Cells from Lymphoid Organs.....	27
2.4.2	Isolation of Lymphoid Cells from Blood	27
2.4.3	Cell Counting	27
2.4.4	Flow Cytometry.....	27
2.4.5	Ca ²⁺ -Flux Assay	29
2.4.6	Magnetic Cell Sorting and FACS Sorting.....	30
2.4.7	Proliferation Assay and <i>in vitro</i> B Cell Stimulation	30
2.4.8	Survival Assay.....	31
2.4.9	Culture of <i>ex vivo</i> Splenocytes and Lymphocytes	31
2.4.10	Plasma Cell Differentiation.....	31
2.4.11	Induced Class Switch Recombination.....	31
2.4.12	PCR of Circular Class Switch Transcripts	32
2.4.13	Histological Analysis	33
2.5	Mouse Experiments	33
2.5.1	Mice.....	34
2.5.2	NP-CG, SRBC and NP-Ficoll Immunization.....	34
2.5.3	Antibiotic Treatment to Eliminate Microbiota in the Gut.....	34
2.5.4	Immunglobulin- and Cytokine-ELISA.....	34
2.6	Software.....	36
2.7	Statistic	36
3	Results	37

3.1	Functionality of the Transgenic Akt ^{BOE} Mouse Model	37
3.2	Investigation of Primary and Secondary Lymphoid Organs	39
3.3	Dramatic Increase of MZ-like B Cells in Akt ^{BOE} Mice	51
3.4	Constitutive Akt1 Signaling Overcomes CD19 Deficiency During MZ B Cell Differentiation	54
3.5	Investigation of MZ B Cell Surface Marker Expression	56
3.6	Investigation of MZ-like B Cell Precursors in Akt ^{BOE} Mice	57
3.7	MZ-like B Cells of Akt ^{BOE} Mice do not Behave as Normal MZ B Cells	60
3.8	Akt1 Expression Prolongs the Survival of Akt ^{BOE} B Cells <i>in vitro</i>	63
3.9	MZ-like B Cells of Akt ^{BOE} Mice do not Class Switch as Normal MZ B Cells	64
3.10	MZ-like B Cells Leave the Spleen and Migrate into other Lymphatic Organs	65
3.11	Loss of CD23 Expression Due to Constitutive Akt1 Signaling	66
3.12	Defects in Class Switch Recombination in Akt ^{BOE} Mice	68
3.13	Germinal Center Formation in Akt ^{BOE} Mice	70
3.14	Investigation of Plasma Cell Formation in Akt ^{BOE} Mice	74
3.15	Influence of Akt1 Signaling on Downstream Signaling Pathways	76
3.16	Proposed Tumor Development in Akt ^{BOE} Mice	80
3.17	Detailed Analysis of IgM ⁺ , IgD ⁺ Double Negative B Cell Population	81
3.18	Overexpression of Akt1 in a Later Phase of B Cell Development	87
4	Discussion	110
4.1	Constitutive Akt1 expression Leads to MZ-like B Cell Development Directly From T1 B Cell Precursors	111
4.2	Overexpression of Akt1 in Akt ^{BOE} Mice Leads to a Loss of the Surface Marker CD23	111
4.3	Constitutive Akt1 Signaling Leads to MZ-like B Cell Development Independent of CD19	112
4.4	FOXO1 and Notch2 Regulation in Akt ^{BOE} Mice	113
4.5	The Loss of BCR Signaling in Akt ^{BOE} Mice	114
4.6	MZ-like B Cells Show Normal Surface Marker but are not Able to Class Switch	116
4.7	Constitutive Akt1 Signaling Leads to the Impairment of CSR, GC Formation and Plasma Cell Differentiation	117
4.8	κ and λ Expression in B Cells of Akt ^{BOE} Mice	119
4.9	Constitutive Akt1 Expressing CD19 ⁺ B Cells Lacking Surface IgM, IgD, Ig κ and Ig λ Can be Restored in JHT ^{-/-} Mice	120
4.10	Signaling Pathways Downstream of Akt: mTOR and GSK-3	121
4.11	B Cell Specific Activation of Akt1 Signaling Itself is not Sufficient to Induce B Cell Lymphomagenesis	122
4.12	Overexpression of Akt1 in Mature B Cells Leads to Malignancy	124
5	Summary	126
6	Zusammenfassung	128
7	References	130
8	Acknowledgments	152
9	Versicherung	153
10	Lebenslauf	154

List of Figures

Figure 1.1: Early B cell development in the bone marrow.....	2
Figure 1.2: Overview of B cell development.	3
Figure 1.3: Mechanism of the class switch recombination.	7
Figure 1.4: Primary structure of activation-induced cytidin deaminase (AID).	8
Figure 1.5: Structure and function of the pre-BCR and BCR complex.	10
Figure 1.6: Structure of Akt1, Akt2 and Akt3.....	12
Figure 1.7: Components of mTORC1 and mTORC2 and its best known substrates..	14
Figure 1.8: Shows how the Akt-FOXO axis controls the B cell differentiation of activated B cells.....	15
Figure 3.1: Generation of Akt ^{BOE} mice.	39
Figure 3.2: B cell distribution in BM.....	40
Figure 3.3: Mature macrophages, monocytes and neutrophils in BM of Akt ^{BOE} mice vs. controls.....	41
Figure 3.4: Increased splenic mature macrophages, monocytes and neutrophils in Akt ^{BOE} mice.	42
Figure 3.5: Effect of Akt1 overexpression on splenic B and T cell numbers in Akt ^{BOE} mice.	43
Figure 3.6: B and T cell distribution in pLN of Akt ^{BOE} mice.....	44
Figure 3.7: B and T cell distribution in mLN is not affected by Akt1 overexpression.	45
Figure 3.8: Overexpression of Akt1 leads to reduced numbers of B cells in PP.	46
Figure 3.9: Increased B and T cell populations in PerC of Akt ^{BOE} mice.	47
Figure 3.10: B1 and B2 B cells in PerC and pLN.	48
Figure 3.11: IgM vs. IgD expression on B cells of spleen, pLN, PP and PerC.....	50
Figure 3.12: Splenic B1 and B2 B cell subsets.	51
Figure 3.13: Distribution of splenic MZ, FO and T1 B cells in Akt ^{BOE} mice vs. controls.....	53
Figure 3.14: Akt1 overexpression leads to splenic MZ-like B cells in Akt ^{+/-} CD19-Cre ^{-/-} mice.	55
Figure 3.15: MZ B cell surface marker expression in Akt ^{BOE} vs. Akt ^{+/-} CD19-Cre ^{-/-} mice and the corresponding controls in spleen.	57
Figure 3.16: Lack of T2 and T3 B cells in spleen of Akt ^{BOE} mice.....	59
Figure 3.17: Influence of Akt1 overexpression after stimulation, BCR induced signaling.	61
Figure 3.18: Less tyrosine phosphorylation, no Syk phosphorylation but Lyn phosphorylation in Akt ^{BOE} splenic B cells after BCR crosslinking.	62
Figure 3.19: Influence of Akt1 overexpression to B cell survival.	63
Figure 3.20: No IgM and IgG3 secretion from B cells of Akt ^{BOE} mice.	64
Figure 3.21: MZ-like B cells in pLN of Akt ^{BOE} and Akt ^{+/-} CD19-Cre ^{-/-} mice.	65
Figure 3.22: MZ-like B cells in mLN and PP of Akt ^{BOE} mice.....	66
Figure 3.23: CD23 secretion in blood sera and CD23 RNA levels.....	67
Figure 3.24: Akt ^{BOE} mice are not able to secrete and express immunoglobulins.....	69
Figure 3.25: Naive GC of mLN in Akt ^{BOE} and CD19-Cre mice.....	70
Figure 3.26: GC formation in Akt ^{BOE} and CD19-Cre control mice before and after immunization.....	72
Figure 3.27: GC formation after antibiotic treatment.....	74
Figure 3.28: Plasma cell differentiation in spleen.....	75

Figure 3.29: Mechanistic signaling pathway analysis of different pathways regulated by Akt1.....	76
Figure 3.30: Mechanistic signaling pathway analysis of Notch2 and quantitative Real-Time analysis of Notch1, Notch2 and Notch2 target genes in Akt ^{BOE} and CD19-Cre control mice.....	79
Figure 3.31: Weight course of aging mice.....	80
Figure 3.32: Immunoglobulin secretion of blood sera in aged Akt ^{BOE} mice.....	81
Figure 3.33: Distribution of κ and λ positive B cells in BM and spleen.....	82
Figure 3.34: Ig κ of and Ig λ concentration in serum Akt ^{BOE} and CD19-Cre mice.....	83
Figure 3.35: Investigation of CD19 positive B cells in different organs and PerC in Akt ^{+/-} JHT ^{-/-} CD19-Cre ^{+/-} mice.....	84
Figure 3.36: Investigation of CD19 positive and double negative B cells in different organs and PerC of Akt ^{+/-} JHT ^{-/-} CD19-Cre ^{+/-} mice.....	86
Figure 3.37: Survival of Akt ^{+/-} AID-Cre ^{+/-} mice in comparison to EYFP ^{+/-} AID-Cre ^{+/-} controls.....	87
Figure 3.38: Abnormal observations in Akt ^{+/-} AID-Cre ^{+/-} mice.....	88
Figure 3.39: Distribution of splenic B and T cells in Akt ^{+/-} AID-Cre ^{+/-} and EYFP ^{+/-} AID-Cre ^{+/-} control mice.....	89
Figure 3.40: Distribution of splenic T cell subsets in Akt ^{+/-} AID-Cre ^{+/-} and EYFP ^{+/-} AID-Cre ^{+/-} control mice.....	91
Figure 3.41: Distribution of B and T cells in Akt ^{+/-} AID-Cre ^{+/-} and EYFP ^{+/-} AID-Cre ^{+/-} control mice in pLN.....	93
Figure 3.42: Distribution of T cell subsets in Akt ^{+/-} AID-Cre ^{+/-} and EYFP ^{+/-} AID-Cre ^{+/-} control mice in pLN.....	95
Figure 3.43: Distribution of B and T cells in Akt ^{+/-} AID-Cre ^{+/-} and EYFP ^{+/-} AID-Cre ^{+/-} control mice in mLN.....	97
Figure 3.44: Distribution of T cell subsets in Akt ^{+/-} AID-Cre ^{+/-} and EYFP ^{+/-} AID-Cre ^{+/-} control mice in mLN.....	98
Figure 3.45: Distribution of B and T cells in Akt ^{+/-} AID-Cre ^{+/-} and EYFP ^{+/-} AID-Cre ^{+/-} control mice in PP.....	100
Figure 3.46: Distribution of B and T cells in thymus of Akt ^{+/-} AID-Cre ^{+/-} and EYFP ^{+/-} AID-Cre ^{+/-} control mice.....	102
Figure 3.47: Distribution of thymic T cell subsets in Akt ^{+/-} AID-Cre ^{+/-} mice and EYFP ^{+/-} AID-Cre ^{+/-} control mice.....	103
Figure 3.48: FACS analysis of splenic IgM and IgD positive B cells in Akt ^{+/-} AID-Cre ^{+/-} mice and EYFP ^{+/-} AID-Cre ^{+/-} control mice.....	105
Figure 3.49: Distribution of splenic mature and immature B cells as well as transitional B cells in Akt ^{+/-} AID-Cre ^{+/-} mice and EYFP ^{+/-} AID-Cre ^{+/-} control mice.....	106
Figure 3.50: Distribution of splenic MZ, FO and T1 B cell populations in Akt ^{+/-} AID-Cre ^{+/-} mice vs. controls.....	107
Figure 3.51: Surface IgG1 expression in different organs of Akt ^{+/-} AID-Cre ^{+/-} and EYFP ^{+/-} AID-Cre ^{+/-} control mice.....	108

List of Tables

Table 2.1: Used chemicals.....	17
Table 2.2: List of equipment not mentioned in the text.	19
Table 2.3: Table of used materials.	19
Table 2.4: Table of used buffers.....	20
Table 2.5: Medium used to culture B cells.....	21
Table 2.6: Program used for quantitative Real-Time PCR.....	22
Table 2.7: Oligonucleotides used for quantitative Real-Time PCR.	22
Table 2.8: PCR program for DNA genotyping.	23
Table 2.9: Sequences of oligonucleotides used for genotyping.	24
Table 2.10: Used Western blot antibodies.....	26
Table 2.11: Antibodies and compensation beads used for FACS stainings and compensations.	28
Table 2.12: Used stimulants.	31
Table 2.13: Stimuli used to induce class switch to different immunoglobulins.....	32
Table 2.14: PCR program used for the analysis of circular class switch transcripts...	32
Table 2.15: Sequences of oligonucleotides used to analyze slope transcripts.....	33
Table 2.16: Antibodies, biotin-conjugates and standards used for Ig-ELISA.....	35

Abbreviations

°C	temperature in degrees Celsius
3'	three prime end of DNA sequences
4EBPI	eIF4E binding protein-1
5'	five prime end of DNA sequences
α	anti or alpha
A	adenosine
Ab	antibody
AGC kinase	cAMP-dependend protein kinase A/protein kinaseG/ protein kinase C
Aicda	activation-induced cytidine deaminase
AID	activation-induced cytidine deaminase
Akt ^{BOE}	Akt1 B cell overexpression
APC	allophycocyanin
APC	antigen-presenting cell
APOBEC1	apolipoprotein B mRNA-editing enzyme, catalytic polypeptide 1
ATP	adenosine triphosphate
B cells	bone marrow or bursal cells
B-CLL	B cell chronic lymphocytic leukemia
BAFF	B cell activation factor
BCR	B cell receptor
BM	bone marrow
bp	base pair
BSA	bovine serum albumin
Btk	Bruton's tyrosine kinase
C	cytosine
C region	constant region
C region	constant region
CAG promoter	cytomegalovirus enhancer fused to the chicken beta- actin promoter
CCL3	chemokine (C-C motif) ligand 3
CCL4	chemokine (C-C motif) ligand 4

CD	cluster of differentiation
cDNA	complementary DNA
CLP	common lymphoid progenitor
CMV	Cytomgalovirus
CO ₂	carbon dioxide
CpG	cytosine-phosphate-guanine dideoxynucleotide motif
Cre	site-specific recombinase (causes recombination)
CSR	class switch recombination
CTP	cytosine triphosphate
CTs	circular transcripts
Cyc	cychrome
DAM	dissociation activation model
DAPI	4',6-diamidino-2-phenylindole
DCs	dendritic cells
ddH ₂ O	double-distilled water
dH ₂ O	distilled water
DMEM	Dulbecco's modified Eagle medium
DMSO	Dimethyl sulfoxide
DN	double negative
DNA	deoxyribonucleic acid
dNTP	deoxyribonucleotide-triphosphate
DP	double positive
ds	double-stranded
DTT	1,4-Dithio- DL-threitol
Dtx1	Deltex1
DZ	dark zone
EDTA	ethylene-diaminetetraacetic acid
EGTA	ethylene glycol tetraacetic acid
EtBr	ethidium bromide
FACS	fluorescence activated cell sorting
FCS	foetal calf serum
FDC's	follicular dendritic cells
FITC	fluorescein-isothiocyanate
Flp	site-specific recombinase, product of yeast <i>FLP1</i> -gene

forw	forward
FOXO	forkhead box, subgroup O
FP	follicular precursor
FRT	Flp recombination target
g	gram
×g	×gravitation
G	guanosine
GC	germinal center
GFP	green fluorescent protein
GSK-3	glycogen synthase kinase-3
GTP	guanosine triphosphate
H-2	histocompatibility locus 2
HBSS	Hank's Balanced Salt Solution
HEK	human embryonic kidney
HEPES	N-2-hydroxyethylpiperazine-N'-2-ethanesulfonic acid
Hes1	hairy and enhancer of split 1
Hes5	hairy and enhancer of split 5
HPRT	Hypoxanthine-guanine phosphoribosyltransferase
HRP	Horseradish peroxidase
i.p.	intraperitoneally
inhib.	inhibitors
Ig	immunoglobulin
IL	interleukin
ITAM	immunoreceptor tyrosine-based activation motifs
ITIMs	immunoreceptor tyrosine-based inhibitory motifs
kb	kilobase pairs
kDa	kilodalton
l	liter
LA	long arm of homology
LMPPs	lymphoid-primed multipotential progenitors
LN	lymph nodes
loxP	recognition sequence for Cre (locus of x-ing over of
LPS	lipopolysaccharide
Lyn	Lyn tyrosine kinase

LZ	light zone
M	molar
MACS	magnetic cell sorting
MEM NEAA	minimum essential medium non-essential amino acid
MFI	mean fluorescence intensity
mIg	membrane immunoglobulin
min	minute
ml	milli liter
mLN	mesenteric lymph nodes
mLST8	mammalian lethal with sec-13 protein 8
DEPTOR	DEP domain containing mTOR-interacting
mM	milli molar
MMM	metallophilic macrophages
MOPS buffer	3-(<i>N</i> -morpholino)propanesulfonic acid buffer
MPP	multipotential progenitor
mRNA	messenger ribonucleic acid
mTOR	mechanistic target of rapamycin
mut	mutant
MZM	marginal zone macrophages
MZPs	Marginal zone precursors
ns	no significance
NaCl	sodium chloride
NaOH	sodium hydroxide
Neo	neomycin resistance gene
NES	nuclear export signal
NF-milk	non-fatty milk
NKT cells	natural killer T cells
NLS	nuclear localization signal
nm	nano meter
NP-40	tergitol-type nonyl phenoxypolyethoxylethanol-40
NP-CG	4-hydroxy-3-nitrophenylacetyl chicken- γ -globulin
OD	optical density
p70S6K or S6K	p70 ribosomal S6 protein kinase

pAkt	phospho Akt
PBS	phosphate buffered saline
PCR	polymerase chain reaction
PDK-1	phosphoinositide-dependent kinase-1
PE	phycoerythrine
Pen	Penicillin
PerC	peritoneal cavity
PFA	Paraformaldehyde
pH	potential hydrogen
PH domain	pleckstrin homology domain phage P1)
PI3K	phosphatinositol 3 kinase
PKB	Protein Kinase B
PNA	peanut agglutinin
PP	Peyer's patches
PRAS40	proline-rich Akt substrate 40 kDa protein
PTEN	phosphatase and tensin homolog
PtdIns-3,4,5-P ₂	phosphatidylinositol-3,4,5-diphosphate
PtdIns-3,4,5-P ₃	phosphatidylinositol-3,4,5-trisphosphate
PTK's	protein tyrosine kinases
PTPs	protein tyrosine phosphatases
RAPTOR	regulatory-associated protein of mammalian target of rapamycin
rew	reverse
rictor	rapamycin-intensive companion of mTOR
RNA	ribonucleic acid
rpm	revolutions per minute
RSS	recognition signal sequence
RT	room temperature
s	second
SA	Streptavidin
SDS	sodium dodecyl sulfate
sec	second
Ser	serine
SGK	serum- and glucocorticoid induced kinase

SH2	SRC homology 2
SHM	somatic hypermutation
SHP-1	Suppressor of High-copy PP1
Sin1	mammalian stress-activated map kinase interacting protein1
SLC	surrogate light chain
SRBC	sheep red blood cell
ss	single-stranded
Strep	Streptomycin
Syk	spleen tyrosine kinase
T1/ 2 or 3	transitional 1/ 2 or 3
T2-FP	transitional stage 2-follicular precursors
T cells	thymus cells
TAE	tris-acetic acid-EDTA
TARC	Translational Animal Research Center
TBS	tris buffered saline
TD	T cell dependent
TE	tris-EDTA buffer
Thr	threonine
TI	T cell independent
TLR	toll-like receptor
Tris	2-amino-2-(hydroxymethyl)-1,3-propanediol
TTP	tyrosine triphosphate
TWEEN	polyoxyethylene-sorbitan-monolaureate
Tyr	tyrosine
U	units
V region	variable region
vs.	versus
v/v	volume per volume
VDJ	variable diversity and junction
w/v	weight per volume
WT	wild type
YFP	yellow fluorescent protein
α	anti

μg	microgram
μl	microliter
μM	micromolar
β-me	β-mercaptoethanol

1 Introduction

1.1 The Immune System

The immune system of vertebrates consists of different mechanisms for defending the body against infection. In general, two lines of defense exist: the innate and the adaptive immune responses. The innate form of the immune system is directly available and reacts to a wide range of pathogens but is not able to build a lasting immunity and is not specific for individual pathogens. This is why the adaptive immune system is important, as this branch of immunity is able to produce specific antibodies against a particular pathogen or its product. The adaptive immune system can result in memory cells against the respective pathogen and reacts very quickly in case of a reinfection. Examples of innate immunity include macrophages, dendritic cells and neutrophils; T and B cells belong to the adaptive immune system.

1.2 B Cell Development

B (*bone marrow or bursal*) cells develop in the bone marrow after birth and are generated in the fetus from pluripotent hematopoietic stem cells in the fetal liver (reviewed in Hardy and Hayakawa, 2001). The multipotential progenitor (MPP) develop from the murine hematopoietic stem cells (HSC) in the bone marrow, then the lymphoid-primed multipotential progenitors (LMPPs) arise followed by common lymphoid progenitor (CLP) population (Fig. 1.1). Different cell types can develop from these different cell stages, for example erythrocytes and megakaryocytes from MPPs, monocytes from LMPPs, T cells and dendritic cells (DCs) from CLPs. They all express different cell surface markers (Fig. 1.1). After the CLP stage, precursor B cells develop. These are divided in four subsets, termed fractions A, B, C and D (Hardy et al., 1991). *In vitro* analysis has shown that fraction A can develop into fraction B or C, suggesting they are the earliest B cell precursors. They are therefore known as pre-pro-B cells. During their differentiation, B cells undergo an immunoglobulin-gene rearrangement. In B cell precursors, the heavy-chain DJ (diversity and junction) is rearranged and then the heavy-chain variable (V)DJ rearrangement takes place. Most pre-pro-B cells lack heavy-chain DJ rearrangements, making them independent of immunoglobulin-gene rearrangement (Allman et al., 1999). Fractions B and C are called pro-B-cells (early and late pro-B cells), consist of

large, mitotically active cells and have heavy-chain DJ or variable (V)DJ rearrangements (Hardy et al., 1991; Li et al., 1996). Most cells in fraction D are small, resting B cells termed pre-B cells and IgM⁺ immature B cells (Hardy et al., 1991).

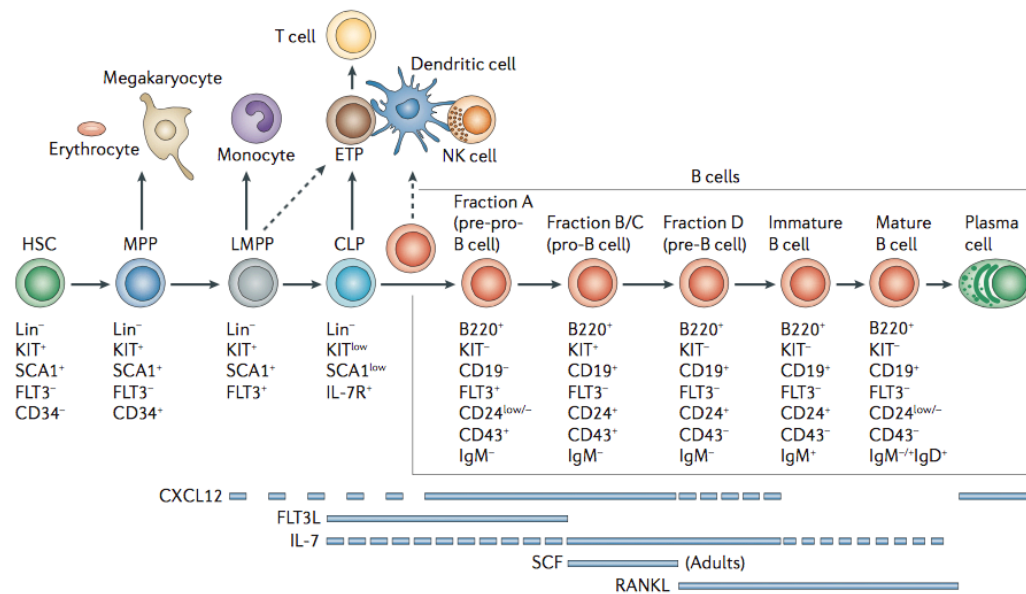


Figure 1.1: Early B cell development in the bone marrow.

B cell precursors, including their surface markers and out of the precursors developing cells. (Nagasawa, 2006)

After a successful rearrangement of their immunoglobulin genes, immature B cells enter the spleen as transitional 1 (T1) B cells. Here, they develop to T2 and possibly T3 B cells and mature to marginal zone (MZ) and follicular (FO) B cells (Fig 1.2) (Allman et al., 2001; Loder et al., 1999). T3 B cells are thought to be anergic B cells (Merrell et al., 2006). The hallmarks of MZ B cells will be described in section 1.2.1. FO B cells are located in the follicles of spleen, lymph node, and ectopic lymphoid aggregates. Ectopic lymphoid organs are also called tertiary lymphoid organs. They are formed after birth and mimic secondary lymphoid tissue structure. They generate local immune responses in tissues (Thompson, 2012). In general, FO B cells need T cell help to develop into plasma cells or memory B cells (Kerfoot et al., 2011; reviewed in Shlomchik and Weisel, 2012). After T cell contact, they proliferate and form small clusters of homogenous clones. These clusters are then able to build short-lived extrafollicular plasmablasts or a long-lived collection of germinal center (GC) B cells (Porto et al., 1998; Coico et al., 1983). In germinal centers, B cells undergo extensive rounds of proliferation, somatic hypermutation and antigen-affinity driven selection (reviewed in Victora and Nussenzweig, 2012; reviewed in Honjo et al.,

2002; Liu et al., 1989).

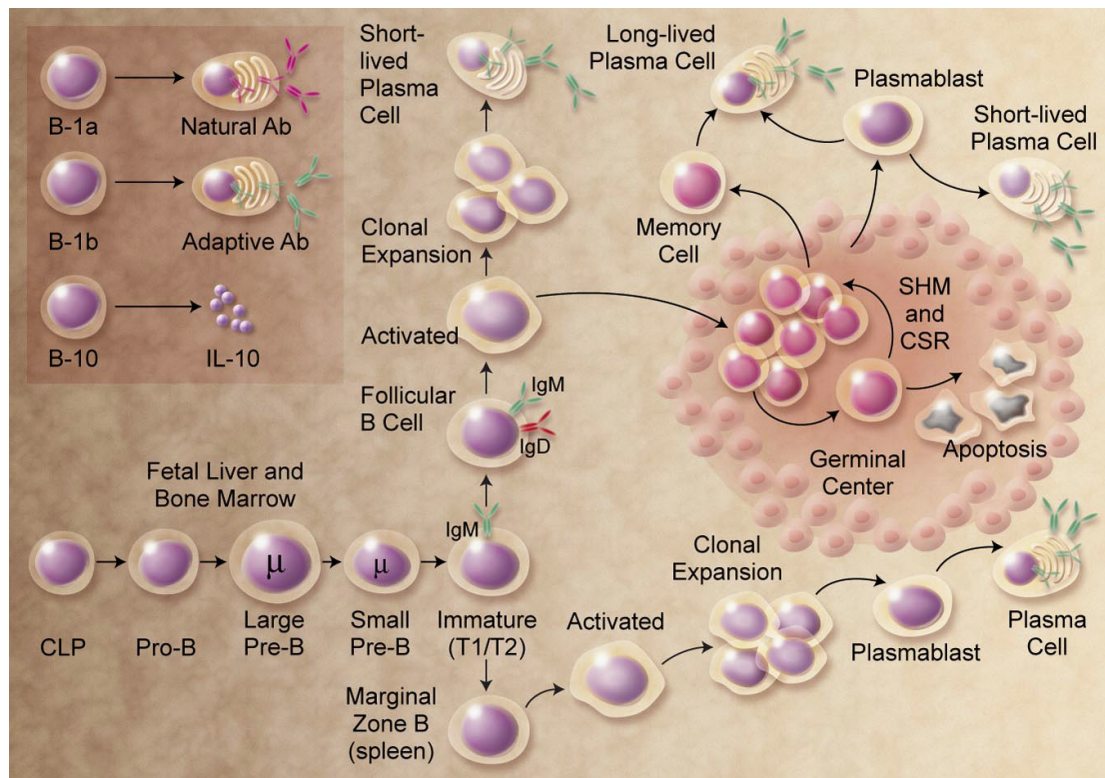


Figure 1.2: Overview of B cell development.

The developmental stages of B cells from the CLP stage via immature B cells to mature B cells. CPL= common lymphoid progenitor, CSR= class switch recombination, SHM= somatic hypermutation (LeBien and Tedder, 2008)

In addition to the B2 B cells, which consists of MZ B cells and the FO B cells, there is another population: B1 B cells. B1 B cells are localized in the peritoneal and pleural cavities but can also be found in lymph nodes and spleen (reviewed in Kantor and Herzenberg, 1993). They can be further divided in two subpopulations: the B1a B cells ($CD5^+$) and B1b B cells ($CD5^-$) (Kantor et al. 1992). In general, B1 B cells have a more restricted immunoglobulin repertoire compared to other immunoglobulin producing B cells and are primarily responsible for innate immunity, reacting to a variety of T cell independent antigens (Kantor et al., 1997; Baumgarth et al., 2005). B1 B cells also have the ability to produce $CD138^+$ plasma cells (Yang et al., 2007; Tung et al., 2007).

1.2.1 Marginal Zone B Cells

The marginal zone is a compartment of the spleen that separates the white pulp from the red pulp and was first described by Weidenreich 1901 as „Knötchenrandzone“

(Weidenreich, 1901; MacNeal, 1929). The marginal zone consists of different cell types: the marginal zone (MZ) B cells, specialized macrophages, reticular fibroblasts and dendritic cells (Nolte et al., 2004). In the MZ, two types of macrophages exist: the marginal metallophilic macrophages (MMM) and the marginal zone macrophages (MZM) (reviewed in Mebius and Kraal, 2005). MMMs cross-present blood-borne antigens by splenic CD8⁺ DCs and CD8⁺ T cells (Backer et al., 2010). MZMs are phagocytotic cells that remove blood-borne pathogens and apoptotic material in the spleen (Aichele et al., 2003; Odermatt et al., 1991). In histology, the marginal zone (MZ) can be detected with MOMA-1 antibody that detects the marginal metallophilic macrophages (MMM) that line the inner face of the marginal sinus (Kraal and Janse, 1986). In addition to using anatomical features to analyze MZ B cells, there are a number of surface markers that can be used to identify them. MZ B cells express high levels of IgM, CD21, CD1d, CD38, CD9 and CD25 and very low levels of IgD and CD23. In addition to these surface markers, they also express high levels of β 2 integrin, LFA-1, α 4 β 1 integrin as well as B7 protein (Gray et al., 1982; Hsu, 1985; Lu et al., 2002; Oliver et al., 1999; Oliver et al., 1997). In contrast to FO B cells that recirculate in the body, MZ B cells cannot circulate because they are sessile (Gray et al., 1982). Another characteristic of MZ B cells is their very long life span. Whether this is because they are long-lived cells or if the spleen contain self-renewing progenitors of MZ B cells is still in discussion (Hao and Rajewsky, 2001; Kumararatne, et al. 1980; reviewed in Pillai et al., 2005).

It has been shown that MZ B cells develop from a different T2 cell type in spleen than FO B cells do. These T2 cells are called T2-MZPs (marginal zone precursors) and are not found in mice that do not have marginal zone B cells, for example Aiolos null mice and conditional Notch2^{-/-} mice (Amano et al., 1998; Roark et al., 1998; reviewed in Pillai et al., 2004; Cariappa et al., 2001; Saito et al., 2003; Kumararatne and MacLennan, 1981).

For the development of MZ B cells only a 'weak' B cell receptor (BCR) signal is needed (Sun et al., 2002). Therefore a signal-strength model is proposed: if the BCR of a transitional stage 2-follicular precursors (T2FP) cell reacts with a self-antigen, the Bruton's tyrosine kinase (Btk) pathway is activated and the cell develops into a FO B cell. If the reaction of the T2-FP to the self-antigen is weak or non-existent, the cells survive because of the B cell activation factor (BAFF) and constitutive BCR

signaling. The absence of stronger BCR stimulation induces signals to develop into MZ B cells (Cariappa et al., 2001; reviewed in Pillai et al., 2004; reviewed in Cariappa and Pillai, 2002). This demonstrates that BAFF is crucial for MZ B cell development and survival (Thien et al., 2004; Batten et al., 2000). The Notch2 signaling also plays an important role for the MZ B cell development. This was first shown in a B cell-specific knockout of RBP-J κ that lead to an MZ B cells loss and an increase in FO B cells (Tanigaki et al., 2002). Other known ways of developing MZ B cells include the activation of PI3K through the BCR, and its subsequent activation of Akt leading to MZ B cell development (Srinivasan et al., 2009; Calamito et al., 2010; reviewed in So and Fruman, 2012).

MZ B cells are able to respond to blood born pathogens in order to defend the body. In this way, they can be part of T cell independent (TI) and T cell dependent (TD) immune reactions (Snapper et al., 1993; Snapper et al., 1995; Oliver et al., 1997; Rubtsov et al., 2008). In general, they react very quickly with a T cell independent humoral response on toll-like receptors (TLRs) and present lipid molecules in association with CD1d (Trembl et al., 2007; Genestier et al., 2007). They also interact with antigens exposed on macrophages, DCs or neutrophils and rapidly differentiate into plasmablasts to produce high amounts of IgM (Martin et al., 2001; Balázs et al., 2002; Ravetch et al., 2000). In addition, they are able to class switch and produce IgG and a little IgA. Antibodies produced by MZ B cells are low affinity antibodies and are required until FO B cells produce high affinity antibodies (Pone et al. 2012).

1.2.2 Germinal Center

Germinal centers (GCs) are found in secondary lymphoid organs. Their development takes place during T cell dependent antibody responses. Therefore, the interaction between antigen specific B cells and CD4⁺ T cells is important (MacLennan, 1994). GCs are mainly involved in antibody diversification through class switch recombination (CSR) and somatic hypermutation (SHM) (Jacob et al., 1991; Berek et al., 1991; Petersen-Mahrt et al., 2002; Hasler et al., 2011). For these two processes, GC B cells express the enzyme activation-induced cytidine deaminase (AID). A GC is divided into two different structural features: the light zone (LZ) and the dark zone (DZ). The LZ is proximal to the lymph node capsule or spleen marginal zone. It contains the antigen-specific GC B cells, follicular dendritic cells (FDCs), and a

subset of naive IgD⁺ B cells (Schwickert et al. 2009; Suzuki et al. 2009). The B cells are mixed among a network of FDCs (Schwickert et al., 2007). In addition to B cells, there are also CD4⁺ and CD8⁺ T cells as well as conventional dendritic cells (DCs) (Grouard et al., 1996). The DZ includes B cells that have a high nucleus to cytoplasm ratio (Nieuwenhuis and Opstelten, 1984).

1.3 Class Switch Recombination

The body has various mechanisms for defending itself against infections. One mechanism is the class switch recombination (CSR), which generates different antibody classes to react against structurally different pathogens. Naive B cells express IgM and IgD on their surfaces. Following infection, they are able to switch to expressing IgG, IgE or IgA (reviewed in Esser and Radbruch 1990). An antibody itself consists of the constant (C) region that has effector function and the variable (V) region where the antigen-binding site is arranged. The V region is built on IgH (heavy) and IgL (light) chains, whereas the IgL chain includes V_L and J_L gene segments and the IgH locus is encoded by V(D)J exons (Alt et al., 2014). The V(D)J exons are composed of variable (V_H), diversity (D) and joining (J) gene segments and are rearranged during early B cell development in the bone marrow (reviewed in Jung et al. 2006). Downstream of the V(D)J exons are eight sets of C_H exons in the following order: 5'-V(D)J-C_μ-C_δ-C_{γ3}-C_{γ1}-C_{γ2b}-C_{γ2a}-C_ε-C_α (Honjo, 1978). During CSR, the constant regions C_μ and C_δ of the C_H locus are replaced with C_{γ3}, C_{γ1}, C_{γ2b}, C_{γ2a}, C_ε or C_α regions, and in the end, one immunoglobulin isotype is produced.

The CSR process can take place both inside and outside the GCs and is induced by AID (Muramatsu et al., 2000). AID targets so-called S regions (repetitive sequences, 1 to 10kb), which are placed upstream before every C_H exon except for C_δ, and places double-strand breaks (DSBs) within them (Kataoka, 1980). AID then links the donor S region (also known as S_μ) to one of the other downstream acceptor S regions (S_{γ3}, S_{γ1}, S_{γ2b}, S_{γ2a}, S_ε or S_α) via a breakage and joining mechanism by which an extra chromosomal circle arises (reviewed in Iwasato et al., 1990; Kataoka, 1980). The “other” ends are joined together by classical non-homologous end-joining (C-NHEJ) or alternative end-joining (A-EJ). This leads to an mRNA in which the C_μ is replaced and a new class of antibody can arise, such as IgG, IgE or IgA. IgE expression can

also take place directly between S_μ and S_ϵ or following IgG switching through sequential CSR between the fused $S_\mu S_{\gamma 1}$ and S_ϵ (Fig. 1.3) (Xiong et al. 2012).

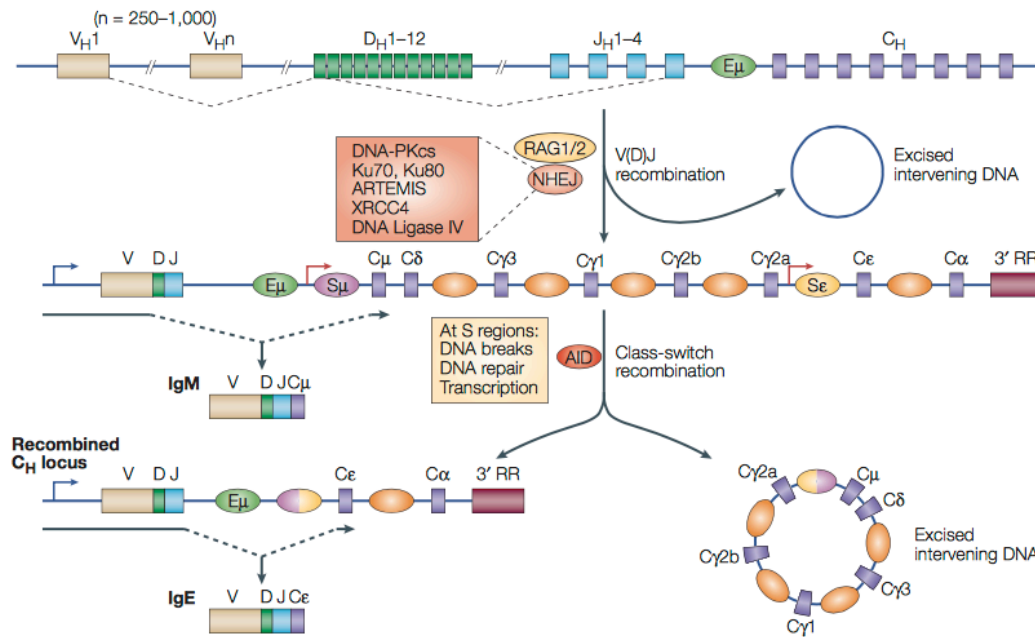


Figure 1.3: Mechanism of the class switch recombination.

After V(D)J recombination, class switch recombination (CSR) takes place. It is induced by activation-induced cytidine deaminase (AID) and leads to an excised intervening DNA and a mRNA sequence encoding for one of the different immunoglobulin isotypes. (Chaudhuri and Alt, 2004)

1.4 Activation-induced Cytidine Deaminase

The activation-induced cytidine deaminase (AID) is a 26kDA enzyme produced by the *Aicda* gene and is an important player and initiator of CSR and somatic hypermutation (SHM) (Muramatsu et al., 2000; Revy et al., 2000; Nagaoka, 2002; Petersen et al., 2001). The initiation of the CSR and SHM through AID starts by deaminating cytosine and creating an uracil (Petersen-Mahrt et al., 2002; Chaudhuri et al., 2003; Sohail et al., 2003; Bransteitter et al., 2003; Dickerson et al., 2003). In addition, AID acts as a mutagen and is involved in tumor genesis in B and non-B cells (Komeno et al., 2010; Pasqualucci et al., 2007; Takizawa et al., 2008; Matsumoto et al., 2007; Kovalchuk et al., 2007). For a long time it was believed that AID is restricted to B cells, but AID expression has also been found in $CD4^+$ T cells, testes, and ovaries (Qin et al., 2011; Schreck et al., 2006; Morgan et al., 2004). The structural composition of AID consists of an N- and a C-terminus that are connected by a cytidine deaminase (CD) catalytic domain and a linker sequence (Ta et al., 2003).

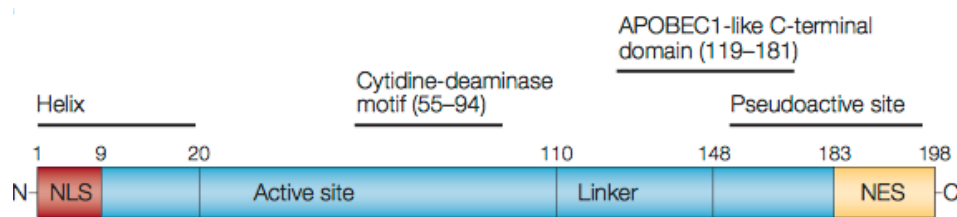


Figure 1.4: Primary structure of activation-induced cytidine deaminase (AID).

AID is composed of a nuclear localization signal (NLS) localized N-terminal, an active site that includes the cytidine-deaminase motif, a linker sequence and a nuclear export signal (NES) that is positioned C-terminal. (Chaudhuri and Alt, 2004, changed by E.-M. Cox)

At the N-terminus, a nuclear localization signal (NLS) can be found; and at the C-terminus, a nuclear export signal (NES) (Ito et al., 2004). The N-terminal region is required for DNA cleavage in CSR and SHM and the C-terminal region is needed for recombination (Ta et al., 2003) (Shinkura et al., 2004; Doi et al., 2009; Shivarov et al., 2008; Wei et al., 2011; Barreto et al., 2003). In addition, AID shows sequence homology with APOBEC1 (apolipoprotein B mRNA-editing enzyme, catalytic polypeptide 1), a RNA-editing cytidine deaminase (Patenaude et al., 2009). Some groups have assumed that AID edits an mRNA to encode a new protein required to activate CSR and SHM (Muramatsu et al., 2000; Revy et al., 2000; Doi et al., 2003), however APOBEC1 seems to be the exception to a family of DNA-cytidine deaminases that evolved to mediate innate immunity, and AID remains a DNA-modifying enzyme, as has been described in various publications (Fig. 1.4) (Harris et al., 2002).

1.5 The B Cell Antigen Receptor

The B cell antigen receptor (BCR) has different important functions. It is very important for clonal selection of B cells and the generation of a humoral immunity and in addition it is needed for the successful development and maintenance of the B cell pool in the periphery. The BCR is composed of a ligand-binding and a signaling domain. The ligand-binding domain includes a transmembrane immunoglobulin heavy chain (IgH) and a covalently associated immunoglobulin light chain (IgL). The antigen binding takes place at the complementary-determining regions (CDRs) that are created by an IgH and IgL in juxtaposition, to create a ligand-binding region that is unique for every BCR. For the signal transduction, a non-covalent-associated heterodimer of Ig α and Ig β signaling protein is provided (Papavasiliou et al., 1995;

Teh, 1997). Both Ig α (CD79a) and Ig β (CD79b) are bound to immune-receptor tyrosine-based activation motifs (ITAMs) that are necessary for signal transduction (Fig. 1.5). The BCR remains in a resting state until antigen binding activates it. There are two models for BCR activation that are currently being discussed. One is the crosslinking hypothesis, which suggests that all the BCR complexes on the resting B-cell surface are monomers, and that the crosslinking of two monomers leads to the activation of the BCR (reviewed in Radbruch et al., 2006). The second model describes an oligomeric structure of the resting BCR called “dissociation activation model” (DAM). This model describes an oligomeric structure for the activation of the BCR (Schamel et al., 2000; Yang and Reth, 2010). Downstream of the inactive BCR, the SRC-family protein tyrosine kinases (PTKs) Lyn tyrosine kinase (Lyn) and spleen tyrosine kinase (Syk) can be found (Campbell and Sefton et al. 1992; Yamanashi et al., 1991). Both act as initiators for BCR signaling. After the binding of an antigen through the BCR, LYN phosphorylates the ITAMs of Ig α and Ig β at the first tyrosine residue (Schmitz et al., 1996). The phosphorylation of ITAM-associated tyrosine residues forms docking sites for SRC homology 2 (SH2)-domain-containing proteins that are important for the activation of Syk, a PTK that contains such an SH2-domain (Fütterer et al., 1998; Grucza et al., 1999; Rowley et al., 1995). The ITAM phosphorylation therefore leads to the activation of Syk and Btk (reviewed in Kurosaki, 1999). Syk plays a key role in B cell signaling and phosphorylates both ITAM tyrosines (Y182 and Y193) of Ig α . A Syk disruption inhibits most downstream BCR signaling and leads to a block in B cell development. This underlines the importance of Syk in the BCR signaling (Abb. 1.4 right) (Jiang et al., 1998; Takata et al., 1994; Turner et al., 1995).

For a successful BCR signaling, positive and negative co-receptors are important. These modulate the signaling of the BCR and are transiently or constitutively localized with the BCR. CD19 and CD45 are positive co-regulators of the pre-BCR and BCR signaling (reviewed in Tedder et al., 1997; reviewed in Hermiston et al., 2003). CD45 is a phosphatase and dephosphorylates an inhibitory residue on the signal-initiating SRC-family PTKs that are responsible for the ITAM phosphorylation (Thomas and Brown, 1999). CD19 functions in a complex with CD21 and CD81 and is able to increase the BCR signaling in multiple ways (Carter and Fearon, 1992). The association of CD19 and CD21 is important for transduction signals that are triggered by the combined binding of complement C3d-coupled antigens to the BCR and CD21

(Fearon et al., 2000). The association of CD19 and CD81 is needed for CD19 surface expression and links the membrane protein complex to the cytoskeleton (Mattila et al., 2013). Examples for negative regulation of the BCR through co-receptors are CD5, CD22, CD72 and paired immunoglobulin-like receptor B (PIRB). They are transmembrane proteins that contain immune-receptor tyrosine-based inhibitory motifs (ITIMs) (Chacko et al., 1996). ITIMs are targets for SRC family proteins and their phosphorylation leads to the recruitment of SH2-domain-containing protein tyrosine phosphatases (PTPs) (reviewed in Nitschke, 2005; reviewed in Gergely et al., 1999).

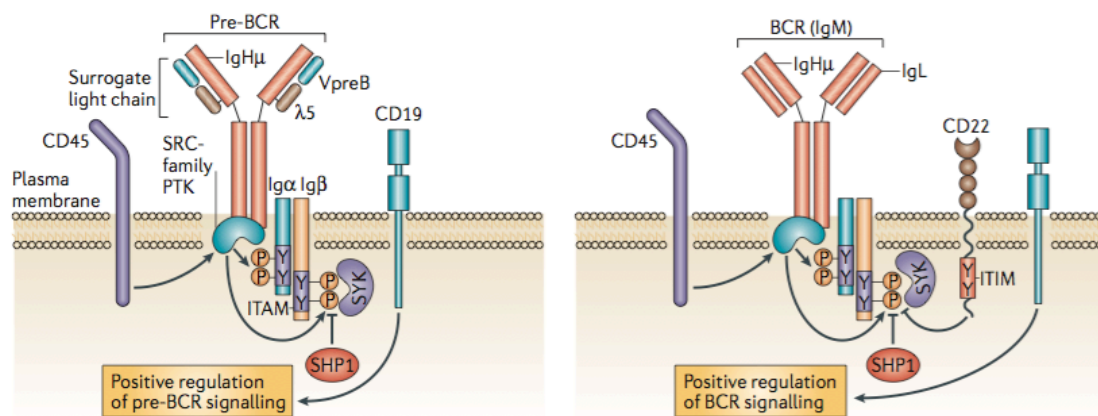


Figure 1.5: Structure and function of the pre-BCR and BCR complex. (Monroe, 2006)

The pre-BCR consist of the same components as the BCR except for the IgL chain at the ligand-binding domain. Instead of the IgL chain, there is a surrogate light chain (SLC) that is formed by Vpre-B and the $\lambda 5$ (Sakaguchi and Melchers, 1986; reviewed in Melchers et al., 1993; Karasuyama et al., 1990) (Fig. 1.5). Although the pre-BCR lacks the original antigen-binding site, the pre-BCR is able to generate signals. These signals and their regulation are similar to those from the BCR (reviewed in Benschop and Cambier, 1999; reviewed in Meffre et al., 2000). The pre-BCR signals are important for all pre-B cell dependent processes such as the IgH allelic exclusion, IL-7-dependend pro-B cell expansion, maturation through the pro-B cell pre-B cell checkpoint and the initiation of IgL gene recombination (reviewed in Monroe, 2006).

1.6 Akt, the Protein Kinase B (PKB)

Akt plays an important role in human diseases such as diabetes, hypertrophy and cancer (Cross et al., 1995; George, 2004; Cho, 2001; Shiojima et al., 2005; Roy, 2002; Cheng et al., 1996; Staal, 1987). This is due to the different ways of signal transduction that Akt influences. Akt is, for example, crucial for cell growth, survival,

proliferation and metabolism (Cho, 2001; Cho et al., 2001; Peng et al., 2003). To get a better understanding of how Akt acts in cases of malignancy in the immune system, we generated a mouse strain that constitutively overexpresses Akt1 in B cells. The Akt/protein kinase B (PKB) is a serine/threonine kinase which belongs to the cAMP-dependent protein kinase A/protein kinase G/protein kinase C (AGC) super family of protein kinases. Three different isoforms exist: Akt1/PKB α /RAC-PK α , Akt2/PKB β /RAC-PK β and Akt3/PKB γ /RAC-PK γ (Jones et al., 1991b; Jones et al., 1991a; Cheng et al., 1992; Staal et al., 1987; Konishi et al., 1995; Nakatani et al., 1999). These are all expressed in mice and humans and show high structural and functional similarity, but are differentially expressed on mRNA and protein levels (reviewed in Yang et al., 2004b; Altomare et al., 1998; Brodbeck et al., 1999). All isoforms consists of an amino terminal pleckstrin homology (PH) domain, a central kinase domain and a regulatory domain at the C-terminus (Fig. 1.6) (Bellacosa et al., 1991; Coffey and Woodgett, 1991; Datta et al., 1995).

The regulatory domain includes the hydrophobic and proline-rich motif characteristic of AGC kinases (Hanada et al., 2004). The phosphatidylinositol 3 kinase (PI3K) builds membrane lipid products such as phosphatidylinositol-3,4,5-diphosphate (PtdIns-3,4,5-P₂) and -trisphosphate (PtdIns-3,4,5-P₃) that become bound by the PH Domain of Akt with similar affinity (Frech et al., 1997; James, 1996). The kinase domain of Akt shares a high similarity with other AGC kinases and contains a conserved threonine (Thr) and serine (Ser) residue (Bellacosa et al., 1991; Coffey and Woodgett, 1991). This threonine residue is important for enzymatic activation. The carboxy terminus contains a 40 acids tail. In this region, a hydrophobic motif characteristic of AGC kinases can be found. To become fully activated, phosphorylation of the serine and threonine residue in this hydrophobic motif is important (Alessi et al., 1996; Hanada et al., 2004; Takeuchi, 1996). In case of Akt1, the residues are Thr308 in the activation loop and Ser473 in the hydrophobic motif (Alessi et al., 1996). Akt can be activated in several ways, but the most significant upstream activation is activation through PI3K (Franke et al., 1995; Burgering and Coffey, 1995).

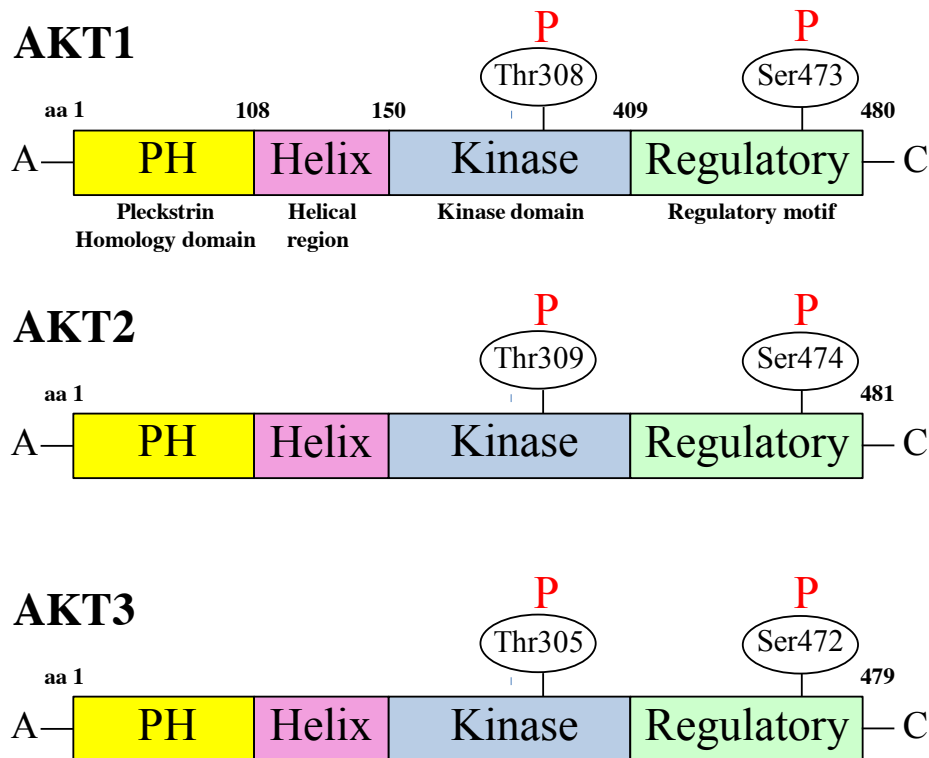


Figure 1.6: Structure of Akt1, Akt2 and Akt3.

Shown are the structures of Akt1, Akt2 and Akt3. They all consist of a pleckstrin homology (PH) domain, a helical region, a kinase domain and a regulatory motif. The kinase domain bears a threonine (Thr) and the regulatory motif a serine (Ser) phosphorylation site. These phosphorylation sites differ between the three isoforms. (Cohen, 2013, adapted by E.-M. Cox)

One mechanism by which PI3K is able to activate Akt is through the binding of phosphoinositides directly to the PH domain (James, 1996; Franke, 1997; Frech et al., 1997). This leads to the translocation of Akt from the cytoplasm to the inner surface of the plasma membrane, where PI3K generates 3'-phosphorylated phospholipid residues (Andjelkovic et al., 1997; Meier et al., 1997; Wijkander et al., 1997; Zhang and Vik, 1997; Sable et al., 1998; Currie et al., 1999). After Akt is constitutively active the relocation of Akt to the plasma membrane is very important for the Akt activation (Burgering and Coffey, 1995; Kohn et al., 1996). Through the relocation to the plasma membrane Akt comes in proximity to regulatory kinases that phosphorylate and activate Akt (Bellacosa et al., 1991; Coffey and Woodgett, 1991; Burgering and Coffey, 1995; Andjelkovic et al., 1996; Kohn et al., 1996; Soskic et al., 1999). Akt1 has four different phosphorylation sites (Ser124, Thr308, Thr450, Ser473) (Alessi et al., 1996). After an extracellular stimulation of cells Thr308 and Ser473 get phosphorylated, whereas Ser124 and Thr450 are basally phosphorylated

and gets dephosphorylated when activated.

1.6.1 Akt in B Cells

Activation of the BCR and its strengthening through the CD19 co-receptor leads to the activation of PI3K (Otero et al., 2001; Pogue et al., 2000). This activation is important for BCR-dependent proliferation and BCR-dependent tonic survival signaling. PI3K binds to the PH domain of Akt and phosphoinositide-dependent kinase-1 (PDK-1) (Stephens, 1998; Stokoe, 1997; Alessi et al., 1997a; Alessi et al., 1997b). PDK-1 activates Akt through phosphorylation of its threonine residue in the activation loop, in a PI3K-dependent manner in the case of Akt1 Thr308 (Aman, 1998; Astoul et al., 1999; Pogue et al., 2000; Alessi et al., 1996; Alessi et al., 1997b). In the case of Akt1 Ser473, for maximal activation of Akt a serine residue in the hydrophobic motif, has to be phosphorylated by another kinase, for example mTORC2 (Alessi et al., 1996). Activated Akt can promote different signaling pathways and substrates including mTOR pathway and FOXO1.

The mTOR kinase takes part in two different multi-protein complexes, mTORC1 and mTORC2 (Brown et al., 1994; Sabatini et al., 1994; Sabers et al., 1995; Cafferkey et al., 1993; Kunz et al., 1993). mTORC1 is composed of the mTOR enzyme, RAPTOR (regulatory-associated protein of mammalian target of rapamycin), PRAS40 (proline-rich Akt substrate 40 kDa), mLST8 (mammalian lethal with sec-13 protein 8) and DEPTOR (DEP domain containing mTOR-interacting protein) (Fig 1.7) (Jacinto et al., 2004; Kim et al., 2003; Peterson et al., 2009; Hara et al., 2002; Kim et al., 2002; Sancak et al., 2007; Thedieck et al., 2007; Haar et al., 2007; Wang et al., 2007). It regulates protein translation, cell size, intracellular transport, metabolism and lipid biogenesis (reviewed in Schmelzle and Hall; Kim et al. 2002). mTORC1 has the ability to sense nutrient and mitogen signals and can be activated by growth factors. The activation of mTORC1 can occur through Akt by phosphorylation (reviewed in Limon and Fruman, 2012).

In addition to the catalytic mTOR subunit, mTORC2 includes the activity components rictor (rapamycin-intensive companion of mTOR), Sin1 (mammalian stress-activated map kinase-interacting protein1) and mLST8, and the regulatory components DEPTOR and Protor1/2 (Sarbasov et al., 2004; Frias et al., 2006; Jacinto et al., 2006; Jacinto et al., 2004; Kim et al., 2003; Peterson et al., 2009; Pearce et al., 2007; Thedieck et al., 2007). As well as phosphorylation of serum- and

glucocorticoid-induced kinase (SGK) and PKC, mTORC2 phosphorylates Akt on Ser473 (Fig. 1.7) (Sarbasov et al., 2005). mTORC2 regulates cell survival and cytoskeleton dynamics (Jacinto et al., 2004).

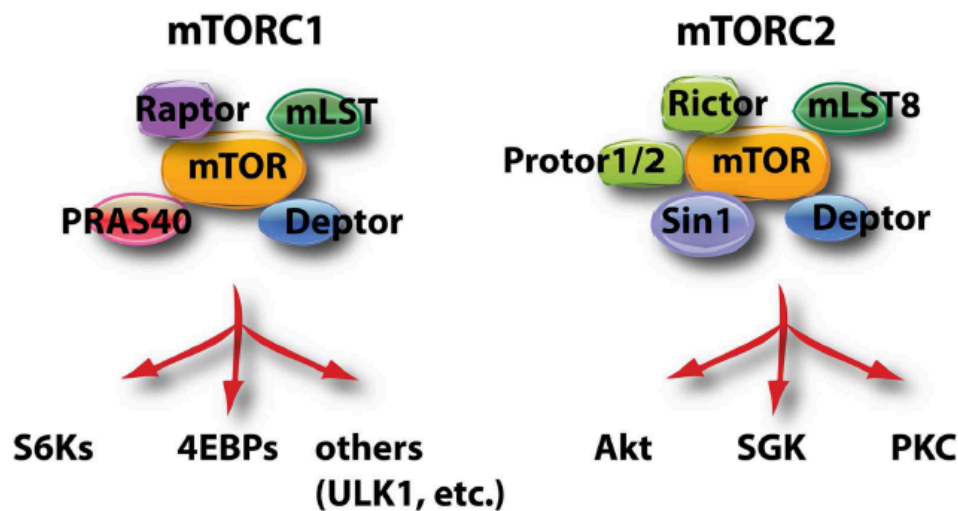


Figure 1.7: Components of mTORC1 and mTORC2 and its best known substrates.

Short cuts see text. (Limon and Fruman, 2012)

FOXO1 and FOXO3 are important players in B cell development and Akt is able to regulate them through phosphorylation (Dengler et al., 2008; Hinman et al., 2009; Lin et al., 2010). *FOXO1* is needed for a successful B cell development, whereas *FOXO3* is crucial for pre-B cell development (Dengler et al., 2008; Hinman et al., 2009). It has been shown that Akt and FOXO are able to regulate each other and the model of the Akt-FOXO axis has therefore been proposed, which can influence B cell development in two ways (reviewed in Limon and Fruman, 2012). In the case of a lower level of FOXO and higher levels of Akt, B cells undergo a fast differentiation into antibody secreting plasma cells that secrete low affinity IgM. A high FOXO and low Akt expression leads to GC formation and after 1-2 weeks memory or plasma cells with high affinity antibodies are generated (SHM and CSR) (Dengler et al., 2008). In resting B cells, FOXO factors are nuclear and force cell cycle arrest, longevity and recirculation (Essers et al., 2005; Takaishi et al., 1999). Akt is activated through B cell activation before entering the nucleus and phosphorylates FOXO at three different serine and threonine residues (Thr24, Ser256, Ser319) (Burgering et al., 1999; Rena et al., 1999; Takaishi et al., 1999; Tang et al., 1999). This leads to the export of FOXO into the cytoplasm, where it is degraded (Brunet et al., 1999; Biggs

et al., 1999; Brownawell et al., 2001). Taken together, the Akt-FOXO axis is a key control point for various B cell functions (Fig. 1.8).

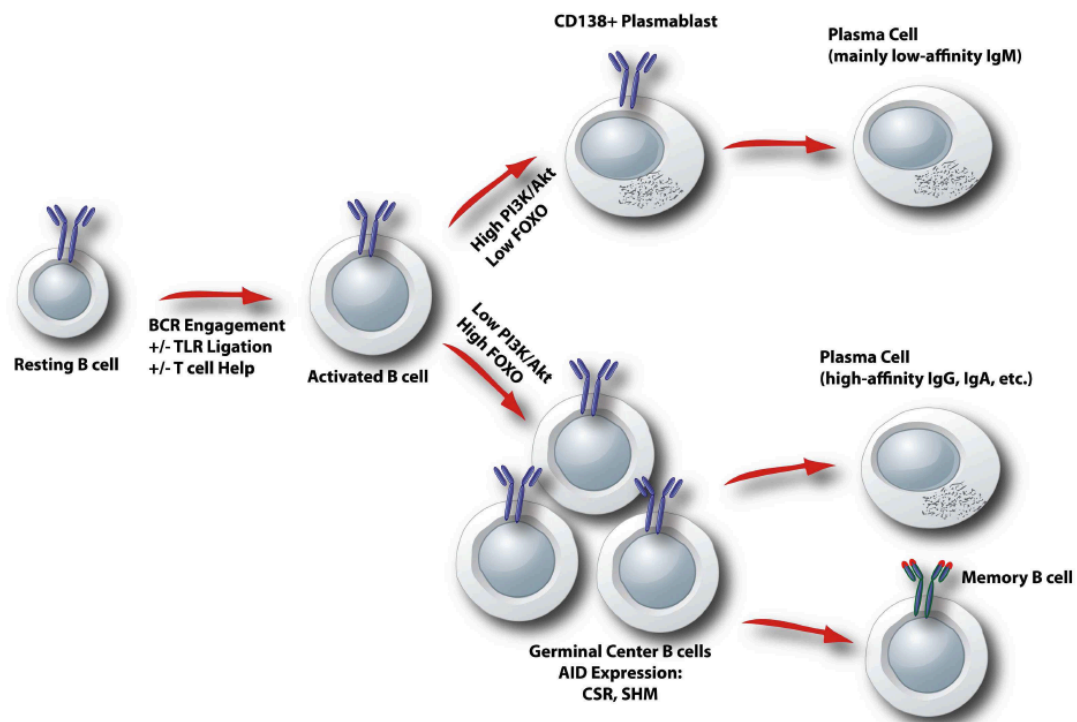


Figure 1.8: Shows how the Akt-FOXO axis controls the B cell differentiation of activated B cells.

The activity of PI3K/Akt signaling defines the nuclear activity of FOXO. High PI3K/Akt activity leads to low FOXO activity and plasmablast differentiation. When PI3K/Akt activity is low, FOXO activity is high and germinal center B cell fate can occur. (Limon and Fruman, 2012)

1.7 Objectives

The Akt pathway has multiple functions. Besides the regulation of cell growth, proliferation, differentiation, and survival it is also known for its role in malignancy. Akt was shown to be overexpressed in various carcinomas and appears to play an important role in cancer and other diseases in humans. The aim of this study was to investigate the role of constitutive Akt1 activation in B cell development, maturation, and possible B cell tumor formation. Therefore, we used a mouse strain allowing for the conditional expression of an N-terminally myristoylated Akt1 (Rosa-Akt-C) in cell types expressing the Cre recombinase. In this mouse, the myristoylation tag recruits Akt1 to the plasma membrane where Akt1 becomes constantly phosphorylated and therefore activated. The Rosa-Akt-C mouse was crossed to CD19-Cre mouse, leading to the B cell-specific overexpression of Akt1 (referred to as Akt^{BOE}) already from pro-B cell or early pre-B cell stages on. To investigate the influence of Akt1 overexpression in mature B cells, the Rosa-Akt-C mouse was crossed to AID-Cre mouse strain, deleting in germinal center cells.

2 Material and Methods

2.1 Used Material

2.1.1 Chemicals and Reagents

Chemicals were purchased from BD Biosciences (USA), Sigma-Aldrich (Steinheim), Carl Roth (Karlsruhe), Fluka (Steinheim), Merck (Darmstadt), or AppliChem (Darmstadt) unless stated otherwise. Solutions were prepared with double distilled water (ddH₂O).

Sterility of solutions and chemicals used in cell culture was maintained by working under a sterile hood (Heraeus[®], HeraSafe[®], Thermo Fisher Scientific, Langenselbold, Germany).

Table 2.1: Used chemicals.

Name of chemical	Supplier
Acetic acid (C ₂ H ₄ O ₂)	Merck, Darmstadt, Germany
Agarose, electrophoresis grade	Biozym, Hess. Oldendorf, Germany
Ammonium Chloride (NH ₄ Cl)	Sigma-Aldrich Chemie, Steinheim, Germany
Aqua	B. Braun, Melsungen, Germany
Bovine serum albumin (BSA)	Pan Biotech, Aidenbach, Germany
Dimethylsulfoxide (DMSO)	Lifetechnologies, Ober-Olm, Germany
DL-Dithiothreitol (DTT)	Sigma-Aldrich Chemie, Steinheim, Germany
Dubelco's Modified Eagle's Medium (DMEM)	Sigma-Aldrich, Sigma [®] Life Science, Buchs, Switzerland
EGTA	Sigma-Aldrich Chemie, Steinheim, Germany
Ethanol, abs. (EtOH)	Carl Roth, Karlsruhe, Germany
Ethidium bromide (EtBr)	Fluka, Sigma-Aldrich Chemie, Steinheim, Germany
Ethylendiamine tetraacetate (EDTA)	Sigma-Aldrich Chemie, Steinheim, Germany
FACS Clean	BD Biosciences, San Diego, USA

FACS Rinse	BD Biosciences, San Diego, USA
FACSFlow TM	BD Biosciences, San Diego, USA
Fetal calf serum (FCS)	Gibco [®] , Life Technologies TM , Paisley, UK
Glycine	Merck, Darmstadt, Germany
HBSS	Gibco [®] , Life Technologies TM , Paisley, UK
HEPES Buffer	Sigma-Aldrich, Sigma [®] Life Science, Buchs, Switzerland
Hydrochloric acid Fuming (37 %) (HCl)	Merck, Darmstadt, Germany
Ionomycin	PromoKine, Heidelberg, Germany
Isofluran, Forene [®] 100% (V/V)	Abbvie, Ludwigshafen, Germany
Isopropanol	Hedinger, Stuttgart, Germany
L-Glutamine 200mM	Gibco [®] , Life Technologies TM , Paisley, UK
Magnesium chloride (MgCl ₂)	Carl Roth, Karlsruhe, Germany
Methanol (MeOH)	Carl Roth, Karlsruhe, Germany
Minimum Essential Medium Non Essential Amino Acids (MEM NEAA)	Gibco [®] , Life Technologies TM , Paisley, UK
MOPS	Carl Roth, Karlsruhe, Germany
NP-40	Merck Millipore, Calbiochem, Schwalbach, Germany
Paraformaldehyde (PFA)	Sigma-Aldrich Chemie, Steinheim, Germany
PBS	Sigma-Aldrich, Sigma [®] Life Science, Buchs, Switzerland
PBS++	Gibco [®] , Life Technologies TM , Paisley, UK
Penicillin Streptomycin	Gibco [®] , Life Technologies TM , Paisley, UK
Phosphoric Acid (H ₃ PO ₄)	Carl Roth, Karlsruhe, Germany
Potassium acetate (C ₂ H ₃ KO ₂)	Merck, Darmstadt, Germany
Potassium chloride (KCl)	Merck, Darmstadt, Germany
Potassium Hydrogen Carbonat (KHCO ₃)	Carl Roth, Karlsruhe, Germany
Proteinase K	Roche, Mannheim, Germany
Sodium dodecyl sulfat (SDS)	Serva, Heidelberg, Germany

Skim Milk Powder	Fluka, Sigma-Aldrich Chemie, Steinheim, Germany
Sodium azide (NaN ₃)	Carl Roth, Karlsruhe, Germany
Sodium chloride (NaCl)	Carl Roth, Karlsruhe, Germany
Sodium hydrogencarbonate (NaHCO ₃)	Carl Roth, Karlsruhe, Germany
Sodium hydroxide (NaOH)	Merck, Darmstadt, Germany
Sodium pyruvate 100mM	Gibco [®] , Life Technologies [™] , Paisley, UK
Sulfuric Acid (H ₂ SO ₄)	Carl Roth, Karlsruhe, Germany
Tris	Carl Roth, Karlsruhe, Germany
Tween [®] 20	Sigma-Aldrich Chemie, Steinheim, Germany
b-Mercaptoethanol (b-ME)	AppliChem, Darmstadt, Germany

2.1.2 Equipment

Table 2.2: List of equipment not mentioned in the text.

Equipment	Supplier
CO ₂ -Incubator	BBD 6220, Heraeus [®] , Thermo Fisher Scientific, Dreieich, Germany
Gel documentation system	Gel-Doc XR, Bio-Rad Laboratories GmbH, Munich, Germany
Heating-Thermo Shaker	Multifunctional Thermo Shaker MHR 13, Ditabis Digital biomedical imaging system AG, Pforzheim, Germany
Magnetic stirrer	MR 3001 K, Heidolph, Schwabach, Germany
Multichannel pipette	Transferpette [®] S-12, Brand, Wertheim, Germany
pH meter	inoLab pH720, WTW, Weilheim, Germany
Pipettes	Pipetman, Gilson, Middleton, USA
Pipettor	MATRIX CellMate II, Thermo Scientific, New Hampshire, USA
Power supply	Power PAC 200 & Power PAC Basic, Bio-Rad Laboratories GmbH, Munich, Germany
Roller mixer	Roller mixer SRT9, Bio Cote Stuart, Stone, Staffordshire, UK
Scale	BP 1200, Sartorius, Sigma-Aldrich, Munich, Germany
Shaker	IKA-VIBRAX-VX12, IKA, Staufen, Germany
Table centrifuge	Galaxy MiniStar, silverline, VWR, Darmstadt, Germany
Vortex	REAX 2000, Heidolph, Schwabach, Germany
Waterbath	Memmert, Schwabach, Germany

2.1.3 Disposable Materials

Table 2.3: Table of used materials.

Expendable materials	Supplier
15 ml and 50 ml Tubes	Greiner Bio-one, Frickenhausen, Germany

6-well plate	Macroplatte, Greiner Bio-one, Frickenhausen, Germany
96-well plates, pointed bottom	Nunc, Thermo Fisher Scientific, Dreieich, Germany
96-well reaction plates for Real-Time analysis	MicroAmp [®] Fast 96-Well Reaction Plate, Applied Biosystems [®] (Life Technologies GmbH, Darmstadt, Germany).
Cryo-Tubes	CryoTube TM vials, Thermo Fisher Scientific, Dreieich, Germany
Cuvette	Roti [®] Lab, single-use cell, PS, Carl Roth, Karlsruhe, Germany
Extra Thick Blot Paper	Bio-Rad Laboratories GmbH, Munich, Germany
Gloves	Sempermed [®] , Sempercare [®] , Wien, Austria
Immobilon Transfer membrane	Immobilon P, Millipore 20orporation, Billerica, USA
Micro tube 1.5 ml	Sarstedt, Nümbrecht, Germany
Sterile 96-well plates, flat and round bottom	Nuncclon Delta Surface, Thermo Fisher Scientific, Dreieich, Germany
Sterile serological pipettes	Cell star, Greiner Bio-one, Frickenhausen, Germany
Sterile syringe filter (0.45 µm)	VWR, Darmstadt, Germany
Syringe 1ml	Luer-Lok TM Tip, BD Biosciences, San Diego, USA
Syringe	Omnifix [®] -F, Tuberculin, B. Braun, Melsungen, Germany
Tips	Nerbe Plus, Winsen/ Luhe, Germany

2.1.4 Buffer and Media

Table 2.4: Table of used buffers.

Buffer	Concentration	Composition
1× RIPA buffer	20mM	Tris-HCl (pH 7.5)
	150m	NaCl
	1mM	Na ₂ EDTA
	1mM	EGTA
	1%	NP-40
	1%	sodium deoxycholate
	2.5mM	sodium pyrophosphate
	1mM	β-glycerophosphate
	1mM	Na ₃ VO ₄
	1µg/ml	leupetin
Buffer A	10mM	HEPES
	10mM	KCl
	0.1mM	EDTA
		DTT and protease inhib., freshly added
1× MOPS buffer	0.05M	Tris
	0.05M	MOPS
	1.03mM	EDTA
	3.5mM	SDS
1× transfer buffer	192mM	Glycine

	25mM 10%	Tris MeOH
TBS	50mM 150mM	Tris NaCl, pH 7.4
10× Ack (Ammonium-Chloride-Potassium) lysis buffer	150mM 100mM 1.25mM	NH ₄ Cl KHCO ₃ EDTA
PBS-EDTA-BSA	2mM 0.5%	EDTA BSA
Tail Lysis buffer	100mM 5mM 2% 200mM 100-400µg/ml	Tris-HCl, pH 8.5 EDTA SDS NaCl Proteinase K, putted freshly
TE buffer	10mM 1mM	Tris-HCl, pH 8 EDTA
1× TAE	0.04M 0.001M 0.02M	Tris, pH 8 EDTA acetic acid

Table 2.5: Medium used to culture B cells.

Name of Medium	Composition
B cell medium	500ml DMEM 1.2% Pen (10.000Units/ml) Strep (10.000µg/ml) 1.2% MEM NEAA (100×) 1.2% L-Glutamin (200mM) 1.2% Sodium Pyruvat (100mM) 1.2% Hepes (1M) 0.12% MeOH 10% FCS
Resting B cell medium	500ml DMEM 1.2% Pen (10.000Units/ml) Strep (10.000µg/ml) 1.2% MEM NEAA (100×) 1.2% L-Glutamin (200mM) 1.2% Sodium Pyruvat (100mM) 1.2% HEPES (1M) 0.12% MeOH 1% FCS

2.2 Molecular Biology

2.2.1 Preparation of Genomic DNA

Tail biopsies were lysed overnight at 56°C in lysis buffer. Undigested tissue was pelleted by centrifugation for 10min at 20,000×g. To precipitate genomic DNA, the supernatant was mixed with an equal volume of isopropanol and collected by centrifugation 10min at 20,000×g. The DNA was washed with 70% (v/v) EtOH 10min at 20,000×g, dried at 37°C and solved in TE buffer.

2.2.2 RNA Isolation and Quantitative Real-Time PCR

RNA from murine cells was prepared using the peqGOLD Total RNA Kit (PEQLAB Biotechnologies GmbH, Erlangen, Germany). The SuperScript® II reverse transcriptase protocol (Invitrogen™ by life technologies™, Carlsbad, USA) was used to synthesize cDNA. cDNA was subsequently used for Real-Time PCR. Quantitative Real-Time PCR was performed with QuantiTect® primers from QIAGEN (Hilden, Germany) as described on their homepage: <https://www.qiagen.com/de/resources/resource-detail?id=882a8baa-29df-4182-a2a5-17083f4dbe11&lang=en>. Reaction took place in StepOnePlus™ Realtime System of Applied Biosystems (Life Technologies GmbH, Darmstadt, Germany). Expression of all genes was normalized to HPRT.

Table 2.6: Program used for quantitative Real-Time PCR.

Step	T °C	Time	Cycles/T °C	Description
1	95	15min		Holding stage
2	95	15sec		Cycling stage
3	55	30sec		Cycling stage
4	72	30sec	40× step 2-4	Cycling stage
5	90	15sec		Melt curve stage
6	60	1min	+0.5°C till 90°C for step 7 are reached	Melt curve stage
7	90	15sec		Melt curve stage

Table 2.7: Oligonucleotides used for quantitative Real-Time PCR.

Name of primer	Sequence (5'-3')/ Order no.	Company
Aicda	QT00123676	QIAGEN (Hilden, Germany),
CD23	QT00099540	QIAGEN (Hilden, Germany),

Deltex1	QT00097139	QIAGEN (Hilden, Germany),
Hes1	QT00313537	QIAGEN (Hilden, Germany),
Hes5	QT00268044	QIAGEN (Hilden, Germany),
IgG1	C μ R- AAT GGT GCT GGG CAG GAA I γ 1F- GGC CCT TCC AGA TCT TTG	Metabion(Planegg/ Steinkirchen, Germany)
Notch1	QT00156982	QIAGEN (Hilden, Germany),
Notch2	QT00153496	QIAGEN (Hilden, Germany),

2.2.3 Agarose Gel Electrophoresis

Separation of DNA fragments by size was achieved by electrophoresis in agarose gels (2% (w/v), 1 \times TAE ((Sambrook, 1989), 0.5mg/ml EtBr).

2.2.4 Quantification of DNA and RNA

The concentration of nucleic acids was determined by measuring the absorption of the sample at 260nm and 280nm in a multimode microplate reader (Infinite[®] M200Pro NanoQuant, Tecan, Männedorf, Switzerland). An OD₂₆₀ of 1 corresponds to approximately 50 μ g/ml for double stranded DNA or 40 μ g/ml for RNA and single stranded DNA. Purity of nucleic acids was estimated by the ratio OD₂₆₀/OD₂₈₀, with 1.8 and 2.0 optimal for DNA and RNA respectively. Alternatively, the DNA was separated by electrophoresis in an agarose gel and the concentration was evaluated from the band intensity in comparison to a standard. A third method for quantification was use of the NanoDrop[®] N-1000 (PEQLAB Biotechnologies GmbH, Erlangen, Germany).

2.2.5 Polymerase Chain Reaction (PCR)

PCR (Mullis and Faloona, 1987; Saiki et al., 1988) was used to genotype mice for the presence of targeted alleles or transgenes from tail DNA. The PCRs were carried out in Biometra T3000 Thermocycler (LABRepCo, Horsham, USA) or in Arctic[™] Thermal Cycler (Thermoscientific, Waltham, USA). Genotyping of mice DNA was performed in a total volume of 20 μ l, using the PCR program shown in Table 2.8. Blood of Akt^{BOE} mice was analyzed by FACS to screen for GFP expression.

Table 2.8: PCR program for DNA genotyping.

Step	T °C	Time	Cycles	Description
1	95	5min		Denaturation
2	96	30sec		Denaturation
3	60	1min		Primer hybridization

4	72	2min	34× step 2-4	Elongation
5	72	10min		Final elongation
6	4	∞		Cooling

PCR mix for 1 sample

10µl REDTaq[®] ReadyMix[™] PCR Reaction Mix*

0.1µl Primer1 (100µM)

0.1µl Primer2 (100µM)

1µl DNA

8.8µl dH₂O

*REDTaq[®] ReadyMix[™] PCR Reaction Mix with MgCl₂ (Sigma-Aldrich, St. Louis, USA) (20mM Tris-HCl, pH 8.3, 100mM KCl, 3mM MgCl₂, 0.002% gelatin, 0.4mM dNTP mix (dATP, dCTP, dGTP, TTP), stabilizers, 0.06unit/µl *Taq* DNA Polymerase).

Table 2.9: Sequences of oligonucleotides used for genotyping.

Name of primer	Sequence (5'-3')	T _{Ann} °C	Expected band sizes (bp)
Cre7	TCA GCT ACA CCA GAG ACG G	63	WT 452 mut 715
CD19c Cre	AAC CAG TCA ACA CCC TTC C	57	
CD19d2 Cre	CCA GAC TAG ATA CAG ACC AGG	62	
Cre rev	CCC GGC AAA ACA GGT AGT TA	58	310
Cre forw	GCA CTG ATT TCG ACC AGG TT	58	
Actin forw	TGT TAC CAA CTG GGA CGA CA	58	510
Actin rew	GAC ATG CAA GGA GTG CAA GA	58	
Rosa FA	AAA GTC GCT CTG AGT TGT TAT	55	WT 600 mut 250
Rosa Spi	CAT CAA GGA AAC CCT GGA CTA CTG	65	
Rosa RA	GGA GCG GGA GAA ATG GAT ATG	61	
5 eGFP	CGC CGT AGG TCA GGG TGG T	62	200
3 Rosa (eGFP)	CGC CGT AGG TCA GGG TGG T	64	
hCD2t forw2	GAC AAG AAA AAG ATT GCA CAA TTC AGA AAA GAG	68	146
hCD2t rev2	GTA TCA TAT ATT GAT ACC TTG TAG ATA TCC TGA TC	68	
JHT1	CAG TGA ATG ACA GAT GGA CCT CC	65	WT 400 mut 600
JHT2 mut	GCA GAA GCC ACA ACC ATA CAT TC	63	
JHT3 WT	CAC AGT AAC TCG TTC TTC TCT GC	63	

2.3 Biochemistry

2.3.1 Protein Extract Preparations

For preparation of whole cell lysates, frozen cell pellets were lysed on ice in appropriate amounts of RIPA buffer (Cell Signaling, Danvers & Boston, USA) to which protease inhibitor cocktail (Roche, Mannheim, Germany) and Phosphatase inhibitor (Roche, Mannheim, Germany) was added. Cells were gently pipetted up and down every 5min for 15min.

Cell suspensions were centrifuged at 20,000×g for 10min to separate debris from supernatant. Supernatants were transferred to fresh tubes. Protein concentration was determined in a photometer (Bio Photometer plus, Eppendorf, Hamburg, Germany) using Bio-Rad reagent (Bio-Rad Protein Assay Dye Reagent Concentrate, Bio-Rad Laboratories GmbH, Munich, Germany) and Bradford assay.

For preparation of nuclear and cytosolic protein fractions, freshly MACS purified B cells were used. Cells were lysed with Buffer A and placed for 15min on ice. Afterwards, 1% NP-40 was added and incubated at RT for 3min. The suspension was subsequently vortexed for 15s and spun down with 1500×g at 4°C. The resulting supernatant was the cytoplasm fraction. The pellet was washed three times in Buffer A and resuspended in RIPA buffer with 1% NP-40, DTT and protease inhibitors and incubated for 30min on ice. After a spin down for 10min at 4°C, the supernatant was transferred into a fresh tube (nuclear fraction). The protein concentrations were determined as described above (section 2.3.1).

2.3.2 Western Blot

20-100µg of protein was mixed with 4× loading dye (NuPAGE® LDS Sample Buffer, Novex® by life technologies™, Carlsbad, USA), 33mM DTT and aqua dest. and denatured at 70°C for 10min. Lysates were run on 4-12% gradient SDS-PAGE gels (NuPAGE® Novex® Gel Systems, Invitrogen™ by life technologies™, Carlsbad, USA) in gel electrophoresis chambers (X Cell Sure Lock™ Mini-Cell, life technologies, Carlsbad, USA) in 1× MOPS buffer and blotted with a semi-dry blot system (Trans-Blot® SD Semi-Dry Transfer Cell, Bio-Rad Laboratories GmbH, HEIDEL, Munich, Germany) in 1× transfer buffer (w/v) NF-milk/TBS/0.01% Tween

for 1 h at RT. Primary antibodies were incubated overnight at 4°C in either 5% (w/v) NF-milk/TBS/0.01% Tween or 5% (w/v) BSA/TBS/0.01% Tween. Membranes were then incubated for 1h at RT with secondary HRP conjugated donkey- α -rabbit or goat- α -mouse antibodies in 5% (w/v) NF-milk/TBS/0.01% Tween, except for Actin, which is directly HRP conjugated, was dissolved in NF-milk/TBS/0.01% Tween and the membranes were incubated for 1h at RT. AmershamTM ECL Prime Western blotting reagent (GE Healthcare Life Science, Freiburg, Germany) was used as a substrate for the HRP reaction and exposed in Molecular Imager[®] Gel DocTM XR System (Universal HoodIII, Bio-Rad Laboratories GmbH, Munich, Germany).

Table 2.10: Used Western blot antibodies.

Antibody	Band size (kDa)	Source	Supplier
Actin (I-19) HRP	43	Goat	Santa Cruz, Dallas, USA
Akt	60	Rabbit	Cell Signaling, Danvers & Boston, USA
A-Rabbit		Donkey	GE Healthcare Life Science, Freiburg, Germany
FOXO1 (C29H4)	78-82	Rabbit	Cell Signaling, Danvers & Boston, USA
Goat- α -Mouse		Goat	Bio-Rad Laboratories GmbH, Munich, Germany
GSK-3 β (27C10)	46	Rabbit	Cell Signaling, Danvers & Boston, USA
Lyn	56	Rabbit	Cell Signaling, Danvers & Boston, USA
mTOR (7C10)	289	Rabbit	Cell Signaling, Danvers & Boston, USA
Notch2 (D76A6) XP [®]	110, 120, 300	Rabbit	Cell Signaling, Danvers & Boston, USA
Phospho-Akt (Ser473)	60	Rabbit	Cell Signaling, Danvers & Boston, USA
Phospho-Akt (Thr308)	60	Rabbit	Cell Signaling, Danvers & Boston, USA
Phospho-GSK-3 β (Ser9) (D85E12)	46	Rabbit	Cell Signaling, Danvers & Boston, USA
Phospho-Lyn (Tyr507)	53, 56	Rabbit	Cell Signaling, Danvers & Boston, USA
Phospho-mTOR (Ser2448)	289	Rabbit	Cell Signaling, Danvers & Boston, USA
Phospho-Syk (Tyr525/526) (C87C1)	72	Rabbit	Cell Signaling, Danvers & Boston, USA
Phospho-Tyr (PY99)		Mouse	Santa Cruz, Dallas, USA
Syk (D3Z1E) XP [®]	72	Rabbit	Cell Signaling, Danvers & Boston, USA
α/β Tubulin	55	Rabbit	Cell Signaling, Danvers & Boston, USA

2.4 Cell Biology

2.4.1 Single Cell Suspensions of Cells from Lymphoid Organs

Murine lymphoid organs were taken and placed into ice-cold PBS/2% FCS. Spleen (Spl), lymph nodes (LN), Peyer's patches (PP) and mesenteric lymph nodes (mLN) were passed through a nylon cell strainer (40 μ M, Falcon[®], Corning, Durham, USA). Bone marrow was flushed with PBS/2% FCS and scattered with a syringe. Erythrocytes of spleen and bone marrow preparations were lysed with Ack lysis buffer for 2min. The reaction was stopped with ice-cold PBS/2% FCS and the erythrocyte debris was removed by centrifugation (300 \times g, 7min). Cells were then resuspended in an appropriate amount of ice cold PBS/2% FCS and counted (see section 2.4.3).

2.4.2 Isolation of Lymphoid Cells from Blood

Blood from the tail vein was collected in a tube with two drops Heparin (Heparin-Natrium-25000, Ratiopharm, Ulm, Germany) and layered on top of 7% (w/v) Ficoll 400 (LSM 1077 Lymphocyte separation medium, PAA Laboratories GmbH, Egelsbach, Germany) at a 1:1 ratio. Tubes were centrifuged at 3500rpm for 7min at RT. Lymphocytes were collected from the interphase of the gradients, resuspended in PBS/2% FCS and stored on ice.

2.4.3 Cell Counting

A Neubauer chamber (Marienfeld-Superior, Lauda-Königshofen, Germany) and trypan blue dye exclusion test were used to determine the number of viable cells. A small amount of cell suspension was diluted with physiological trypan blue solution (Gibco[®], Life Technologies[™], Paisley, UK), which stains dead cells blue. Live cells cannot take up the dye because of their intact membrane. After counting 16 single quadrants, the average counted cell number (N) was multiplied by the dilution factor (V) and the chamber factor (10⁴), resulting in the number of live cells per ml (Cell number/ml = $N \times V \times 10^4$).

2.4.4 Flow Cytometry

1 $\times 10^6$ cells per sample of prepared and counted single cell suspensions from organs were treated with Fc-block (BioXCell, West Lebanon, USA) to block free Fc receptors. The cells were then surface-stained in 40 μ l PBS/2% FCS with

combinations of fluorescein isothiocyanate (FITC), phycoerythrin (PE), peridin-chlorophyll protein complex (PerCP), allophycocyanin (APC), the tandem conjugates phycoerythrin cyanine dye (Pe-Cy7) and allophycocyanin cyanine dye (APC-Cy7), Pacific Blue, AmCyan and/ or biotin-conjugated monoclonal antibodies for 10min at 4°C. Stainings that contained biotinylated mAbs were then stained for a second time with Streptavidin (SA)-PE, SA-APC, SA-PE-Cy7, SA-APC-Cy7, SA-V500, SA-PerCP for 10 min at 4°C. The samples were subsequently washed and resuspended in PBS/2% FCS and analyzed on a FACSCanto™ II (BD Biosciences, Heidelberg, Germany) or FACSscan (BD Biosciences, Heidelberg, Germany). FLOWJO software (FLOWJO, LLC data analysis software, USA) or Cell Quest™ software (BD Biosciences, Heidelberg, Germany) was used to evaluate the results.

Table 2.11: Antibodies and compensation beads used for FACS stainings and compensations.

Specificity	Clone	Vendor
AA4.1/ CD93	AA4.1	eBioscience
B220/ CD45R	104 & RA3-6B2 RA3-6B2	eBioscience Biolegend, Caltag Lab, BD Bioscience
CD1d	1B1	eBioscience
CD3	145-2C11	BD Bioscience
CD4	GK 1.5 & RM4-5 RM4-5 & GK1.5	eBioscience BD Bioscience, eBioscience
CD5	53-7.3	eBioscience, BD Bioscience
CD8	YTS 169.4 53-6.7 5H10	Immunotools Biolegend, eBioscience, BD Bioscience Invitrogen
CD11b	M1/70	eBioscience
CD19	PeCa1 6D5 MB 19-1 1D3	Immunotools Biolegend eBioscience BD Bioscience
CD21/ CD35	7E9 8D9	Biolegend eBioscience
CD23	B3B4	BD Bioscience, eBioscience
CD24	M1/69	Biolegend
CD38	90	eBioscience
CD43	S7	BD Bioscience
CD44	IM7 IM8	eBioscience Biolegend

CD62L (L-Selectin)	MEL-14	Immunotools, eBioscience
CD90.2/ Thy1.2	53-2.1	eBioscience, Biolegend, BD Bioscience
CD138	281-2	BD Bioscience
F4/80	BM8	eBioscience
FAS/ CD95	Jo2	BD Bioscience
GR-1/ Ly6C+Ly6G	RB6-8C5	BD Bioscience
IgD	11-26c.2a 11-26c	BD Bioscience eBioscience
IgG1	A85-1	BD Bioscience
IgM	R6-60.2 II/41	BD Bioscience eBioscience
Igκ	187.1	BD Bioscience
Igλ		SouthernBiotech
IRF4	3E4	eBioscience
PNA		Sigma life science
PO-PRO TM -1 iodide		Invitrogen
SA Ab's		Biolegend, BD Bioscience, eBioscience
Fixable via dyes		eBioscience, BD Bioscience
Comp beads α-mouse negative control		BD Biosciences
Comp beads α-rat and α-hamster/ negative control		BD Biosciences

2.4.5 Ca²⁺-Flux Assay

To measure the flux of the second-messenger Ca²⁺ in cells, a chelate system was used. Chelators can bind Ca²⁺ in a high affinity. Therefore, fluorescent chelate-antibodies that change their spectral abilities in dependence to the loading condition with Ca²⁺ were used. The taken antibodies are FuraRedTM (PerCP) and Flou4 (FITC) (InvitrogenTM by life technologiesTM, Eugene, USA). The fluorescence intensity of FuraRedTM decreases with the uptake of Ca²⁺. For Flou4, the fluorescence intensity goes up with the Ca²⁺-binding. The FACS CantoTM II (BD Biosciences, Heidelberg, Germany) was used to measure the fluorescence. 10×10⁶ CD19 MACS purified B cells were stained and afterwards 4×10⁶ B cells were used for the measurement. Sit flush was shut down at the FACSCantoTM II to measure Ca²⁺ flux before the reaction was completed. First, the baseline of the B cells was recorded for 1min. Measurement was paused and 5μg/ml αIgM added to the cells to activate them and trigger the Ca²⁺ release. Ca²⁺ flux is a very fast reaction; therefore cells were immediately measured

for 4min after α IgM addition. As a positive control, 5 μ M Ionomycin was added to trigger a Ca^{2+} release and measured for 1 min; as a negative control, 10mM EGTA was used for the uptake of Ca^{2+} and measured for 2min.

Since efficiency of dye uptake differ from cell to cell, the intensity of only one dye cannot be used for comparison. Therefore, for the analysis the ratio between the fluorescence intensities of the two chelating-antibodies was calculated.

2.4.6 Magnetic Cell Sorting and FACS Sorting

Specific cell populations were either sorted or depleted from a heterogeneous cell suspension by magnetic cell sorting (MACS; Miltenyi Biotec, Bergisch Gladbach, Germany). Cell populations were labeled with antibody-coupled microbeads (10 μ l beads, 90 μ l PBS-EDTA-BSA per 10⁷ cells) and separated on LS or LD MACS columns (Miltenyi Biotec, Bergisch Gladbach, Germany) in a magnetic field (Miltenyi et al., 1990). For MACS purification, CD19 or CD43 Micro beads for mouse (Miltenyi Biotec, Bergisch Gladbach, Germany) were used. The purity of isolated cell populations was verified by FACS analysis. The purity of isolated B cells was between 93 and 98%. For cell sorting, B cells were purified by MACS and then stained with antibodies against various cell surface markers. Individual B cell subsets were then sorted using a FACS AriaTM II (Becton Dickinson, Franklin Lakes, USA).

2.4.7 Proliferation Assay and *in vitro* B Cell Stimulation

The CellTraceTM Violet Cell Proliferation Kit (Invitrogen, Paisley, UK) was used for cell labeling. This dye diffuses into cells, where it is cleaved by intracellular esterases to form a highly fluorescent compound. This compound binds covalently to intracellular amines, resulting in a stable fluorescent staining. The dye is unable to diffuse out of the cell. After one cycle of cell division, the stain is halved in each of the daughter cells. This can be detected by flow cytometry. For proliferation analysis, MACS-sorted (see section 2.4.6) B cells were labeled with CellTrace dye. For proliferation assays, B cells were resuspended in 1ml 37°C warm PBS per 10⁶ cells and 5 μ M CellTrace (5mM stock in DMSO, Molecular probes) and incubated in the dark for 20min at RT. The reaction was stopped by addition of 10ml B cell media (see table 2.5). After centrifugation (300 \times g, 7min), unbound CellTrace was washed away twice with PBS. Triplicates of 300,000 labeled cells were plated in a 96-well round bottom plate. The cells were incubated in B cell media (see table 2.5), treated with

α CD40, α IgM, LPS, BAFF or CpG (concentrations see table 2.12) and incubated at 37°C, 5% CO₂. Labeled cells were analyzed by flow cytometry after four days.

Table 2.12: Used stimulants.

Stimulus	Stock conc.	End conc.	Vendor
α IgM	1.2mg/ml	10 μ g/ml	Jackson ImmunoResearch, West Baltimore Pike, USA
BAFF	10 μ g/ml	50ng/ml	R&D Systems, Minneapolis, USA).
CpG	500 μ M	0.1 μ M	InvivoGen, San Diego, USA
LPS	1mg/ml	20 μ g/ml	Sigma-Aldrich, St. Louis, USA
α CD40	500 μ g/ml	2.5 μ g/ml	BioXCell West Lebanon. USA

2.4.8 Survival Assay

Two triplicates of 300,000 MACSed B cells were plated in a 96-well, round bottom plate and cultured for four days in B cell media (see table 2.5) at 37°C, 5% CO₂. The living cell number was determined daily by counting (see section 2.4.3) and cells were analyzed by flow cytometry.

2.4.9 Culture of *ex vivo* Splenocytes and Lymphocytes

Single cell suspensions of spleen and lymph nodes were prepared as described in section 2.4.1 and MACS either purified or not. B cells of spleens or lymph nodes were then resuspended in B cell media (see table 2.5) supplemented with various stimuli in the indicated concentration (see table 2.12) and cultured (37°C, 5% CO₂) for no longer than four days.

2.4.10 Plasma Cell Differentiation

For *in vitro* plasma cell differentiation triplicates of 300,000 MACS, purified B cells were plated in a 96-well round bottom plate and cultured in B cell media (see table 2.5) with IL4 and LPS (see table 2.13) at 37°C, 5% CO₂. After four days, cells were analyzed by flow cytometry.

2.4.11 Induced Class Switch Recombination

Splenic B cells were isolated using the MACS system. Triplicates of 300,000 cells per well were incubated in a 96-flat bottom plate for four days in the presence of different stimuli (concentrations see table 2.12). After this, B cells were either analyzed for the expression of IgA (BAFF, IL4, IL5, LPS, TGF β , α δ Dextran), IgG1 (IL4, LPS),

IgG2b (BAFF, LPS, TGF β) and IgG3 (LPS) by flow cytometry or used to generate PCR of circular class switch transcripts.

Table 2.13: Stimuli used to induce class switch to different immunoglobulins.

Stimulus	Stock conc.	End conc.	Vendor
BAFF	10 μ g/ml	100ng/ml	R&D Systems, Minneapolis, USA).
IL4	10 μ g/ml	20ng/ml	R&D Systems, Minneapolis, USA).
IL5	5 μ g/ml	1.5ng/ml	R&D Systems, Minneapolis, USA).
LPS	1mg/ml	50 μ g/ml	Sigma-Aldrich, St. Louis, USA
TGF β 1	2 μ g/ml	2ng/ml	R&D Systems, Minneapolis, USA).
α δ Dextran	25 μ g/ml	3ng/ml	Fina Biosolutins (Rockville, USA)

2.4.12 PCR of Circular Class Switch Transcripts

During class switch recombination, slope transcripts are formed. These transcripts can be detected via PCR.

Table 2.14: PCR program used for the analysis of circular class switch transcripts.

Step	T °C	Time	Cycles	Description
1	95	9min		Denaturation
2	94	30sec		Denaturation
3	58	1min		Primer hybridization
4	72	1min	35 \times step 2-4	Elongation
5	72	10min		Final elongation
6	4	∞		Cooling

PCR mix for 1 sample

10 μ l REDTaq[®] ReadyMix[™] PCR Reaction Mix*

0.1 μ l Primer1 (100 μ M)

0.1 μ l Primer2 (100 μ M)

1 μ l DNA

8.8 μ l dH₂O

*REDTaq[®] ReadyMix[™] PCR Reaction Mix with MgCl₂ (Sigma-Aldrich, St. Louis, USA) (20 mM Tris-HCl, pH 8.3, 100 mM KCl, 3 mM MgCl₂, 0.002 % gelatin, 0.4 mM dNTP mix (dATP, dCTP, dGTP, dTTP), stabilizers, 0.06 unit/ μ l *Taq* DNA Polymerase).

Table 2.15: Sequences of oligonucleotides used to analyze slope transcripts.

Name of primer	Sequence (5'-3')	T _{Ann} °C
C μ R	AAT GGT GCT GGG CAG GAA GT	60
I γ 1F	GGC CCT TCC AGA TCT TTG AG	60
I γ 3F	TGG GCA AGT GGA TCT GAA CA	58
Actin rew	GAC ATG CAA GGA GTG CAA GA	58
Actin forw	TGT TAC CAA CTG GGA CGA CA	58

2.4.13 Histological Analysis

Shock-frozen organs were cut in 8-10 μ m slices in a cryostat (LEICA CM1900, Leica, Wetzlar, Deutschland), transferred onto glass slides and stored at -80°C till needed. For immunofluorescence staining, sections were thawed, air dried, fixed with 4% PFA (Sigma-Aldrich Chemie, Steinheim, Germany) and stained with primary antibody overnight at 4°C in a humidified chamber. Used antibodies: α -B220 (BD Pharmingen, Hatfield, United Kingdom), α -CD1d (eBioscience, Hatfield, United Kingdom), α -CD3 (eBioscience, Hatfield, United Kingdom) and α -MOMA-1 (BMA biomedicals, Augst, Switzerland). Slides were incubated for 30min, RT with a biotinylated secondary antibody (Dianova, Hamburg, Germany). Finally, slides were treated with streptavidin-HRP and stained with Tyramide (Cy3). Before investigation, nuclei were counterstained for 5min at RT with Hoechst 3342. Slides were covered with Mounting Medium with DAPI (Vector H-1200, Vector Laboratories, Inc. Burlingame, USA). Analysis was carried out with a fluorescence microscope (Olympus IX81, Shuichi, Tokio, Japan). Stainings and fluorescence microscope pictures were performed by Alexei Nikolaev (Institute for Molecular Medicine, University Medical Center of the Johannes Gutenberg-University).

For the manufacture of 4% PFA, 900ml of dH₂O were heated up to 60°C. During stirring, 40g of PFA (Sigma-Aldrich Chemie, Steinheim, Germany) were added. To dissolve PFA 10 drops of 2N NaOH were added and after the solution had become clear, 100ml of 10 \times PBS were added. After this the pH was adjusted to 7.2.

2.5 Mouse Experiments

Tail bleeding as well as the general handling of mice was performed according to Hogan (Hogan et al., 1987) and Silver (Silver, 1995).

2.5.1 Mice

C57BL/6 mice were obtained from Harlan Laboratories. CD19-Cre mice (Rickert et al., 1997) and AID-Cre mice (Kwon, Busslinger et al., 2008) were crossed to Rosa-Akt-C mice (F. T. Wunderlich, unpublished). JHT knockout mice (Gu et al., 1993) were crossed to CD19-Cre mice and then to Rosa-Akt-C mice. The crossings were carried out in the standard facilities of the University Medical Center Mainz TARC (Translational Animal Research Center).

2.5.2 NP-CG, SRBC and NP-Ficoll Immunization

Primary T cell dependent (TD) responses were induced with alum precipitated NP-CG (4-hydroxy-3-nitrophenylacetyl chicken- γ -globulin) (Weiss and Rajewsky, 1990; Rickert et al., 1995) and sheep red blood cells (SRBC). The antigen was prepared by mixing 1 volume of NP₂₀-CG (100 μ g) (Biosearch Technologies, Petaluma, USA) with 1 volume of PBS (100 μ l). Mice were immunized with i.p. injections of 100 μ g NP₂₀-CG in a volume of 200 μ l. For an immunization with SRBC, 1 volume SRBC (Sheep Blood in Alsevers Solutions, Oxoid, Thermo Fisher Scientific, Hampshire, UK) was mixed with 50 volumes of PBS, centrifuged for 10min, 300 \times g at 4°C. Then it was washed three times with 50 volumes PBS. The cells were counted and resuspended in PBS (10⁹ cells/ml). The mice were i.p. injected with 100 μ l of the diluted SRBC. NP-Ficoll generated a T cell independent (TI) type 2 antigen reaction. For NP₂₇-Ficoll (Biosearch Technologies, Petaluma, USA), immunization mice were injected i.p. with 5 μ g/mouse NP₂₇-Ficoll. The antigen was dissolved in 10 μ l PBS.

2.5.3 Antibiotic Treatment to Eliminate Microbiota in the Gut

4.5 week-old mice were treated for 5.5 weeks with a mixture of antibiotics in their drinking water, which was changed twice a week and kept in the dark. The following antibiotics were dissolved in autoclaved water: Metronidazole (2.15mg/ml) (Sigma-Aldrich Chemie, Steinheim, Germany), kanamycin sulfate salt (4mg/ml) (Sigma-Aldrich Chemie, Steinheim, Germany), gentamicin sulfate salt (350 μ g/ml) (Sigma-Aldrich Chemie, Steinheim), Germany and ampicillin (2.5mg/ml) (Ratiopharm, Ulm, Germany).

2.5.4 Immunglobulin- and Cytokine-ELISA

For the Ig-ELISA, Ig serum concentrations to NP (4-hydroxy-3-nitrophenylacetyl) were determined with ELISA as has been described previously (Roes and Rajewsky,

1993). Microtiter plates (Greiner Bio-one, Frickenhausen, Germany) were coated overnight at 4°C with a for Ig class specific coating antibody in PBS or when NP-specific with NP BSA (Biosearch Technologies, Petaluma, USA). The next day, the microtiter plate was blocked with PBS/0,5% BSA for 30min at RT. Serially diluted sera samples, standard and blank, were applied to the wells and incubated for 1h at 37°C. The secondary biotinylated antibody was added for 1h at 37°C. Streptavidine-AP (Roche, Mannheim, Germany) was pipetted onto the microtiter plate and incubated for 30min at RT. Afterward this, the substrate (ALP Roche Hitachi, Mannheim, Germany) was incubated for 10-20min in the dark at RT. Following each incubation step, unbound antibodies, streptavidin-enzyme or substrate were removed by a three times 5min washing step with tap water. The probes were measured in a multimode microplate reader (Infinite® M200Pro NanoQuant, Tecan, Männedorf, Switzerland) at 405nm and a reference at 570nm. The relative antibody concentration was determined by calculating the association constant as described by Cumano and Rajewsky (Cumano and Rajewsky, 1985), following a method developed by Herzenberg et al. (Herzenberg et al., 1980). SoftMax® Pro (Molecular Devices Corporation, Sunnyvale, California, USA) software was used to analyze the data. For the CD23 ELISA, a Kit was used and performed as instructed by the manufactures (mouse CD23/Fcε RII, DuoSet® ELISA Development Systems, R&D Systems, Minneapolis, USA).

Table 2.16: Antibodies, biotin-conjugates and standards used for Ig-ELISA.

Coating	Biotin-Conjugate	Specificity	Standard
Goat α-Mouse IgM	Rat α-Mouse IgM	IgM	Homemade, Clone: B1-8μ
Goat α-Mouse IgG1	Rat α-Mouse IgG1	IgG1	Homemade, Clone: N1G9
Goat α-Mouse IgG2a	Goat α-Mouse IgG2a	IgG2a	Homemade, Clone: 41.2-3
Goat α-Mouse IgG2b	Goat α-Mouse IgG2b	IgG2b	Homemade, Clone: D3-13F1
Goat α-Mouse IgG3	Goat α-Mouse IgG3	IgG3	Homemade, Clone: S24/63
Goat α-Mouse IgA	Goat α-Mouse IgA	IgA	SouthernBiotech
Rat α-Mouse IgE	Rat α-Mouse IgE	IgE	Homemade, Clone: B1-8
Goat α-Mouse κ	Goat α-Mouse κ		Homemade, Clone: S8
Goat α-Mouse λ	Rat α-Mouse λ		Homemade, Clone: N1G9

All used antibodies and biotin-conjugates were from SouthernBiotech (Birmingham, USA).

2.6 Software

For analyzing flow cytometry data, Cell QuestTM (BD Biosciences, Heidelberg, Germany) and FLOWJO (FLOWJO, LLC data analysis software, USA) were used. SoftMax[®] Pro (Molecular Devices Corporation, Sunnyvale, California, USA) software was used for ELISA data and StepOneTM Software v2.2 (Life Technologies GmbH, Darmstadt, Germany) for quantitative Real-Time analysis. For statistics, Prism[®] (GraphPad Software Inc., USA) and Microsoft Excel (Microsoft Corporation, USA) were used. For preparing figures, Adobe Illustrator CS4, Adobe Acrobat Pro and Adobe Photoshop CS4 (Adobe Systems, USA) were used. For text processing Microsoft Word (Microsoft Corporation, USA) was used.

2.7 Statistic

Values are typically represented as mean \pm SEM (standard error of mean). Statistical significance was assessed using 2-tailed Student *t* test or 2-way ANOVA test. P-values $< 0,5$ were regarded as significant, displayed by * in the figures (*= p-value < 0.05 , **= p-value < 0.01 , ***= p-value < 0.001).

3 Results

3.1 Functionality of the Transgenic Akt^{BOE} Mouse Model

Akt is an important serine/threonine kinase with functions that encompass cell growth, proliferation, differentiation, survival, and metabolism (Cho et al., 2001; Peng et al., 2003). Besides these essential roles, Akt also plays an important role in certain diseases, including diabetes, hypertrophy, and cancer (Roy, 2002; Shiojima et al., 2005; Staal, 1987). For instance, Akt was shown to be activated in cancer (Staal, 1987). For example, in a special form of non-Hodgkin lymphoma, the B cell chronic lymphocytic leukemia (B-CLL) activation of Akt was observed and direct inhibition of Akt led to apoptosis of B-CLL cells (Hofbauer et al., 2010). In general, Akt gets activated through the phosphorylation of serine (Ser) and threonine (Thr) residues. In B cells, Akt is phosphorylated at Ser473 and Thr308, which either activates or inactivates target proteins, influencing processes such as survival, proliferation, differentiation, metabolism, and certain diseases. (Cheng et al., 1992; Alessi et al., 1996; Alessi et al., 1997b; reviewed in Limon and Fruman, 2012).

For experiments the Rosa-Akt-C mouse (unpublished mouse made by F. T. Wunderlich) was used. The Rosa-Akt-C mouse strain allows for the conditional expression of an N-terminally myristoylated Akt1 in cells expressing the Cre recombinase. The myristoylation tag recruits Akt1 to the plasma membrane where Akt1 is constantly phosphorylated. As an internal control, green fluorescent protein (GFP) serves to monitor recombination efficiency through an Internal Ribosome Entry Site (IRES-element) (Fig. 3.1A). IRES in general leads to an efficient co-expression of two genes under the same promoter (Kozak, 2005). In order to investigate the role of B cell specific overexpression of Akt1 in B cell maintenance, differentiation and possible B cell tumor formation, the Rosa-Akt-C mouse was crossed to the CD19-Cre mouse (Rickert et al., 1997). In the resulting strain the Cre recombination deletes a loxP flanked STOP cassette, allowing for the B cell specific overexpression of Akt1, under control of the CAG promoter (Fig. 3.1A). The CAG promoter consists of the Cytomegalovirus (CMV) early enhancer and the chicken β -actin promoter and rabbit β -globin which is a strong synthetic promoter that drives

high levels of gene expression allowing Akt1 to be consistently active (Niwa et al., 1991).

The CD19-Cre mouse strain deletes loxP flanked alleles specifically in the B cell lineage from the pro-B cell or early pre-B cell stages on with a deletion efficiency of 75-80% in the bone marrow (BM) and over 90-95% in splenic B cells (Rickert et al., 1997).

In this thesis, the Rosa-Akt-C mouse crossed to the CD19-Cre mouse is referred to as Akt^{BOE} mice and expresses both Akt1 and CD19-Cre heterozygously. As controls we used CD19-Cre heterozygous mice, due to the fact that they already have a reduced number of marginal zone (MZ) B cells and B1 B cells. B cell populations that are shown in FACS stainings are always gated on GFP⁺ B cells to exclude cells that escaped Cre-mediated recombination with the exception of stainings including T cells, since T cells do not overexpress Akt1 and are not GFP⁺. For the calculation of total B and T cells, all cells were used. In our hands, the Cre deletion efficiency in B cells of Akt^{BOE} mice was different for each organ and for the peritoneal cavity (PerC). In spleen, (Spl) the deletion efficiency was 92-96%; in peripheral lymph nodes (pLN, including: superficial cervicals, axillary, brachial, and inguinal lymph nodes) 35-76%; in mesenteric lymph nodes (mLN) 70-96%; in Peyer's patches (PP) 89-97%; and in PerC 98-99.8%.

The phosphorylation of Akt1 at the site Thr308 is mediated through phosphoinositide-dependent kinase-1 (PDK-1) in a phosphoinositide 3-kinase (PI3K) dependent manner, whereas the Ser473 becomes phosphorylated by mTORC2 (Alessi et al., 1996; Alessi et al., 1997b; reviewed in Limon and Fruman, 2012). For maximal activation of Akt, both amino acid residues need to be phosphorylated (Alessi et al., 1996). To confirm the overexpression and the activation of Akt1 in unstimulated B cells of Akt^{BOE} mice, we performed Western blot analysis. Therefore, antibodies that recognize the phosphorylation of Akt at Ser473 and Thr308 were used and, as expected, the phosphorylated amino acid residues could be detected at 60kDa in the Akt^{BOE} MACS purified B cell lysates. Akt^{BOE} B cell lysates showed, in addition to the phosphorylated Akt variants, a slightly larger pAkt band when compared to B cell lysates from CD19-Cre controls (Fig. 3.1B). Endogenous Akt was, as expected, detected in MACS purified B cell lysates from spleen of Akt^{BOE} mice and CD19-Cre controls at 60kDa. An additional larger band was also seen here in cell lysates of Akt^{BOE} when compared to CD19-Cre controls (Fig. 3.1B). This additional band could

be due to the myristoylation tag and the triple FLAG tag at the C-terminus, which are absent in controls. A slight phosphorylation of Akt at Ser473 and Thr308 was also observed in control lysates. This is possibly due to the MACS purification since the process of MACS purification with CD19 beads leads to direct binding of the co-receptor CD19 on B cells, causing activation, which might explain the weak phosphorylation in controls.

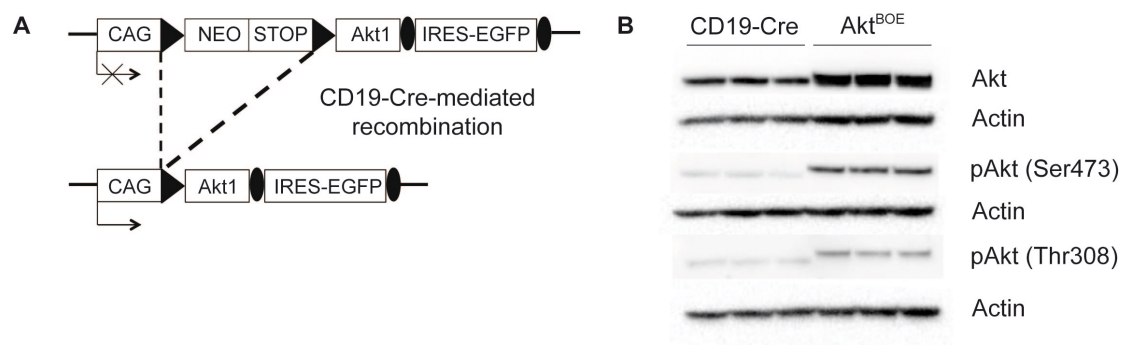


Figure 3.1: Generation of Akt^{BOE} mice.

(A) Schematic representation of the targeting strategy in a Rosa locus. B cell specific overexpression of Akt1 (Akt^{BOE}) was generated through CD19-Cre-loxP mediated recombination. Filled triangles represent loxP sites; filled ovals represent FRT sites. After Cre recombination, the Neomycin (NEO) and the Stop cassette, flanked by loxP, are excised. Akt1 and GFP are expressed under the control of the CAG promoter. **(B)** Western blot analysis of 45µg protein lysates from CD19 purified splenic B cells using α -Akt (60kDa), α -phospho-Akt Ser473 (60kDa), and α -phospho-Akt Thr308 (60kDa) antibodies. α -Actin (43kDa) was used as loading control.

3.2 Investigation of Primary and Secondary Lymphoid Organs

The bone marrow (BM) is the primary lymphoid organ where B cells are ‘born’. Here, precursor B cells develop into pro and pre-B cells followed by an immature B cell stage. Immature B cells leave the BM and enter the spleen as transitional 1 (T1) B cells (AA4⁺CD23⁻IgM^{hi}). In the spleen they mature to transitional 2 (T2) B cells (AA4⁺CD23⁺IgM^{hi}) and possibly to transitional 3 (T3) B cells (AA4⁺CD23⁺IgM^{low}) (Allman et al., 2001). T2 B cells are precursors of mature B cells whereas T3 B cells are suggested to be anergic B cells (Merrell et al., 2006). Akt1 overexpression induced by CD19-Cre revealed significantly reduced total numbers of pro/pre, immature, and mature recirculating B cells in the BM of Akt^{BOE} mice in comparison to controls (Fig. 3.2A, B).

Taken together, Akt1 overexpression at the stage of pro/pre-B cell development resulted in reduced B cell development and also caused a reduction of mature recirculating B cells in the BM.

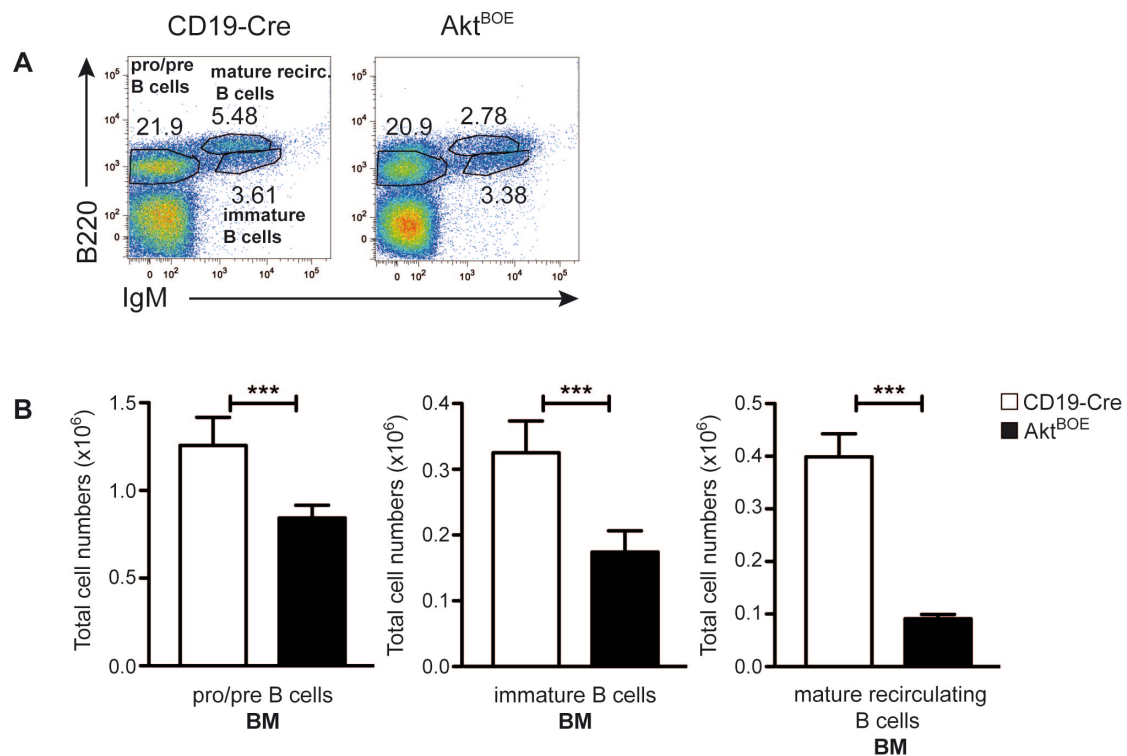


Figure 3.2: B cell distribution in BM.

(A) FACS analysis of 6-8 week-old Akt^{BOE} and CD19-Cre control mice. Genotypes and antibodies used are indicated. The numbers close to the gates of lymphocyte populations refer to the percentage of live cells in the gates. Representative plots are shown, experiment was repeated 9 times with $n = 2-3$ mice per genotype. **(B)** Total cell numbers of immature (B220⁺, IgM⁺), pro/pre (B220⁺, IgM^{low}) and mature recirculating (recirc.) B cells (B220^{high}, IgM⁺) in BM. For total cell numbers, all experiments are combined. Horizontal bars mark the mean value \pm SEM. *** $P < 0.001$, as calculated using 2-tailed Student t test.

In different B cell malignancies, including B-CLL, the microenvironment is very important for tumor growth and survival (Steidl et al., 2010; reviewed in Burger et al., 2009a). Apoptosis of B-CLL cells can be rescued in the presence of macrophages, T cells or stromal follicular dendritic cells which provide survival stimuli such as chemokines and angiogenic factors (reviewed in Burger et al., 2009a; Pedersen et al., 2002; Tsukada, 2002; reviewed in Chiorazzi et al., 2005).

Two groups observed overexpression of the T cell chemokines CCL3 and CCL4 in B-CLL cells (Burger et al., 2009b; Zucchetto et al., 2010). It was shown that these

chemokines recruit monocytes and macrophages to the B-CLL cells and, in addition, these recruited cells secrete stimuli that prevent B-CLL apoptosis (Zucchetto et al., 2010; Burger et al., 2009b; Burger et al., 2000). With the knowledge that these cells are important in B-CLL survival and growth, further investigation through FACS analysis of mature macrophages, monocytes and neutrophils were performed. In BM the investigation of mature macrophages, monocytes and neutrophils revealed no significant difference between Akt^{BOE} mice and CD19-Cre controls (Fig. 3.3A, B), but in spleen of Akt^{BOE} mice a significant increase in total numbers of mature macrophages, monocytes and neutrophils was observed (Fig. 3.4A, B).

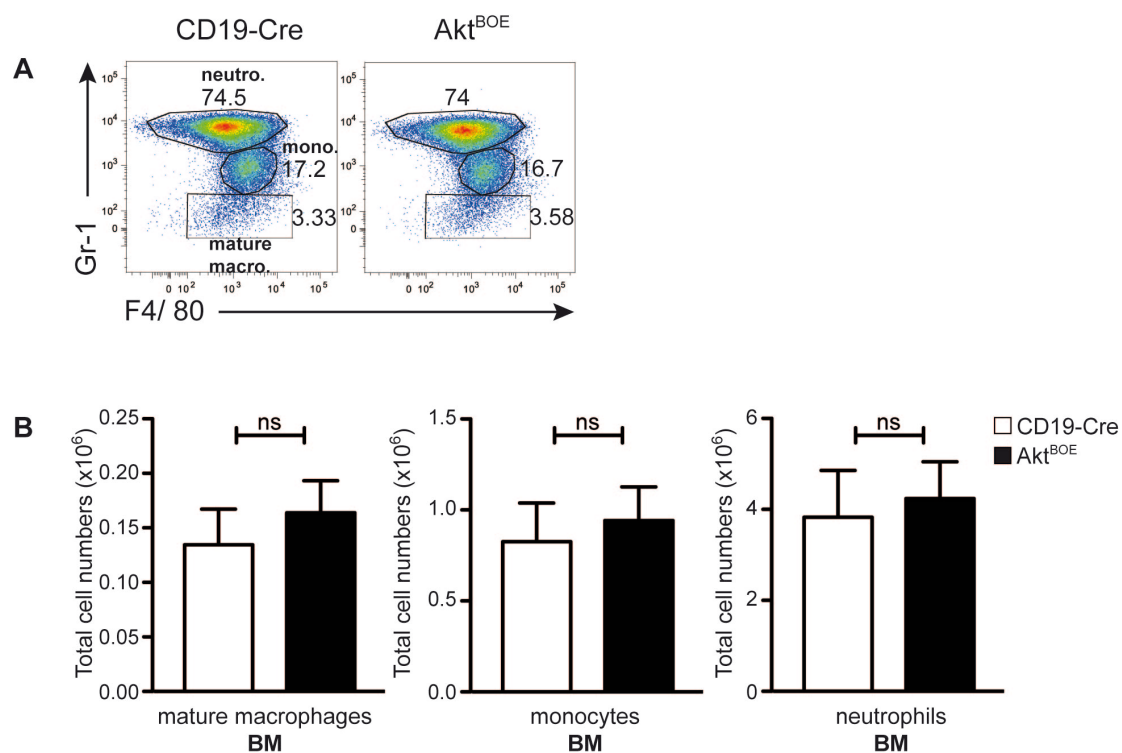


Figure 3.3: Mature macrophages, monocytes and neutrophils in BM of Akt^{BOE} mice vs. controls.

(A) FACS analysis of 6-8 week-old Akt^{BOE} and CD19-Cre control mice. Genotypes and antibodies are indicated. The numbers close to the boxes of cell populations refer to the percentage of live cells in the gates. Cells were gated on $B220^{-}$, $CD3^{-}$ and $CD11b^{+}$ cells. Representative plots are shown, experiment was repeated 4 times with $n = 2-3$ mice per genotype. **(B)** Total cell numbers of mature macrophages (mature macro.) ($F4/80^{+}$, $Gr-1^{-}$), monocytes (mono.) ($F4/80^{+}$, $Gr-1^{inter}$) and neutrophils (neutro.) ($F4/80^{+}$, $Gr-1^{high}$) in BM. For total cell numbers, 2 experiments are combined with 7 Akt^{BOE} mice vs. 7 CD19-Cre control mice. Horizontal bars mark the mean value \pm SEM, ns = not significant, as calculated using 2-tailed Student t test.

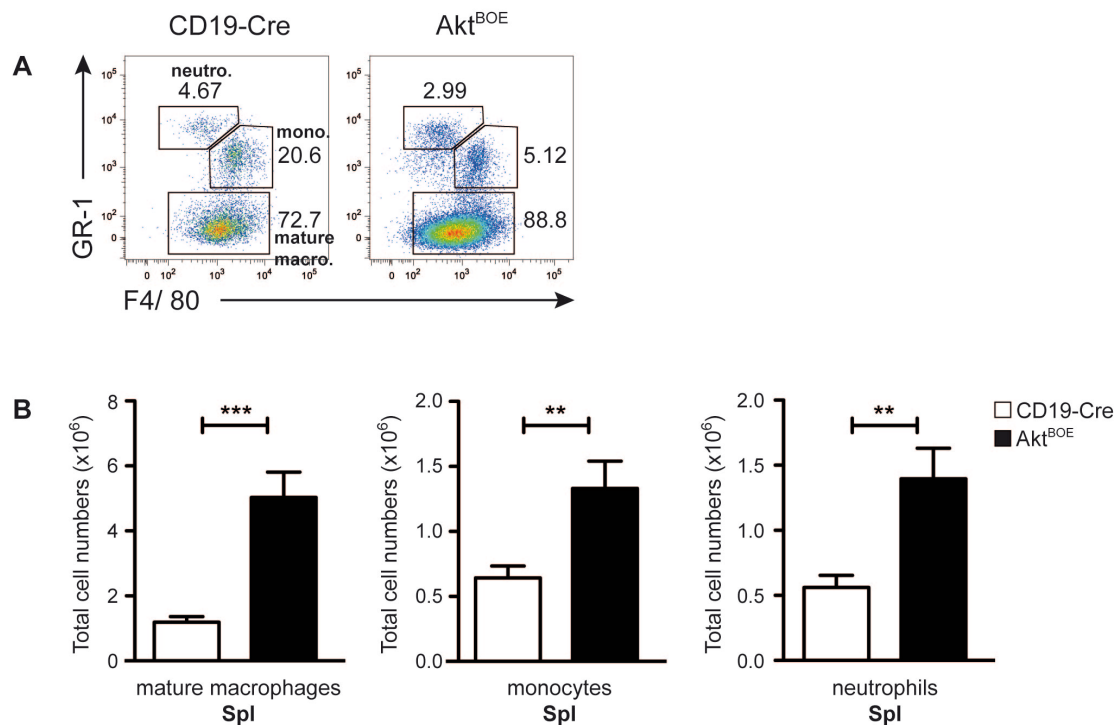


Figure 3.4: Increased splenic mature macrophages, monocytes and neutrophils in Akt^{BOE} mice.

(A) FACS analysis of 6-8 week-old Akt^{BOE} and CD19-Cre control mice. Genotypes and antibodies used are indicated. The numbers close to the boxes of lymphocyte populations refer to the percentage of live cells in the gates. Cells were gated on B220⁻, CD4⁺, CD8⁻ and CD11b⁺ cells. Representative plots are shown, experiment was repeated 5 times with n = 3-4 mice per genotype. **(B)** Total cell numbers of splenic mature macrophages (mature macro.) (F4/80⁺, Gr-1⁻), monocytes (mono.) (F4/80⁺, Gr-1^{inter}) and neutrophils (neutro.) (F4/80⁺, Gr-1^{high}). For total cell numbers, all experiments are combined. Horizontal bars mark the mean value \pm SEM. ***P < 0.001, **P < 0.01, as calculated using 2-tailed Student *t* test.

Macroscopic analysis of secondary lymphoid organs revealed a dramatic enlargement of the spleens in Akt^{BOE} mice as early as 6 weeks of age, accompanied by significantly higher total splenic cell numbers (Fig. 3.5A, B).

To address which population could account for the enlargement of the spleen, FACS analysis was performed, using B220 as a B cell marker and CD90.2 as a T cell marker. This analysis revealed significantly elevated total numbers of B and T cells in the spleen of Akt^{BOE} mice compared to controls (Fig. 3.5C, D).

To investigate if the splenic structure of Akt^{BOE} mice was normal, histological analysis of the B and T cell compartments was performed, using antibodies against B220 and CD3. The histological analysis showed normal follicles of B and T cells in Akt^{BOE} spleens compared to controls (Fig. 3.5E). The follicles that were observed

showed CD3⁺ T cells surrounded by B220⁺ B cells. Taken together, Akt1 overexpression leads to higher total numbers of B and T cells as well as increased total cell numbers of mature macrophages, monocytes and neutrophils and therefore to the enlargement of the spleen in Akt^{BOE} mice while the structure looks normal.

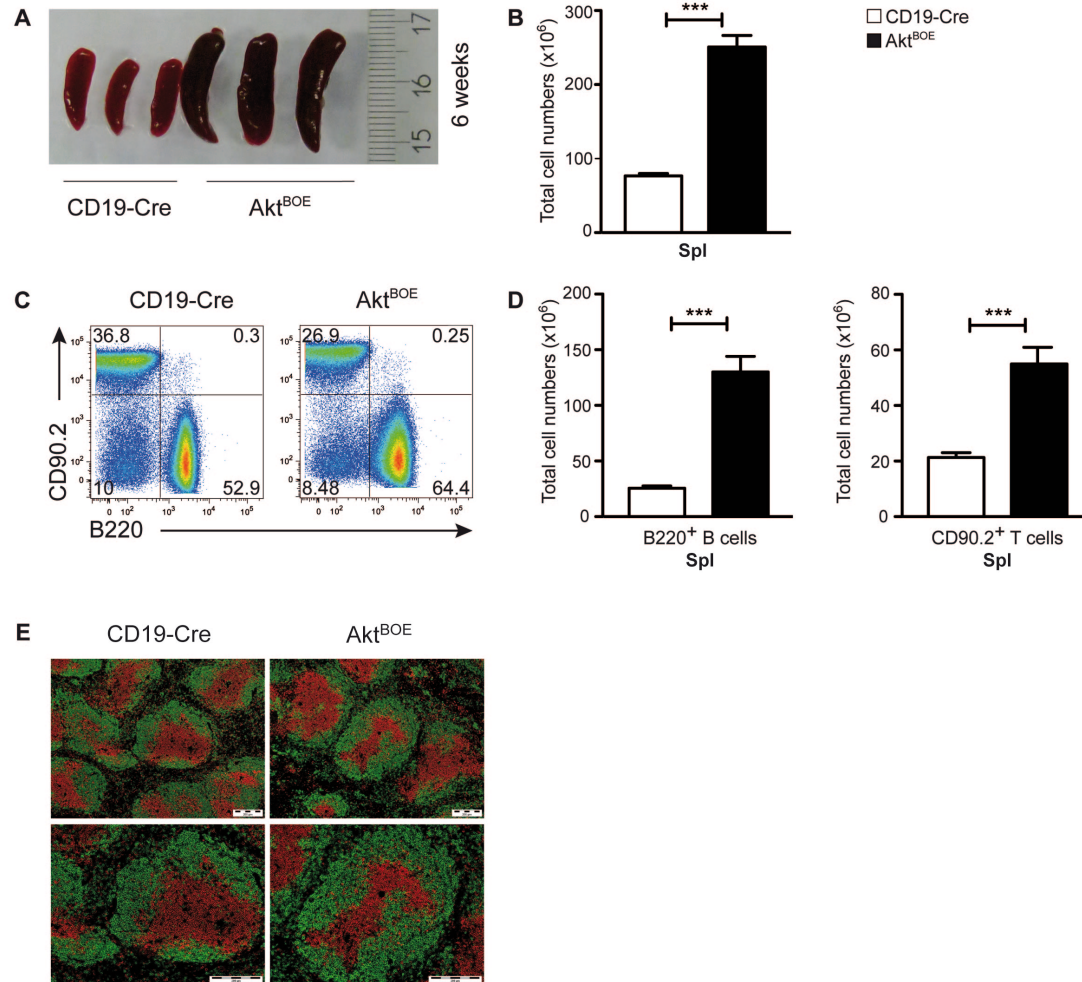


Figure 3.5: Effect of Akt1 overexpression on splenic B and T cell numbers in Akt^{BOE} mice.

(A) Splenomegaly of Akt^{BOE} mice already at the age of 6 weeks. (B) Total splenic B cell numbers. Experiment was repeated 9 times with n = 3-4 mice per genotype. (C) FACS analysis of 6-8 week-old Akt^{BOE} and CD19-Cre control mice. Genotypes and antibodies used are indicated. The numbers close to the boxes of lymphocyte populations refer to the percentage of live cells in the gates. Representative plots are shown, experiment was repeated 7 times with n = 3-4 mice per genotype. (D) Total cell numbers of B220⁺ B cells and CD90.2⁺ T cells in spleen. For total cell numbers, all experiments are combined. (E) Histological analysis of the B and T cell compartments in spleen. α-CD3 (red) antibody was used to detect T cells and α-B220 (green) antibody was used to detect B cells. Scale bar = 200 μm. B, D Horizontal bars mark the mean value +/- SEM. ***P < 0.001 as calculated using 2-tailed Student *t* test.

In contrast to the enlarged spleens in Akt^{BOE} mice, all pLN were normal in size compared to CD19-Cre controls (data not shown). As expected, total cell numbers of pLN were unchanged between Akt^{BOE} mice and CD19-Cre controls (Fig. 3.6A). Unexpectedly, FACS analysis of B and T cells of Akt^{BOE} mice showed significantly decreased numbers of B220⁺ B cells and a tendency to increased CD90.2⁺ T cell numbers in comparison to CD19-Cre mice (Fig. 3.6B, C). The tendency of more T cells and fewer total B220⁺ B cell numbers in Akt^{BOE} mice in comparison to controls can explain same total cell numbers in Akt^{BOE} mice and controls.

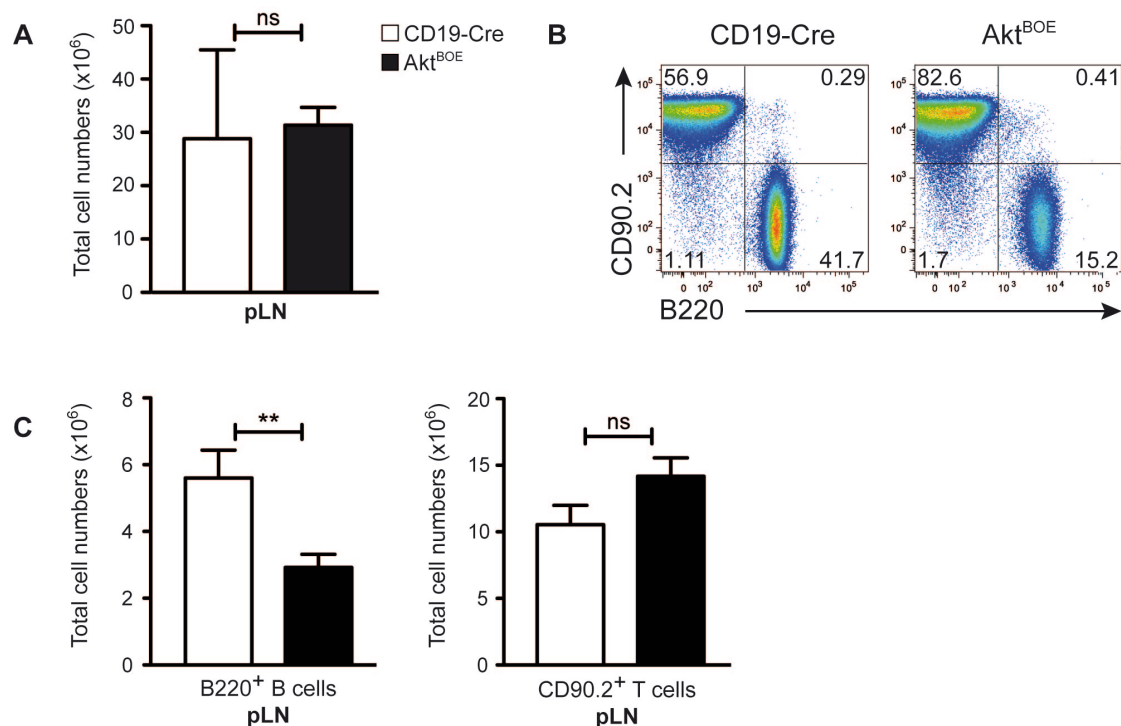


Figure 3.6: B and T cell distribution in pLN of Akt^{BOE} mice.

(A) Total cell numbers of pLN. Experiment was repeated 9 times with n = 3-4 mice per genotype. (B) FACS analysis of 6-8 week-old Akt^{BOE} and CD19-Cre control mice. Genotypes and antibodies were used as indicated. The numbers close to the boxes of lymphocyte populations refer to the percentage of live cells in the gates. Representative plots are shown, experiment was repeated 6 times with n = 3 mice per genotype. (C) Total cell numbers of B220⁺ B cells and CD90.2⁺ T cells in pLN. For total cell numbers, all experiments are combined. A, C Horizontal bars mark the mean value +/- SEM. **P < 0.01, ns = not significant, as calculated using 2-tailed Student *t* test.

Analysis of mLN from Akt^{BOE} mice displayed significantly increased total cell numbers compared to mLN from controls (Fig. 3.7A). FACS analysis of mLN revealed no significant difference in total cell numbers of B and T cells in Akt^{BOE} mice compared to CD19-Cre controls (Fig. 3.7B, C). Possibly due to the

overexpression of Akt1 in B cells of Akt^{BOE} mice, other cell types are attracted and either accumulate or migrate for example due to the secretion of chemokines into the mLN. This is displayed by the high amount of B220⁺, CD90.2⁺ double positive (DP) cells (13% in CD19-Cre control mice compared to 51% in Akt^{BOE} mice), which could lead to this increase in total cell number in Akt^{BOE} mice.

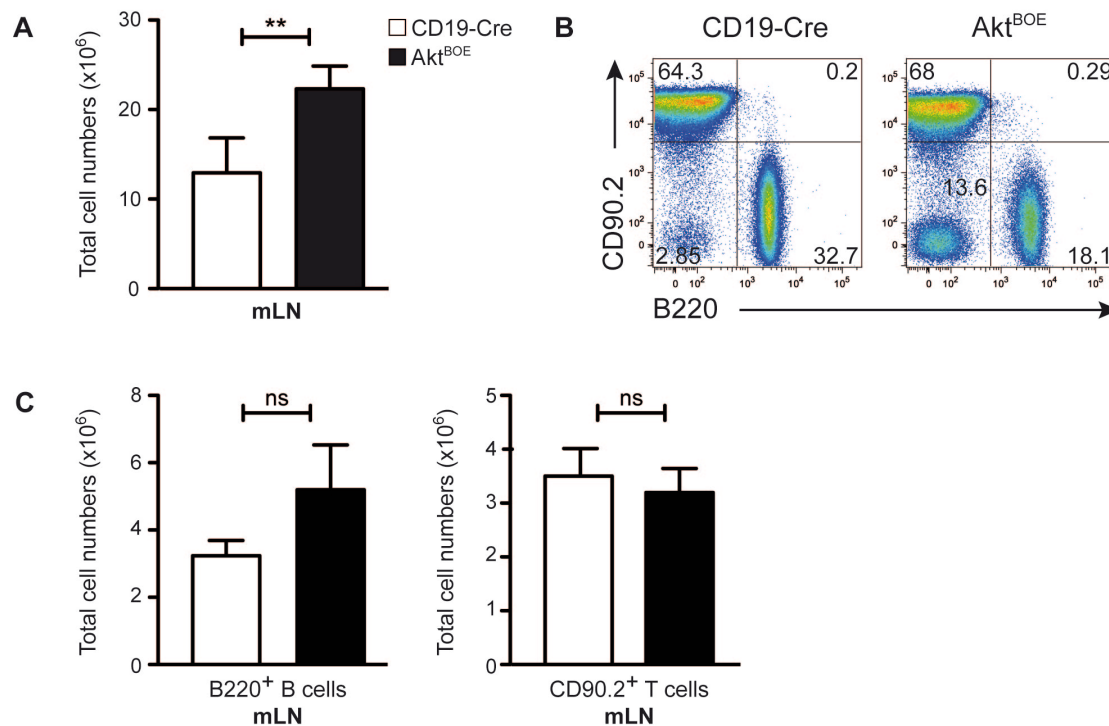


Figure 3.7: B and T cell distribution in mLN is not affected by Akt1 overexpression.

(A) Total cell numbers of mLN. Experiment was repeated 4 times with $n = 3$ mice per genotype. (B) FACS analysis of 6-8 week-old Akt^{BOE} and CD19-Cre control mice. Genotypes and antibodies are indicated. The numbers close to the boxes of lymphocyte populations refer to the percentage of live cells in the gates. Representative plots are shown, experiment was repeated 4 times with $n = 3$ mice per genotype. (C) Total cell numbers of B220⁺ B cells and CD90.2⁺ T cells in mLN. For total cell numbers, all experiments are combined. A, C Horizontal bars mark the mean value \pm SEM. ** $P < 0.01$, ns = not significant, as calculated using 2-tailed Student t test.

PP are secondary lymphoid organs located outside of the gut that include B cell follicles, follicular dendritic cells (FDCs), T cells, and dendritic cells (DCs) (Barreau et al., 2007; reviewed in Jung et al., 2010). In PP, the total cell number did not significantly differ between CD19-Cre and Akt^{BOE} mice. PP of Akt^{BOE} mice revealed significantly decreased numbers of B cells whereas T cell numbers showed no significant difference between Akt^{BOE} mice and controls (Fig. 3.8A, B, C). Similar to what we observed in mLN, we also detected in the PP an increase in the percentage of

B220⁺, CD90⁺ DN cells (51%) compared to CD19-Cre controls (13%) (Fig. 3.8B, C). Due to the increase in the DN cell population, total cell numbers of Akt^{BOE} mice and CD19-Cre controls did not differ. Possibly this DN cells are FDCs and DCs.

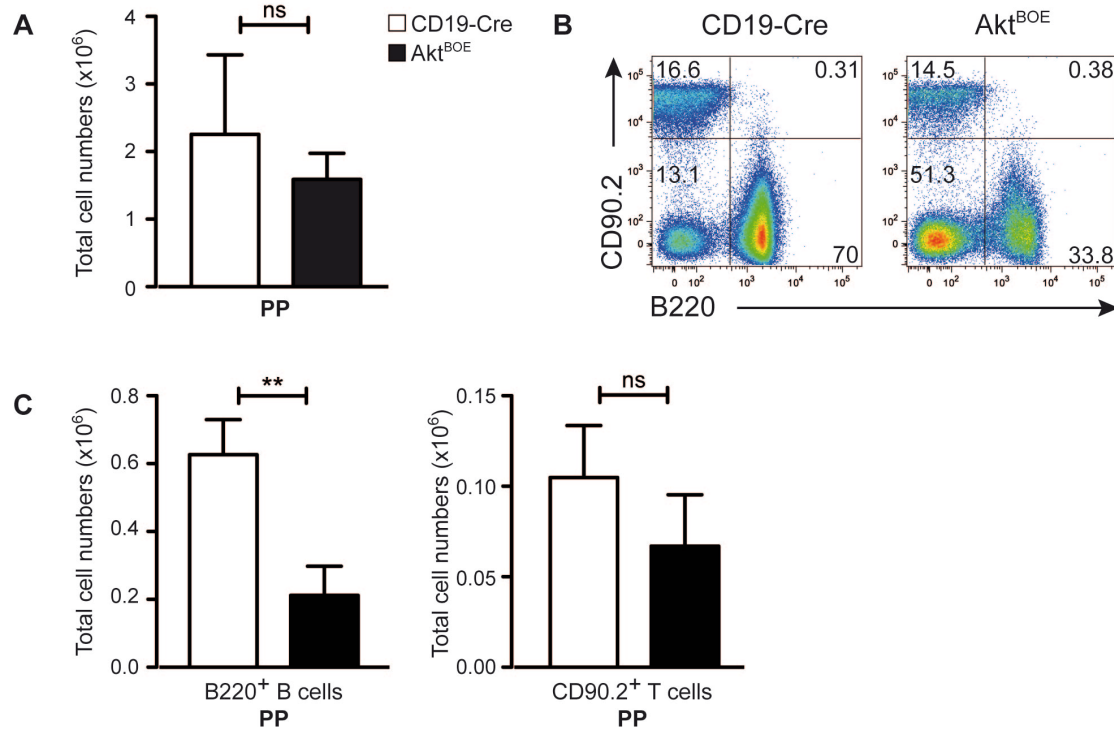


Figure 3.8: Overexpression of Akt1 leads to reduced numbers of B cells in PP.

(A) Total cell numbers of PP. Experiment was repeated 5 times with $n = 5$ mice per genotype, 5 PP were taken from each mouse. (B) FACS analysis of 6-8 week-old Akt^{BOE} and CD19-Cre control mice. Genotypes and antibodies were used as indicated. The numbers close to the boxes of lymphocyte populations refer to the percentage of live cells in the gates. Representative plots are shown, experiment was repeated 4 times with $n = 3$ mice per genotype, 5 PP per mouse. (C) Total cell numbers of B220⁺ B cells and CD90.2⁺ T cells in PP. For total cell numbers, all experiments are combined. A, C Horizontal bars mark the mean value \pm SEM. ** $P < 0.01$, ns = not significant, as calculated using 2-tailed Student t test.

The PerC is located between the parietal peritoneum and the visceral peritoneum. In this cavity, immune cells such as monocytes/macrophages, natural killer (NK) cells, dendritic cells (DCs), T cells, FO and B1 B cells can be found (reviewed in Broche and Tellado, 2001). FACS analysis of the PerC revealed increased numbers of both B and T cell populations in Akt^{BOE} mice, leading to a highly significant difference in total cell numbers (Fig. 3.9A, B, C).

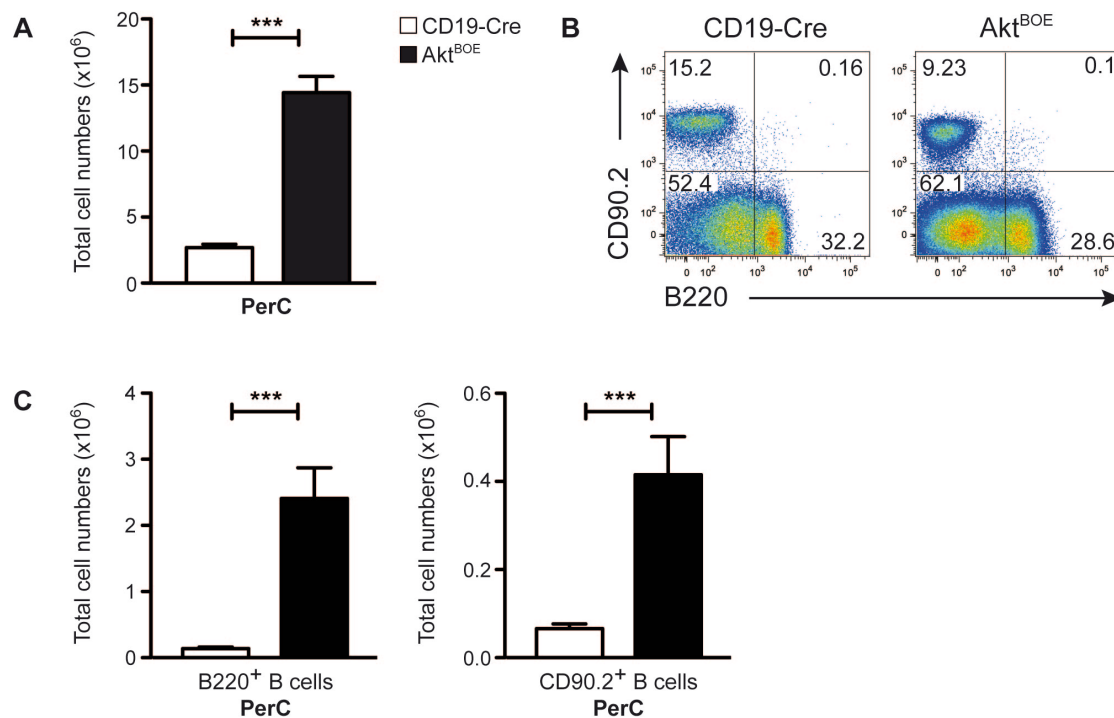


Figure 3.9: Increased B and T cell populations in PerC of Akt^{BOE} mice.

(A) Total cell numbers of PerC. Experiment was repeated 14 times with $n = 3-4$ mice per genotype. **(B)** FACS analysis of 6-8 week-old Akt^{BOE} and CD19-Cre control mice. Genotypes and antibodies were used as indicated. The numbers close to the boxes of lymphocyte populations refer to the percentage of live cells in the gates. Representative plots are shown, experiment was repeated 5 times with $n = 3$ mice per genotype. **(C)** Total cell numbers of B220⁺ B cells and CD90.2⁺ T cells in PerC. For total cell numbers, all experiments are combined. **A, C** Horizontal bars mark the mean value \pm SEM. *** $P < 0.001$, as calculated using 2-tailed Student t test.

In summary, Akt1 overexpression significantly increased the total cell numbers in the spleen and PerC. This increase was due to more B and surprisingly also more T cells. In addition, the spleen showed elevated numbers of mature macrophages, monocytes and neutrophils.

Also in mLN, overall total cell numbers were elevated but the Akt1 overexpression had no influence on total B and T cell numbers when compared to controls. Perhaps an increase in other cell types is responsible for the increase in total cells numbers.

Total cell numbers of pLN and PP in Akt^{BOE} mice were not changed when compared to control mice. In pLN of Akt^{BOE} mice Akt1 overexpression led to the tendency of increased T cells but to a reduction of B cells. In PP, an increased DN cell population in Akt^{BOE} mice could account for the equivalent total cell numbers in Akt^{BOE} mice and controls, but reduced total B cell numbers in Akt^{BOE} mice.

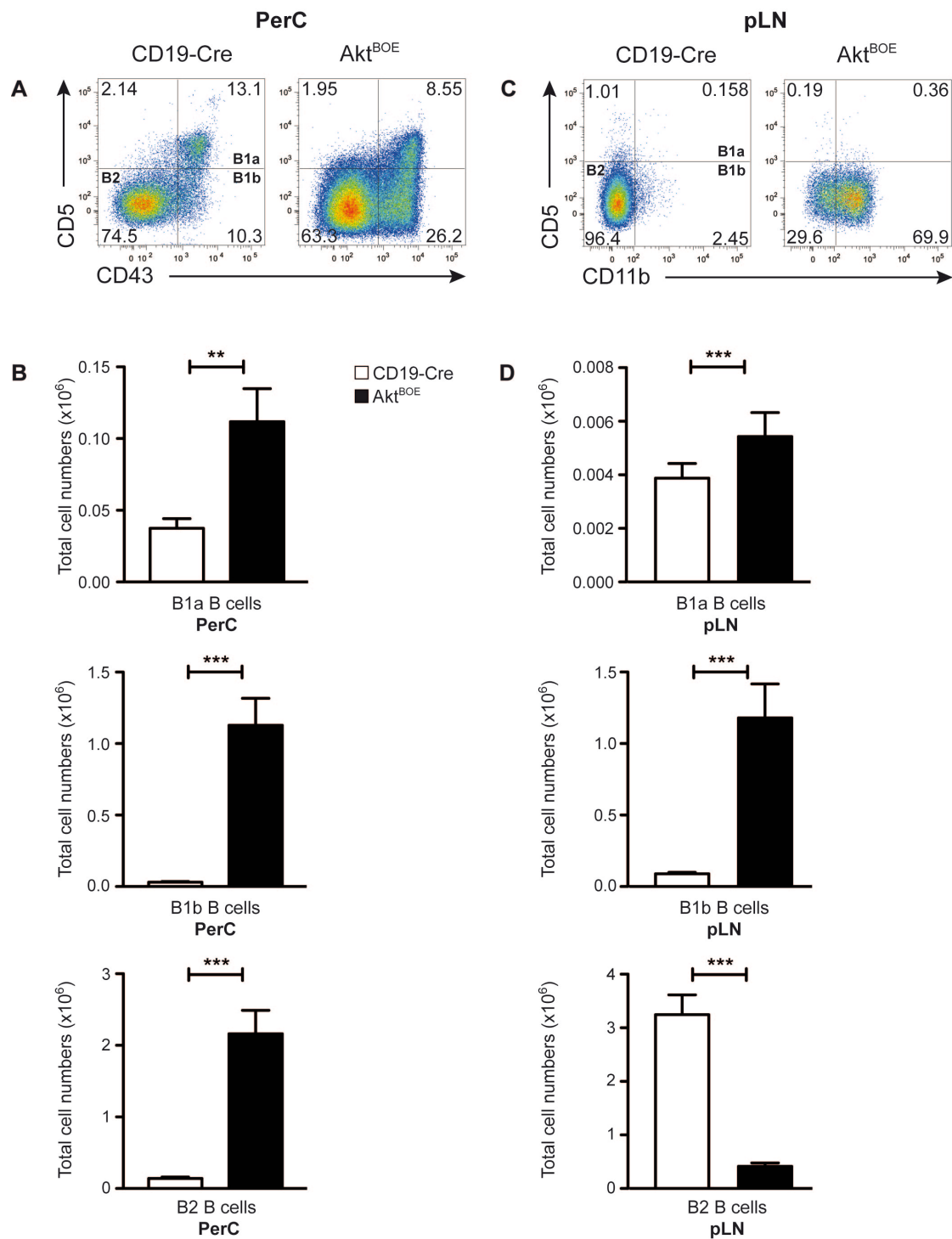


Figure 3.10: B1 and B2 B cells in PerC and pLN.

(A) FACS analysis of PerC cells from 6-8 week-old Akt^{BOE} and CD19-Cre control mice. Genotypes and antibodies used are indicated. The numbers close to the boxes of lymphocyte populations refer to the percentage of CD19⁺ live cells in the gates. Akt^{BOE} mice were additionally gated on GFP⁺ cells to exclude escapees. Representative plots are shown. Experiment was repeated 9 times with $n = 3$ mice per genotype. (B) Total cell numbers of B1a (CD5⁺, CD43⁺), B1b (CD5⁺, CD43⁺) and B2 (CD5⁺, CD43⁺) B cells of PerC. For total cell numbers, 8 experiments are combined. (C) FACS analysis of 6-8

week-old Akt^{BOE} and CD19-Cre control mice of pLN. Genotypes and antibodies are indicated. The numbers close to the boxes of lymphocyte populations refer to the percentage of CD19⁺ and B220⁺ live cells. Akt^{BOE} mice were additionally gated on GFP⁺ cells to exclude escapees. Representative plots are shown. Experiment was repeated 4 times with n = 2-3 mice per genotype. **(D)** Total cell numbers of B1a (CD5⁺, CD11b⁺), B1b (CD5⁻, CD11b⁺) and B2 (CD5⁻, CD11b⁻) B cells in pLN. For total cell numbers, 3 experiments are combined. **B, D** Horizontal bars mark the mean value \pm SEM. ***P < 0.001, **P < 0.01, as calculated using 2-tailed Student *t* test.

In PerC B1 B cells that can be sub-divided into B1a (CD5⁺) and B1b B cells (CD5⁻), are found predominantly beside B2 B cells. Recently, Calamito et al. could show that Akt1 and Akt2 play a determining role in B1 B cell development, the B1 B cell development was hindered in Akt1 and Akt2 deficient chimeras (Calamito et al., 2010). Thus, we aimed to analyze B1 and B2 B cell subsets in PerC and pLN via FACS analysis.

In PerC of Akt^{BOE} mice a significant increase in total cell numbers of B2, B1a and B1b B cells was observed compared to CD19-Cre controls (Fig. 3.10A, B). Collectively, in PerC this indicates a strong influence of Akt1 on B1a, B1b and B2 B cell numbers.

As expected, pLN of CD19-Cre controls mainly consist of B2 B cells. In contrast, Akt^{BOE} mice had a significantly diminished B2 B cell population but increased numbers of B1a and B1b B cells (Fig. 3.10C, D).

The Akt1 overexpression in B cells of Akt^{BOE} mice led to a dramatic shift of total cell numbers of B1a, B1b, and B2 B cells in comparison to controls. Possibly the increase of CD5⁺ B1a B cells in PerC and pLN as well as the dramatic increase of B2 B cells in PerC hint to the development of B-CLL cells in Akt^{BOE} mice, because it is assumed that B1 and MZ B cells (belonging to the B2 B cell population) are the precursors of B-CLL (Caligaris-Cappio et al., 1982; reviewed in Chiorazzi and Ferrarini, 2003; reviewed in Chiorazzi et al., 2005).

It is known that immature B cells (AA4.1⁺, IgM⁺, IgD⁻) express membrane IgM (mIgM) whereas mature B cells express membrane IgM/IgD or just IgD (mIgD) (Benschop and Cambier, 1999; Havran et al., 1984; Scher et al., 1976). FACS analysis of mature vs. immature B cells was performed to investigate the maturation of IgM and IgD expressing B cells in the lymphatic organs and the PerC.

Interestingly, splenic B cells of Akt^{BOE} mice expressed only IgM⁺ B cells, but no mature IgD⁺ B cells, indicating an immature population (Fig. 3.11 upper left). Surprisingly, we detected a CD19⁺ IgM⁻, IgD⁻ DN population, which was absent in CD19-Cre controls (Fig. 3.11 upper left). Further assumptions regarding this IgM⁻, IgD⁻ DN population can be found in chapter 3.6.

pLN of WT mice are usually composed of mature IgD⁺ B cells. Therefore, it was surprising that, similarly to what was observed in the spleen, B cells of pLN of Akt^{BOE} mice showed only IgM⁺ B cells and no IgD⁺ B cells in comparison to CD19-Cre mice (Fig. 3.11 lower left). Furthermore, in pLN of Akt^{BOE} mice, the IgM⁻, IgD⁻ DN population was detected whereas this population was absent in controls (Fig. 3.11 lower left).

In PP the same observation was made for Akt^{BOE} mice, whereas controls showed normal IgD⁺ B cells and IgM⁻, IgD⁻ DN population (Fig. 3.11 upper right).

Also in PerC of Akt^{BOE} mice, mainly IgM⁺ and IgM⁻, IgD⁻ DN B cells were detected, whereas the controls displayed normal IgM⁺ and IgD⁺ B cells and no IgM⁻, IgD⁻ DN cells (Fig. 3.11 lower right).

In conclusion, all tested organs and PerC of Akt^{BOE} mice consisted of a population of IgM⁺ B cells whereas mature IgD⁺ B cells were absent. In addition, in all tested organs and PerC we detected a population of B cells that is DN for IgM and IgD.

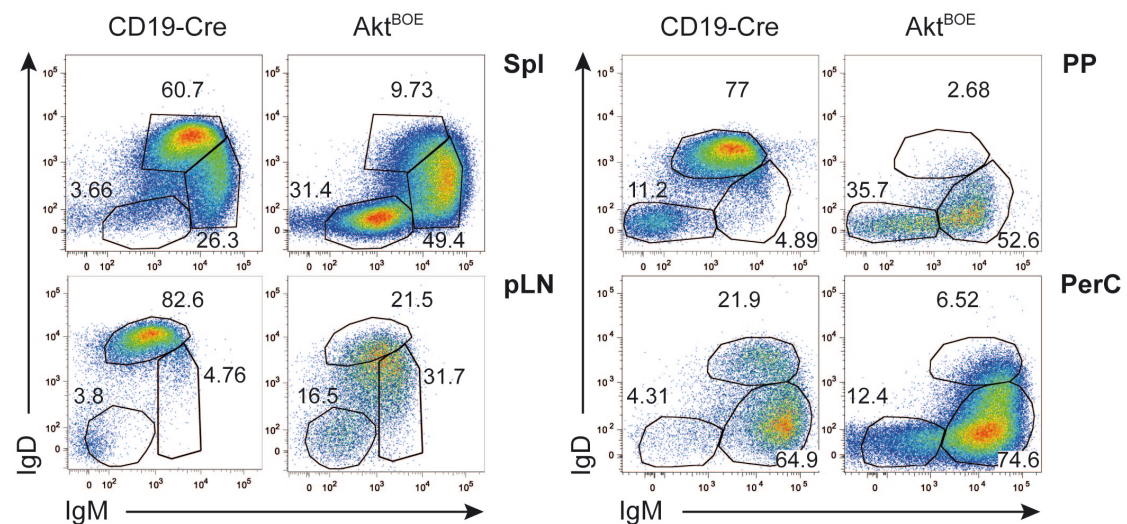


Figure 3.11: IgM vs. IgD expression on B cells of spleen, pLN, PP and PerC.

FACS analysis of 6-8 week-old Akt^{BOE} and CD19-Cre control mice. Genotypes and antibodies used are indicated. The numbers close to the boxes of lymphocyte populations refer to the percentage of CD19⁺ live cells in the gates. Akt^{BOE} mice are additionally gated on GFP⁺ cells to exclude escapees. Representative plots are shown for all organs. Spleen: Experiment was repeated 10 times with n = 2-3 mice per genotype. pLN: Experiment was repeated 5 times with n = 3 mice per genotype. PP:

Experiment was repeated 3 times with $n = 3$ mice per genotype. 5 PP each mouse. PerC: Experiment was repeated 4 times with $n = 2$ mice per genotype.

3.3 Dramatic Increase of MZ-like B Cells in Akt^{BOE} Mice

Due to the findings that in pLN and PerC B1 and B2 B cell numbers were elevated, we investigated B1 and B2 B cell subsets in spleen. Interestingly, FACS analysis of splenic B cells of Akt^{BOE} mice revealed significantly increased numbers of B2 and B1b B cells when compared to CD19-Cre controls. Splenic B1a B cells of Akt^{BOE} mice were not significantly changed, but slightly reduced in total cell number, when compared to CD19-Cre control animals (Fig. 3.12A, B). In order to investigate, due to which B cell population the B2 B cells were increased, MZ B cells, and FO B cells were analyzed.

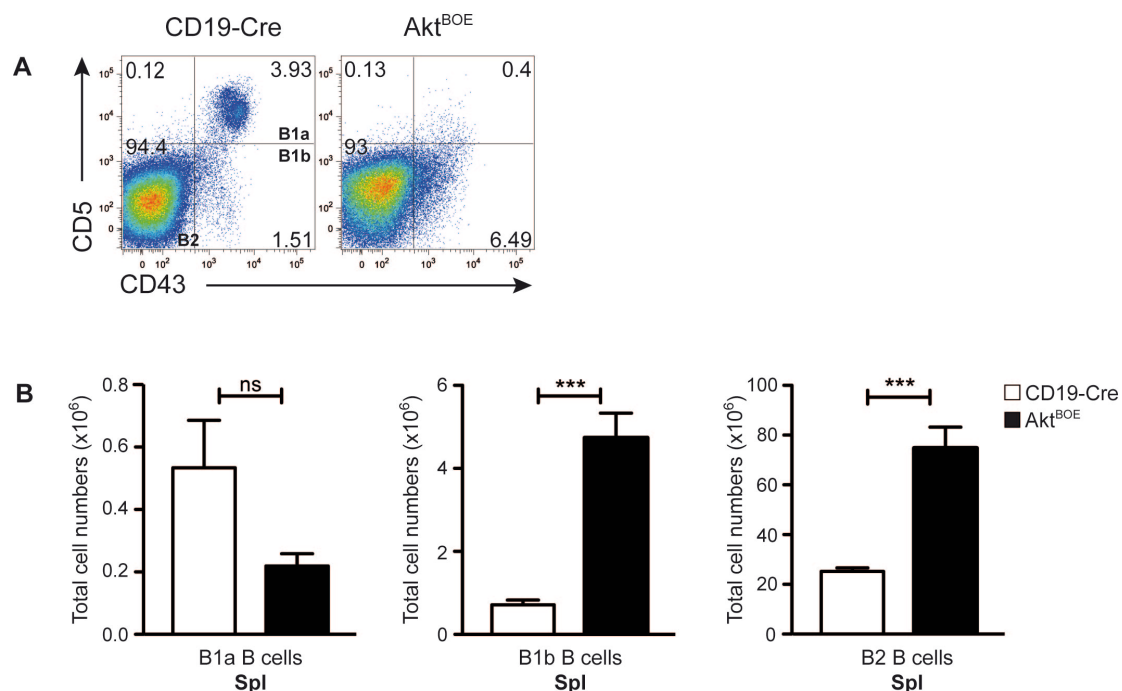


Figure 3.12: Splenic B1 and B2 B cell subsets.

(A) FACS analysis of 6-8 week-old Akt^{BOE} and CD19-Cre control mice. Genotypes and antibodies used are indicated. The numbers close to the boxes of lymphocyte populations refer to the percentage of CD19⁺ and B220⁺ live cells in the gates. Akt^{BOE} mice were additionally gated on GFP⁺ cells to exclude escapees. Representative plots are shown. Experiment was repeated 6 times with $n = 3$ mice per genotype. **(B)** Total cell numbers of splenic B1a (CD5⁺, CD43⁺), B1b (CD5⁺, CD43⁺) and B2 (CD5⁺, CD43⁺) B cells. For total cell numbers, all experiments are combined. Horizontal bars mark the mean value \pm SEM. *** $P < 0.001$, ns = not significant, as calculated using 2-tailed Student t test.

Spleens of wild type mice normally consist of mature B cells expressing IgM^{high}, IgD^{low} for MZ and IgM^{low}, IgD^{high} for FO B cells. It was interesting to find out whether increased numbers of IgM⁺ B cells were due to a developmental block or if they were MZ B cells.

In order to investigate the B2 B cell population and the IgM⁺ B cells we performed FACS analysis to discriminate between FO and MZ B cells (Fig. 3.13A).

MZ B cells, identified as CD1d^{high}, CD21^{high} and CD23⁻, are located in the marginal zone of the spleen, which separates the white pulp from the red pulp (Weidenreich, 1901; MacNeal, 1929; Nolte et al., 2004).

FACS analysis of splenic B cells of Akt^{BOE} mice displayed significantly higher numbers of CD1d^{high}, CD21^{high} MZ-like B cells, while FO B cells, which are CD23⁺, were completely absent in comparison to CD19-Cre controls (Fig. 3.13A, B).

In summary, we could show that IgM⁺ B cell populations detected in spleen (Fig. 3.11) were due to increased numbers of MZ-like B cells. In addition, the elevated number of B2 B cells and the general increase in B cell numbers could also be explained by the enlarged population of MZ-like B cells.

Normally, MZ B cells can be found in the MZ surrounding the MOMA ring. In order to investigate if MZ-like B cells in spleen show a normal distribution around the MOMA ring, histological analysis using α -MOMA to detect metallophilic macrophages located at the inner border of the MZ, and α -CD1d, to detect MZ B cells surrounding the MOMA ring, was performed. The size of the CD1d^{high} MZ-like B cell population was strongly increased and, interestingly, was observed both in- and outside of the MOMA ring in Akt^{BOE} mice (Fig. 3.13,C). These data show a strong shift to the MZ-like B cell compartment at the expense of FO B cells due to constitutive Akt1 signaling.

T1 B cells are precursor cells that develop to T2 B cells, which are then direct precursors of MZ and FO B cells (Loder et al., 1999). By FACS analysis we detected an increased T1 B cell population in Akt^{BOE} mice (Fig. 3.13A, B). Detailed analysis of transitional B cells can be found in chapter 3.8.

The investigation of surface IgM clearly revealed higher IgM expression on the surface of B cells of Akt^{BOE} mice in comparison to CD19-Cre controls (Fig. 3.13D). This observation underlines the finding of mostly MZ-like B cells in Akt^{BOE} mice,

due to the knowledge, that MZ B cells are IgM^{high} and IgD^{low} in comparison to FO B cells that are IgM^{low} and IgD^{high} (Martin et al., 2001; reviewed in Pillai et al., 2005). Significant increased T1 B cells are also reasonable to account to the high surface expression of IgM in Akt^{BOE} mice in comparison to CD19-Cre controls, because T1 B cells are, as MZ B cells IgM^{high} and IgD^{low} (reviewed in Pillai et al., 2005).

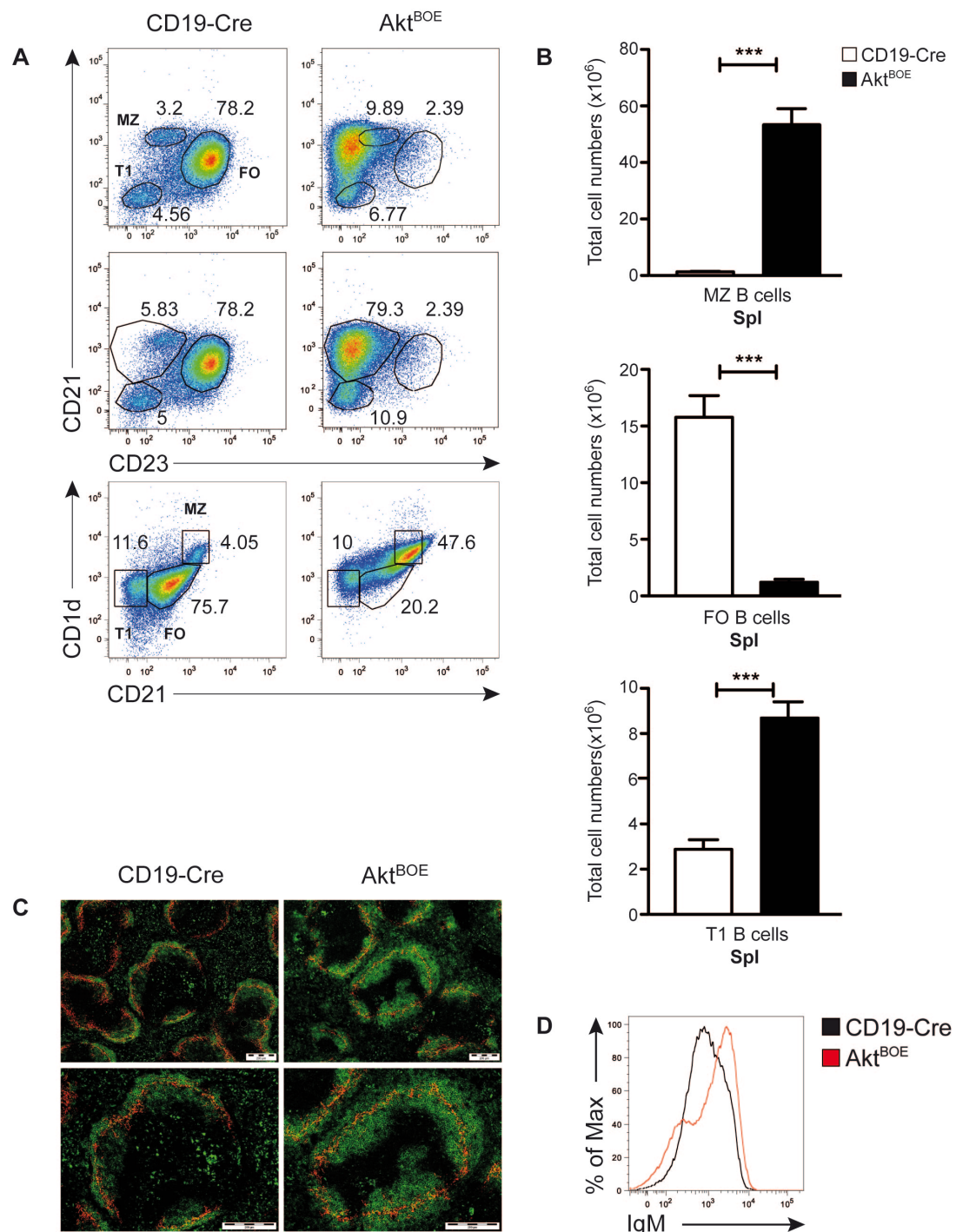


Figure 3.13: Distribution of splenic MZ, FO and T1 B cells in Akt^{BOE} mice vs. controls.

(A) FACS analysis of splenic B cells from 6-8 week-old Akt^{BOE} and CD19-Cre control mice. Displayed are 2 different stainings to show MZ, FO and T1 B cells. To calculate the cell numbers of

the different populations, the upper staining shows different gates for the MZ B cell population ($CD21^{high}$, $CD23^{-}$) and the T1 ($CD21^{low}$, $CD23^{-}$) B cells. In the upper 2 plots, FO ($CD21^{inter}$, $CD23^{+}$), MZ ($CD21^{high}$, $CD23^{-}$) and T1 ($CD21^{low}$, $CD23^{-}$) B cells are shown. In the lower 2 plots, FO ($CD21^{int}$, $CD1d^{low}$), MZ ($CD21^{high}$, $CD1d^{high}$) and T1 ($CD21^{low}$, $CD1d^{low}$) B cells are displayed. The numbers close to the boxes of lymphocyte populations refer to the percentage of B220⁺ live cells in the gates. Akt^{BOE} mice are additionally gated on GFP⁺ cells to exclude escapees. CD23 vs. CD21 staining: Experiment was repeated 4 times with n = 2-3 mice per genotype. CD1d vs. 21 staining: Experiment was repeated 4 times with n = 2-3 mice per genotype. **(B)** Total cell numbers of splenic MZ, FO and T1 B cells were calculated based on the lower CD21 vs. CD23 staining. For total cell numbers, 3 experiments are combined. **(C)** Histological analysis of the MZ in spleen. α -MOMA (red) antibody was used to detect the MOMA ring and α -CD1d (green) antibody was used to detect MZ B cells. Scale bar = 200 μ m. **(D)** Surface expression of IgM in splenic B cells of Akt^{BOE} mice and CD19-Cre controls. Cells were gated on live cells and CD19⁺ cells. Akt^{BOE} mice were additionally gated on GFP⁺ cells. Histogram is representative of all experiments. **B** Horizontal bars mark the mean value \pm SEM. ***P < 0.001, as calculated using 2-tailed Student *t* test.

3.4 Constitutive Akt1 Signaling Overcomes CD19 Deficiency During MZ B Cell Differentiation

In CD19 deficient mice it was shown that the co-receptor CD19 of the BCR is very important for BCR-derived MZ B cell generation (Rickert et al., 1995; Engel et al., 1995). Activation of the BCR and its strengthening of the signaling through the CD19 co-receptor prominently leads to the activation of PI3K (Otero et al., 2001; Pogue et al., 2000). Also, further observations that the lack of the PI3K isoform p110 δ leads to a defective MZ B cell development, hints that PI3K signaling might be responsible for a lack of MZ B cell development. The main downstream target of PI3K is Akt (James, 1996; Franke, 1997; Frech et al., 1997). Therefore, we investigated whether constitutive Akt1 can overcome the absence of CD19 and restore MZ B cell development. In mice homozygous insertion of Cre into the CD19 locus leads to a knockout of CD19 and therefore to CD19 deficiency (Rickert et al., 1997). The CD19 knockout mouse was crossed to the Rosa-Akt-C mouse (Akt^{+/-}CD19-Cre^{-/-}).

Similar to what we observed for Akt^{BOE} mice, splenic total cell numbers of Akt^{+/-}CD19-Cre^{-/-} mice were increased in comparison to CD19-Cre^{-/-} controls (Fig. 3.14A). FACS analysis of Akt^{+/-}CD19-Cre^{-/-} mice revealed that although CD19 is absent, an enlarged splenic MZ-like B cell population, similar as in Akt^{BOE} mice, was present

(Fig. 3.14B, C; Fig. 3.13A, B). As expected, CD19-Cre^{-/-} controls developed no MZ B cells (Fig. 3.14B, C).

In conclusion, Akt1 overexpression is able to overcome CD19 deficiency and allows for the development of MZ-like B cells at the expense of FO B cells.

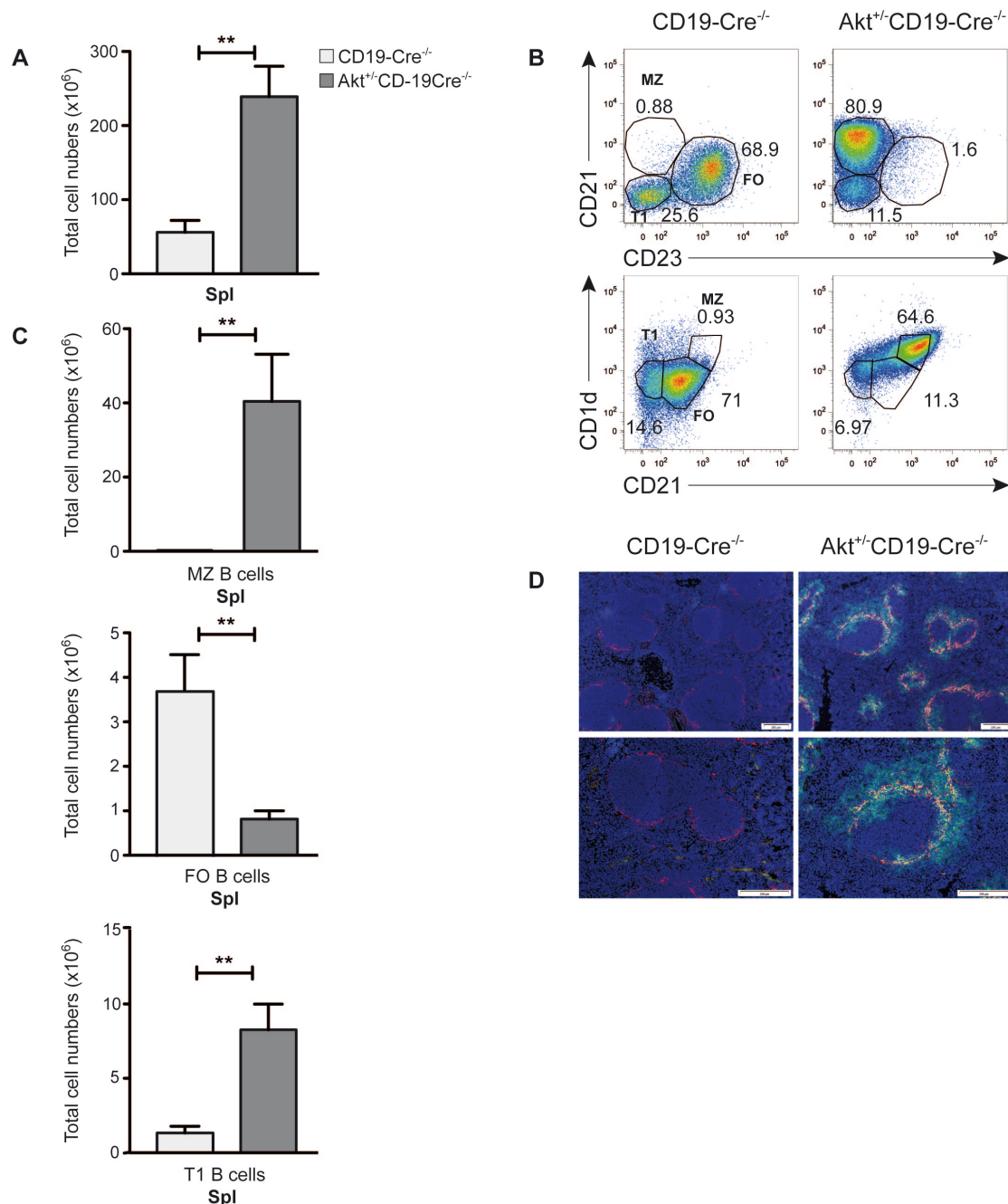


Figure 3.14: Akt1 overexpression leads to splenic MZ-like B cells in Akt^{+/+}CD19-Cre^{-/-} mice.

(A) Total splenic cell numbers of 8.5 week-old Akt^{+/+}CD19-Cre^{-/-} and CD19-Cre^{-/-} control mice. **(B)** FACS analysis of splenic B cells Akt^{+/+}CD19-Cre^{-/-} and CD19-Cre^{-/-} control mice. 2 different stainings are shown to differentiate MZ, FO and T1 B cells. In the upper 2 plots, FO (CD21^{inter}, CD23⁺), MZ (CD21^{high}, CD23⁻) and T1 (CD21^{low}, CD23⁻) B cells are shown. In the lower 2 plots, FO (CD21^{inter}, CD1d^{low}), MZ (CD21^{high}, CD1d^{high}) and T1 (CD21^{low}, CD1d^{low}) B cells are shown. The numbers close

to the boxes of lymphocyte populations refer to the percentage of B220⁺ live cells in the gates. Akt^{+/-} CD19-Cre^{-/-} mice are additionally gated on GFP⁺ cells to exclude escapees. Representative plots are shown, experiment was twice with n = 2-3 mice per genotype. **(C)** Total cell numbers of splenic MZ, FO and T1 B cells were calculated based on the CD21 vs. CD23 staining. For total cell numbers, the experiments were combined. **(D)** Histological analysis of the MZ in spleen. α -MOMA (red) antibody was used to detect the MOMA ring, α -CD1d (green) antibody was used to detect MZ B cells, and DAPI (blue) to detect the nuclei. Scale bar = 200 μ m. **A, C** Horizontal bars mark the mean value \pm SEM. **P < 0.01, as calculated using 2-tailed Student *t* test.

In order to investigate the localization of MZ-like B cells and the structure of spleen in Akt^{+/-}CD19-Cre^{-/-} mice, splenic sections were stained with α -MOMA, α -CD1d and DAPI. Akt^{+/-}CD19-Cre^{-/-} mice showed a similar follicular organization including an enlarged MZ as in the Akt^{BOE} mice, whereas in CD19-Cre^{-/-} controls only the MOMA-ring was observed (Fig. 3.14D; Fig. 3.13C). The investigation of the structure of the spleen by histology also displayed MZ-like B cells in- and outside of the MOMA ring equivalent to the Akt^{BOE} mice (Fig. 3.14D; Fig. 3.13C). In general, MZ B cells are only located outside of the MOMA ring, so it is possible that due to increased numbers of MZ-like B cells in the spleens of Akt^{+/-}CD19-Cre^{-/-} and Akt^{BOE} mice, they also begin to accumulate inside of the MOMA ring.

Collectively, we could show that the overexpression of Akt1 can overcome the CD19 deficiency and induce the MZ-like B cell development.

3.5 Investigation of MZ B Cell Surface Marker Expression

Hallmarks of MZ B cells are their characteristic surface markers, their location in the MZ and their ability to respond rapidly to T cell independent antigens. To monitor whether the MZ-like B cells of Akt^{BOE} and Akt^{+/-}CD19-Cre^{-/-} mice are ‘real’ MZ B cells, the expression levels of two typical MZ B cell markers (CD21 and CD1d), were analyzed by FACS. Akt^{BOE}, Akt^{+/-}CD19-Cre^{-/-} mice and their controls expressed CD21 in similar levels (Fig. 3.15, left). CD1d presents self and non-self glycolipids, and activates, through this presentation, natural killer (NK) T cells via interaction with the T cell receptor (TCR) of NKT cells (Chen et al., 2007). CD1d expression in MZ-like B cells of Akt^{BOE} mice was similar to CD1d expression of MZ B cells of CD19-Cre control mice. MZ-like B cells of Akt^{+/-}CD19-Cre^{-/-} mice showed

significant increased expression of CD1d on the surface in comparison to MZ B cells of CD19-Cre^{-/-} controls (Fig. 3.15, right).

MZ-like B cells of Akt^{BOE} and Akt^{+/-}CD19-Cre^{-/-} mice express the characteristic MZ B cell marker CD21 and CD1d and therefore, have a similar phenotype to typical MZ B cells.

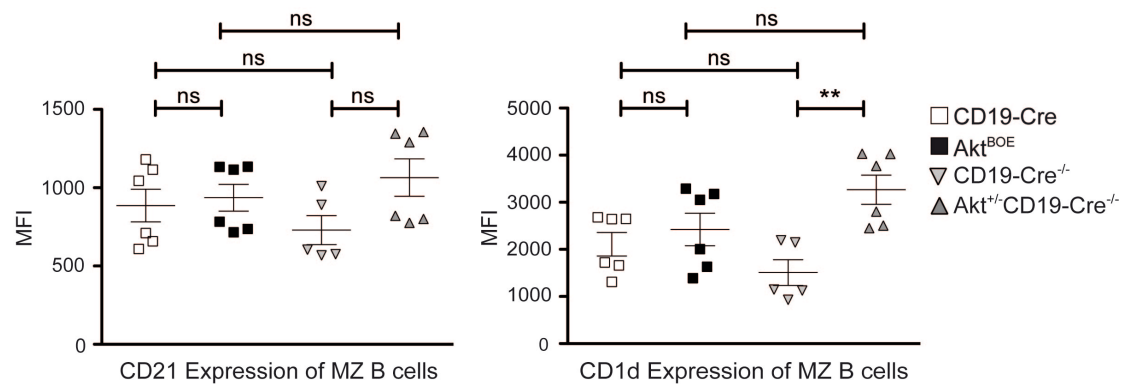


Figure 3.15: MZ B cell surface marker expression in Akt^{BOE} vs. Akt^{+/-}CD19-Cre^{-/-} mice and the corresponding controls in spleen.

Determination of MFI (mean fluorescence intensity) through FACS analysis of the MZ surface markers CD21 and CD1d. Cells are gated on splenic live cells and MZ B cells. Akt^{BOE} and Akt^{+/-}CD19-Cre^{-/-} mice were additionally gated on GFP. Experiment was repeated twice with n = 2-3 mice per genotype. Horizontal bars mark the mean value \pm SEM. **P < 0.01, ns = not significant, as calculated using 2-tailed Student *t* test.

3.6 Investigation of MZ-like B Cell Precursors in Akt^{BOE} Mice

It is known that immature B cells express mIgM⁺ B cells and AA4.1 while the mature ones express mIgM and mIgD. AA4.1 is an early marker for immature B cells (Li et al., 1996). The investigation of mature and immature B cells in spleen revealed that while Akt^{BOE} mice showed significantly increased mature B cells (B220⁺, AA4.1⁻) as compared to controls, there were no differences in the immature B cell (B220⁻, AA4.1⁺) population (Fig. 3.16A, B). The larger mature B cell population in Akt^{BOE} mice could be due to the increased MZ-like B cell populations in spleen (Fig. 3.13).

To study the different subpopulations of immature B cells, FACS analysis was performed. Splenic immature B cells of Akt^{BOE} mice revealed strongly increased T1 (CD23⁻, IgD^{high}) and extremely decreased T2 (CD23⁺, IgD^{high}) and T3 (CD23⁺, IgD⁻) B cell populations (Fig. 3.16C, D). It is still elusive whether MZ B cells differentiate only from the T2 B cell stage or also from T1 B cell stages. Some groups assumed

that MZ B cells can also develop from T1 B cells (Loder et al., 1999; Hampel et al., 2011; Roundy et al., 2010). The dramatic increase of T1 B cells in Akt^{BOE} mice could indicate that MZ-like B cells can develop directly from T1 B cells. T2 B cells are important for the FO fate decision (reviewed in Pillai and Cariappa, 2009). They are highly decreased in Akt^{BOE} mice and could therefore explain the loss of FO B cells in Akt^{BOE} mice.

In summary, the overexpression of Akt1 leads to a block in the early precursor development from T1 to T2 B cells.

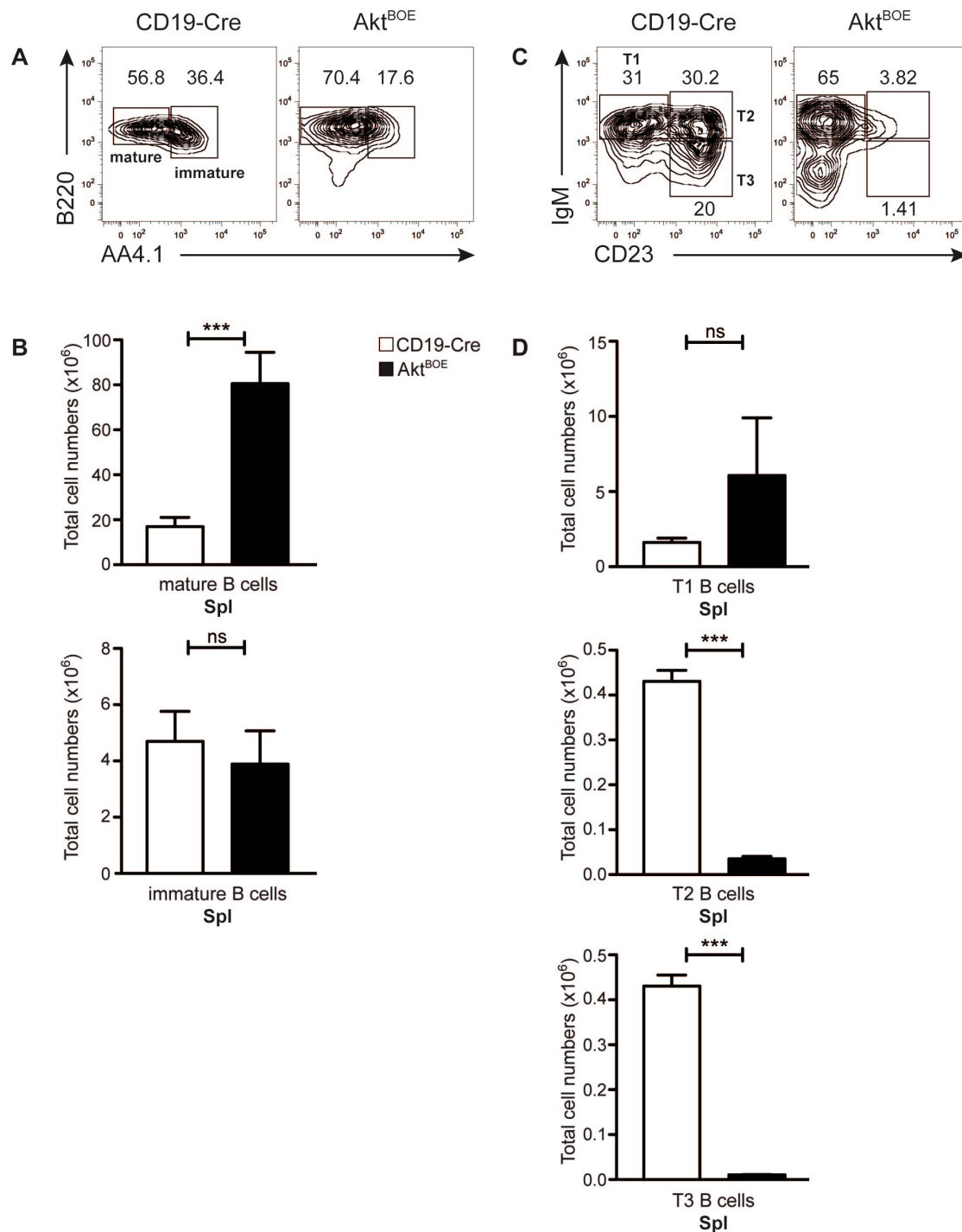


Figure 3.16: Lack of T2 and T3 B cells in spleen of Akt^{BOE} mice.

(A) FACS analysis of splenic B cells from 6-8 week-old Akt^{BOE} and CD19-Cre control mice. Shown is a staining for mature (B220⁺, AA4.1⁻) and immature B cells (B220⁺, AA4.1⁺). The numbers close to the boxes of lymphocyte populations refer to the percentage of CD19⁺ live cells in the gates. Akt^{BOE} mice were additionally gated on GFP⁺ cells to exclude escapees. Representative plots are shown, experiment was repeated 4 times with n = 2-3 mice per genotype. (B) Total cell numbers of mature and immature B cells in spleen. For total cell numbers, 2 experiments are combined. (C) FACS analysis of splenic B cells from 6-8 week-old Akt^{BOE} and CD19-Cre control mice. Shown is a staining for T1 (IgM^{high}, CD23⁻) T2 (IgM^{high}, CD23⁺) and T3 (IgM^{low}, CD23⁺) B cells. The numbers close to the boxes

of lymphocyte populations refer to the percentage of live cells in the gates. Cells were additionally gated on CD19⁺, B220⁺ and AA4.1⁺ cells. Akt^{BOE} mice were additionally gated on GFP⁺ cells to exclude escapees. Representative gates are shown, experiment was repeated 4 times with n = 2-3 mice per genotype. **(D)** Total cell numbers of transitional B cell subsets in spleen. For total cell numbers, 2 experiments are combined. **B, D** Horizontal bars mark the mean value +/- SEM. ***P < 0.001, ns = not significant, as calculated using 2-tailed Student *t* test.

3.7 MZ-like B Cells of Akt^{BOE} Mice do not Behave as Normal MZ B Cells

We hypothesized that the increased MZ-like B cell population could be due to either a survival advantage or increased proliferation of these cells. To answer this, a proliferation assay was performed. B cells were labeled with Violet CellTrace, which is a dye that intercalates into the cell. Due to cell cycle division fluorescence intensity is halved in each of the daughter cells after one cycle of cell division. These labeled splenic B cells were cultured for four days. B cells were either left untreated or were treated with α IgM (BCR), CpG (TLR9), or LPS (TLR4). Unstimulated B cells were treated with BAFF (B cell activation factor) to keep them alive.

FACS analysis of the proliferation assay revealed normal response of Akt^{BOE} B cells to stimulation of TLR9 (Fig. 3.17A, B). Oliver et al. postulated that MZ B cells after LPS stimulation proliferate better than FO B cells (Oliver et al., 1997). However, although the B cell population of Akt^{BOE} mice mainly consists of MZ-like B cells, they did not proliferate better than control B cells after LPS stimulation (Fig. 3.17A, B). Interestingly, stimulation of the BCR of B cells from Akt^{BOE} mice with α IgM showed no proliferation at all compared to controls (Fig. 3.17A, B).

The crosslinking and activation of the BCR, leads to the activation of a cascade of molecules that drives a Ca²⁺ release (reviewed in Cambier et al., 1994). This Ca²⁺ release is important for many intracellular processes including apoptosis, cell adhesion and migration, and in general, Ca²⁺ release also plays a role in cell-fate decisions in B cells (reviewed in Scharenberg et al., 2007). To test whether B cells of Akt^{BOE} mice are able to flux after BCR stimulation, Ca²⁺ flux experiments were performed. Induction of a Ca²⁺ output in Akt^{BOE} B cells with α IgM activation failed, although they do show a higher baseline level than CD19-Cre control B cells (Fig. 3.17C).

In conclusion, it seems that the BCR of Akt^{BOE} mice is not able to respond to α IgM

stimulation (shown by proliferation assay and Ca^{2+} flux analysis) and is, as was the case with the CD19 co-receptor, not necessary to generate and keep MZ-like B cells alive in case of constitutively active Akt1 expression.

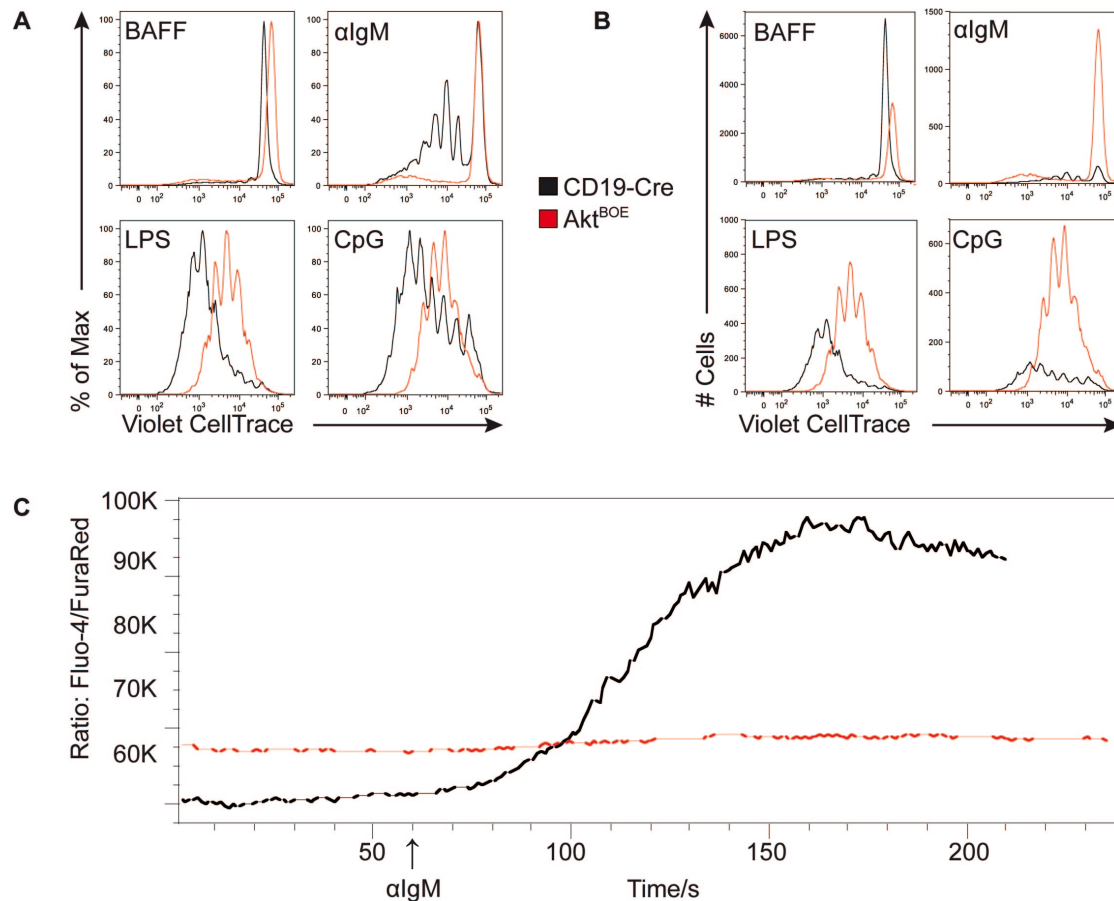


Figure 3.17: Influence of Akt1 overexpression after stimulation, BCR induced signaling.

(A) *In vitro* analysis of Violet CellTrace labeled B cells stimulated with BAFF, αIgM, CpG and LPS for 4 days. Plots are displayed in % of Max. Experiment was repeated 4 times with $n = 3$ mice per genotype. Cells were gated on live cells and CD19⁺ cells. Akt^{BOE} mice were additionally gated on GFP⁺ cells to exclude escapees. **(B)** Same experiment as in A, but with cell numbers. **(C)** Ca^{2+} flux of splenic B cells of Akt^{BOE} and CD19-Cre controls after stimulation with αIgM (5μg/ml, indicated by arrow). Cells were gated on live cells and CD19⁺ cells. Experiment was repeated 4 times with $n = 1$ mouse per genotype. A-C For both experiments, CD19⁺ MACS purified splenic B cells were used.

In general, the activation of the BCR leads to phosphorylation of tyrosine residues, such as the Igα and Igβ ITAM tyrosines, as well as to binding and activation of src-family and spleen tyrosine kinase (Syk), which, for their part, phosphorylate other signal transduction molecules (reviewed in Kurosaki, 1999). To prove whether B cells of Akt^{BOE} mice get phosphorylated at all tyrosine residues through the activation of

the BCR, a pTyr Western blot was performed using α IgM stimulated splenic B cells (Fig. 3.18A). The Western blot revealed mostly less tyrosine phosphorylation in Akt^{BOE} B cells compared to controls, but also two bands (≈ 110 kDa, >160 kDa) in the upper part of the blot were highly phosphorylated (Fig. 3.18A).

Lyn tyrosine kinase (Lyn) and Syk are both tyrosine kinases that are activated through the ITAMS of the BCR (reviewed in Fruman et al., 2000). It was shown that Lyn can potentially act as an inhibitor of BCR mediated activation of Akt (Li et al., 1999). To test Syk and Lyn activation another Western blot with α IgM stimulated B cells was performed. Preliminary data showed that, as expected, Syk was not phosphorylated, whereas phosphorylation of Lyn was the same as in controls (Fig. 3.18B, C). Since phosphorylation of Lyn can be caused by Akt, observed Lyn phosphorylation is due to constitutively active Akt1.

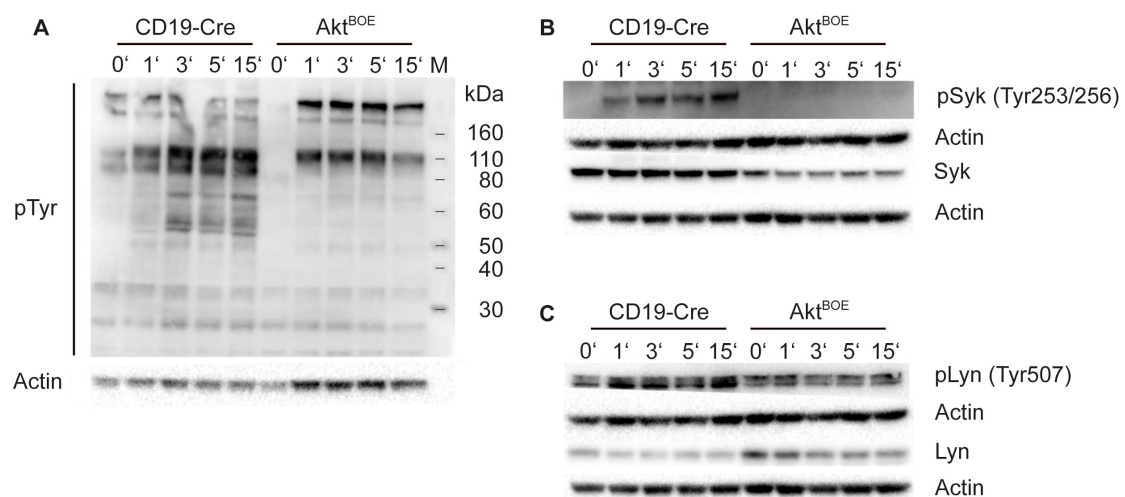


Figure 3.18: Less tyrosine phosphorylation, no Syk phosphorylation but Lyn phosphorylation in Akt^{BOE} splenic B cells after BCR crosslinking.

(A) α -phospho-Tyr Western blot of CD19 MACS purified splenic B cells rested for 4h and stimulated with 10 μ g/ml α IgM for the indicated time points. 24 μ g protein of each lysate was used. (B) Western blot of α -phospho-Syk (72kDa) and α -Syk (72kDa) from depleted CD43 MACS purified splenic B cells stimulated with 10 μ g/ml α IgM for the indicated time points. 30 μ g protein of each lysate was used. (C) Western blot of α -phospho-Lyn (53/56kDa) and α -Lyn (56kDa) from depleted CD43 MACS purified splenic B cells stimulated with 10 μ g/ml α IgM for the indicated time points. 30 μ g protein of each lysate was used. A-C As loading control in all blots, α -Actin (43kDa) were used.

3.8 Akt1 Expression Prolongs the Survival of Akt^{BOE} B Cells *in vitro*

We could already show that increased cell numbers of MZ-like B cells in Akt^{BOE} mice could not be due to increased proliferation (Fig. 3.17A, B), therefore we investigated if B cells of Akt^{BOE} mice survive better than B cells of CD19-Cre controls. To answer this, CD19 MACS purified splenic B cells were cultured for four days without additional stimulation. Every day the number of living cells was determined by counting and flow cytometry. The survival assay revealed a survival advantage of B cells of Akt^{BOE} mice in comparison to B cells of CD19-Cre controls (Fig. 3.19A, B). Already at day two B cells of Akt^{BOE} mice showed significant better survival than B cells of CD19-Cre controls (Fig. 3.19A, B). After four days, all CD19-Cre B cells were dead, whereas 50% of Akt^{BOE} B cell were still alive (Fig. 3.19B). Increased B cell numbers in Akt^{BOE} mice thus seem to be a consequence of better survival, and not due to increased proliferation.

Taken together, these results showed that Akt1 overexpression in B cells led to a prolonged survival of B cells in Akt^{BOE} mice *in vitro* and indicated that constitutive Akt1 signaling is able to rescue B cells of Akt^{BOE} mice from cell death to some extent.

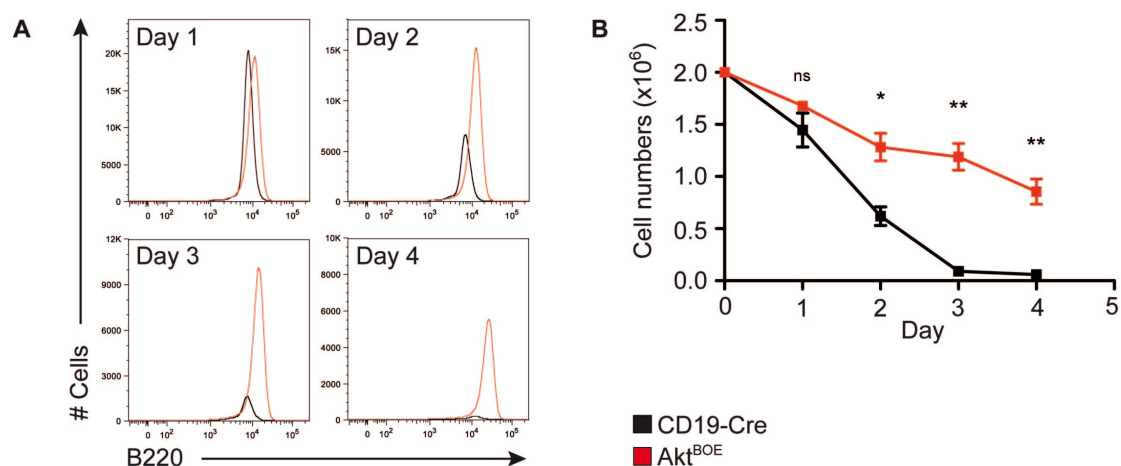


Figure 3.19: Influence of Akt1 overexpression to B cell survival.

(A) FACS analysis of survival assay. Splenic B cells were taken for 4 days in culture without any stimulus to determine the survival of the cells. Experiment was repeated 4 times with $n = 3$ mice per genotype. **(B)** Cell numbers of survival assay. \pm SEM. $**P < 0.001$, $*P < 0.05$, ns = not significant, as calculated using 2-tailed Student t test. For the experiment, CD19⁺ MACS purified splenic B cells were used.

3.9 MZ-like B Cells of Akt^{BOE} Mice do not Class Switch as Normal MZ B Cells

One hallmark of MZ B cells is to secrete immunoglobulin IgM und IgG3 in a TI manner (Martin et al., 2001). To analyze the immunoglobulin secretion of the Akt1 overexpressing MZ-like B cells, Akt^{BOE} and CD19-Cre mice were immunized with NP-Ficoll to generate a TI immune response. Therefore, serum from blood taken on day 0, 7, 14, 21 and 28 were used to determine IgM and IgG3 secretion using NP-specific ELISA. Surprisingly, we detected significant less IgM in the blood sera of Akt^{BOE} mice in comparison to controls (Fig. 3.20A left, B left). Furthermore, IgG3 was not secreted by MZ-like B cells of Akt^{BOE} mice (Fig. 3.20B right, C right). To illustrate that the sera of Akt^{BOE} mice mostly do not secrete IgM and no IgG3, we also display the values on a linear scale, to show zero values (Fig. 3.20B).

In conclusion, MZ-like B cells of Akt^{BOE} mice were not able to initiate an immune response after TI immunization.

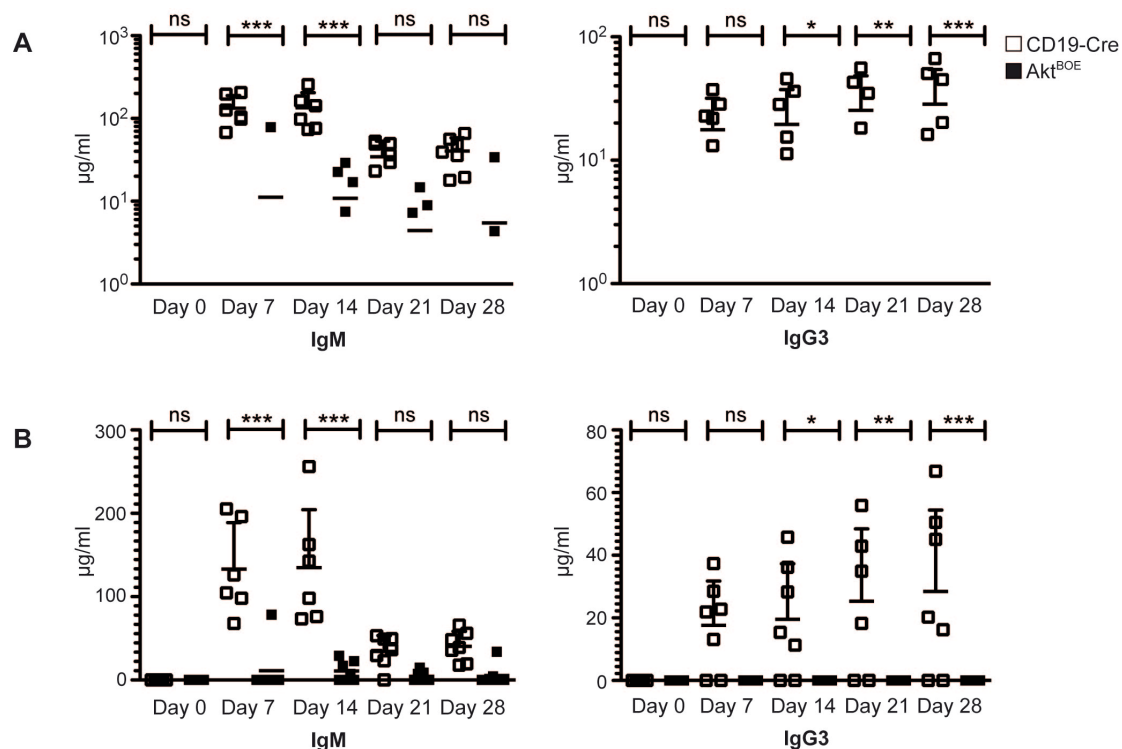


Figure 3.20: No IgM and IgG3 secretion from B cells of Akt^{BOE} mice.

(A) NP-specific immunoglobulin ELISA of blood sera from NP-Ficoll immunized Akt^{BOE} mice and CD19-Cre controls. Experiment was carried out once with $n = 7$ mice per genotype. (B) Same data as in (A) but y-axis is linear, to also display 0 values. Horizontal bars mark the mean value \pm SEM. *** $P < 0.001$, ** $P < 0.01$, * $P < 0.05$, ns = not significant, as calculated using 2-way ANOVA test.

3.10 MZ-like B Cells Leave the Spleen and Migrate into other Lymphatic Organs

MZ B cells are sessile cells that are located exclusively in the MZ in wild type mice (Gray et al., 1982; Nolte et al., 2004). Due to the fact that nearly all splenic GFP⁺ B cells of Akt^{BOE} mice are MZ-like B cells, we assumed that these cells start to migrate into other lymphoid organs because the splenic niche, the MZ, is replenished. In order to prove this theory, FACS analysis of pLN, mLN, and PP was performed.

Interestingly, MZ-like B cells were found in pLN of Akt^{BOE} mice. Nodal B cells of Akt^{BOE} mice showed a shift from FO B cells to MZ-like B cells (Fig. 3.21).

In Akt^{+/-}CD19-Cre^{-/-} mice we could already show that splenic MZ-like B cells could develop independently of the CD19 co-receptor due to Akt1 signaling. Interestingly, also in the pLN of Akt^{+/-}CD19-Cre^{-/-} mice MZ-like B cells could be observed, whereas in pLN of CD19-Cre^{-/-} controls FO B cells were detected (Fig. 3.21).

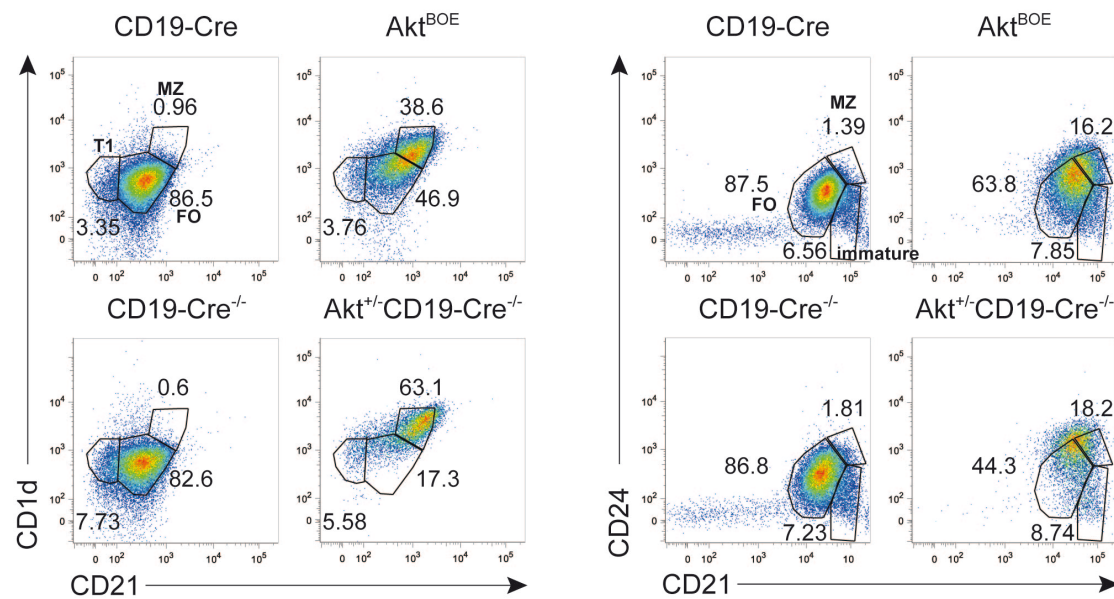


Figure 3.21: MZ-like B cells in pLN of Akt^{BOE} and Akt^{+/-}CD19-Cre^{-/-} mice.

FACS analysis of nodal B cells from 6-8 week-old Akt^{BOE} and Akt^{+/-}CD19-Cre^{-/-} mice with corresponding control mice. Displayed are 2 different stainings showing MZ, FO and T1 B cells. In the left staining, FO (CD21^{int}, CD1d^{low}), MZ (CD21^{high}, CD1d^{high}) and T1 (CD21^{low}, CD1d^{low}) B cells are shown. The right staining shows FO (CD21^{inter}, CD24^{inter}), MZ (CD21^{high}, CD24⁺) and immature (CD21^{high}, CD24^{inter}) B cells. The numbers close to the boxes of lymphocyte populations refer to the percentage of B220⁺ live cells in the gates. Akt^{BOE} and Akt^{+/-}CD19-Cre^{-/-} mice were additionally gated on GFP⁺ cells to exclude escapees. Representative plots are shown, Akt^{BOE} and CD19-Cre mice: n = 2-3 and Akt^{+/-}CD19-Cre^{-/-} CD19-Cre^{-/-} mice: n = 2-3, experiment was repeated twice.

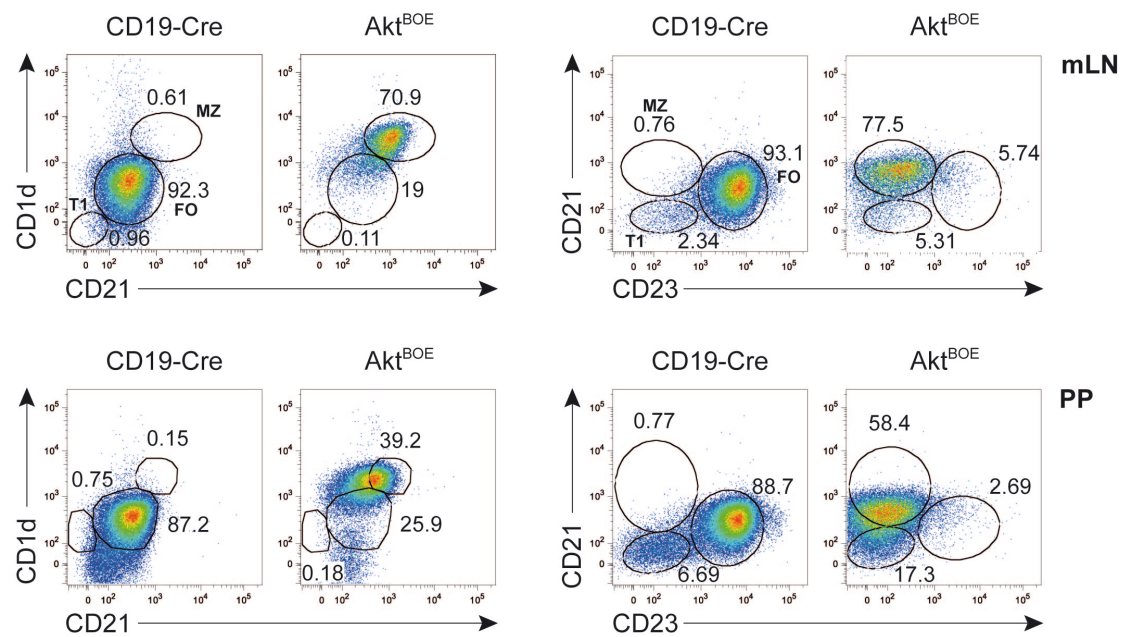


Figure 3.22: MZ-like B cells in mLN and PP of Akt^{BOE} mice.

FACS analysis of mLN and PP from 6-8 week-old Akt^{BOE} and CD19-Cre control mice. Displayed are 2 different stainings showing MZ, FO and T1 B cells. In the left staining, FO (CD21^{inter}, CD1d^{low}), MZ (CD21^{high}, CD1d^{high}) and T1 (CD21^{low}, CD1d^{low}) B cells are shown. The right staining shows FO (CD21⁺, CD23⁺), MZ (CD21⁺, CD23⁻) and T1 (CD21^{low}, CD23⁻) B cells. The numbers close to the boxes of lymphocyte populations refer to the percentage of live cells in the gates. Cells were gated on live cells and CD19⁺ cells. Akt^{BOE} mice were additionally gated on GFP⁺ cells to exclude escapees. mLN: Experiment was repeated 3 times with n = 3 mice per genotype. PP: Experiment was repeated 3 times with n = 3 mice per genotype, 5 PP per mouse.

FACS analysis of MZ B cells in mLN and PP revealed MZ-like B cells in Akt^{BOE} mice whereas in the controls only FO B cells were detected (Fig. 3.22). MZ-like B cells of Akt^{BOE} mice are also able to migrate into mLN and PP.

In conclusion, constitutive Akt1 signaling leads to the accumulation of dramatically increased splenic MZ-like B cell population. Despite the fact that MZ B cells are sessile cells, these MZ-like B cells migrate into other lymphatic organs, probably due to restricted space in the spleen.

3.11 Loss of CD23 Expression Due to Constitutive Akt1 Signaling

CD23 was shown as an important surface marker for T2, T3 and FO B cells (Loder et al., 1999; Allman et al., 2001; reviewed in Pillai and Cariappa, 2009). As already

shown, FACS analysis of transitional B cells of Akt^{BOE} mice revealed strongly diminished T2 and T3 B cell populations and the investigation of mature B cells showed an absence of FO B cell populations (Fig. 3.16C, D; Fig. 3.13A, B). In general, T2 and T3 B cells as well as FO B cells express CD23, but this surface marker was not detectable in B cells of Akt^{BOE} mice by FACS. It is known that ADAM10 is the *in vivo* sheddase of CD23 (Gibb et al., 2010). In order to investigate if CD23 was completely cleaved and therefore not detectable on the cell surface of Akt^{BOE} B cells a CD23 ELISA was performed. CD23 ELISA from blood sera of Akt^{BOE} mice revealed a significant reduction of CD23 in sera of Akt^{BOE} mice in comparison to sera of CD19-Cre controls (Fig. 3.23A).

Thus, Real-Time analysis was performed to investigate if already *CD23* mRNA levels are reduced. The investigation of *CD23* levels revealed a significant reduction of *CD23* mRNA levels in B cells of Akt^{BOE} mice in comparison to B cells of CD19-Cre controls (Fig. 3.23B).

Collectively, Akt1 signaling is a negative regulator of *CD23* mRNA levels, as we could show that B cells of Akt^{BOE} mice express no CD23.

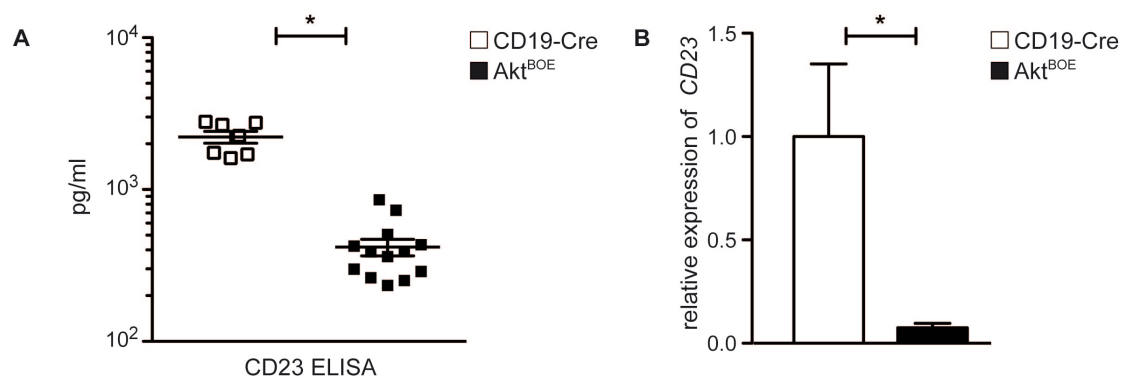


Figure 3.23: CD23 secretion in blood sera and *CD23* RNA levels.

(A) CD23 ELISA of blood sera from Akt^{BOE} mice and CD19-Cre controls. Experiment was carried out once with $n = 7-13$ mice per genotype. **(B)** Quantitative Real-Time PCR of CD19 MACS purified splenic B cells. Relative expression levels of *CD23* with indicated genotypes. Gene expression levels were normalized to HPRT from each mRNA preparation. The fold change was calculated in comparison with the results obtained from CD19-Cre controls. Experiment was carried out once with $n = 3$ mice per genotype. A, B, Horizontal bars mark the mean value \pm SEM. *** $P < 0.001$, * $P < 0.05$, as calculated using 2-tailed Student *t* test.

3.12 Defects in Class Switch Recombination in Akt^{BOE} Mice

CSR is a very important mechanism to defend the body from antigens. To investigate if CSR in B cells of Akt^{BOE} mice is functional we performed ELISA, FACS and Real-Time analysis. Pierau et al. could show that overexpression of Akt1 in all cells of the body leads to increased levels of IgM, IgG1 and IgG3 after TI immunization. After stimulation with LPS they could detect an increase in IgM, IgG and IgA secretion in Akt1 overexpressing mouse line in comparison to controls (Pierau et al., 2012).

First, immunoglobulin ELISAs from blood sera from naive animals was performed. B cells of Akt^{BOE} mice in comparison to B cells of CD19-Cre controls secreted significantly less of all tested immunoglobulins (Fig. 3.24A, B). We assumed that detected immunoglobulin titers were due to Cre escapee cells that do not overexpress Akt1 and cannot be excluded in blood sera.

Nevertheless B cells of Akt^{BOE} mice do not secrete immunoglobulins, it is possible, that they switch but not secrete them. To test this, *in vitro* stimulation with LPS and IL4 was performed, which cause a switch to IgG1. Stimulation of Akt^{BOE} B cells did not induce class switch to IgG1, whereas as expected for CD19-Cre controls, 19% control B cells switched to IgG1 (Fig. 3.24C).

To assess if B cells of Akt^{BOE} mice in general are able to perform the process of class switching, this process was investigated. One requirement for B cells to switch is the generation of circular transcripts (CTs). These CTs can be verified by PCR of *in vitro* stimulated splenic B cells. During the process of CSR activation-induced cytidine deaminase (AID) targets so called S regions, inserts two double-strand breaks and links the donor S region (S_μ) to one of the other downstream acceptor S regions, in the case of IgG1: S_{γ1} (Muramatsu et al., 2000; Kataoka et al., 1980). Therefore, an extra chromosomal circle arises and the CTs are generated (reviewed in Iwasato et al., 1990; Kataoka et al., 1980). The performed PCR for _{γ1} CTs is specific for IgG1. After *in vitro* stimulation of splenic B cells with LPS and IL4, a clear band for the _{γ1} CTs could be detected in the DNA of control mice, whereas the Akt^{BOE} mice cells did not show this band (Fig. 3.24D).

IgG1 expression can also be detected via quantitative Real-Time PCR. RNA levels of *IgG1* were dramatically reduced in B cells of Akt^{BOE} mice whereas B cells of CD19-Cre mice showed normal RNA expression levels of *IgG1* (Fig. 3.24E).

Given that there is no CSR detectable, it was interesting to investigate the gene expression levels of *Aicda*. Its protein, the AID, is very important in initiating the mechanism of CSR (Muramatsu et al., 2000). Quantitative Real-Time analysis revealed significantly less *Aicda* gene expression in RNA of Akt^{BOE} mice.

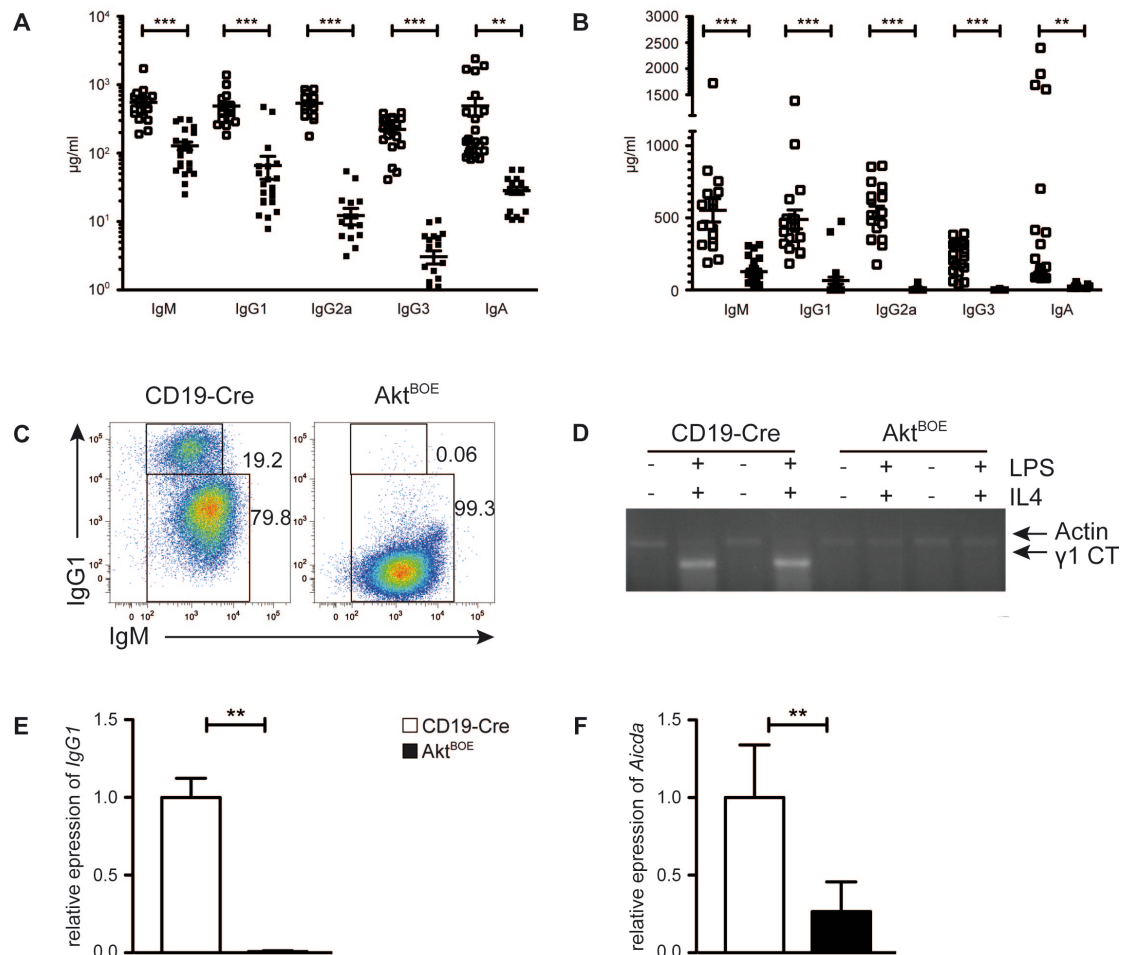


Figure 3.24: Akt^{BOE} mice are not able to secrete and express immunoglobulins.

(A) Analysis of immunoglobulins in blood sera using ELISA assay. Depending on immunoglobulin, 18-25 blood probes were used. Y-axis shows logarithmic scale. (B) Different way of representing ELISA assay of immunoglobulins. Y-axis is linear pictured in order to show data of zero. (C) FACS analysis of CD19⁺ MACS purified splenic B cells after 4 days of *in vitro* stimulation (LPS and IL-4) to achieve an IgG1 switch (LPS 50µg/ml and IL-4 20ng/ml). Mice used were 6-8 weeks old. Numbers next to the gates refer to percentage of CD19⁺ live cells. Akt^{BOE} mice were additionally gated on GFP to exclude escapees. Representative plots are shown, experiment was repeated 3 times with n = 3 mice per genotype. (D) PCR analysis of IgG1 circular transcripts (γ1 CT) for splenic B cells of Akt^{BOE} and CD19-Cre control mice after *in vitro* stimulation. Actin was detected at a size of 510bp and γ1 CT at a band size of 408bp. Experiment was repeated 3 times with n = 3 mice per genotype. (E) Quantitative Real-Time analysis of IgG1 from *in vitro* stimulated CD19 MACS purified splenic B cells. Experiment was performed once with n = 3 mice per genotype. (F) Quantitative Real-Time PCR of CD19 MACS

purified splenic B cells. Relative expression levels of *Aicda* with indicated genotypes. Gene expression levels were normalized by HPRT from each mRNA preparation. The fold change was calculated in comparison with the results obtained from CD19-Cre controls. Experiment was repeated twice with $n = 3$ mice per genotype. **A, B, E, F** Horizontal bars mark the mean value \pm SEM. $**P < 0.01$, $*P < 0.05$, as calculated using 2-tailed Student t test.

In summary, Akt^{BOE} B cells do not secrete immunoglobulins, and the process of class switching is, due to Akt1 overexpression, inhibited in these mice. For CSR important features such as *Aicda* expression and generation of CTs are absent.

3.13 Germinal Center Formation in Akt^{BOE} Mice

One place where CSR can take place are germinal centers (GCs) which are located in secondary lymphoid organs and arise in follicles after TD immune responses (Jacob et al., 1991; Berek et al., 1991; Petersen-Mahrt et al., 2002; Hasler et al., 2011; MacLennan, 1994).

Surprisingly, the investigation of GC B cells in mLN of naive Akt^{BOE} mice revealed GC B cells, although the total cell numbers of GC B cells in Akt^{BOE} mice were decreased in comparison to CD19-Cre controls (Fig. 3.25A, B).

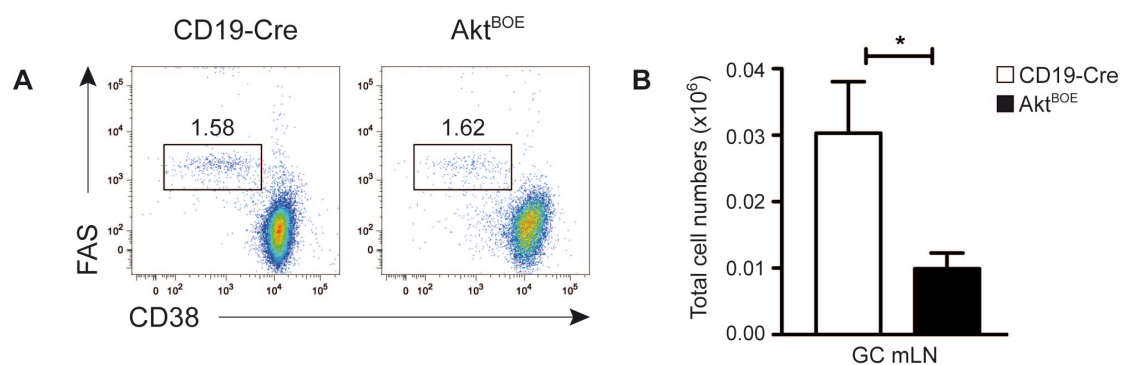


Figure 3.25: Naive GC of mLN in Akt^{BOE} and CD19-Cre mice.

(A) FACS analysis of naive GC in mLN. Mice were 6-8 weeks old. Genotypes and antibodies used are indicated. The numbers close to the boxes of lymphocyte populations refer to the percentage of CD19^+ live cells in the gates. Akt^{BOE} mice were additionally gated on GFP^+ cells to exclude escapees. Representative plots are shown, experiment was repeated twice with $n = 3$ mice per genotype. (B) Displays the total cell numbers of GC of mLN in the different mouse strains. For total cell numbers, all experiments are combined. **C, D** Horizontal bars mark the mean value \pm SEM. $*P < 0.05$, as calculated using 2-tailed Student t test.

To investigate the immune response of Akt^{BOE} mice after T cell dependent (TD) immunization, GC formation was verified. GC B cells can be detected by FACS without immunization and 10 days after immunization with either sheep red blood cells (SRBC) or 4-hydroxy-3-nitrophenylacetyl chicken- γ -globulin (NP-CG). Naive splenic B cells of Akt^{BOE} mice showed no GC formation whereas CD19-Cre mice already had a small population of GC B cells before immunization (Fig. 3.26A), as expected since the animals are not kept germfree in the animal facility. Following TD immunization with NP-CG and SRBC, total cell numbers of GC B cells were drastically reduced in spleen of Akt^{BOE} mice in comparison to control mice. After NP-CG immunization in spleen of Akt^{BOE} 0.03% GCs could be detected, whereas CD19-Cre controls showed 1.6% of GC formation. In spleen of Akt^{BOE} mice the SRBC immunization led to 0.3% GC formation and 5% in CD19-Cre controls (Fig. 3.26C). In PP, B cells of CD19-Cre controls and Akt^{BOE} mice in the naive state already showed GC formation (Fig. 3.26B). After TD immunization with NP-CG in Akt^{BOE} mice, the total cell numbers of GCs strongly decreased compared to controls (Fig. 3.26D).

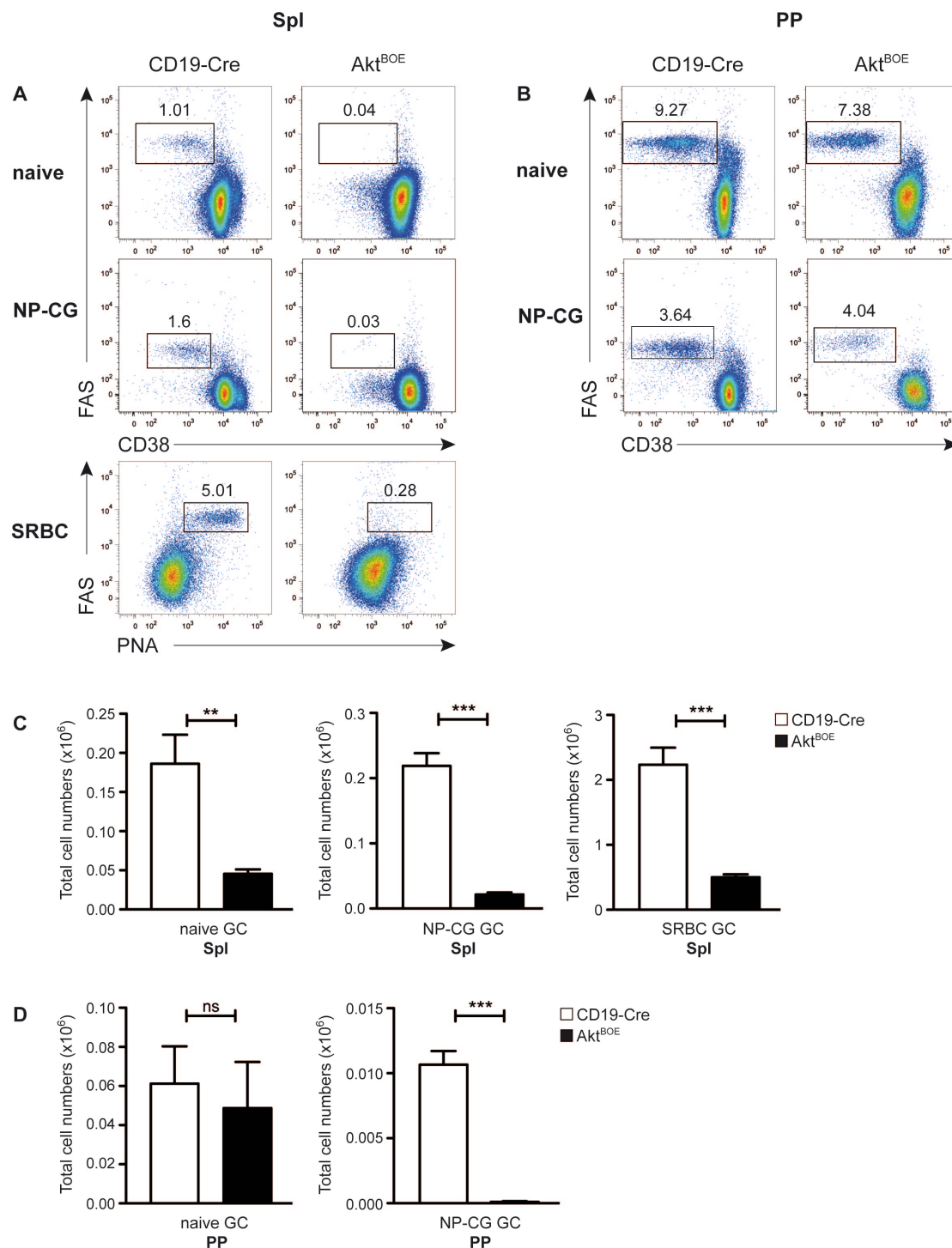


Figure 3.26: GC formation in Akt^{BOE} and CD19-Cre control mice before and after immunization.

(A) FACS analysis of splenic B cells. Shown are 3 independent experiments, unimmunized and immunized Akt^{BOE} and CD19-Cre control mice. Unimmunized mice were 6-8 weeks old. Representative plots are shown, experiment was repeated 3 times with n = 3 mice per genotype. For immunization, SRBC and NP-CG were used. Immunized mice were analyzed 10 days after immunization. Mice immunized with SRBC were 7 weeks old. Experiment was repeated once with n = 3 mice per genotype. Mice immunized with NP-CG were 12 weeks old. Experiment was carried out once with n = 4 mice per genotype. Genotypes and antibodies used are indicated. The numbers close to

the boxes of lymphocyte populations refer to the percentage of CD19⁺ live cells in the gates. Akt^{BOE} mice are additionally gated on GFP⁺ cells to exclude escapees. **(B)** FACS analysis of GC in PP. Shown are 2 independent experiments, unimmunized and immunized with NP-CG. Unimmunized mice were 6-8 weeks old, experiment was done once with n = 3 mice per genotype. Immunized mice were 12 weeks old and analyzed 10 days after immunization. Genotypes and antibodies were used as indicated. The numbers close to the boxes of lymphocyte populations refer to the percentage of CD19⁺ live cells in the gates. Akt^{BOE} mice were additionally gated on GFP⁺ cells to exclude escapees. **(C)** Displays the total cell numbers of GC of the different conditions and the different mouse strains in spleen. Experiment was carried out once with n = 3 mice per genotype. **(D)** Displays the total cell numbers of GC of the different conditions and the different mouse strains in PP. Experiment was carried out once with n = 3 mice per genotype, 5 PP per mouse. Horizontal bars mark the mean value +/- SEM. ***P< 0.001, **P< 0.01, ns = not significant as calculated using 2-tailed Student *t* test.

In summary, due to constitutive Akt1 signaling splenic B cells of Akt^{BOE} mice cannot form GC B cells even after TD immunization. In contrast, GC formation in PP of Akt^{BOE} mice could be detected in naive cells whereas TD immunization led to reduced numbers of GC B cells.

Why do B cells of PP and mLN in Akt^{BOE} mice form GC B cells, particularly without immunization? Casola et al. could show that 3 week-old transgenic mice treated for 2 weeks with a cocktail of broad-spectrum antibiotics display a reduction in GCs of PP. He claimed that the GCs in PP are microbiota derived (Casola et al., 2004).

To determine if the development of GCs in PP and mLN of Akt^{BOE} mice was dependent on bacteria 4.5 week-old mice were treated for 5.5 weeks with a mixture of broad-spectrum antibiotics. FACS analysis of PP B cells showed no significant decrease in GC B cell numbers of antibiotic-treated Akt^{BOE} mice in comparison to treated controls and naive GC B cells of Akt^{BOE} mice and controls (Fig. 3.27A, D). FACS analysis of mLN revealed an increase of GC B cells in percentage in Akt^{BOE} mice and no difference in CD19-Cre controls after antibiotic treatment (Fig. 3.27B). As expected, splenic B cells showed no GC B cells (Fig. 3.27C).

In summary, antibiotic treatment of Akt^{BOE} mice did not reduce total GC B cell numbers in PP as well as in mLN in comparison to CD19-Cre controls.

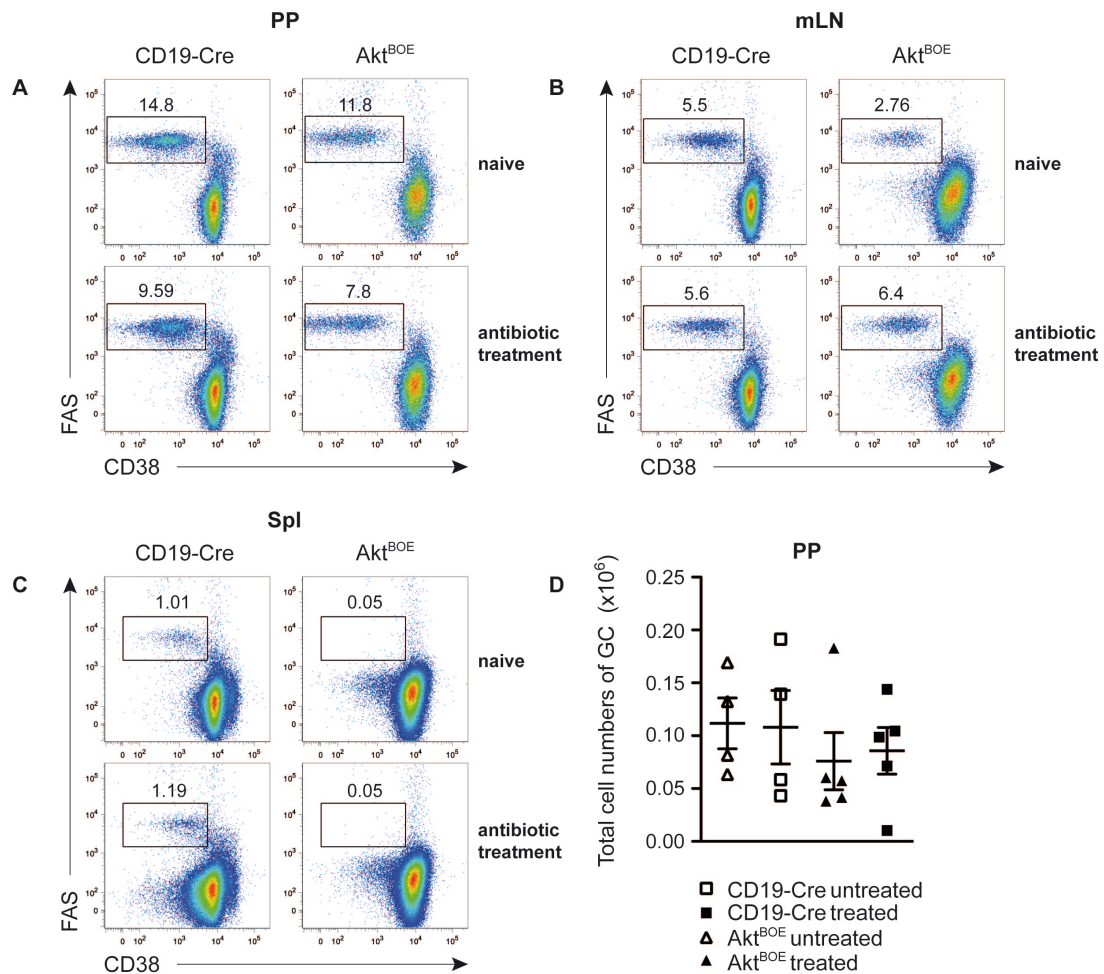


Figure 3.27: GC formation after antibiotic treatment.

FACS analysis of GC in different organs. Mice were 10 weeks old. Genotypes and antibodies were used as indicated. The numbers close to the boxes of lymphocyte populations refer to the percentage of CD19⁺ live cells in the gates. Akt^{BOE} mice were additionally gated on GFP⁺ cells to exclude escapees. Representative plots are shown, 4 mice per genotype of untreated mice and 5 mice per genotype of treated mice, experiment was done once. Antibiotic treatment started with the age of 4.5 weeks and was given for 5.5 weeks. **(A)** GC in PP, 5 PP each mouse. **(B)** GC in mLN. **(C)** Splenic GC. **(D)** Displays the total cell numbers of GC in PP, 5 PP each mouse. Graph shows no significances.

3.14 Investigation of Plasma Cell Formation in Akt^{BOE} Mice

Plasma cells are terminally differentiated B cells that secrete high-affinity antibodies (reviewed in Calame et al., 2003). Due to strongly decreased GC formation and no observed CSR in Akt^{BOE} mice, plasma cell formation in these mice were investigated. Based on the fact that Akt^{BOE} mice had mostly MZ-like B cells, and that MZ B cells are able to differentiate into plasma cells, the B cells of Akt^{BOE} mice should develop into plasma cells, provided that they are functional MZ B cells.

To investigate “natural” plasma cell formation without stimuli leading to plasma cell differentiation FACS analysis was performed. It revealed no significant difference in plasma cell numbers between Akt^{BOE} mice and controls (Fig. 3.28A, B).

Next, an *in vitro* experiment was performed to induce B cell differentiation into plasma cells. Therefore, splenic B cells were stimulated with LPS and IL4 for 4 days and afterwards analyzed by FACS. B cells of CD19-Cre mice were able to differentiate into plasma cells after stimulation, whereas B cells of Akt^{BOE} mice were not (Fig. 3.28C).

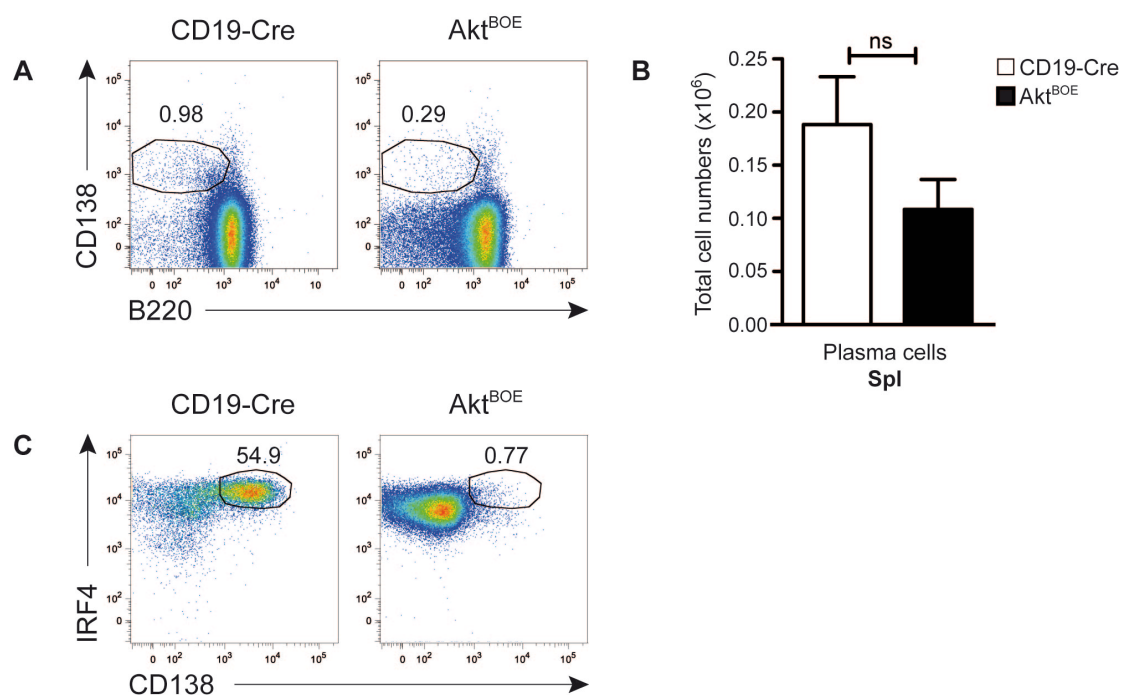


Figure 3.28: Plasma cell differentiation in spleen.

(A) FACS analysis of plasma cells in spleen. Mice were 11 weeks old. Representative plots are shown. Experiment was performed once with $n = 4$ mice per genotype. Genotypes and antibodies were used as indicated. The numbers close to the boxes of lymphocyte populations refer to the percentage of CD19⁺ live cells in the gates. Akt^{BOE} mice were additionally gated on GFP⁺ cells to exclude escapees. **(B)** Displays the total cell numbers of plasma cells in spleen of Akt^{BOE} and CD19-Cre mice. **(C)** FACS analysis of *in vitro* plasma cell differentiation via stimulation with LPS (50μg/ml) and IL4 (20ng/ml) for 4 days. Mice used for this experiment were 10 weeks old. The numbers close to the boxes of lymphocyte populations refer to the percentage of CD19⁺ live cells in the gates. Experiment was carried out once with $n = 3$ mice per genotype. **B** Horizontal bars mark the mean value \pm SEM, ns = not significant as calculated using 2-tailed Student *t* test.

In summary, Akt^{BOE} B cells cannot differentiate into plasma cells, although Akt1 is known to provide the signal for differentiation into plasma cells (reviewed in Limon

and Fruman, 2012). These data show evidence that MZ-like B cells in Akt^{BOE} mice are not functional.

3.15 Influence of Akt1 Signaling on Downstream Signaling Pathways

It was important to know how the constitutive Akt1 signaling in B cells of Akt^{BOE} mice influenced downstream pathways. In general, Akt^{BOE} B cells had more total protein than the same cell numbers of B cells from CD19-Cre mice. Mechanistic pathway analysis was performed to investigate signaling downstream of Akt1 in Akt^{BOE} mice.

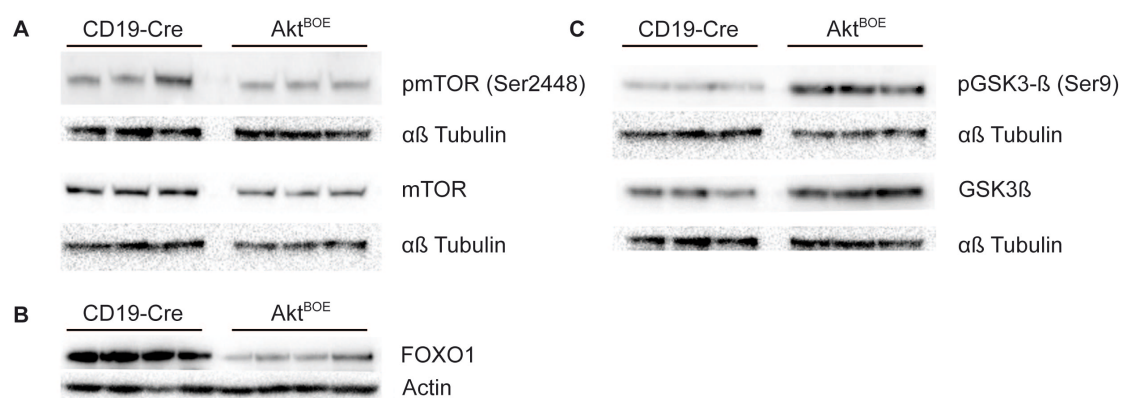


Figure 3.29: Mechanistic signaling pathway analysis of different pathways regulated by Akt1.

(A) Western blot analysis of the mTOR pathway. Shown are protein levels of α -phospho-mTOR Ser2448 (289kDa) and α -mTOR (289kDa). 67 μ g of total protein lysate were used. (B) Western blot analysis of α -FOXO1 (78-82kDa). 25 μ g of total protein lysate were used (C) Western blot analysis of α -phospho-GSK-3 β Ser9 (46kDa) and α -GSK3- β (46kDa). 67 μ g of total protein lysate were used. A - C As loading control α - $\alpha\beta$ Tubulin (55kDa) or α -Actin (43kDa) were used. For all blots CD19 MACS purified splenic B cells rested for 4 hours were used.

For HEK-293 cells it could be shown that the growth factor-induced PI3K/Akt signaling pathway phosphorylates mTOR at Ser2448 and leads to an elevated activity of mTOR (Navé, 1999). So we expected, due to Akt1 activation, to detect higher levels of pmTOR in Akt^{BOE} mice than in controls, but in Akt^{BOE} mice the overexpression of Akt1 did not lead to a higher activation of mTOR (Fig. 3.29A). In contrast, mTOR itself seems to be less expressed in Akt^{BOE} mice in comparison to CD19-Cre controls and pmTor Ser2448 shows similar protein levels compared to controls (Fig. 3.29A).

Beside mTOR and many other substrates, also FOXO transcription factors play an important role in B cells. In B cells only FOXO1 and FOXO3a are expressed and Akt is known to phosphorylate FOXO (Kerdiles et al., 2009; reviewed in Peng, 2008). This harms its transcriptional activity and leads to the transport of pFOXO into the nucleus where it gets degraded (Brunet et al., 1999; Brownawell et al., 2001). Western blot analysis of FOXO1 revealed less protein levels of FOXO1 in B cell lysates of Akt^{BOE} mice in comparison to CD19-Cre controls, which could hint that overexpression of Akt1 leads to the degradation of FOXO1 (Fig. 3.29B).

Furthermore, the glycogen synthase kinase-3 (GSK-3) is regulated through Akt. GSK-3 is a serine/threonine protein kinase that regulates several physiological processes such as the phosphorylation and inactivation of glycogen synthase 3 (reviewed in Welsh et al., 1996). Phosphorylation of GSK-3 α at Ser21 and phosphorylation of GSK-3 β at Ser9 through Akt leads to its inhibition (Cross et al., 1995; Sutherland et al., 1993; Sutherland et al., 1994; reviewed in Li et al., 2015). Analysis of GSK-3 β and pGSK-3 β revealed slightly higher amounts of GSK3- β and noticeably more pGSK3- β in lysates of Akt^{BOE} mice (Fig. 3.29C). Therefore, Akt1 overexpression leads to the phosphorylation of GSK3- β at Ser9 and could lead to its inhibition.

In general, Notch2 could be observed as an important player in B cell development and it was shown that MZ B cell development is Notch2 dependent (Hampel et al., 2011; Saito et al., 2003; Shimizu et al., 2000; Tan-Pertel et al., 2000). Besides Notch2, Notch1 is also expressed in B cells. Notch1 can also increase MZ B cell development and plays a role in peripheral B cell activation and antibody secretion (Kang et al., 2014). To investigate Notch signaling, Western blot and quantitative Real-Time analysis for *Notch1*, *Notch2* and the target genes of Notch2 were performed. The analysis of Notch2 protein revealed more Notch2 protein levels in B cells of Akt^{BOE} mice in comparison to CD19-Cre controls.

Quantitative Real-Time analysis showed significantly less *Notch2* expression independent of whether cells were CD19 positive, CD43 depleted and MACS purified, or sorted for only MZ B cells (Fig. 3.30A, B). Notch1 is also downregulated at the RNA level in B cells of Akt^{BOE} mice (Fig. 3.30C). In addition to Notch2 and Notch1, the Notch2 target genes *hairy and enhancer of split 1 (Hes1)*, *hairy and enhancer of split 5 (Hes5)* and *Deltex1 (Dtx1)* were investigated. Hes1 and Hes5 are

direct downstream targets of Notch2 and their activation through Notch1 leads to a disruption of B cell development (Shimizu et al., 2000; Tan-Pertel et al., 2000; Kawamata et al., 2002). *Dtx1* is a Notch signal modulator and a transcriptional target of Notch and gets regulated by Notch2 (Saito et al., 2003). Previous quantitative Real-Time analysis of Notch2 target genes *Hes1*, *Hes5* and *Dtx1* revealed different results (Saito et al., 2003; Shimizu et al., 2000; Tan-Pertel et al., 2000). Saito et al. could show that Notch2 regulates *Dtx1* expression and that both play a role in MZ B cell development, whereas *Hes1* and *Hes5* expression are less affected when Notch2 is absent (Saito et al., 2003). The data shown here also suggests that downregulation of *Notch2* RNA transcripts in MZ B cells of Akt^{BOE} mice leads to downregulation of *Dtx1* transcription in MZ B cells of Akt^{BOE} mice in comparison to RNA transcripts of MZ B cells in control mice (Fig. 3.30B, F). The opposite could be observed for immature and mature resting B cells of Akt^{BOE} mice (negative purified for CD43) (Fig. 3.30B, F). The latter showed an increase of *Dtx1* RNA levels in comparison to immature and mature resting B cells of controls (Fig. 3.30B, F). *Hes1* RNA levels of MZ B cells from Akt^{BOE} mice were not affected and showed similar transcription levels as CD19-Cre controls even when *Notch2* RNA levels were downregulated (Fig. 3.30B, D). The same was true for immature and mature resting B cells (Fig. 3.30B, D). However, the downregulation of *Notch2* seems to downregulate *Hes5* in all investigated B cell populations (Fig. 3.30B, E),

Through the Akt1 overexpression in B cells of Akt^{BOE} mice, Notch2 protein levels are increased, which could explain the increased number of MZ-like B cells. The increased Notch2 protein levels lead to a reduction in *Notch2* RNA levels, and its target genes *Hes1*, *Hes5* and *Dtx1* are differentially regulated. Whereas *Hes1* RNA levels seemed to be independent of Notch2 protein and RNA levels, *Hes5* RNA transcription levels decreased with increased Notch2 protein levels and downregulated RNA levels. *Dtx1* RNA levels seemed to be differentially regulated through Notch2 in the different B cell subsets. In MZ-like B cells, the higher levels of Notch2 protein and the lower levels of RNA seemed to also reduce the relative expression levels of *Dtx1*, whereas in immature and mature resting B cells, RNA levels of *Dtx1* were upregulated.

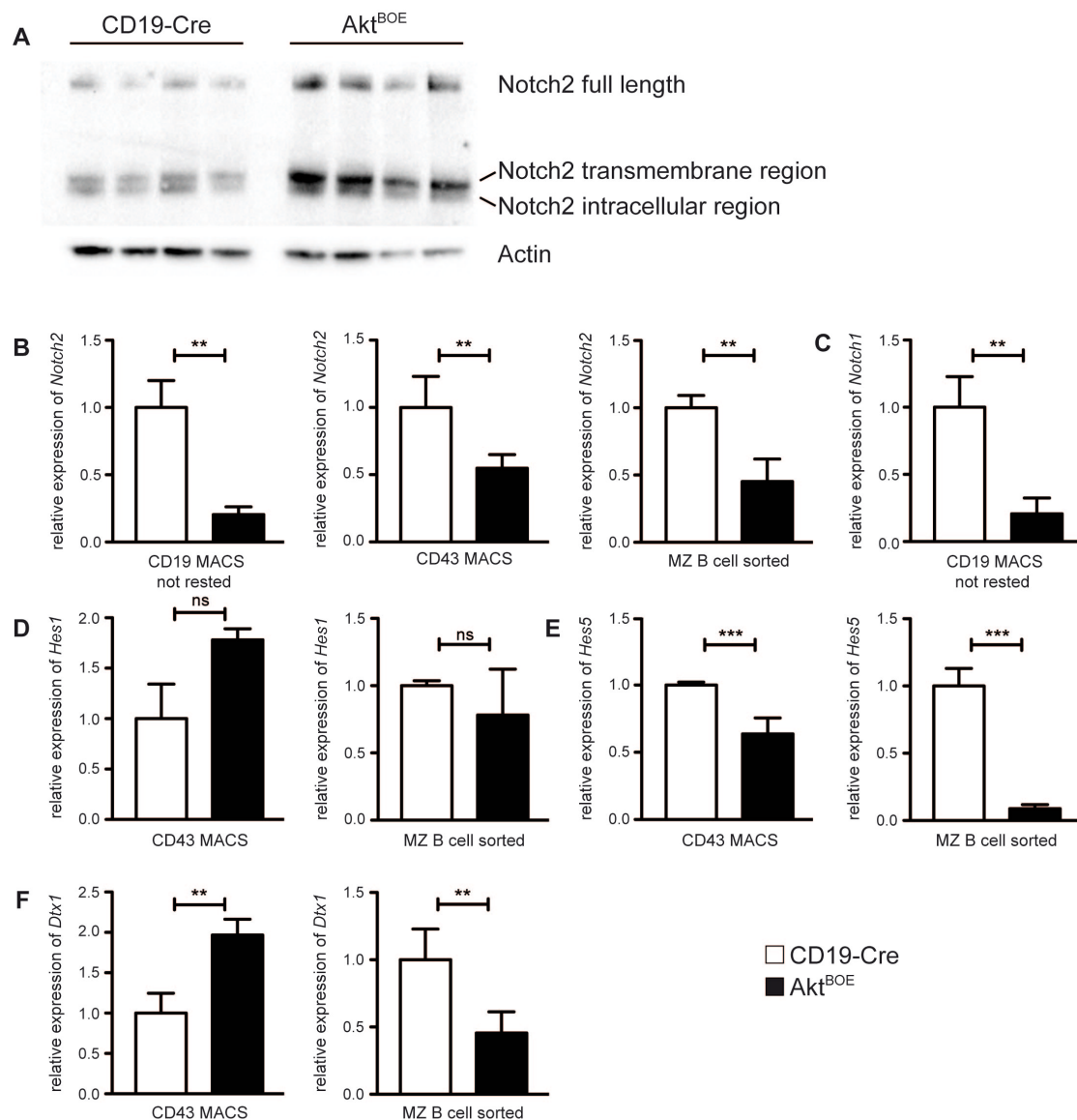


Figure 3.30: Mechanistic signaling pathway analysis of Notch2 and quantitative Real-Time analysis of Notch1, Notch2 and Notch2 target genes in Akt^{BOE} and CD19-Cre control mice.

(A) CD43 MACS depleted purified B cells were used to prepare total protein lysates for α -Notch2 Western blot. Shown is Notch2 full length (300kDa), Notch2 transmembrane (120kDa) and Notch2 intracellular region (100kDa). 60 μ g of total protein lysate were used. α -Actin (43kDa) was used as a loading control. (B) The relative expression level of *Notch2* in CD19/CD43 MACS purified splenic B cells and MZ-like B cells is shown. (C) Relative *Notch1* expression in CD19 MACS purified splenic B cells. (D-F) Relative gene expression levels of the target genes *Hes1*, *Hes5* and *Deltex1* (*Dtx1*) of Notch2 in CD43 MACS purified splenic B cells and MZ-like B cells. (B-F) Gene expression levels were normalized to HPRT from each mRNA preparation. The fold change was calculated in comparison to the results obtained from CD19-Cre controls. B-F Horizontal bars mark the mean value \pm SEM. ***P < 0.001, **P < 0.01, ns = not significant as calculated using 2-tailed Student *t* test.

3.16 Proposed Tumor Development in Akt^{BOE} Mice

It is known that Akt is overexpressed in many kinds of tumors; therefore, we expected to generate a B cell tumor model by overexpressing Akt1 in B cells. Possibly due to the young age of Akt^{BOE} mice (6-8 weeks old) we did not detect tumor formation, so far. B-CLL is by definition, “a proliferation of B lymphocytes that express CD19 or CD20, CD5, CD23 and low levels of Ig on their surface” (Chiorazzi and Ferrarini, 2003). In this disease, an accumulation of slowly proliferating CD5⁺ B lymphocytes can be observed that develops with age. To find out if constitutive Akt1 leads to an accumulation of these cells, mice were left to age. These experiments are just in the beginning stages and no mice have yet been analyzed, but thus far we could observe a tendency in aged Akt^{BOE} mice (≥ 72 weeks) to lose weight as compared to controls (Fig. 3.31).

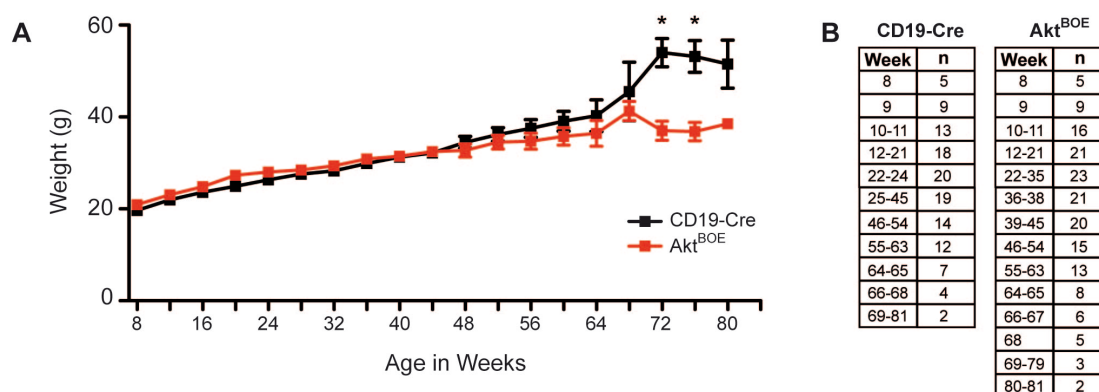


Figure 3.31: Weight course of aging mice.

(A) The relationship between weight and age in Akt^{BOE} mice in comparison to CD19-Cre controls is shown. Differences between groups are not significant, except in week 72 and 76. Horizontal bars mark the mean value \pm SEM. * $P < 0.05$, as calculated using 2-tailed Student *t* test. (B) Table that displays the number (n) of mice in the corresponding week.

To proof a possible immunoglobulin production with age, ELISA of blood sera from 17-29 week-old mice was performed. Curiously, the blood sera of aged Akt^{BOE} mice showed no IgM secretion in comparison to CD19-Cre mice (Fig. 3.32A). In addition, IgG1 and IgG3 were not detectable compared to CD19-Cre controls (Fig. 3.32B, C). B cells of aged Akt^{BOE} mice did not secrete immunoglobulins.

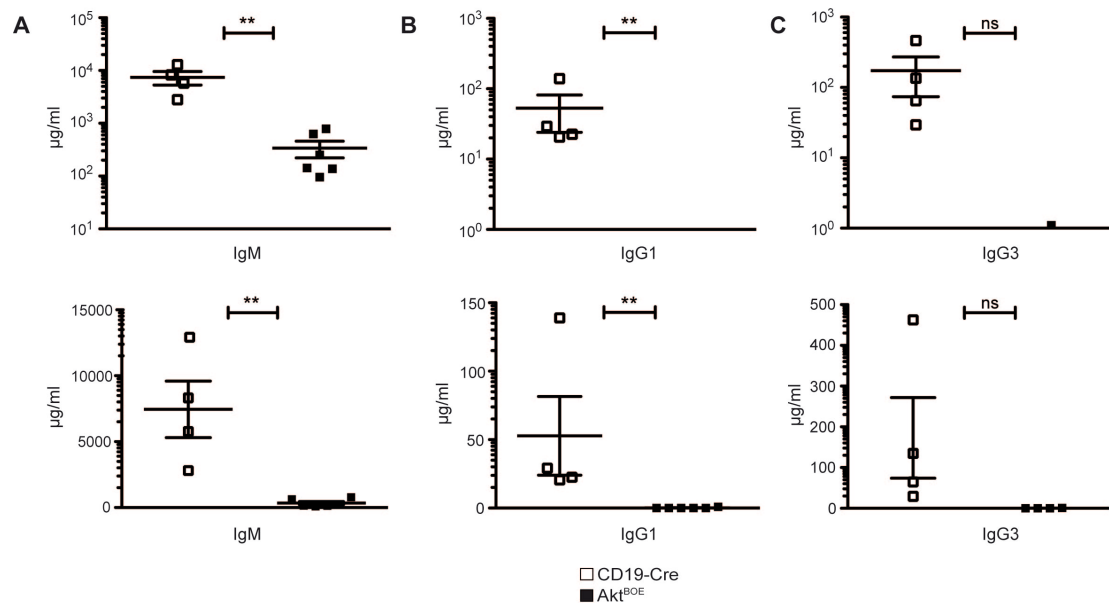


Figure 3.32: Immunoglobulin secretion of blood sera in aged Akt^{BOE} mice.

ELISA for Immunoglobulins of blood sera from 17-29 week-old Akt^{BOE} mice and controls (A) IgM ELISA (B) IgG1 ELISA (C) IgG3 ELISA. The upper figures show logarithmic scale; lower figures display linear scale to also include values of zero. Experiment was done once with $n = 4-6$ mice per genotype. A-C Horizontal bars mark the mean value \pm SEM. ** $P < 0.01$, ns = not significant as calculated using 2-tailed Student t test.

3.17 Detailed Analysis of IgM⁻, IgD⁻ Double Negative B Cell Population

Ig κ (Ig kappa) and Ig λ (Ig lambda) are the two existing light chains and are important markers for mature B cells (Bernier and Cebra, 1964; Pernis et al., 1965). An immunoglobulin has either κ or λ chains and in the BM of wild type mice the ratio of κ to λ is 95 to 5 (Takeda et al., 1996; Alt et al., 1980; Langman and Cohn, 1995). Some B cell tumors showed a shifted Ig κ , Ig λ ratio and therefore we investigated Ig κ and Ig λ (Niewmierzycka et al., 2015; reviewed in Jenner, 2014).

The investigation of κ^+ and λ^+ B cells in BM and spleen of Akt^{BOE} mice revealed an opposite picture. In BM Akt^{BOE} mice showed significantly reduced κ^+ , λ^+ and double negative B cells as compared to CD19-Cre controls (Fig. 3.33A, B).

Spleens of Akt^{BOE} mice had significantly more total cell numbers of κ^+ and λ^+ B cells than controls, due to more B cells in Akt^{BOE} mice (Fig. 3.33C, D). Also numbers of B cell negative for κ and λ (DN) are significantly increased in spleen of Akt^{BOE} mice in comparison to CD19-Cre controls (Fig. 3.33D). The same DN population could be detected in the IgM vs. IgD staining in spleen, PP and PerC (Fig. 3.11). It seems that

these B cells do not express Ig κ , Ig λ , IgM and IgD and are not normal B cells, but express the surface marker CD19.

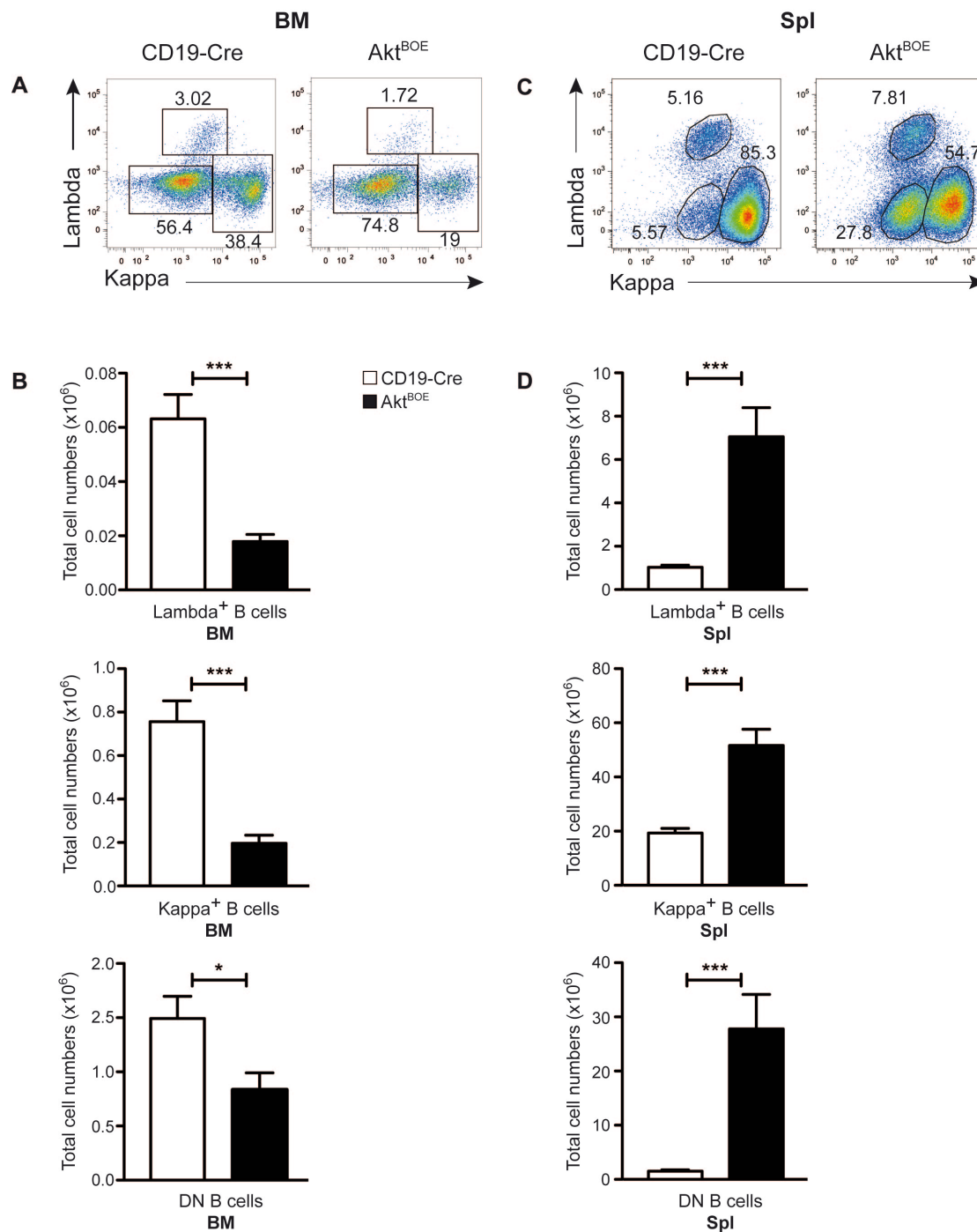


Figure 3.33: Distribution of κ and λ positive B cells in BM and spleen.

(A) FACS analysis of 6-8 week-old Akt^{BOE} and CD19-Cre control mice in BM. Genotypes and antibodies are used as indicated. The numbers close to the boxes of lymphocyte populations refer to the percentage of CD19⁺ live cells in the gates. Akt^{BOE} mice were additionally gated on GFP⁺ cells to exclude escapees. Representative plots are shown, experiment was repeated 3 times with n = 3-4 mice per genotype. (B) Total cell numbers of κ , λ and double negative cells of BM B cells. For total cell numbers, all experiments are combined. (C) FACS analysis of splenic cells from 6-8 week-old Akt^{BOE}

and CD19-Cre control mice. Genotypes and antibodies were used as indicated. The numbers close to the boxes of lymphocyte populations refer to the percentage of live cells in the gates. Cells were gated on live cells and CD19⁺ cells. Akt^{BOE} mice were additionally gated on GFP to exclude escapees. The experiment was performed 4 times with 12 mice per genotype each time. **(D)** Total cell numbers of κ , λ and double negative cells in spleen. For total cell numbers, all experiments are combined. **B, D** DN stands for double negative. Horizontal bars mark the mean value \pm SEM. *** P < 0.001, * P < 0.05 as calculated using 2-tailed Student t test.

To investigate if Ig κ and Ig λ are secreted in the blood sera of Akt^{BOE} mice, ELISA was performed. Amazingly the blood sera showed less κ and λ in the blood sera of Akt^{BOE} mice than in controls (Fig. 3.34A, B). That means that Akt^{BOE} mice express significantly increased splenic κ ⁺ and λ ⁺ B cells but soluble Ig κ and Ig λ is significantly reduced in comparison to the CD19-Cre control mice.

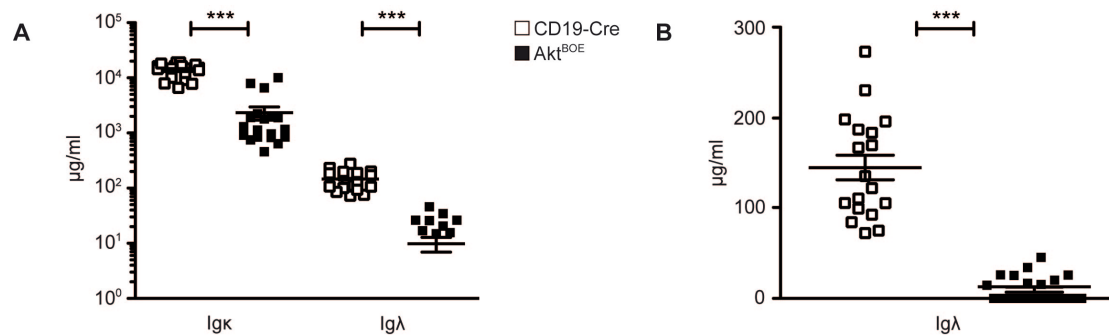


Figure 3.34: Ig κ and Ig λ concentration in serum Akt^{BOE} and CD19-Cre mice.

(A) Ig λ and Ig κ concentrations in serum of Akt^{BOE} and CD19-Cre mice determined by ELISA. **(B)** Figure shows linear y-axis to display also data of zero from Ig λ . Ig κ had no zero values and therefore no other way of representing data is needed.

During the investigation of surface IgM and IgD in B cells of Akt^{BOE} mice a population negative for IgM and IgD was observed (Fig. 3.11). The study of the κ and λ light chains also revealed this DN population (Fig. 3.33). We assumed that these CD19⁺ B cells that do not express BCR are able to bypass the process of selection in the BM. To verify this, Akt^{BOE} mice were crossed to JHT^{-/-} mice. The JHT^{-/-} mice carry a deletion of the J_H segments and the intron enhancer in the IgH locus. This mouse strain cannot generate functional B cells, because the formation of heavy V region genes through somatic V_H-D_H-J_H recombination is not functional (Gu et al., 1993). In this thesis Akt^{BOE} mice crossed to JHT^{-/-} mice are called Akt^{+/+}JHT^{-/-}CD19-Cre^{+/+} mice. As controls C57BL/6 mice called wild type (WT) and JHT^{-/-}CD19-Cre^{+/+}

mice were used. During our investigations it was observed that $JHT^{-/-}CD19-Cre^{+/-}$ and $Akt^{+/-}JHT^{-/-}CD19-Cre^{+/-}$ did not form PP.

First, we investigated if $CD19^{+}$ B cells developed. As expected in $JHT^{-/-}CD19-Cre^{+/-}$ controls, no $CD19^{+}$ B cells could be detected in the analyzed organs whereas in WT mice normal $CD19^{+}$ B cells were observed. Amazingly, in $Akt^{+/-}JHT^{-/-}CD19-Cre^{+/-}$ mice $CD19^{+}$ cells could be found in all organs. Spleen and PerC showed the most impressive $CD19^{+}$ population followed by the population in pLN and mLN (Fig. 3.35).

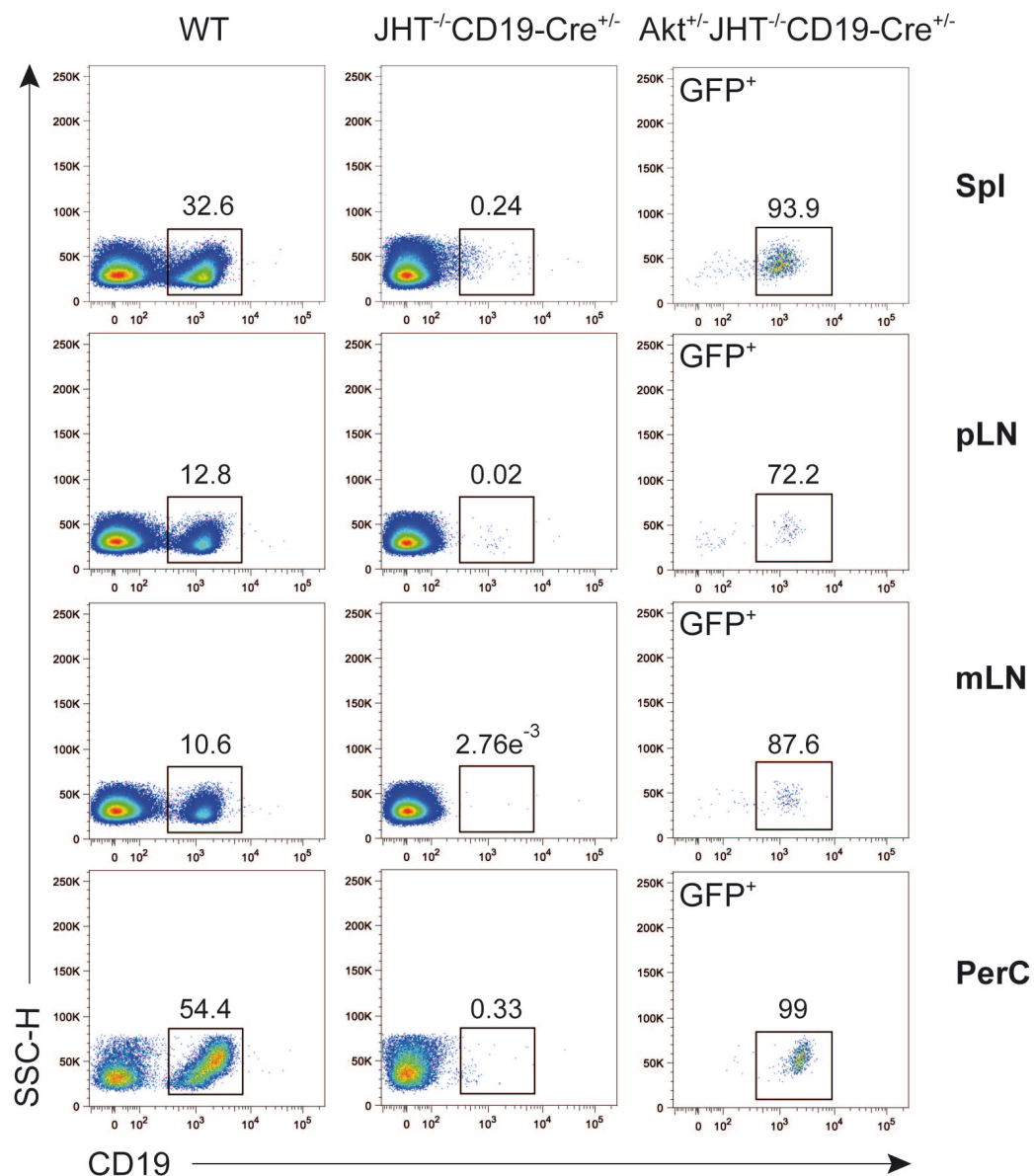


Figure 3.35: Investigation of CD19 positive B cells in different organs and PerC in $Akt^{+/-}JHT^{-/-}CD19-Cre^{+/-}$ mice.

FACS analysis of 7.5 week-old $Akt^{+/-}JHT^{-/-}CD19-Cre^{+/-}$, WT and $JHT^{-/-}CD19-Cre^{+/-}$ control mice in spleen, pLN, mLN and PerC. Antibodies used are indicated. The numbers close to the boxes of

lymphocyte populations refer to the percentage of live cells in the gates. Akt^{+/-}JHT^{-/-}CD19-Cre^{+/-} mice were additionally gated on GFP⁺ cells to exclude escapees. The experiment was done 3 times with mice of different ages: firstly, 7.5 weeks (2 WT, 2 JHT^{-/-}CD19-Cre^{+/-} and 4 Akt^{+/-}JHT^{-/-}CD19-Cre^{+/-} mice), secondly, 9.5 weeks (2 WT, 2 JHT^{-/-}CD19-Cre^{+/-} and 4 Akt^{+/-}JHT^{-/-}CD19-Cre^{+/-} mice) and thirdly, 12 weeks (2 WT, 2 JHT^{-/-}CD19-Cre^{+/-} and 4 Akt^{+/-}JHT^{-/-}CD19-Cre^{+/-} mice).

In order to identify the type of CD19⁺ cells found in the Akt^{+/-}JHT^{-/-}CD19-Cre^{+/-} mice, stainings for IgM vs. IgD and κ vs. λ were performed. We assumed that these CD19⁺ B cells are the DN B cells that already could be observed in the κ vs. λ and IgM vs. IgD stainings of Akt^{BOE} B cells (Fig. 3.33; Fig. 3.11). As expected, B cells of WT mice in spleens and PerC showed IgM⁺ and IgD⁺ cells, whereas in pLN and mLN only IgD⁺ cell could be observed (Fig. 3.36A-D upper staining). WT mice showed no DN population (Fig. 3.36A-D upper staining). In spleen, pLN, mLN and PerC κ ⁺ and λ ⁺ B cells could be detected in WT and no DN cells could be seen. Due to no CD19⁺ B cells in JHT^{-/-}CD19-Cre^{+/-} controls no κ ⁺, λ ⁺ nor DN cells could be observed. Also in Akt^{+/-}JHT^{-/-}CD19-Cre^{+/-} mice no κ ⁺ and λ ⁺ cells could be detected in all investigated organs and PerC but all CD19⁺ cells were DN (Fig. 3.36A-D middle staining). This was most impressive in spleen and PerC, whereas in pLN and mLN few DN cells could be detected, even when the number of cells next to the gates seemed to be high (Fig. 3.36A-D upper staining).

Next we gated on the DN cell population of the κ vs. λ staining and following on IgM and IgD (Fig. 3.36A-D lower staining). Obviously the CD19⁺ DN cells found in Akt^{+/-}JHT^{-/-}CD19-Cre^{+/-} mice were the same DN cell population detected in the IgM vs. IgD staining. This was true for all organs and PerC, whereas this population was also most impressive in spleen and PerC (Fig. 3.36A-D lower staining). It seems that through the constitutive Akt1 overexpression in Akt^{+/-}JHT^{-/-}CD19-Cre^{+/-} mice B cells do not undergo BCR selection and leave the BM without a functional BCR. So the Akt1 overexpression leads to the generation of CD19⁺ B cells that can leave the BM even without a functional BCR.

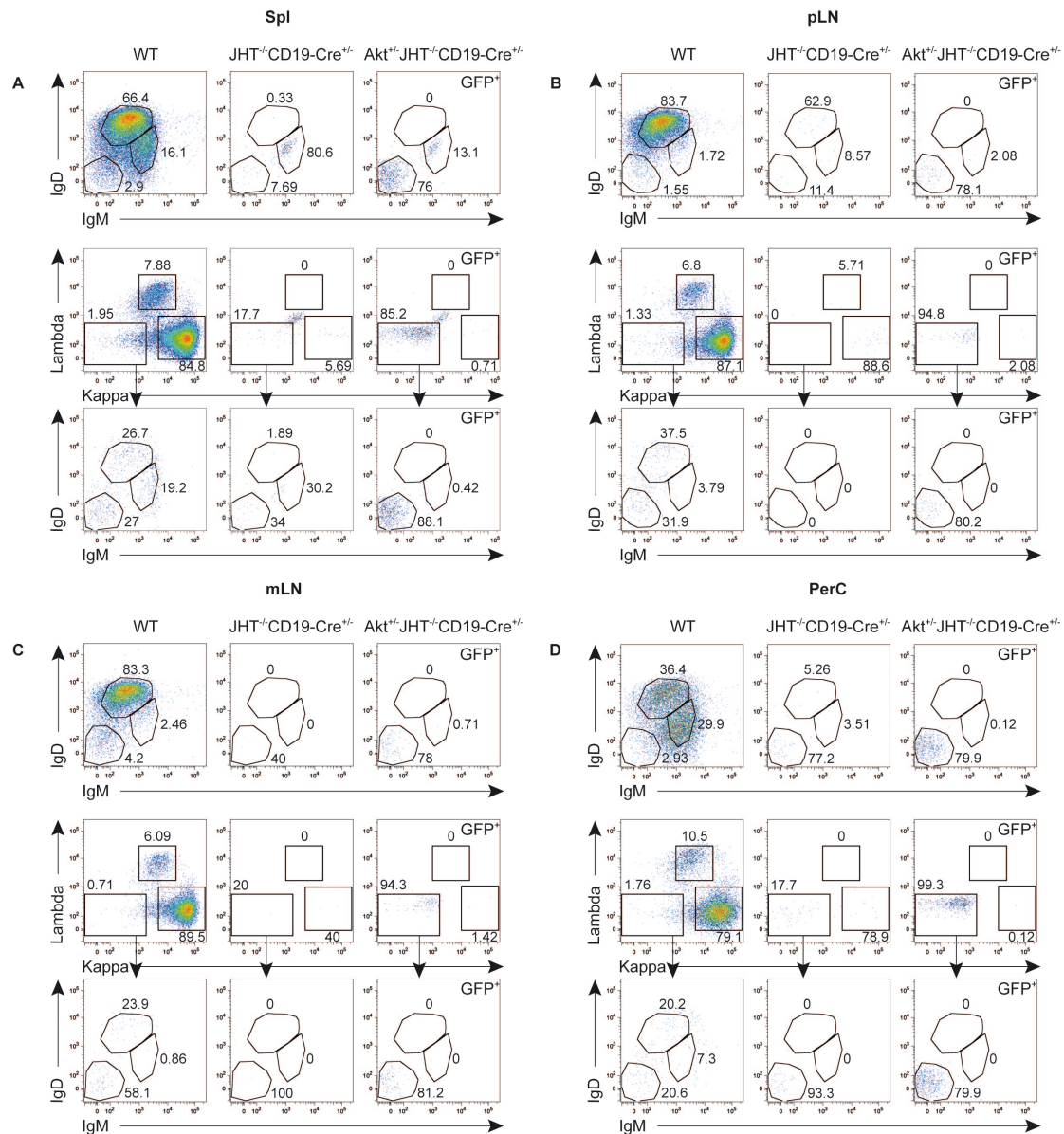


Figure 3.36: Investigation of CD19 positive and double negative B cells in different organs and PerC of $Akt^{+/-}JHT^{-/-}CD19-Cre^{+/-}$ mice.

FACS analysis of 7.5 week-old $Akt^{+/-}JHT^{-/-}CD19-Cre^{+/-}$, WT and $JHT^{-/-}CD19-Cre^{+/-}$ control mice in (A) spleen (B) pLN, (C) mLN and (D) PerC Antibodies used are indicated. The numbers next to the gates refer to the percentage of CD19⁺ live cells. $Akt^{+/-}JHT^{-/-}CD19-Cre^{+/-}$ mice were additionally gated on GFP⁺ cells to exclude escapees. The experiment was performed 3 times with mice of different ages: firstly, 7.5 weeks (2 WT, 2 $JHT^{-/-}CD19-Cre^{+/-}$ and 4 $Akt^{+/-}JHT^{-/-}CD19-Cre^{+/-}$ mice), secondly, 9.5 weeks (2 WT, 2 $JHT^{-/-}CD19-Cre^{+/-}$ and 4 $Akt^{+/-}JHT^{-/-}CD19-Cre^{+/-}$ mice) and thirdly, 12 weeks (2 WT, 2 $JHT^{-/-}CD19-Cre^{+/-}$ and 4 $Akt^{+/-}JHT^{-/-}CD19-Cre^{+/-}$ mice).

3.18 Overexpression of Akt1 in a Later Phase of B Cell Development

The CD19-Cre mouse used for the previous experiments leads to recombination already at the pro-B cell or early pre-B cell stages in the B cell development of the BM (Rickert et al., 1997; Engel et al., 1995). To investigate, if the observed influence of a constitutively active overexpression of Akt1 in Akt^{BOE} mice is due to very early Akt1 overexpression already in the BM, Akt1 overexpression in a later phase of B cell development had to be investigated. Therefore the *Aicda*-Cre mouse was crossed to the Rosa-Akt-C mouse (Akt^{+/-}AID-Cre^{+/-}) (Qin et al., 2011; Kwon et al., 2008). In B cells the *Aicda*-Cre deletes in GC B cells (Kwon et al., 2008; Muramatsu et al., 2000). It is known that *Aicda* expression is not unique for B cells; it is also expressed in CD4⁺ T cells and in different organs such as mouse ovary and human testis (Morgan et al., 2004; Qin et al., 2011; Schreck et al., 2006). To be able to detect in which cells beside B cells *Aicda* is expressed *Aicda*-Cre mice were crossed to EYFP mice (EYFP^{+/-}AID-Cre^{+/-}). EYFP mice express the reporter yellow fluorescent protein (YFP) and then *Aicda* expression is visible.

The first impressive observation was that Akt^{+/-}AID-Cre^{+/-} mice died very early. Females die already at the age of 6.5-12.5 weeks while males die between 8-24 weeks of age (Fig 3.37). In Akt^{+/-}AID-Cre^{+/-} mice a weight loss of about 1 gram was observed \approx one week before they died. The weight loss correlated with the sickness of the Akt^{+/-}AID-Cre^{+/-} mice.

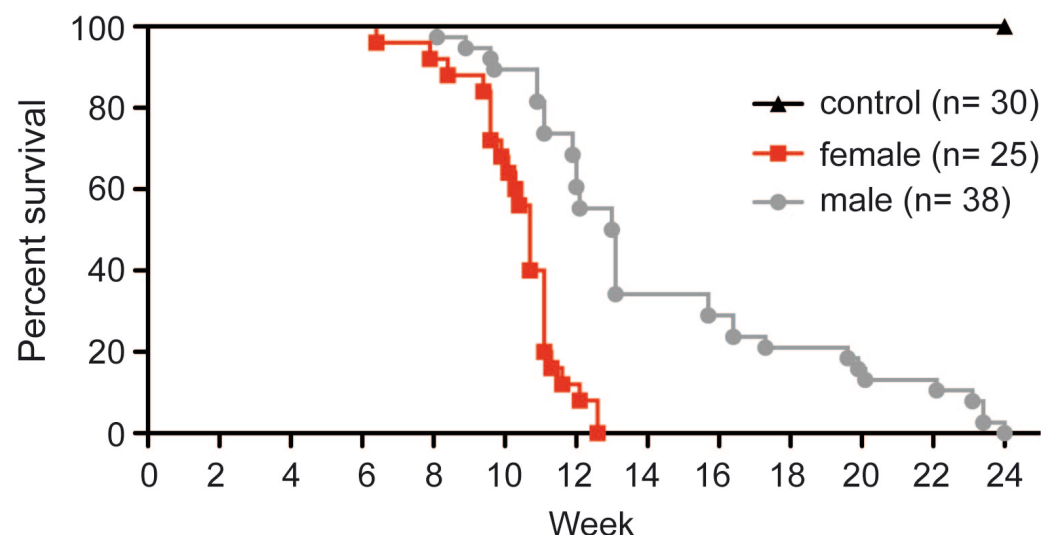


Figure 3.37: Survival of Akt^{+/-}AID-Cre^{+/-} mice in comparison to EYFP^{+/-}AID-Cre^{+/-} controls.

Shown is the percentage per week of survival of female (red) and male Akt^{+/-}AID-Cre^{+/-} mice (grey) in comparison to EYFP^{+/-}AID-Cre^{+/-} controls (black) in week.

The second very interesting observation was that $Akt^{+/-}AID-Cre^{+/-}$ mice showed large pLN that were partly encapsulated, and in females extreme enlarged ovaries could be detected (Fig. 3.38 A-C, G, H). Spleen sizes of $Akt^{+/-}AID-Cre^{+/-}$ mice and $EYFP^{+/-}AID-Cre^{+/-}$ controls were comparable (data not shown). In one $Akt^{+/-}AID-Cre^{+/-}$ male a large thymus was seen and in 10 females and 2 males just relicts of thymi could be observed (Fig. 3.38 E, F). Another exciting observation was that most of the males develop long grey hair with age. The male in the picture was 20 weeks old (Fig. 3.38 D).

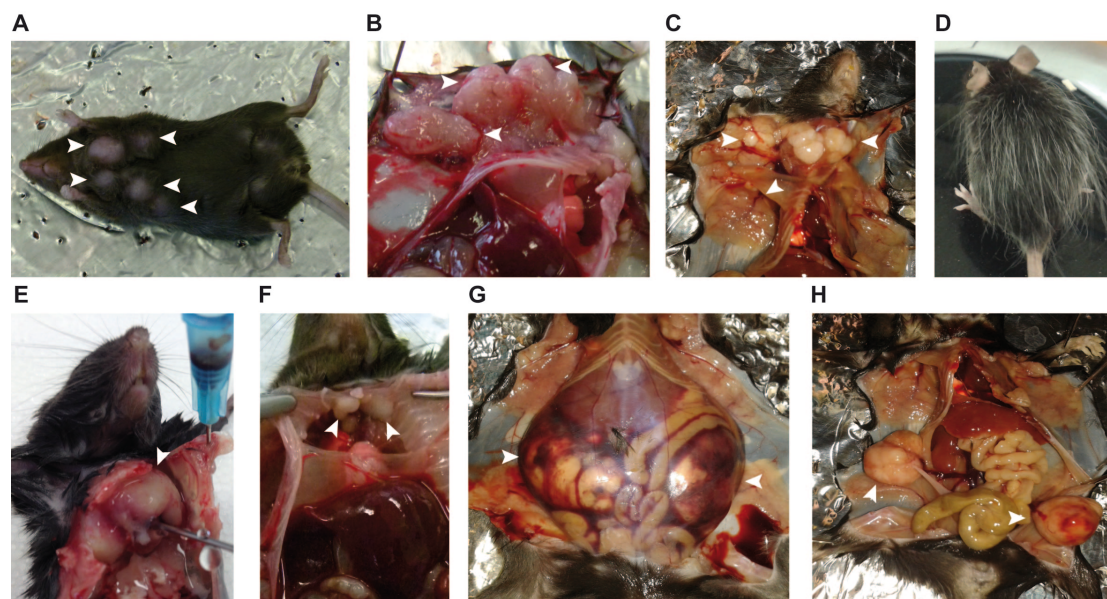


Figure 3.38: Abnormal observations in $Akt^{+/-}AID-Cre^{+/-}$ mice.

(A) Shown is a female $Akt^{+/-}AID-Cre^{+/-}$ mouse with swollen abdomen (see white darts). (B) The white darts indicate the altered pLN of the $Akt^{+/-}AID-Cre^{+/-}$ mouse in (A). (C) Shown are the large and encapsulated pLN of $Akt^{+/-}AID-Cre^{+/-}$ mouse marked with white arrows. (D) $Akt^{+/-}AID-Cre^{+/-}$ male that has long, grey hair. The mouse displayed is 20 weeks old. (E) Enlarged thymus in $Akt^{+/-}AID-Cre^{+/-}$ mouse (see white dart). (F) Relicts of thymus marked with white darts. (G) Top view abdomen. Darts mark enlarged ovaries in $Akt^{+/-}AID-Cre^{+/-}$ mouse. (H) Shown are the enlarged ovaries of $Akt^{+/-}AID-Cre^{+/-}$ mouse, marked with white darts.

After all these interesting observations, FACS analysis was performed to investigate the influence of constitutive Akt1 expression in later phases of B cells. The investigation of B and T cell distribution in spleen revealed YFP^{+}/GFP^{+} cells not only in B cells. Interestingly, YFP^{+}/GFP^{+} cells could also be seen in T cells in $EYFP^{+/-}AID-Cre^{+/-}$ controls and in $Akt^{+/-}AID-Cre^{+/-}$ mice (Fig. 3.39A, B, C). DN cells also expressed YFP^{+}/GFP^{+} cells (Fig. 3.39D). Therefore *Aicda* expression is not restricted

to B cells, and thus Akt1 is overexpressed also in a minor population of T cells of $Akt^{+/-}AID-Cre^{+/-}$ mice.

In conclusion, in splenic B, T and DN cells *Aicda* is expressed and therefore, also Akt1 is constitutively active in these cells, which implicates a role for *Aicda* in cell types other than B cells.

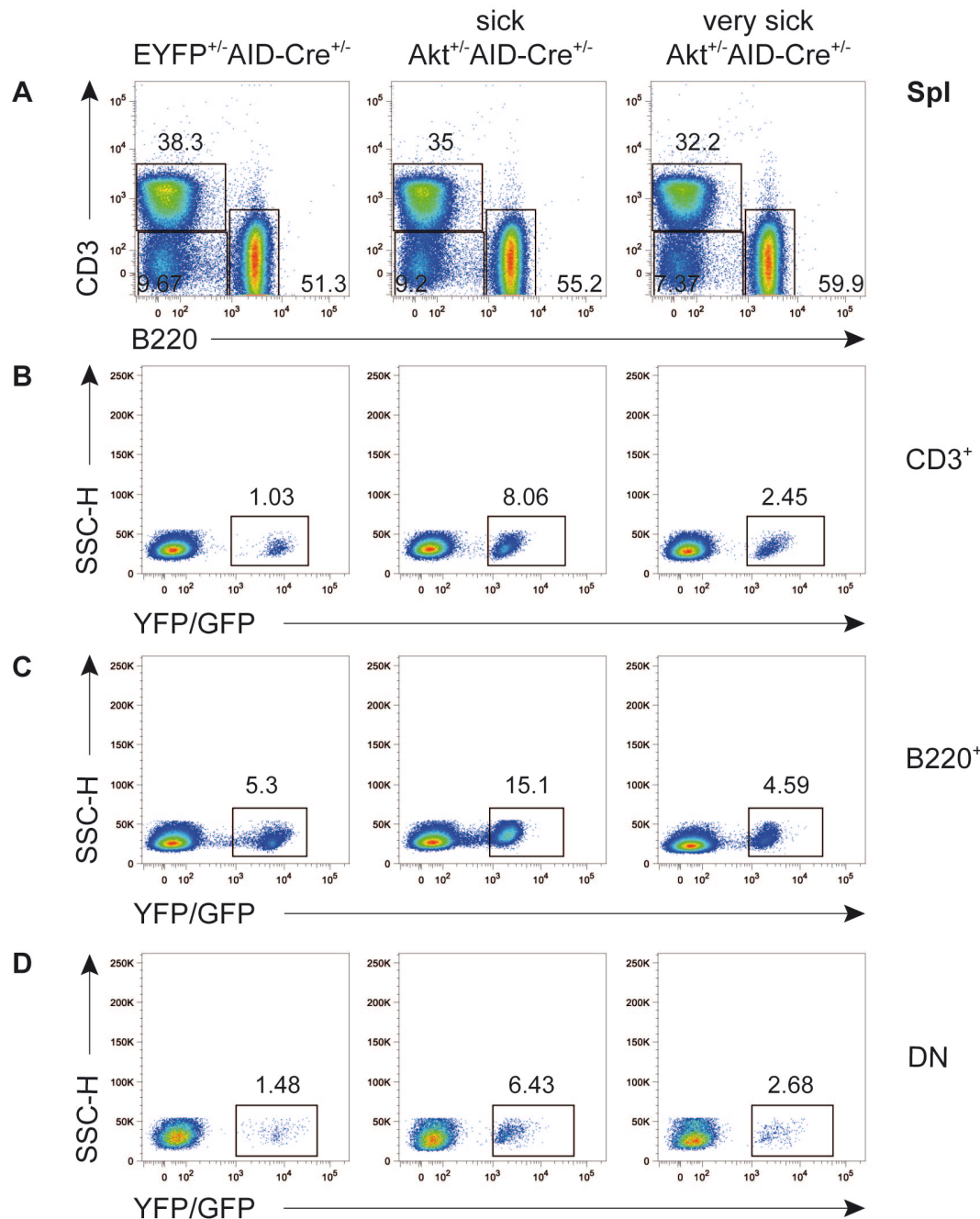


Figure 3.39: Distribution of splenic B and T cells in $Akt^{+/-}AID-Cre^{+/-}$ and $EYFP^{+/-}AID-Cre^{+/-}$ control mice.

(A-D) FACS analysis of $Akt^{+/-}AID-Cre^{+/-}$ and $EYFP^{+/-}AID-Cre^{+/-}$ mice. Antibodies were used as indicated. The numbers close to the boxes of lymphocyte populations refer to the percentage of live

cells in the gates. Experiment was repeated 3 times with $n = 3$ mice per genotype. DN stands for double negative.

Since we detected YFP⁺ cells (*Aicda* expressing cells) also in T cells, different T cell subsets were analyzed. By FACS analysis we could show a similar distribution between splenic CD4⁺ and CD8⁺ T cell populations between the genotypes and both populations showed YFP⁺/GFP⁺ cells. In Akt^{+/-}AID-Cre^{+/-} mice, GFP⁺ cells showed increased percentages in comparison to YFP⁺ cells in controls due to the Akt1 overexpression in Akt^{+/-}AID-Cre^{+/-} mice (Fig. 3.40A).

To show which T cell population express GFP/YFP on the surface and therefore constitutively express Akt1, CD4⁺ and CD8⁺ T cell subsets were investigated. The investigation of CD8⁺ naive, memory effector and effector T cells revealed that YFP⁺/GFP⁺, CD8⁺ T cells are effector T cells (Fig. 3.40B). The same was true for CD4⁺ T cell subpopulations, but here the population of YFP⁺/GFP⁺ memory effector T cells was larger than in the CD8⁺ T effector cell populations (Fig. 3.40C).

Collectively, GFP/YFP expression was observed in CD8⁺ effector T cells and CD4⁺ memory effector T cells and therefore, constitutive Akt1 expression in T cells of Akt^{+/-}AID-Cre^{+/-} mice seemed to be restricted to these T cell populations.

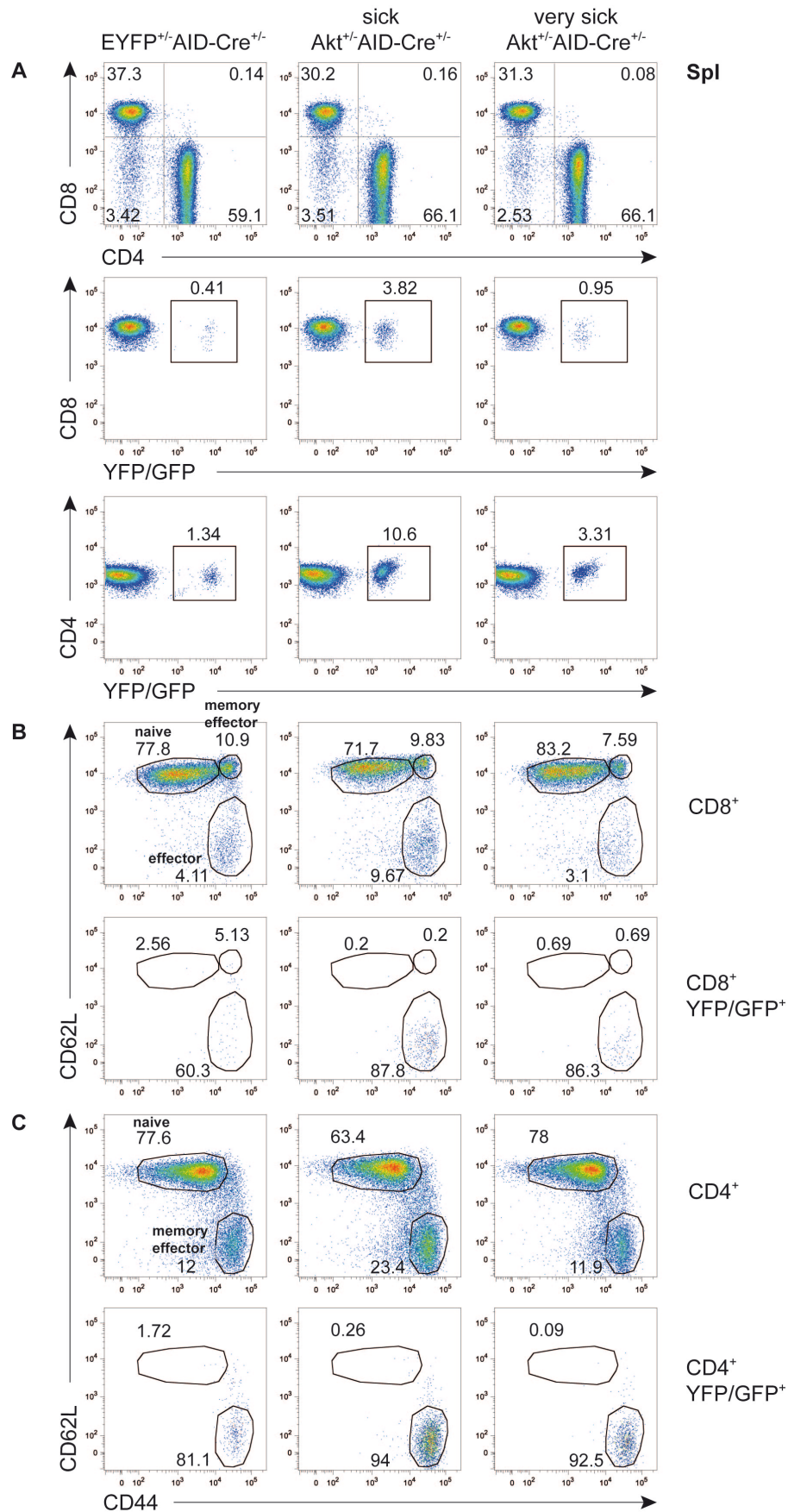


Figure 3.40: Distribution of splenic T cell subsets in *Akt*^{+/-} AID-Cre^{+/-} and *EYFP*^{+/-} AID-Cre^{+/-} control mice.

(A) FACS analysis of CD8⁺ and CD4⁺ T cells in spleen. Genotypes were used as indicated. The numbers close to the boxes of lymphocyte populations refer to the percentage of CD3⁺ live cells in the gates. Experiment was repeated 3 times with n = 3 mice per genotype. **(B)** Displays CD8⁺ naive (CD62L⁺, CD44⁻), memory effector (CD62L⁺, CD44⁺) and effector T cells (CD62L⁻, CD44⁺). The numbers close to the boxes of lymphocyte populations refer to the percentage of CD3⁺ live cells in the gates. **(C)** Displays CD4⁺ naive (CD62L⁺, CD44⁻) and memory effector T cells (CD62L⁻, CD44⁺). The numbers close to the boxes of lymphocyte populations refer to the percentage of CD3⁺ live cells in the gates.

In pLN more B cells and less T cells could be observed in Akt^{+/-}AID-Cre^{+/-} mice in comparison to the EYFP^{+/-}AID-Cre^{+/-} control mice (Fig. 3.41A-C). Similarly to spleen, in pLN B as well as T cells were positive for YFP/GFP and also DN (CD3⁻, B220⁻) cells were YFP⁺/GFP⁺ (Fig. 3.41B-D).

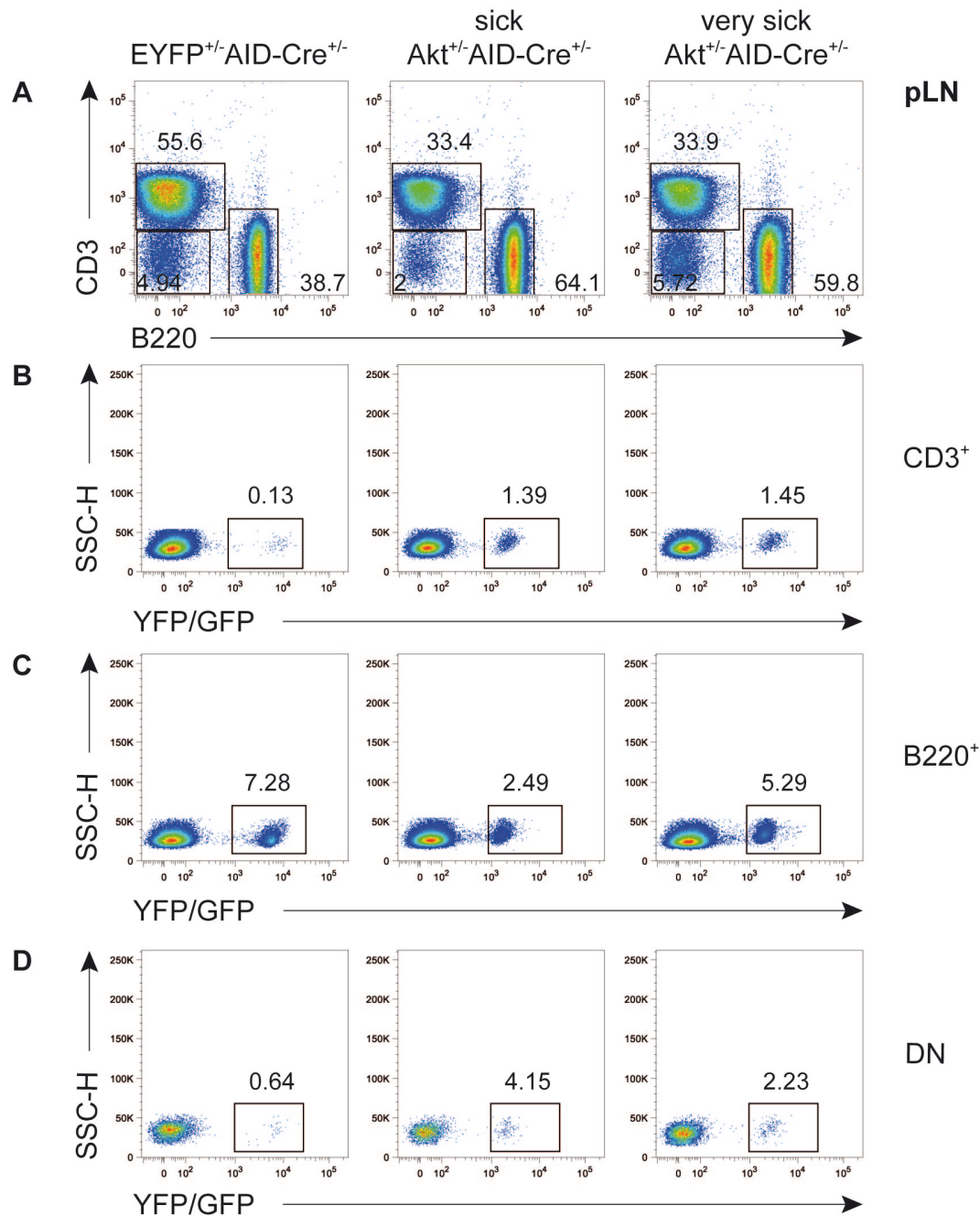


Figure 3.41: Distribution of B and T cells in Akt^{+/-} AID-Cre^{+/-} and EYFP^{+/-} AID-Cre^{+/-} control mice in pLN.

(A-D) FACS analysis of Akt^{+/-} AID-Cre^{+/-} and EYFP^{+/-} AID-Cre^{+/-} in pLN. Antibodies are used as indicated. The numbers close to the boxes of lymphocyte populations refer to the percentage of live cells in the gates. Experiment was repeated 3 times with n = 3 mice per genotype. DN stands for double negative.

We also investigated the different T cells subsets in pLN. In general, CD4⁺ and CD8⁺ T cells showed a population of YFP⁺/GFP⁺ cells (Fig. 3.42A). The analysis of CD8⁺ naive, memory effector, and effector T cells revealed mainly YFP⁺/GFP⁺ effector T

cells (Fig. 3.42B). Also in CD4⁺ T cell subsets of memory effector T cells were the affected cells that expressed YFP and GFP (Fig. 3.42C).

In summary, CD4⁺ T cells of Akt^{+/-}AID-Cre^{+/-} mice showed in general more GFP expression than CD8⁺ T cells and therefore higher numbers of CD4⁺ T cells of Akt^{+/-}AID-Cre^{+/-} express Akt1 constitutively. In general, CD4⁺ memory effector and CD8⁺ effector T cells are the subpopulation of T cells that express *Aicda* and therefore overexpress Akt1.

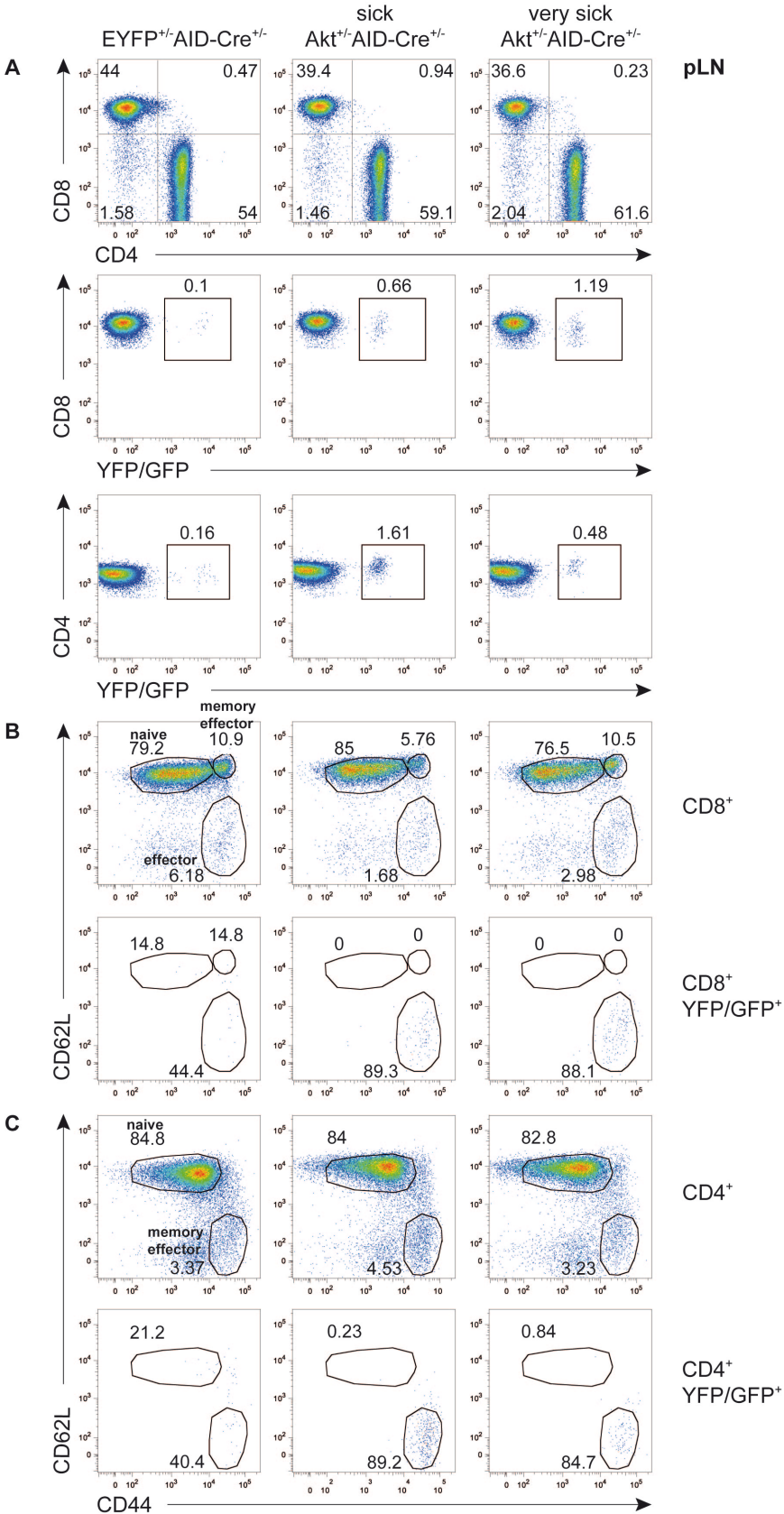


Figure 3.42: Distribution of T cell subsets in Akt^{+/-}AID-Cre^{+/-} and EYFP^{+/-}AID-Cre^{+/-} control mice in pLN.

(A) FACS analysis of CD8⁺ and CD4⁺ T cells in pLN. Genotypes are used as indicated. The numbers close to the boxes of lymphocyte populations refer to the percentage of CD3⁺ live cells in the gates. Experiment was repeated 3 times with n = 3 mice per genotype. (B) Displays CD8⁺ naive (CD62L⁺, CD44⁻), memory effector (CD62L⁺, CD44⁺) and effector T cells (CD62L⁻, CD44⁺). The numbers close to the boxes of lymphocyte populations refer to the percentage of CD3⁺ live cells in the gates. (C) Displays CD4⁺ naive (CD62L⁺, CD44⁻) and memory effector T cells (CD62L⁻, CD44⁺). The numbers close to the boxes of lymphocyte populations refer to the percentage of CD3⁺ live cells in the gates.

In mLN it was the same as in spleen and pLN: YFP⁺ and GFP⁺ cells could be detected in B, T and DN cells (Fig. 3.43B-D). Further analysis of CD8⁺ and CD4⁺ T cells showed that CD4⁺ T cell had more YFP⁺/GFP⁺ cells than CD8⁺ T cells (Fig. 3.44A). The investigation of CD4⁺ and CD8⁺ T cells subsets again showed YFP⁺/GFP⁺ CD4⁺ memory effector T cells and CD8⁺ effector T cells, whereas CD4⁺ memory effector T cells of Akt^{+/-}AID-Cre^{+/-} mice display a real dominant subset (Fig. 3.44B, C).

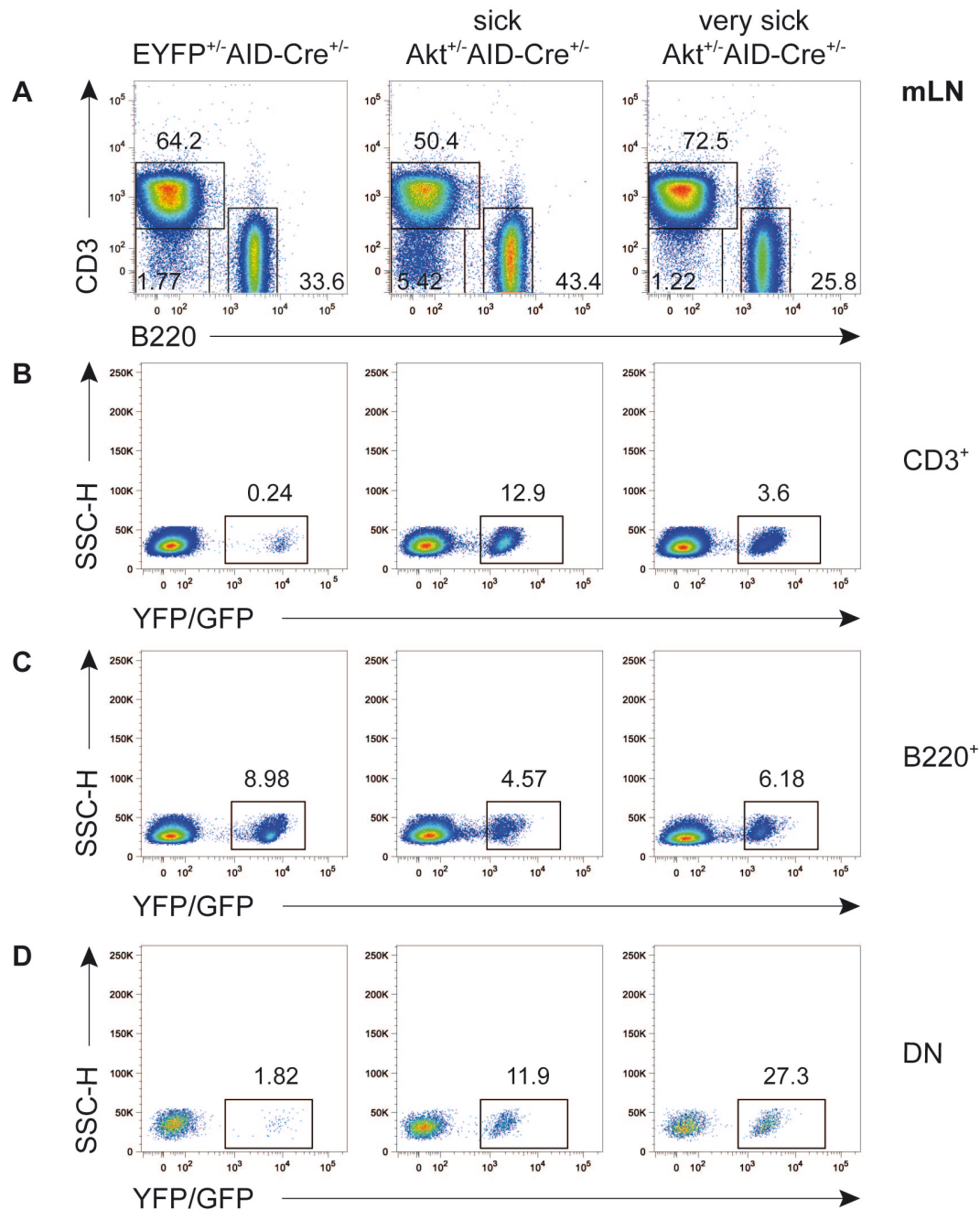


Figure 3.43: Distribution of B and T cells in Akt^{+/-}AID-Cre^{+/-} and EYFP^{+/-}AID-Cre^{+/-} control mice in mLN.

(A-D) FACS analysis of mLN of B and T cells in Akt^{+/-}AID-Cre^{+/-} and EYFP^{+/-}AID-Cre^{+/-} mice. Antibodies are used as indicated. The numbers close to the boxes of lymphocyte populations refer to the percentage of live cells in the gates. Experiment was repeated 3 times with n = 3 mice per genotype. DN stands for double negative.

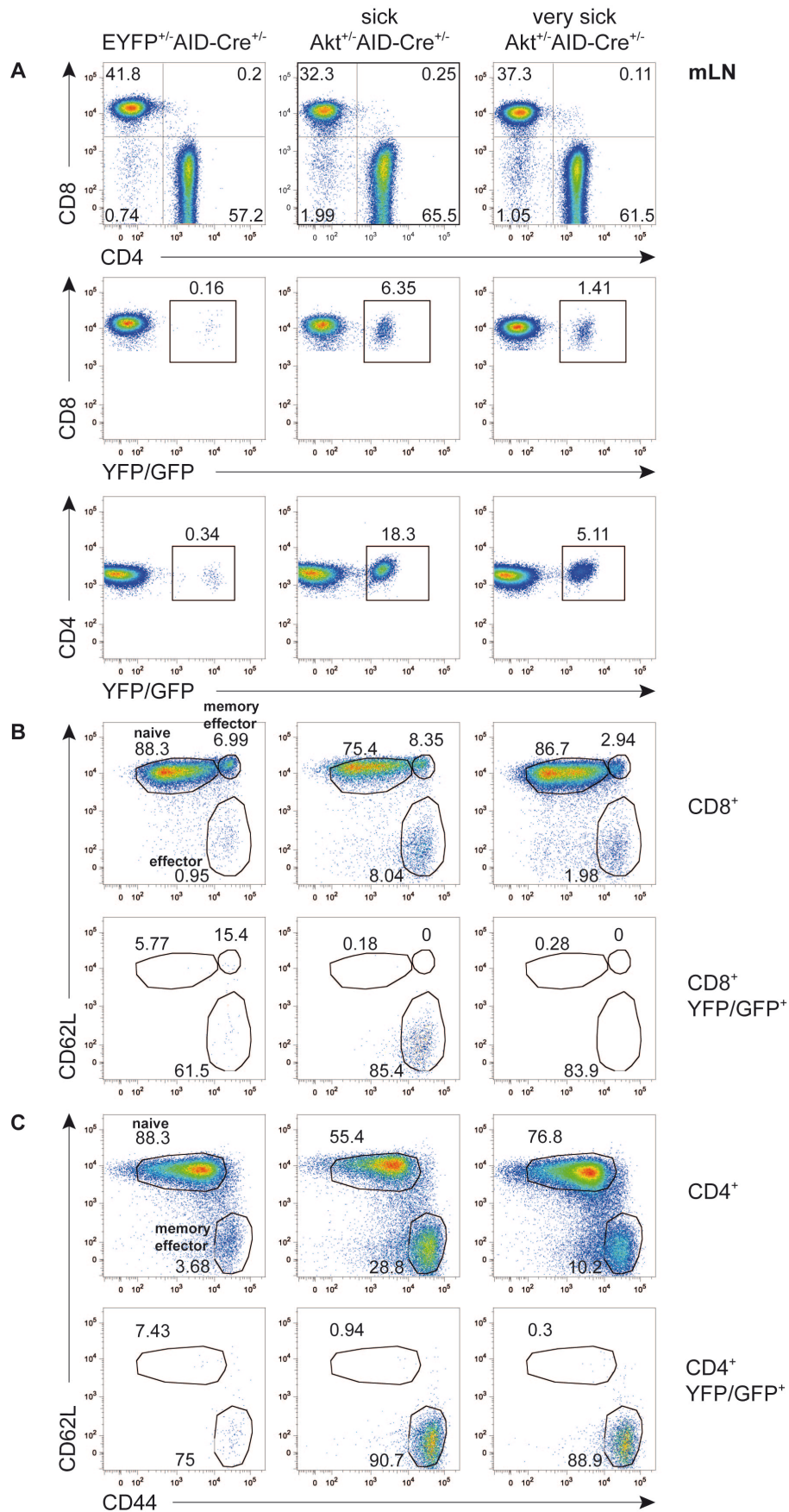


Figure 3.44: Distribution of T cell subsets in *Akt*^{+/-} AID-Cre^{+/-} and *EYFP*^{+/-} AID-Cre^{+/-} control mice in mLN.

(A) FACS analysis of CD8⁺ and CD4⁺ T cells in mLN. Genotypes are used as indicated. The numbers close to the boxes of lymphocyte populations refer to the percentage of CD3⁺ live cells in the gates. Experiment was repeated 3 times with n = 3 mice per genotype. **(B)** Displays CD8⁺ naive (CD62L⁺, CD44⁻), memory effector (CD62L⁺, CD44⁺) and effector T cells (CD62L⁻, CD44⁺). The numbers close to the boxes of lymphocyte populations refer to the percentage of live cells in the gates. **(C)** Displays CD4⁺ naive (CD62L⁺, CD44⁻) and memory effector T cells (CD62L⁻, CD44⁺). The numbers close to the boxes of lymphocyte populations refer to the percentage of CD3⁺ live cells in the gates.

As already observed in spleen, pLN and mLN, also in PP T cells as well as B cells and DN cells showed YFP⁺/GFP⁺ cells (Fig. 3.45A-D).

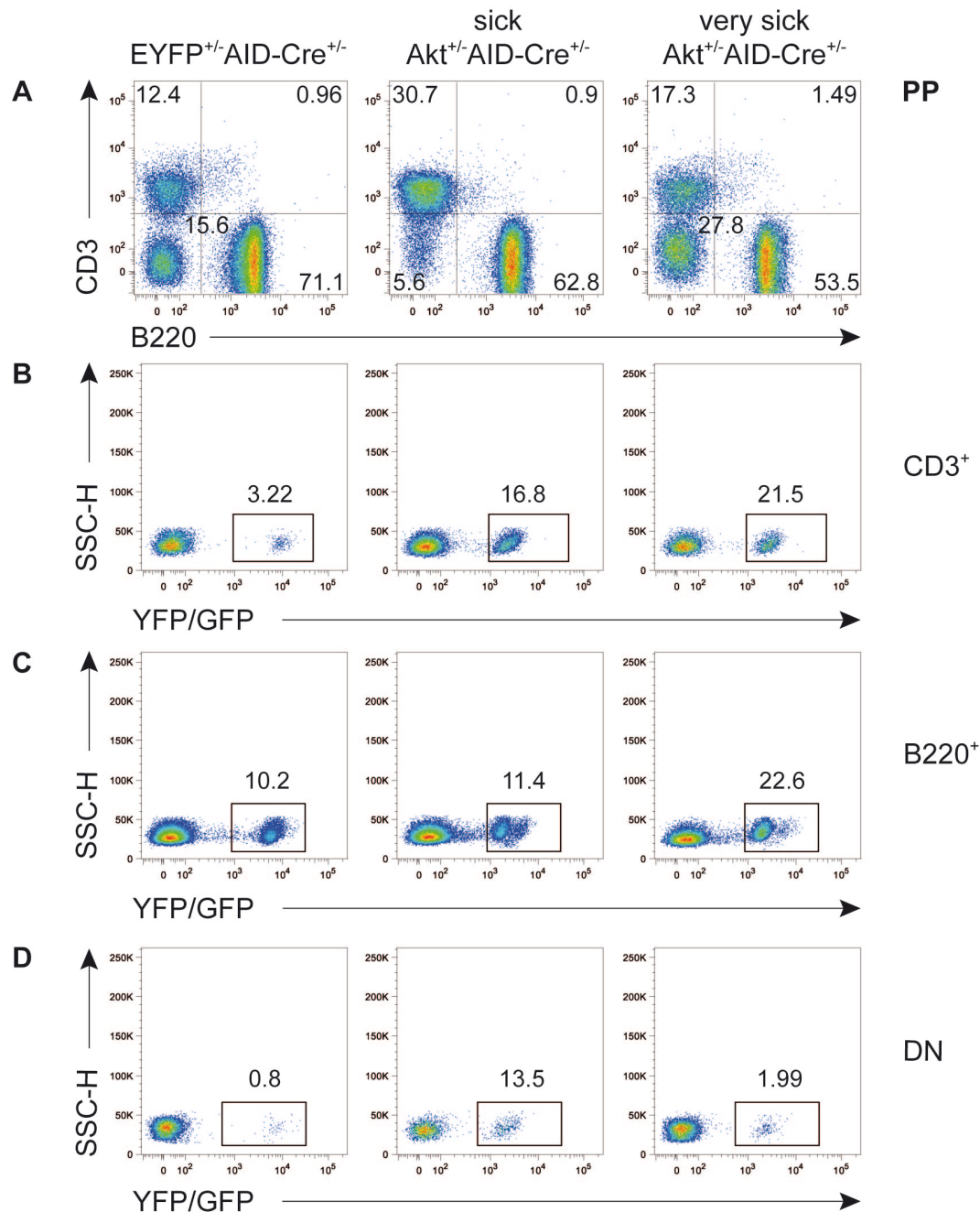


Figure 3.45: Distribution of B and T cells in Akt^{+/-}AID-Cre^{+/-} and EYFP^{+/-}AID-Cre^{+/-} control mice in PP.

(A-D) FACS analysis of PP of B and T cells in Akt^{+/-}AID-Cre^{+/-} and EYFP^{+/-}AID-Cre^{+/-} mice. Antibodies are used as indicated. The numbers close to the boxes of lymphocyte populations refer to the percentage of live cells in the gates. Experiment was repeated 3 times with n = 3 mice per genotype, 5 PP each mouse. DN stands for double negative.

In conclusion, in all investigated organs, B and T cells as well as DN cells showed YFP expression and therefore constitutively active Akt1 expression in B, T and DN cells of Akt^{+/-}AID-Cre^{+/-} mice. Nevertheless, T cell subset analysis showed YFP

expression and resulting constitutive Akt1 expression in both CD8⁺ effector T cells and CD4⁺ memory effector T cells, although expression was stronger in CD4⁺ memory effector T cells.

Due to the observed expression of YFP in T cells and that some mice showed an enlarged thymus and some showed only small relicts of the thymus, it was also relevant to investigate the thymus of Akt^{+/-}AID-Cre^{+/-} mice. Interestingly, with sickness progression of Akt^{+/-}AID-Cre^{+/-} mice, more B cells migrated into the thymus. Whereas in controls nearly no B cells (0.7%) were detected, in mildly sick Akt^{+/-}AID-Cre^{+/-} mice were 2.5% and in very sick Akt^{+/-}AID-Cre^{+/-} mice enormous 52% B cells were detectable (Fig. 3.46A). A proportion of these B cells show GFP expression (Fig. 3.46C). Also very few T cells of Akt^{+/-}AID-Cre^{+/-} mice showed GFP (Fig. 3.46B). With the increasing number of B cells that migrate into the thymus, the DN population decreased (Fig. 3.46A). The DN cells in Akt^{+/-}AID-Cre^{+/-} mice also contained GFP⁺ cells (Fig. 3.46D).

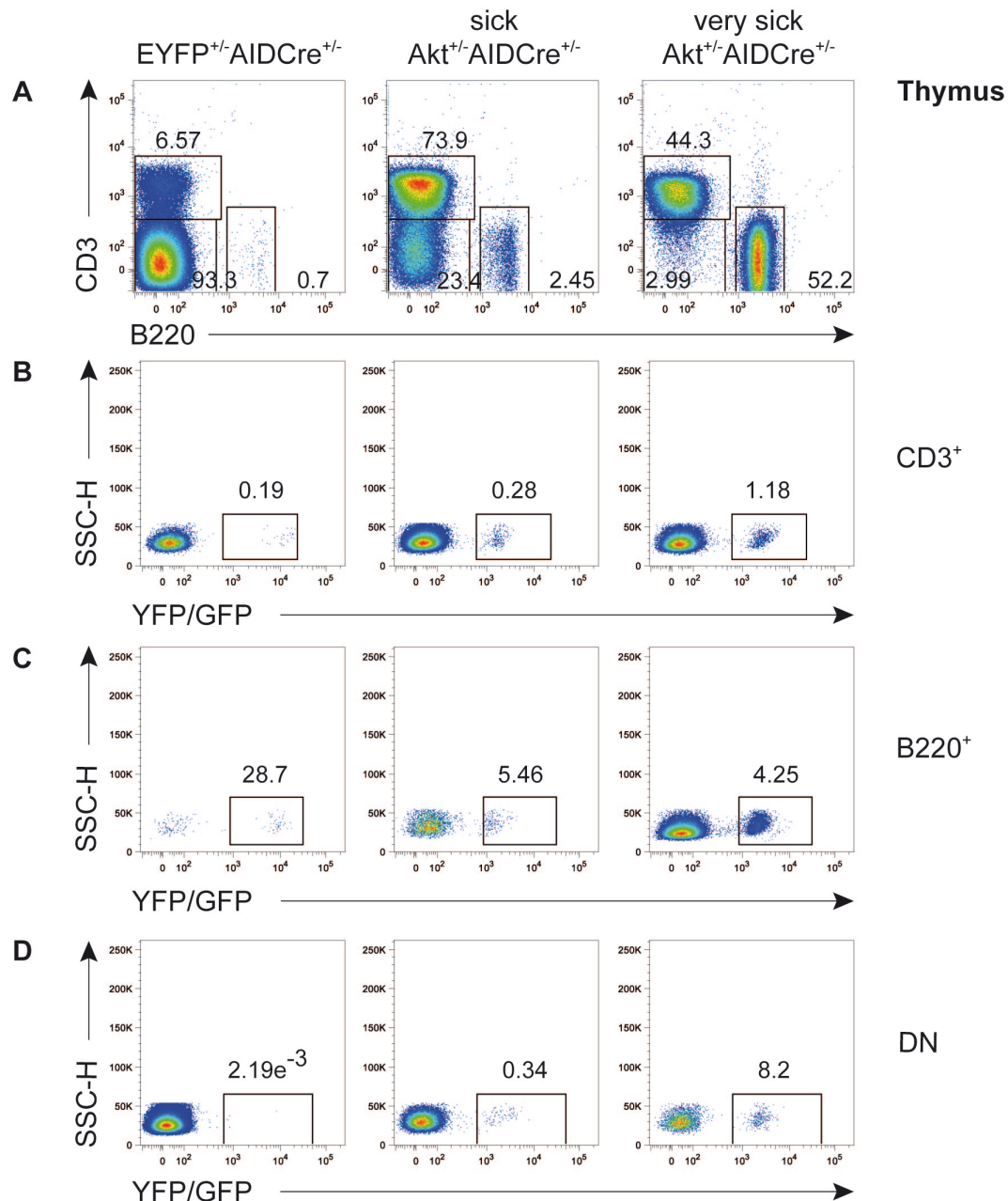


Figure 3.46: Distribution of B and T cells in thymus of Akt^{+/-}AID-Cre^{+/-} and EYFP^{+/-}AID-Cre^{+/-} control mice.

(A-D) FACS analysis of thymic B and T cells in Akt^{+/-}AID-Cre^{+/-} and EYFP^{+/-}AID-Cre^{+/-} mice. Antibodies are used as indicated. The numbers close to the boxes of lymphocyte populations refer to the percentage of live cells in the gates. Experiment was repeated 3 times with n = 3 mice per genotype. DN stands for double negative. Plots are gated on live cells.

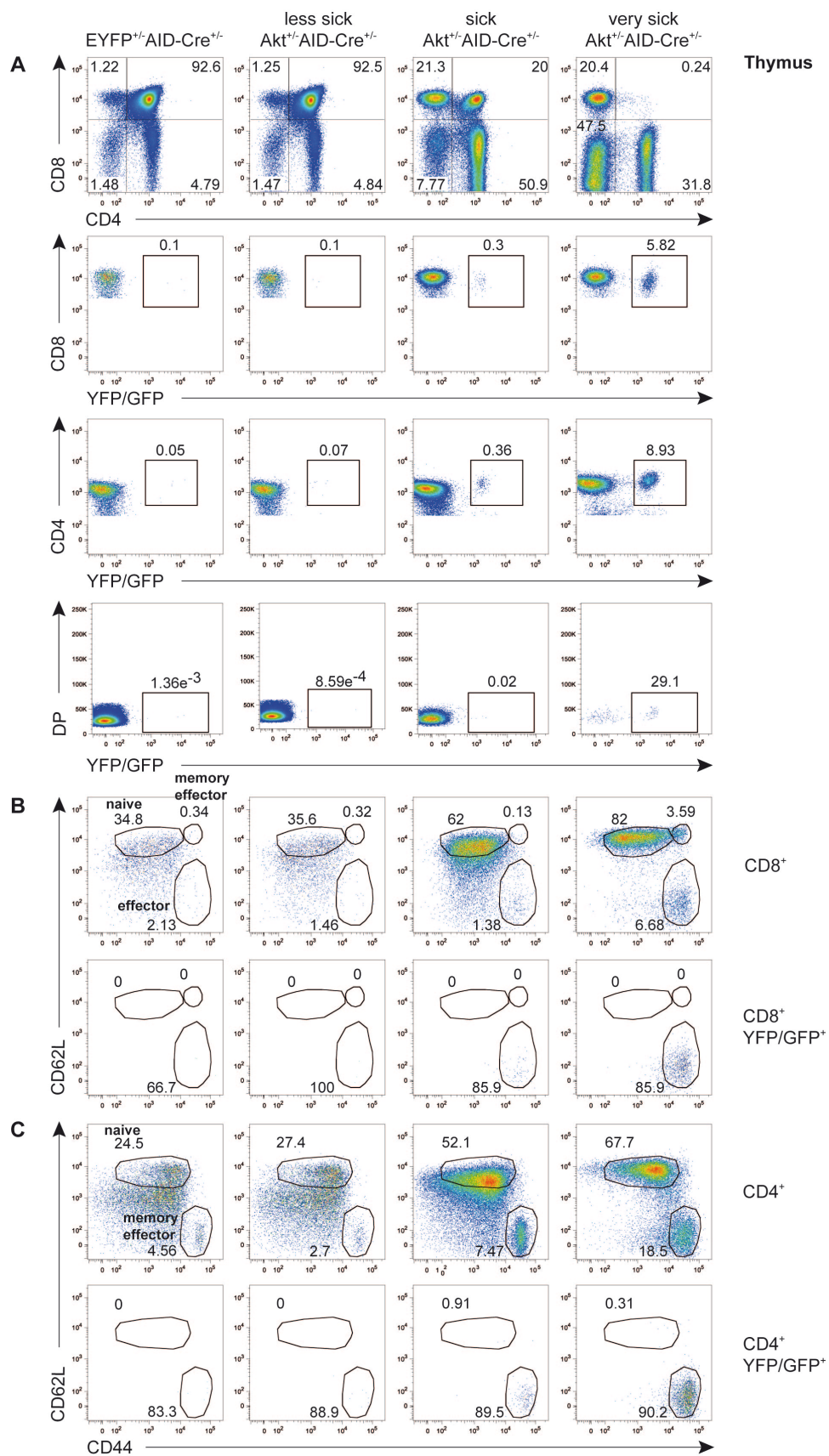


Figure 3.47: Distribution of thymic T cell subsets in Akt^{+/+}AID-Cre^{+/+} mice and YFP^{+/+}AID-Cre^{+/+} control mice.

(A) FACS analysis of CD8⁺ and CD4⁺ T cells in thymus. Genotypes were used as indicated. The numbers close to the boxes of lymphocyte populations refer to the percentage of live cells in the gates. Experiment was repeated 3 times with $n = 3$ mice per genotype. DP stands for double positive. **(B)** Displays CD8⁺ naive (CD62L⁺, CD44⁻), memory effector (CD62L⁺, CD44⁺) and effector T cells (CD62L⁻, CD44⁺). The numbers close to the boxes of lymphocyte populations refer to the percentage of CD3⁺ live cells in the gates. **(C)** Displays CD4⁺ naive (CD62L⁺, CD44⁻) and memory effector T cells (CD62L⁻, CD44⁺). The numbers close to the boxes of lymphocyte populations refer to the percentage of CD3⁺ live cells in the gates.

Analysis of CD8⁺ and CD4⁺ T cells in thymus showed a normal T cell development in EYFP^{+/-}AID-Cre^{+/-} controls and less sick Akt^{+/-}AID-Cre^{+/-} mice (Fig. 3.47A). In general, sick Akt^{+/-}AID-Cre^{+/-} mice showed a strongly decreased double positive (DP) T cell population and increased CD4⁺, CD8⁺ T cells and DN cells (Fig. 3.47A). In contrast, in very sick Akt^{+/-}AID-Cre^{+/-} mice CD4⁺, CD8⁺ DP T cells are not detectable anymore and DN cells as well as CD4⁺ and CD8⁺ T cells were increased in comparison to controls (Fig. 3.47A). GFP expression in CD8⁺ and CD4⁺ T cells and therefore Akt1 overexpression was only detectable in sick and very sick mice, whereas EYFP^{+/-}AID-Cre^{+/-} controls and less sick Akt^{+/-}AID-Cre^{+/-} showed no YFP⁺/GFP⁺ CD8⁺ and CD4⁺ T cells (Fig. 3.47A). This was also true for CD4⁺ memory effector and CD8⁺ effector T cells (Fig. 3.47B, C). It is amazing, that due to the Akt1 overexpression mice get really sick and in this very sick mice the thymus look as a secondary lymphoid organ.

After the investigation of T cell subsets, B cell subsets in spleen were also studied. The splenic distribution of IgM⁺ and IgD⁺ B cells showed only IgM⁺ GFP⁺ B cells in Akt^{+/-}AID-Cre^{+/-} mice, whereas EYFP^{+/-}AID-Cre^{+/-} mice displayed also IgD⁺ YFP⁺ B cells (Fig. 3.48). So in Akt^{+/-}AID-Cre^{+/-} mice the Akt1 overexpression led to the same phenotype as already observed in Akt^{BOE} mice (Fig. 3.48; Fig. 3.11).

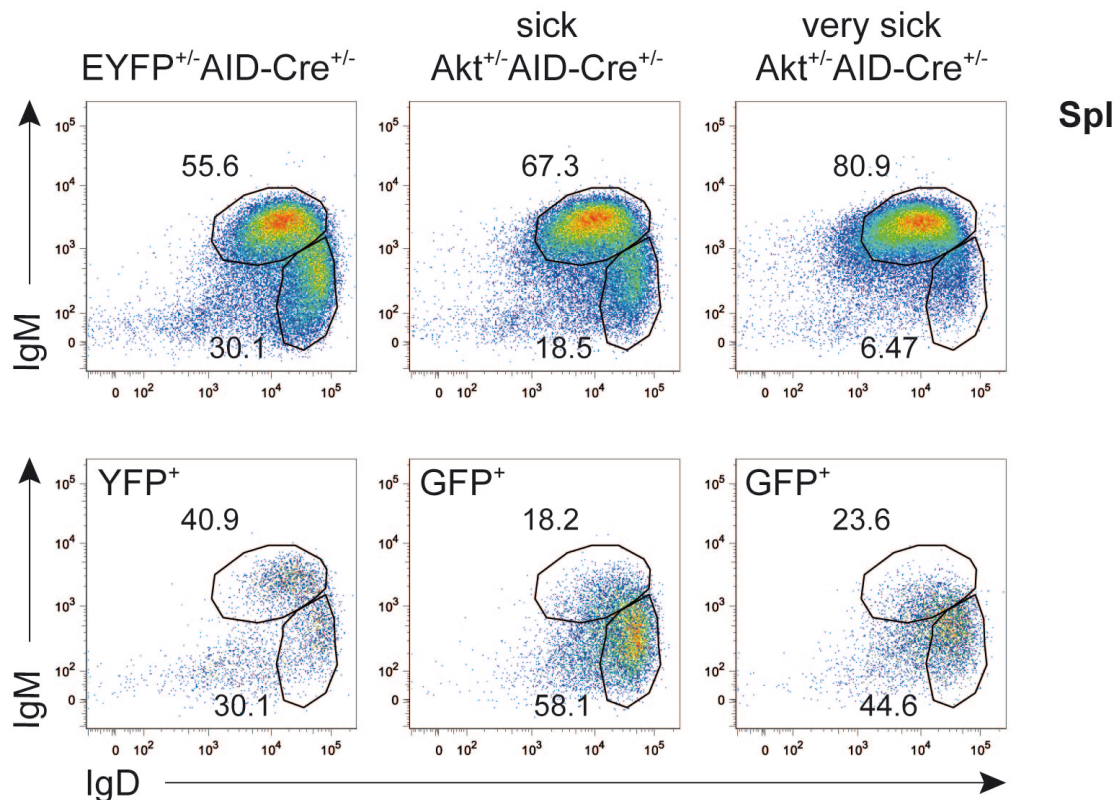


Figure 3.48: FACS analysis of splenic IgM and IgD positive B cells in Akt^{+/-}AID-Cre^{+/-} mice and EYFP^{+/+}AID-Cre^{+/+} control mice.

FACS analysis of Akt^{+/-}AID-Cre^{+/-} and EYFP^{+/+}AID-Cre^{+/+} mice. Antibodies were used as indicated. The numbers close to the boxes of lymphocyte populations refer to the percentage of CD19⁺ live cells in the gates. Experiment was repeated 3 times with n = 3 mice per genotype.

Also analysis of splenic immature and mature B cells in Akt^{+/-}AID-Cre^{+/-} mice showed, as in Akt^{BOE} mice, decreased immature B cell populations in comparison to controls (Fig. 3.49A; Fig. 3.16A, B). The same was true for splenic T2 and T3 B cells of Akt^{+/-}AID-Cre^{+/-} mice in comparison to EYFP^{+/+}AID-Cre^{+/+} control mice. In Akt^{+/-}AID-Cre^{+/-} mice T1 B cells strongly increased in comparison to EYFP^{+/+}AID-Cre^{+/+} controls and T2 and T3 populations are highly reduced (Fig. 3.49B). This was already shown for Akt^{BOE} mice and leads to the assumption that the influence of constitutive Akt1 expression in B cells is not dependent of the time point at which it gets expressed (Fig. 3.16C, D).

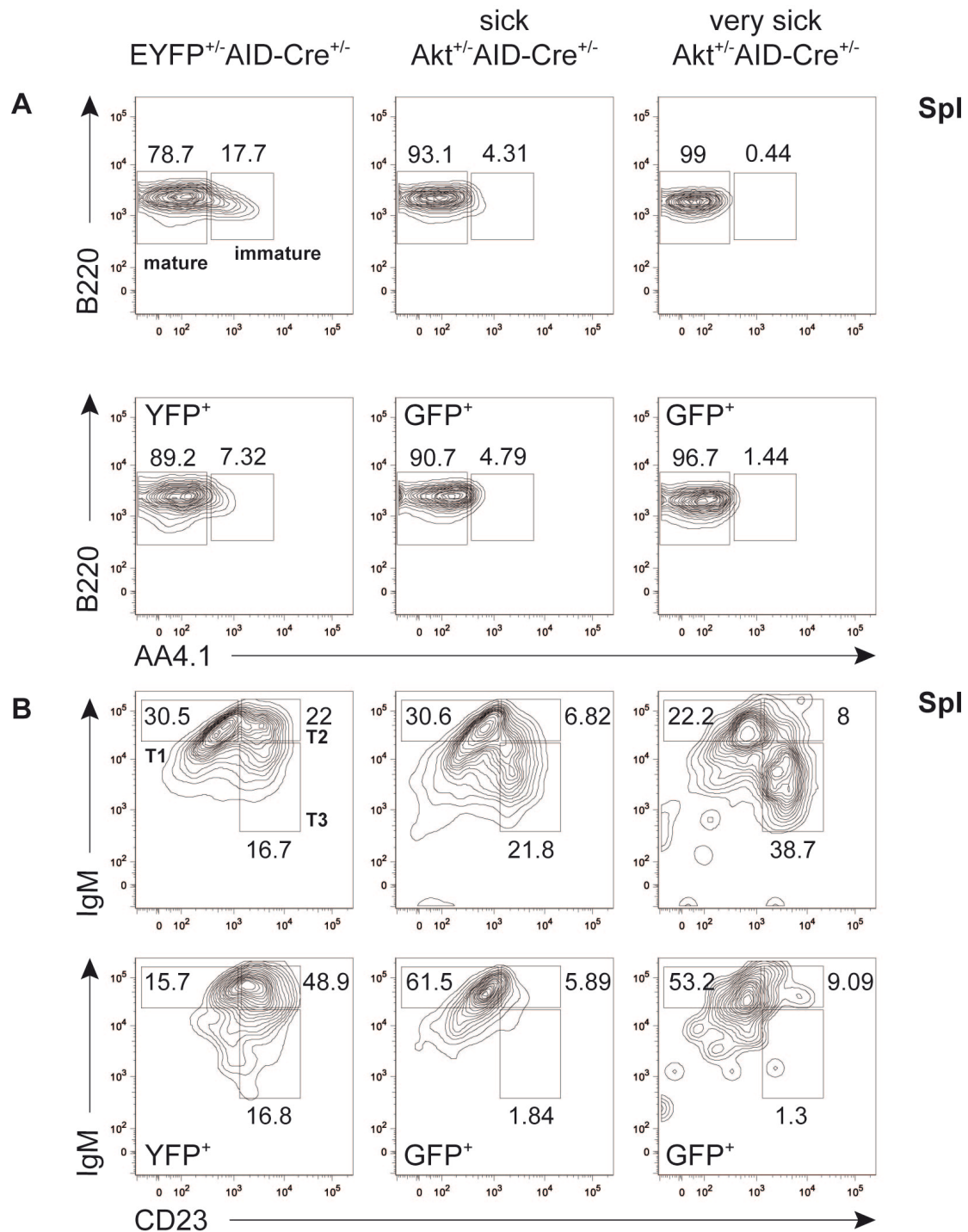


Figure 3.49: Distribution of splenic mature and immature B cells as well as transitional B cells in Akt^{+/+}-AID-Cre^{+/+} mice and EYFP^{+/+}-AID-Cre^{+/+} control mice.

(A) FACS analysis of splenic mature (B220⁺, AA4.1⁻) and immature (B220⁺, AA4.1⁺) B cells in Akt^{+/+}-AID-Cre^{+/+} and EYFP^{+/+}-AID-Cre^{+/+} mice. Antibodies were used as indicated. The numbers close to the boxes of lymphocyte populations refer to the percentage of CD19⁺ live cells in the gates. Experiment was repeated 3 times with n = 3 mice per genotype. **(B)** FACS analysis of splenic T1 (IgM^{high}, CD23⁻), T2 (IgM^{high}, CD23⁺) and T3 (IgM^{low}, CD23⁺) B cells in Akt^{+/+}-AID-Cre^{+/+} and EYFP^{+/+}-AID-Cre^{+/+} mice. Antibodies were used as indicated. The numbers close to the boxes of lymphocyte populations refer to

the percentage of live cells in the gates. Plots are additionally gated on CD19⁺ B cells and AA4.1⁺ cells. Experiment was repeated 3 times with n = 3 mice per genotype.

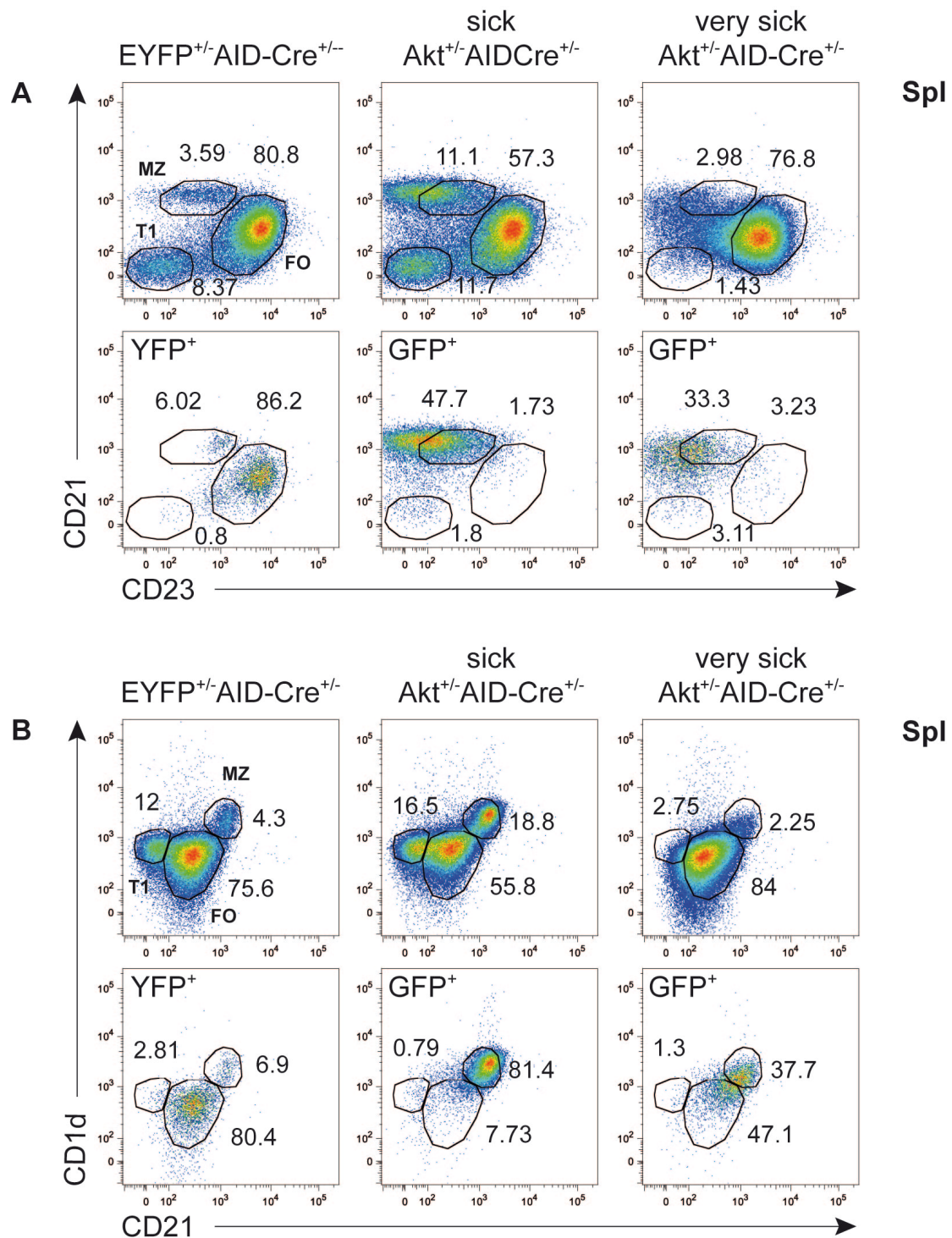


Figure 3.50: Distribution of splenic MZ, FO and T1 B cell populations in Akt^{+/-} AID-Cre^{+/-} mice vs. controls.

(A) FACS analysis of splenic B cells from Akt^{+/-} AID-Cre^{+/-} and YFP⁺ AID-Cre^{+/-} control mice. Displayed are FO (CD21^{inter}, CD23⁺), MZ (CD21^{high}, CD23⁻) and the T1 (CD21^{low}, CD23⁻) B cells. The numbers close to the boxes of lymphocyte populations refer to the percentage of live cells in the gates.

Cells were gated on live cells and CD19⁺ cells. Experiment was repeated 3 times with n = 3 mice per genotype. **(B)** Shown are FO (CD21^{inter}, CD1d^{low}), MZ (CD21^{high}, CD1d^{high}) and T1 (CD21^{low}, CD1d^{low}) B cells. The numbers close to the boxes of lymphocyte populations refer to the percentage of CD19⁺ live cells in the gates. Experiment was repeated 3 times with n = 3 mice per genotype.

The investigation of MZ B cell populations in the spleen revealed, as in the Akt^{BOE} mice, mainly MZ-like B cells, no FO B cells, and a small population of T1 B cells in Akt^{+/-}AID-Cre^{+/-} in comparison to B cells of EYFP^{+/-}AID-Cre^{+/-} controls (Fig. 3.50A, B; Fig. 3.13A, B).

In summary the influence of constitutively expression of Akt1 on MZ B cell fate decision seemed not to be dependent at the time point of expression, cause Akt^{BOE} mice and Akt^{+/-}AID-Cre^{+/-} showed the same strong MZ-like B cell population.

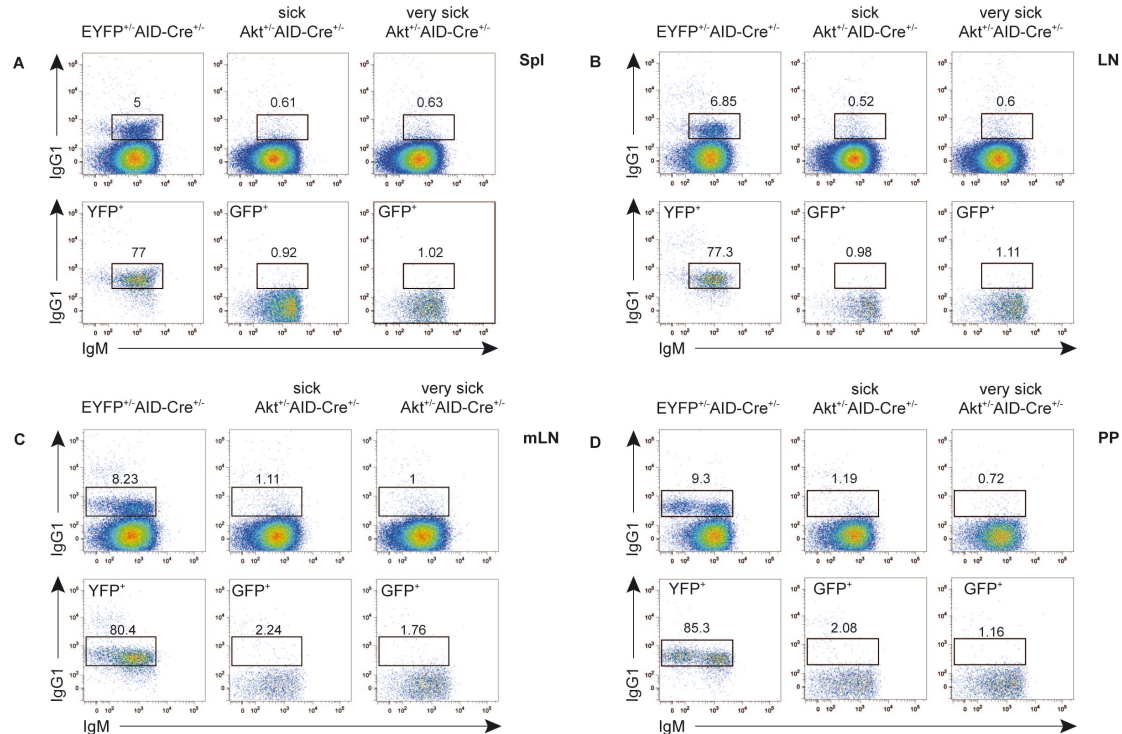


Figure 3.51: Surface IgG1 expression in different organs of Akt^{+/-}AID-Cre^{+/-} and EYFP^{+/-}AID-Cre^{+/-} control mice.

(A-D) FACS analysis of IgG1 expression in B cells from different organs of Akt^{+/-}AID-Cre^{+/-} and EYFP^{+/-}AID-Cre^{+/-} control mice. The numbers close to the boxes of lymphocyte populations refer to the percentage of CD19⁺ live cells in the gates. Experiment was repeated 3 times with n = 3 mice per genotype. **(A)** Spleen **(B)** pLN **(C)** mLN **(D)** PP, 5 PP each mouse.

Surface IgG1 could be detected in EYFP^{+/+}AID-Cre^{+/+} controls but not in Akt^{+/+}AID-Cre^{+/+} mice in spleen, pLN, mLN and PP (Fig. 3.51A-D). The overexpression of Akt1 also seem to have an influence on the GFP⁻ B cells, because also these cell do not switch to IgG1. So the overexpression of Akt1 also led to a block of surface IgG1 expression in a later phase of B cell development.

Taken together in Akt^{+/+}AID-Cre^{+/+} mice the MZ-like B cell phenotype could be observed as well as the inability to produce surface IgG1 as in Akt^{BOE} mice. As with Akt^{BOE} mice, all B cells in Akt^{+/+}AID-Cre^{+/+} mice were IgM⁺ and did not express IgD. From the three different transitional B cell populations, Akt^{+/+}AID-Cre^{+/+} mice showed only T1 B cells, similar to Akt^{BOE} mice. Besides this, Akt^{+/+}AID-Cre^{+/+} mice showed CD4⁺ memory effector and CD8⁺ effector T cells that are GFP⁺ and therefore these cells also overexpress Akt1.

4 Discussion

Akt belongs to the serine/threonine kinases and is overexpressed in many human diseases such as diabetes and hypertrophy, as well as in many different forms of cancer including ovarian carcinomas, colon carcinogenesis, gastric adenocarcinomas and B cell chronic lymphocytic leukemia (B-CLL) (Cross et al., 1995; George, 2004; Cho, 2001; Shiojima et al., 2005; Roy, 2002; Cheng et al., 1992; Staal, 1987; Hofbauer et al., 2010). It exists in three different isoforms: Akt1/PKB α /RAC-PK α , Akt2/PKB β /RAC-PK β and Akt3/PKB γ /RAC-PK γ , which share similar structures and functions (Jones et al., 1991b; Coffey and Woodgett, 1991; Staal, 1987; Konishi et al., 1995; reviewed in Yang et al., 2004b; Altomare et al., 1998; Brodbeck et al., 1999; reviewed in Cohen, 2013).

Gene ablations showed that besides BCR, NF κ B, and Notch2 signaling also PI3K/Akt signaling is critically involved in MZ B cell differentiation or maintenance or both (Rickert et al., 1995; Engel et al., 1995; Gu et al., 1993; Cariappa et al., 2000; Saito et al., 2003; Fruman et al., 1999; Clayton et al., 2002; Calamito et al., 2010). However, until now the effects of constitutive Akt signaling on B cell differentiation and activation are still under debate. In this thesis, we describe the analysis of a transgenic mouse strain, expressing Akt1 upon Cre-mediated recombination in B cells. The Rosa-Akt-C mouse was crossed to a CD19-Cre mouse, to overexpress Akt1 in B cells already at the pro-B cell or early pre-B cell stage (termed Akt^{BOE} mice). It is known that Akt is activated in B-CLL and therefore the aim of the project was to generate a mouse line that possibly develops B cell cancer, such as a B-CLL. B-CLL is a special form of non-Hodgkin lymphoma where an activation of Akt could be detected and where the direct inhibition of Akt leads to the apoptosis of B-CLL cells (Hofbauer et al., 2010). Besides studies of Akt1 overexpression at early stages of B cell development using the CD19-Cre, the Rosa-Akt-C mouse was also crossed to *Aicda* (AID)-Cre mice to investigate the influence of Akt1 overexpression in later stages of B cell development.

4.1 Constitutive Akt1 expression Leads to MZ-like B Cell Development Directly From T1 B Cell Precursors

Akt^{BOE} mice showed increased size of spleens due to significantly increased numbers of B and T cells as well as mature macrophages, monocytes, and neutrophils as compared to controls. The increased number of B cells was due to a massive accumulation of MZ-like B cells at the expense of FO B cells.

Immature B cells that migrate as T1 B cells into the spleen and further differentiate to T2 B cells. T1 B cells are AA4⁺, IgM^{high} and negative for CD23 whereas T2 B cells are AA4⁺, IgM^{low} and CD23⁺ (Allman et al., 2001). It is still in discussion at which developmental stage immature B cells are committed to become either a FO or a MZ B cell. However, in general, T2 B cells are thought to be direct precursors of MZ and FO B cells (Merrell et al., 2006).

The Akt1 overexpression in B cells led to the development of T1 B cells exclusively, therefore we propose that Akt1 expressing MZ-like B cells are generated from T1 B cells. This is in accordance with other reports suggesting that MZ B cells mainly branch from T1 B cells (Loder et al., 1999; Hampel et al., 2011; Roundy et al., 2010). For example, mice overexpressing Notch2 only in B cells have a MZ phenotype and also show an accumulation of T1 B cells, suggesting that in this mouse model MZ B cells develop directly from the T1 stage (Hampel et al., 2011). Further, Roundy et al. showed that cells *in vitro* with a MZ phenotype which developed from CD23⁻ populations were more robust than cells from CD23⁺ transitional B cells, suggesting a direct maturation from T1 B cells to MZ cells (Roundy et al., 2010).

In summary, constitutive Akt1 expression in B cells leads to a developmental block from T1 to T2 B cell stages possibly due to the inability to express CD23 and MZ-like B cells seems to develop from T1 B cells. The loss of CD23 expression is discussed in the next section (4.2).

4.2 Overexpression of Akt1 in Akt^{BOE} Mice Leads to a Loss of the Surface Marker CD23

FO B cells are, besides other important surface markers, defined through CD23 (FcεRII) expression (reviewed in Pillai and Cariappa, 2009). CD23 is expressed on mouse B cells and follicular DCs (FDCs) and functions as a low-affinity receptor for IgE (Bonney et al., 1987; reviewed in Gould et al., 2008). It is involved in the

regulation of IgE production and is important for the survival of GC B cells (Vander-Mallie et al., 1982; Liu et al., 1991). Due to the fact that B cells from Akt^{BOE} mice revealed no CD23 expression on the surface, the loss of FO B cells in Akt^{BOE} mice can be explained.

In general, CD23 can be found in soluble form in sera when cleaved by ADAM10 (Gibb et al., 2010). However, sCD23 was not detectable in blood sera of Akt^{BOE} mice and, in addition, *CD23* RNA expression levels in B cells of Akt^{BOE} mice were decreased.

Knockout of CD23 in mice led to the absence of B cells that express CD23 (Fujiwara et al., 1994). This was also true for mice that constitutively express Akt1; therefore, Akt1 overexpression can regulate the expression of CD23 and lead to MZ B cell fate decision.

Pierau et al. could show similar MZ B cell numbers in controls and transgenic mice overexpressing Akt1 constitutively active, whereas FO B cells revealed only a slight reduction in this Akt1 overexpressing mouse model compared to controls (Pierau et al., 2012). Due to an overexpression of Akt1 in all cells and not specifically in B cells as in Akt^{BOE} mice, it is possible that general Akt1 overexpression leads to a different phenotype as seen in Akt^{BOE} mice.

In conclusion, constitutive Akt1 signaling prohibits CD23 expression and therefore leads to MZ fate decision and FO B cell development is underprivileged.

4.3 Constitutive Akt1 Signaling Leads to MZ-like B Cell Development Independent of CD19

An established scenario is that MZ B cell development is dependent on PI3K activation downstream of BCR signaling and subsequent activation of Akt (Srinivasan et al., 2009; Calamito et al., 2010; reviewed in So and Fruman, 2012). Deficiency of the BCR co-receptor CD19 leads to a defective MZ B cell development, as well as mutations in the PI3K isoforms p110 δ (Rickert et al., 1997; Clayton et al., 2002). The constitutive activation of PI3K through deficiency of phosphatase and tensin homolog (PTEN), a negative regulator of PI3K signaling, leads to a significant increase in MZ B cells (Suzuki et al., 2003). In this work, we show that constitutive Akt1 expression in CD19-deficient B cells can overcome the defect in MZ B cell differentiation. Therefore, the differentiation into MZ-like B cells is independent of the BCR CD19 co-receptor in the case of B cell specific Akt1 overexpression.

This could also be shown for constitutive Notch2 activity in transgenic Notch2IC//CD19-Cre^{-/-} mice (called Notch2IC//CD19-Cre^{+/+} in the paper). Here, the activation of B cells through Notch2 leads to the hyper activation of MAPK and PI3K/Akt signaling and, in the case of CD19 knockout, to the generation of MZ B cells nevertheless (Hampel et al., 2011). Also for the inactivation of PTEN in addition to CD19 deficiency, MZ B cell development through PI3K/Akt signaling could be observed (Anzelon et al., 2003). That again underlines the dispensability of CD19 in the case of constitutive Akt1 expression during MZ B cell maturation.

4.4 FOXO1 and Notch2 Regulation in Akt^{BOE} Mice

For MZ B cell development, the downregulation of FOXO1 is important (Dengler et al., 2008; Chen et al., 2010). This downregulation is mediated by FOXO phosphorylation through Akt (Dengler et al., 2008; Hinman et al., 2009; Lin et al., 2010). In B cells of Akt^{BOE} mice, the protein level of the transcription factor FOXO1 is downregulated, verifying the theory of the Akt-FOXO axis. That theory is implicated, with high PI3K/Akt activity, in the downregulation of FOXO and the development of MZ B cells, CD138⁺ plasmablasts and low-affinity IgM plasma cells (reviewed in Limon and Fruman, 2012; Dengler et al., 2008). CD138⁺ plasmablasts and low-affinity IgM plasma cells develop in general from MZ B cells (Martin et al., 2001). High FOXO activity and low PI3K/Akt leads to GC development, CSR and SHM followed by the development of high-affinity plasma cells and memory B cells (reviewed in Limon and Fruman, 2012). Chen et al. could show that the deletion of FOXO1 leads to MZ B cell development also in case of CD19 knockout and Calamito et al. showed that the complete knockout of Akt1 and Akt2 leads to the loss of MZ B cells, whereas in mice with a deletion of either Akt1 or Akt2, proper MZ B cell development can still take place (Chen et al., 2010; Calamito et al., 2010). This leads to the assumption that the overexpression of Akt1 and the resulting loss of FOXO1 function impair the cell fate decision to FO B cells, thereby explaining the loss of FO B cells in Akt^{BOE} mice and resulting in MZ B cell development.

In MZ fate decision also Notch2 plays an important role. A strong BCR signal in transitional B cells induces FO B cell maturation, whereas a weak BCR signaling allow cells to develop to MZ B cells due to Notch2 signaling (reviewed in Pillai and Cariappa, 2009). Increased protein levels of Notch2 could also be detected in B cells of Akt^{BOE} mice, indicating an advantage for MZ B cell generation (Saito et al., 2003;

Hampel et al., 2011). Furthermore, *Dtx1* expression is suggested to be regulated by *Notch2* and that both play a role in MZ B cell development, whereas *Hes1* and *Hes5* are only less affected, in the case of *Notch2* deficiency (Saito et al., 2003). Further investigations of *Notch2* target genes such as *Dtx1* and the general Notch receptor targets *Hes1* and *Hes5* in MZ-like B cells of *Akt*^{BOE} mice, revealed only *Hes5* and *Dtx1* are direct downstream targets of *Notch2*; *Hes1* transcription was less affected by downregulation of *Notch2*. In contrast to the findings in MZ B cells of *Akt*^{BOE} mice, Shimizu and Tan-Pertel suggest that besides *Hes5*, *Hes1* also is a downstream target of Notch (Shimizu et al., 2000; Tan-Pertel et al., 2000). Overall, stating that the induction of *Hes1* and *Hes5* disturb B cell development seems to be only partially true for *Akt1* overexpression in MZ B cells (Kawamata et al., 2002).

In summary, MZ-like B cells of *Akt*^{BOE} mice express higher protein levels and lower transcription levels of *Notch2*, affecting the transcription of *Hes5* and *Dtx1*. However, there is no effect on *Hes1* transcription levels. So the overexpression of *Akt1* in MZ-like B cells of *Akt*^{BOE} mice leads to the downregulation of *Notch2* therefore possibly having a direct effect on the downregulation of *Hes5* and *Dtx1*.

4.5 The Loss of BCR Signaling in *Akt*^{BOE} Mice

It is known, that in B cells, ligation of the BCR co-receptor complex consisting of CD19, CD81, or CD21 is needed to activate PI3K and *Akt*, leading to MZ B cell development (Calamito et al., 2010; Otero et al., 2001; Tuveson et al., 1993). In the process of BCR signaling, the receptor phosphorylates and activates Syk and Lyn (reviewed in Campbell, 1999; reviewed in Kurosaki, 1999). Syk subsequently phosphorylates and activates BLNK/SPL-65 and PLC γ ; phosphorylation of BLNK/SLP-65 is required for membrane localization of PLC γ (Fu et al., 1998; Wienands et al., 1998). Lyn phosphorylates the tyrosine kinase Btk that together with Syk activates PLC γ , resulting in BCR mediated Ca²⁺ signaling (Takata et al., 1994; Takata and Kurosaki, 1996; Fluckiger et al., 1998).

Upon activation of the BCR by α IgM stimulation, B cells of *Akt*^{BOE} mice showed no proliferative capacities. In addition, no Ca²⁺ flux could be induced although an increase in basal Ca²⁺ levels was observed when compared to CD19-Cre controls. As seen in B cells of *Akt*^{BOE} mice, anergic cells in general fail to mobilize Ca²⁺ after BCR engagement but show elevated basal intracellular Ca²⁺ levels (reviewed in Cambier et al., 2007; Healy et al., 1997; Cooke et al., 1994). Anergy is a process

where autoreactive B cells able to bind self-antigens through low-affinity recognition, are silenced (Healy et al., 1997; reviewed in Goodnow et al., 2005; reviewed in Goodnow, 1997). It is possible that through the overexpression of Akt1 B cells become anergic and do not react to signals coming from the BCR. Through the possible anergy of MZ-like B cells in Akt^{BOE} mice and the Akt1 overexpression, these cells cannot undergo apoptosis and they remain as anergic MZ-like B cells that are unable to respond to BCR signaling (Bommhardt et al., 2004).

In addition to positive functions as Ca²⁺ flux, Lyn also mediates negative pathways by phosphorylating the BCR co-receptor CD22. CD22 recruits and phosphorylates Suppressor of High-copy PP1 (SHP-1), which leads to the downregulation of the BCR signaling (Nishizumi et al., 1998; Smith et al., 1998; Chan et al., 1998; Cornall et al., 1998). In B cells of Akt^{BOE} mice Lyn phosphorylation was observed, but phosphorylation of Syk could not be detected. It is possible that the constitutively active overexpression of Akt1 in Akt^{BOE} mice leads to a negative feedback loop, which blocks the BCR. pLyn triggers the phosphorylation and activation of the BCR co-receptor CD22, therefore resulting in a downregulation or complete hindering of BCR signaling and blocked phosphorylation of Syk, to avoid more and more MZ-like B cell lineage development.

Whereas B cells of Akt^{BOE} mice did not respond via α IgM stimulation they are responsive to the stimulation of other receptors. After the stimulation of TLR4 and TLR9 through LPS and CpG respectively, B cells of Akt^{BOE} mice proliferate. High responsiveness to LPS ligation is known as a hallmark of MZ B cells, but B cells of Akt^{BOE} mice showed weaker proliferation than controls (Oliver et al., 1997; Allman et al., 2001). In mice overexpressing Akt1 in all cells, a reduced proliferation and a lower Ca²⁺ flux after BCR engagement could be observed, and therefore is different to observations in Akt^{BOE} mice (Pierau et al., 2012). In addition, the CAG promoter used in the Rosa-Akt-C construct strengthens the signal from Akt1, possibly leading to a much stronger Akt1 overexpression in B cells of Akt^{BOE} mice than in the Akt1 overexpression mice of Pierau, and therefore to a stronger phenotype (Pierau et al., 2012). In conclusion, increased numbers of MZ-like B cells are not the result of elevated proliferation through the stimulation of the BCR.

Survival assays revealed a survival advantage of constitutive Akt1 B cells compared to CD19-Cre mice. Akt forces cell survival through many mechanisms, including the

direct phosphorylation and inhibition of pro-apoptotic proteins such as Caspase-9, Bad and Forkhead transcription factors (reviewed in Datta et al., 1999; Cardone et al., 1998; Datta et al., 1997; reviewed in Zhang et al., 2011; Brunet et al., 1999). Also B cells lacking Akt1 and Akt2 showed reduced survival compared to wild type mice (Calamito et al., 2010). Our data indicate that the enormous increased MZ-like B cell population is due to survival as a consequence of constitutive Akt1, that is known to prevent apoptosis and leads to a better survival of B cells (reviewed in Datta et al., 1999; Jeong et al., 2008; Yang et al., 2004a; reviewed in Yang et al., 2004b; Pogue et al., 2000). Furthermore, constitutive Akt1 signaling acts independently of BCR signaling during the induction of MZ-like B cell differentiation.

4.6 MZ-like B Cells Show Normal Surface Marker but are not Able to Class Switch

MZ-like B cells of Akt^{BOE} mice in general do not behave like ‘normal’ MZ B cells. B cells in general can become activated through the BCR and MZ B cells secrete IgG3 after TI dependent. Besides the inability of MZ-like B cells of Akt^{BOE} mice to be activated through the BCR they do not secrete IgG3 immunoglobulins even after TI NP-Ficoll immunization, as normal MZ B cells would do. Although mIgM expression on B cells of Akt^{BOE} mice is higher than in B cells of CD19-Cre control mice and underlines the huge number of MZ-like B cells detected in Akt^{BOE} mice, due to the knowledge, that MZ B cells express higher levels IgM on its surface in comparison to FO B cells (Martin et al., 2001). This was also displayed in the IgM vs. IgD staining where B cells of Akt^{BOE} mice express mainly IgM⁺ cells. Another typical feature for MZ B cells are the expression of CD1d and CD21 surface markers (Gray et al., 1984; reviewed in Pillai et al., 2005). The expression of these surface markers is comparable between MZ-like B cells of Akt^{BOE} mice to those in MZ B cells of controls. Concerning the expression of surface markers IgM, CD1d and CD21, constitutive Akt1 expressing MZ-like B cells seemed to be ‘normal’ MZ B cells. Unexpectedly, after TI immunization with NP-Ficoll MZ-like B cells of Akt^{BOE} mice showed a reduced IgM and no IgG3 secretion, suggesting a defect of these cells to respond to TI antigens as normal MZ B cells would do. In order to investigate whether these MZ-like B cells are ‘real’ MZ B cells one could additionally investigate basal activity of signaling pathways that are active in MZ B cells such as IκBα, c-Myc, Erk and JNK.

In contrast to the general finding that MZ B cells are sessile cells and stay in the marginal zone of spleen, in Akt^{BOE} mice, MZ-like B cells are also detectable in pLN, mLN and PP (Gray et al., 1982). These MZ-like B cells could also be detected in Akt^{+/-}CD19^{-/-} mice, that bear a CD19 co-receptor knockout, whereas CD19^{-/-}-Cre mice do not develop MZ B cells in general and least of all in pLN, mLN or PP. Possibly as a consequence of the highly increased MZ-like B cell population in spleen, the MZ is overcrowded and MZ-like B cells therefore migrate into other lymphoid organs.

In pancreatic LN of 16 week-old NOD mice, MZ-like B cells could be detected, indicating antigen-presenting cell (APC) activity; these cells are thought to be capable of presenting autoantigen *in vivo* (Mariño et al., 2008). Mariño et al. suggested, that these increased numbers of MZ-like B cells in the pancreatic LN of NOD mice are not due to migration but are related to the pathophysiology of diabetes, due to the knowledge, that the pancreatic LN are a site critical for the presentation of autoantigen and self-reactive T cells (Mariño et al., 2008; Höglund et al., 1999; Jaakkola et al., 2003; Gagnerault et al., 2002). These MZ-like B cell populations expanded with age (Mariño et al., 2008). Also for BAFF transgenic mice it could be shown that MZ-like B cells migrate into blood and LN (Batten et al., 2000). These MZ-like B cells also infiltrate into salivary glands of BAFF transgenic mice, the target organ for Sjögren's syndrome, and are therefore suggested to participate tissue damage in Sjögren's syndrome and possibly other autoimmune diseases (Groom et al., 2002). Expanded MZ-like B cells expressing Akt1 constitutively, detected in pLN, mLN and PP could be MZ-like B cells that have migrated out of the spleen, and might develop an autoreactive phenotype possibly leading to autoimmune disease with age. To proof this theory, an autoantibody test can be performed.

4.7 Constitutive Akt1 Signaling Leads to the Impairment of CSR, GC Formation and Plasma Cell Differentiation

To defend the body, one very important function of B cells is to generate immunoglobulins. Therefore, for this function mainly GC B cells and FO B cells are important, although MZ B cells are also able to produce low-affinity IgM and IgG3 (Jacob et al., 1991; Martin et al., 2001; Won and Kearney, 2002).

B cells of Akt^{BOE} mice are not able to secrete immunoglobulins and do not express IgG1. Even after immunization with TI NP-Ficoll no IgG3 could be detected in the sera of Akt^{BOE} mice. This stands in contrast to the finding of Pierau et al. where they

could show more IgG1 and IgG3 secretion after TI-II-TNP Ficoll immunization in mice overexpressing Akt1 (Pierau et al., 2012). In these transgenic mice, stimulation *in vitro* with LPS also leads to an increased secretion of IgM, IgG and IgA in comparison to controls (Pierau et al., 2012).

Discrepancies between our constitutive Akt1 mouse model and theirs could be caused by a B cell specific overexpression of Akt1 in ours vs. an overexpression of Akt1 in the whole body in theirs. The constitutive Akt1 mouse used by Pierau still contain FO B cells and MZ B cells and due to containing FO B cells and normal MZ B cells Ig secretion is not deficient.

For the generation and secretion of immunoglobulins the mechanism of CSR is important. During this process so called circular DNAs and circular transcripts (CTs) appear (Kinoshita et al., 2001). For the initiation of CSR AID plays an important role, and for the generation of AID, FOXO1 is needed (Dengler et al., 2008). For B cells of CD19-Cre controls, IgG1 specific $\gamma 1$ CTs could be observed, but not for B cells of Akt^{BOE} mice. Real-Time analysis revealed that *Aicda* expression levels, the gene encoding for AID, was significantly reduced in B cells of Akt^{BOE} mice. This could be explained by downregulation of FOXO1 protein levels in B cells of Akt^{BOE} mice through the overexpression of Akt1. It was already shown that PI3K activity results in activation of Akt leading to the nuclear exclusion of FOXO and to the inhibition of CSR due to poor AID expression, whereas high expression of AID did not lead to increased CSR (McBride et al., 2004; Omori et al., 2006). CTs also serve as a hallmark for active CSR *in vitro* and *in vivo* and are indispensable during this process of CSR (Kinoshita et al., 2001).

Despite the impaired CSR in B cells of Akt^{BOE} mice GC formation was also investigated. In splenic B cells of Akt^{BOE} mice, no GC formation took place, even after TD immunization with NP-CG and SRBC. Interestingly, it is different in PP and mLN. In these organs GCs could already be observed without stimulation. It was shown that the GC response in the gut associated tissue (GALT) of wild type mice is dependent on the microbial flora (Cebra et al., 1991). Also Casola et al. could show that GCs generated in PP are microbiota derived. He treated D_HLMP2A mice with a cocktail of broad-spectrum antibiotics and could show a reduction of GCs in PP (Casola et al., 2004). The antibiotic treatment to eliminate the microorganisms was also used in Akt^{BOE} mice to investigate GC formation due to microbial influence. The

antibiotic treatment did not lead to a reduction of GCs in PP and mLN in Akt^{BOE} mice. It is possible, that through the antibiotic treatment not the whole microbial flora was eliminated and therefore GCs could still be generated.

The absence of GC formation in spleen after immunization and the loss of CSR and, therefore, no immunoglobulins in B cells of Akt^{BOE} mice, can be explained by the Akt-FOXO axis. In the case of high expression of Akt, FOXO gets degraded and therefore GC formation and CSR cannot take place (reviewed in Limon and Fruman, 2012). In resting B cells, FOXO factors are in the nucleus and influence cell cycle arrest, longevity and recirculation (Essers et al., 2005; Takaishi et al., 1999). Through phosphorylation and therefore activation of Akt, Akt enters the nucleus and phosphorylates FOXO (Burgering et al., 1999; Rena et al., 1999; Takaishi, 1999; Tang et al., 1999). This leads to the export of FOXO into the cytoplasm, where it gets degraded and no GC formation and CSR can take place (Brunet et al., 1999; Biggs et al., 1999; Brownawell et al., 2001).

Due to the increased numbers of MZ-like B cells in Akt^{BOE} mice and the knowledge that MZ B cells differentiate very quickly into plasma cells after very low dose of mitogens, it was expected to find plasma cells in Akt^{BOE} mice (Oliver et al., 1999). *In vivo*, less plasma cell differentiation could be observed in Akt^{BOE} mice and CD19-Cre controls whereas *in vitro* stimulation with IL4 and LPS lead to plasma cell differentiation in CD19-Cre controls but not in Akt^{BOE} mice. This is another hint, that the Akt1 overexpression leads indeed to MZ-like B cell differentiation but that these cells are anergic and not able to react as normal MZ B cells, as already assumed.

These data suggest that Akt1 signaling interfere with non-galt GC formation and differentiation of B cells. It further suggests that Akt1 signaling has to be switched off to allow GC as well as PC differentiation.

4.8 κ and λ Expression in B Cells of Akt^{BOE} Mice

The expression of the κ and λ light chains are important markers for B cells (Bernier and Cebra, 1964; Pernis et al., 1965). Mature B cells express either κ or λ chains and in the bone marrow of wild type mice the ratio between κ and λ is 95 to 5 (Takeda et al., 1996; Alt et al., 1980; Langman and Cohn, 1995). The requirement for light chain rearrangement depends on productive heavy chain rearrangement.

In bone marrow, a reduction of κ and λ expressing B cells could be observed in Akt^{BOE} mice in comparison to CD19-Cre mice, whereas the ratio between κ and λ in Akt^{BOE} mice is still ~93% and ~7% and therefore quite normal. The reduced cell number of κ^+ and λ^+ B cells in case of constitutive Akt1 expression could be due to the general reduction of mature recirculating B cells in the bone marrow of Akt^{BOE} mice.

In splenic Akt^{BOE} B cells, elevated κ and λ levels are detected, although the ratio is still normal (~91% are κ^+ B cells and ~9% are λ^+ B cells). Increased cell numbers of κ^+ and λ^+ B cells were due to a generally increased B cell population in Akt^{BOE} mice in comparison to CD19-Cre controls.

Collectively, light chain rearrangement functions remain normal in case of constitutive Akt1 expression.

4.9 Constitutive Akt1 Expressing CD19⁺ B Cells Lacking Surface IgM, IgD, Ig κ and Ig λ Can be Restored in JHT^{-/-} Mice

The investigation of IgM⁺ and IgD⁺ B cells revealed, as already discussed, mainly IgM⁺ B cells in Akt^{BOE} mice. Besides this, a DN CD19⁺ B cell population lacking surface IgM and IgD could be detected. The investigation of Ig κ and Ig λ chain distribution in spleen also revealed a DN population, negative for Ig κ and Ig λ .

Dengler et al. could detect a similar cell population in mice bearing a deletion of FOXO1 in a CD19-Cre background, but these cells were still able to express little of intracellular κ - or λ -light chains but abundant intracellular μ -heavy chains. They postulate that this cell population is made up of progenitor B cells that could escape the bone marrow because of a changed BCR expression. These mice also show an increase in MZ B cells as Akt^{BOE} mice (Dengler et al., 2008).

Our theory was that through constitutive Akt1 expression also B cells without a functional BCR can leave the bone marrow. These cells are the CD19⁺ B cells negative for IgM, IgD, Ig κ and Ig λ .

With the generation of the Akt^{+/-}JHT^{-/-}CD19-Cre^{+/-} mice it was possible to prove this theory. These mice do not express a functional BCR and therefore there are no B cells in the periphery. Astonishingly, Akt^{+/-}JHT^{-/-}CD19-Cre^{+/-} mice generate CD19⁺ B cells. These cells are, as were the cells in Akt^{BOE} mice, negative for IgM, IgD, Ig κ and Ig λ . In conclusion these immature B cells are able to leave the bone marrow due to constitutively active Akt1 even without a functional BCR and move into the

periphery. It is known that a tonic signal of the BCR is important to keep resting B cells alive and a knockout of the BCR leads to apoptosis of these cells (reviewed in Grande et al., 2007; Stadanlick et al., 2008; Lam et al., 1997; Kraus et al., 2004). Apoptosis of B cells without a BCR can be rescued by overexpression of PI3K and resulting activation of Akt as a downstream target of PI3K (Srinivasan et al., 2009; James, 1996; Franke, 1997; Frech et al., 1997; reviewed in Datta et al., 1999). For that reason in Akt^{BOE} mice also B cells without a BCR can survive, since in the case of Akt1 overexpression BCR signaling is not needed.

4.10 Signaling Pathways Downstream of Akt: mTOR and GSK-3

The mTOR kinase is active in two different multi-protein complexes mTORC1 and mTORC2. mTORC1 can be activated by Akt through phosphorylation and mTORC2 phosphorylates Akt at Ser473 (Navé et al., 1999; Sarbassov et al., 2005). These signaling pathways are important for cell growth, metabolism and proliferation (reviewed in Liu et al., 2009; reviewed in Wullschleger et al., 2006). It was proposed that mTOR Ser2448 gets phosphorylated by Akt and is insulin dependent whereas Chiang et al. proposed that mTOR Ser2448 gets directly phosphorylated *in vitro* by p70 ribosomal S6 protein kinase (p70S6K or S6K; serine/threonine kinase) (Navé et al., 1999; Chiang and Abraham, 2005). In B cells of Akt^{BOE} mice, phosphorylation of mTOR at Ser2448 is not elevated, fitting to the hypothesis that Ser2448 rather becomes phosphorylated by S6K than by Akt (Chiang and Abraham, 2005). Akt can also phosphorylate and inhibit tuberous sclerosis complex TSC1/2, which also leads to the stimulation of S6K, a key regulator of translation and cell growth (Inoki et al., 2002). It would be interesting to investigate the protein levels of TSC1/2 and S6K to show the involvement of Akt in mTOR signaling in our mice.

Another substrate that is regulated by Akt is the serine threonine kinase GSK-3. GSK-3 can regulate a lot of cellular processes as transcription and translation and also controls the synthesis of glycogen and protein by insulin regulation (Parker et al., 1983; Welsh and Proud, 1993). Akt can phosphorylate GSK-3 α at Ser21 and GSK-3 β at Ser9 (Cross et al., 1995; Sutherland et al., 1993; Sutherland et al., 1994). This leads to the inhibition of GSK-3 enzyme activity and to the dephosphorylation and activation of glycogen synthase and the synthesis of glycogen (Cross et al., 1995; Gold et al., 2000; reviewed in Cohen et al., 1997). Gold et al. could show that BCR activation leads to the phosphorylation of GSK-3 α and GSK-3 β . The activity of GSK-

3 α is PI3K dependent and it is still being investigated if this is mediated by Akt (Gold et al., 2000). In the case of B cells of Akt^{BOE} mice, the phosphorylation of GSK-3 β shows significantly more protein phosphorylation, hence inactivating the kinase, than CD19-Cre controls do. This is a hint that Akt1 is able to inactivate GSK3 through phosphorylation of GSK-3 β and confirms the literature, although it is not possible to say how this phosphorylation influences the cellular processes in B cells. To make any conclusions out of this finding, the phosphorylation state of GSK-3 α at Ser21 also has to be investigated in the case of Akt1 overexpression in B cells. Further analysis in the direction of metabolism and insulin regulation through GSK-3 in case of Akt1 overexpression has to be performed.

4.11 B Cell Specific Activation of Akt1 Signaling Itself is not Sufficient to Induce B Cell Lymphomagenesis

During this thesis, some points indicate a possible generation of a B-CLL. A hallmark for B-CLL are accumulations of increased numbers of CD5⁺ B cells (Boumsell et al., 1978; Caligaris-Cappio, 1996). In pLN as well as in PerC, CD5⁺ B1a B cells show elevated cell numbers in Akt^{BOE} mice. Due to functional similarities and phenotypical characteristics between CLL and splenic MZ B cells, we can hypothesize that CLL might be derived from MZ B cells (reviewed in Chiorazzi and Ferrarini, 2011; Caligaris-Cappio and Janossy, 1985). This would fit to the MZ-like B cell phenotype found in Akt^{BOE} mice.

It was already shown that CLL patients with low levels of soluble IgM (sIgM) are not able to mobilize Ca²⁺ response after BCR engagement (Mockridge et al., 2007; Lankester et al., 1995; Michel et al., 1993). This leads to the assumption that B-CLL cells are anergic and survive better because of this anergy (Apollonio et al., 2013). Moreover, B cells of Akt^{BOE} are unable to proliferate in the case of BCR stimulation; they survive better and do not respond with Ca²⁺ flux after BCR engagement. In addition, they secrete less sIgM than CD19-Cre control mice do. All these characteristics would fit to an anergic B-CLL phenotype.

Mature macrophages and neutrophils are increased in splenic Akt^{BOE} B cells. These cells are known to send survival signals through secretion of cytokines to B-CLL cells to prevent apoptosis (Zucchetto et al., 2010; reviewed in Burger et al., 2009a; Pedersen et al., 2002; Tsukada et al., 2002). This also suggests that Akt^{BOE} mice maybe develop a B-CLL.

In general, B-CLL arises with age. Due to the fact that Akt^{BOE} mice investigated in this thesis were very young we put a cohort of mice to age to determine whether these mice will develop a clear B-CLL or other type of cancer. The first observation that could be made was that Akt^{BOE} mice at the age of 70 weeks start to lose weight in comparison to control. This can hint at malignancy, because that often correlates with weight loss.

In Akt^{BOE} proliferation assays revealed normal or no proliferation untypical for tumors, but survival assay revealed an extreme survival advantage against controls that could hinting to tumor development in Akt^{BOE} mice. Some forms of B-CLL are known as a monoclonal B-lymphocyte expansion, therefore it would be interesting to investigate clonality of observed MZ-like B cells (Rawstron et al., 2002).

MZ-like B cells found in the different organs and in PerC can possibly be the precursors for a CLL. In B-CLL, Akt activity could be shown, and inhibition of Akt leads to the apoptosis of B-CLL cells (Hofbauer et al., 2010). The protooncogene T-cell leukemia 1 (Tcl1) is a co-activator of Akt and augments Akt activation (Laine et al., 2000). It is expressed in preleukemic T cells and subsets of naive lymphocytes (Narducci et al., 1995; Said et al., 2001; Herling et al., 2006). Tcl1 is overexpressed in many human B-cell lymphomas, including follicular lymphoma, CLL, mantle cell lymphoma, diffuse large B-cell lymphoma and splenic marginal zone lymphoma (Weng et al., 2012). So it is not far-fetched to assume an eventual development of B-CLL in Akt^{BOE} mice. So during the investigation of the relatively young Akt^{BOE} mice some observations were made that could be linked to a B-CLL. Further investigations are necessary to verify this theory.

Another possibility to explain the migration of MZ-like B cells in other organs is a nodal marginal zone B cell lymphoma (NMZL). In humans this NMZL is known. It poses problems in diagnosis and has morphologic and immunophenotypic similarities with extranodal lymphomas of the MALT lymphoma or splenic marginal zone lymphomas. The exact definition for NMZL according to the World health organisation (WHO) is “a primary nodal B-cell neoplasm that morphologically resembles LN involved by marginal zone lymphomas of extranodal or splenic types, but without evidence of extranodal or splenic disease”. NMZL cells are mature B cells that express the B-cell markers CD20, CD79a and IgM, but do not express CD5, CD23, and cyclin D1, and lack the expression of germinal center markers CD10 and Bcl-6 (Kahl and Yang, 2008). It is possible that the MZ-like B cells observed in pLN

are a NMZL and maybe this form of malignancy also exists for other organs such as mLN and PP. To clarify if the found MZ-like B cells in pLN may be a NMZL, NMZL specific markers, as described above, has to be investigated.

4.12 Overexpression of Akt1 in Mature B Cells Leads to Malignancy

AID is the initiator of CSR and SHM through target DNA cleavages (Muramatsu et al., 2000; Revy et al., 2000; Nagaoka, 2002; Petersen et al., 2001). Besides this important function, AID has mutagenic activity and is known for its involvement in tumorigenesis in B and non-B cells (Rucci et al., 2006; Komeno et al., 2010; Pasqualucci et al., 2007; Takizawa et al., 2008; Matsumoto et al., 2007; Kovalchuk et al., 2007).

The overexpression of Akt1 in later phases of B cell development through the usage of the AID-Cre leads to malignancies in Akt^{+/-}AID-Cre^{+/-} mice. In Akt^{+/-}AID-Cre^{+/-} mice the overexpression of Akt1 leads to enlarged pLN, altered thymi and, in females, to swollen ovaries. Also the expectation of life is dramatically reduced in Akt^{+/-}AID-Cre^{+/-} mice.

It is known that the activation of Akt in general leads to malignancy and tumor development (Cross et al., 1995; George, 2004; Cho, 2001; Shiojima et al., 2005; Roy, 2002; Cheng et al., 1992; Staal, 1987). In human ovarian carcinoma cell lines and primary ovarian tumors, Akt2 is overexpressed (Cheng et al., 1992). Through the knowledge that in MZ B cell generation Akt1 and Akt2 have overlapping functions, it is possible that an Akt1 overexpression can also lead to ovarian tumors in Akt^{+/-}AID-Cre^{+/-} mice (Calamito et al., 2010; Cheng et al., 1992). B and T cell lymphomas as well as lung and liver tumors could be observed in transgenic mice that systemically overexpress AID (Morisawa et al., 2008; Okazaki et al., 2003). The observed enlarged ovaries in Akt^{+/-}AID-Cre^{+/-} mice are not more closely investigated, but it is possible that it is a form of tumor affected by the Akt1 overexpression, leading to early death of the female mice. Also males die very early.

Constitutive Akt1 in later B cell development also led to increased splenic MZ-like B cell populations and mainly mature, IgM⁺ B cells as already observed in Akt^{BOE} mice. Regarding transitional B cells, Akt^{+/-}AID-Cre^{+/-} mice also developed only T1 B cells as already seen with Akt^{BOE} mice. In conclusion, constitutive Akt1 expression influences B cells in a similar way independent at which stage of B cell development

Akt1 is overexpressed, but in Akt^{+/-}AID-Cre^{+/-} mice the mutagenicity of Akt1 is visible.

Besides the expected Akt1 overexpression in B cells detected by GFP expression, Akt^{+/-}AID-Cre^{+/-} mice show also GFP expression in T cells. Here the expression of AID was not only restricted to CD4⁺ T cells, but also CD8⁺ T cells were affected (Qin et al., 2011). Qin et al. could show that AID frequency in CD8⁺ T cells was much lower than in CD4⁺ T cells in LN and PP (Qin et al., 2011). In Akt^{+/-}AID-Cre^{+/-} mice, closer investigation of CD8⁺ and CD4⁺ T cells revealed that CD4⁺ memory effector T cells and CD8⁺ effector T cells are the cells that express GFP and therefore overexpress Akt1. This was true for all organs but the CD4⁺ memory effector T cell population was usually more dominant than the CD8⁺ effector T cell population. Only in pLN were these two populations nearly the same. In pLN, the general GFP expression of CD4⁺ and CD8⁺ T cells was the weakest in comparison to the other investigated organs. Interestingly, in some organs the sickness seems to correlate with a higher GFP expression and therefore higher Akt1 overexpression. Also in thymus a connection between sickness and GFP expression/Akt1 overexpression could be observed. With sickness of the mice DP T cells disappeared and DN cells, probably B cells, increased in thymus, so the thymus looks more like a secondary lymphoid organ.

5 Summary

Akt, also known as PKB, belongs to the serine/threonine kinases and is involved in different human diseases such as diabetes, hypertrophy and cancer. Due to its diverse ways of signaling, Akt is involved in cell growth, survival, proliferation and metabolism. F. T. Wunderlich generated the Rosa-Akt-C mouse strain (unpublished) that leads to an Akt1 overexpression after Cre-mediated recombination. In this thesis, the Rosa-Akt-C mouse was crossed to CD19-Cre mice resulting in mice that overexpress Akt1 in a B cell specific manner (Akt^{BOE} mice). Due to the involvement of Akt1 in different forms of cancer, we aimed to generate a mouse line to investigate the role of Akt1 in B cell development, maintenance, differentiation and possible tumor formation. The overexpression of Akt1 leads to the accumulation of MZ-like B cells in all tested lymphoid organs at the expense of FO B cells. Further, we could show that MZ-like B cells develop independently of CD19 in Akt^{+/-}CD19-Cre^{-/-} mice that bear a knockout for the co-receptor CD19 and normally leads to the absence of MZ B cells. In general the B cells of the Akt^{BOE} mice do not behave as normal B cells and seem to be anergic and not functional. Thus, B cells do not proliferate after BCR induced engagement and do not even show Ca²⁺ flux after BCR specific stimulation. Moreover, the investigation of CSR revealed that B cells of the Akt^{BOE} mice were lacking the ability to class switch. Further, GC formation failed in spleen, whereas in PP and mLN, GCs could be observed. In addition, the investigation of plasma cell development in Akt^{BOE} mice revealed no plasma cells even after induction of plasma cell differentiation *in vitro*. During this thesis, so far no cancer formation in Akt^{BOE} mice could be observed, but aging Akt^{BOE} mice lose weight in comparison to CD19-Cre controls and many of our findings indicate a possible development of B-CLL, possibly with age.

To investigate the role of Akt1 overexpression in later phases of B cell differentiation the Rosa-Akt-C mouse was crossed to the *Aicda*-Cre mouse, where Cre deletes in GC B cells. Lastly, also in these mice (Akt^{+/-}AID-Cre^{+/-}) constitutive Akt1 leads to MZ-like B cell development at the expense of FO B cells in GFP⁺ cells. Unexpectedly, overexpression of Akt1 was observed in CD8⁺ effector T cells and CD4⁺ memory effector T cells. Other interesting observations were enlarged ovaries and pLN, as well as thymi that looked either enlarged or disturbed. These AktAID-Cre^{+/-} mice die

very early and so the very low longevity of these mice displays the strong involvement of Akt1 in malignancies and survival, in case of deregulation.

Akt1 is very important for the maturation of MZ-like B cells and influences the survival of this cells in a positive way in comparison to normal B cells. Due to the loss of regulation of Akt1 in Akt^{BOE} mice, the generated MZ-like B cells are not functional. The data obtained from AktAID-Cre^{+/-} mice underlines the important role of Akt1 in disease and survival.

6 Zusammenfassung

Akt, auch PKB genannt, gehört zur Familie der Serin/Threonin Kinase und ist in verschiedene Erkrankungen wie Diabetes, Hypertrophie und Krebs involviert. Durch die Mannigfaltigkeit seiner Signalwege ist Akt in viele lebenswichtige Prozesse eingebunden, wie dem Zellwachstum, dem Zellüberleben, der Proliferation und dem Metabolismus. F. T. Wunderlich klonierte den Rosa-Akt-C Mausstamm (unpubliziert), der nach einer Cre vermittelten Rekombination zur Überexpression von Akt1 führt. In dieser Arbeit wurde dieser Mausstamm mit der CD19-Cre Maus verpaart, um eine Überexpression von Akt1 in B Zellen zu erreichen (Akt^{BOE} Mäuse). Ziel war es eine Maus zu kreieren, durch die man den Zusammenhang von Akt1 und der B Zell Entwicklung, Erhaltung, Differenzierung und eventuell auch der Krebsentwicklung untersuchen kann. Die Überexpression von Akt1 führte in Akt^{BOE} Mäusen zur Entwicklung von MZ ähnlichen B Zellen in der Milz und einem Verlust von FO B Zellen. In pLN, mLN and PP konnten ebenfalls MZ ähnliche B Zellen gefunden werden. Außerdem konnte gezeigt werden, dass sich diese MZ ähnlichen Zellen in Akt^{+/-}CD19-Cre^{-/-} Mäusen, die Akt1 überexprimieren, unabhängig vom CD19 co-Rezeptor bilden, obwohl dieser Knockout von CD19 normalerweise zum Verlust von MZ B Zellen führt. Generell zeigten B Zellen von Akt^{BOE} Mäusen keine normalen Reaktionen auf Stimulation und scheinen anerg und nicht funktionell zu sein. Nach spezifischer Stimulation des B Zell Rezeptors kommt es weder zur Proliferation der B Zellen, noch zum Ausstoß von Ca²⁺ innerhalb der B Zellen. Versuche zur CSR zeigten deutlich, dass B Zellen von Akt^{BOE} Mäusen nicht in der Lage sind zu class switchen. Die Formation von GC in der Milz blieb ebenfalls aus, wohingegen PP und mLN GC Entwicklung zeigten. Untersuchungen zur Entwicklung von Plasmazellen kamen zu dem Ergebnis, dass B Zellen von Akt^{BOE} Mäusen *in vivo* und *in vitro* nach spezifischer Stimulation keine Plasmazellen entwickeln. Bisher zeigten die Untersuchungen der B Zellen von Akt^{BOE} Mäusen keine Tumorbildung, jedoch weisen viele Beobachtungen auf eine mögliche Entwicklung einer B-CLL hin. Um den Einfluss einer Überexpression von Akt1 in späteren Phasen der B Zell Entwicklung zu untersuchen, wurde der Rosa-Akt-C Mausstamm mit dem *Aicda*-Cre Mausstamm verpaart. Die *Aicda*-Cre deletiert in den GC B Zellen. Auch in diesen Mäusen (Akt^{+/-}AID-Cre^{+/-}) zeigte sich ein Verlust von GFP⁺ FO B Zellen und die

GFP⁺ MZ ähnlichen B Zellen erwiesen sich als dominante B Zell Population. Des Weiteren konnte eine Überexpression von Akt1 in CD8⁺ Effektor und CD4⁺ Memory Effektor T Zellen nachgewiesen werden. Außerdem konnten vergrößerte Ovarien und pLN beobachtet werden sowie Thymi, die entweder vergrößert oder zerstört waren.

Akt1 scheint ein sehr wichtiger Faktor bei der Bildung von MZ ähnlichen B Zellen zu sein und beeinflusst das Überleben dieser Zellen positiv im Vergleich zu normalen B Zellen. Da in Akt^{BOE} Mäusen keine natürliche Regulation von Akt1 mehr stattfindet, zeigen die MZ ähnlichen B Zellen keine normale Funktionalität. Durch die geringe Lebenserwartung der AktAID-Cre^{+/-} Mäuse zeigt sich deutlich, welche wichtige Rolle Akt1 in Krankheit und Überleben spielt.

7 References

- Aichele, P., Zinke, J., Grode, L., Schwendener, R. A., Kaufmann, S. H. E. and Seiler, P. (2003). Macrophages of the splenic marginal zone are essential for trapping of blood-borne particulate antigen but dispensable for induction of specific T cell responses. *J Immunol.* **171**, 1148–1155.
- Alessi, D. R., Andjelkovic, M., Caudwell, B., Cron, P., Morrice, N., Cohen, P. and Hemmings, B.A. (1996). Mechanism of activation of protein kinase B by insulin and IGF-1. *EMBO J* **15**, 6541–6551.
- Alessi, D. R., Deak, M., Casamayor, A., Caudwell, F. B., Morrice, N., Norman, D. G., Gaffney, P., Reese, C. B., MacDougall, C. N., Harbison, D., Ashworth, A. and Bownes, M. (1997a). 3-Phosphoinositide-dependent protein kinase-1 (PDK1): structural and functional homology with the *Drosophila* DSTPK61 kinase. *Curr Biol* **7**, 776–789.
- Alessi, D. R., James, S. R., Downes, C. P., Holmes, A. B., Gaffney, P. R. J., Reese, C. B. and Cohen, P. (1997b). Characterization of a 3-phosphoinositide-dependent protein kinase which phosphorylates and activates protein kinase Ba. *Curr Biol* **7**, 261–269.
- Allman, D., Li, J. and Hardy, R. R. (1999). Commitment to the B Lymphoid Lineage Occurs before DH-JH Recombination. *J Exp Med* **189**, 735–740.
- Allman, D., Lindsley, R. C., DeMuth, W., Rudd, K., Shinton, S. A. and Hardy, R. R. (2001). Resolution of Three Nonproliferative Immature Splenic B Cell Subsets Reveals Multiple Selection Points During Peripheral B Cell Maturation. *J Immunol.* **167**, 6834–6840.
- Alt, F. W., Enea, V., Bothwell, A. L. and Baltimore, D. (1980). Activity of multiple light chain genes in murine myeloma cells producing a single, functional light chain. *Cell* **1980** **21**(1):1-12.
- Alt, F. W., Honjo, T., Radbruch, A. and Reth, M. (2014). Biology of B cells, Second Edition. *Academic Press*.
- Altomare, D. A., Lyons, G. E., Mitsuuchi, Y., Cheng, J. Q. and Testa, J. R. (1998). Akt2 mRNA is highly expressed in embryonic brown fat and the AKT2 kinase is activated by insulin. *Oncogene* **16**, 2407-2411.
- Aman, M. J. (1998). The Inositol Phosphatase SHIP Inhibits Akt/PKB Activation in B Cells. *J Biol Chem* **273**, 33922–33928.
- Amano, M., Baumgarth, N., Dick, M. D., Brossay, L., Kronenberg, M., Herzenberg, L. A. and Strober, S. (1998). CD1 expression defines subsets of follicular and marginal zone B cells in the spleen: β 2-Microglobulin-dependent and independent Forms. *J Immunol* **161**, 1710-1717.
- Andjelkovic, M., Alessi, D. R., Meier, R., Fernandez, A., Lamb, N. J. C., Frech, M., Cron, P., Cohen, P., Lucocq, J. M. and Hemmings, B. A. (1997). Role of translocation in the activation and function of protein kinase B. *J Biol Chem* **272**, 31515–31524.
- Andjelkovic, M., Jakubowicz, T., Cron, P., Ming, X. F., Han, J. W. and Hemmings, B. A. (1996). Activation and phosphorylation of a pleckstrin homology domain containing protein kinase (RAC-PK/PKB) promoted by serum and protein phosphatase inhibitors. *Proc Natl Acad Sci U S A* **93**, 5699-5704.
- Anzelon, A. N., Wu, H. and Rickert, R. C. (2003). Pten inactivation alters peripheral B lymphocyte fate and reconstitutes CD19 function. *Nat Immunol* **4**, 287-294.

- Apollonio, B., Scielzo, C., Bertilaccio, M. T. S., Hacken, Ten, E., Scarfo, L., Ranghetti, P., Stevenson, F., Packham, G., Ghia, P., Muzio, M., et al. (2013). Targeting B-cell anergy in chronic lymphocytic leukemia. *Blood* **121**, 3879–3888.
- Astoul, E., Watton, S. and Cantrell, D. (1999). The Dynamics of Protein Kinase B Regulation during B Cell Antigen Receptor Engagement. *J Cell Biol* **145**, 1511-1520.
- Backer, R., Schwandt, T., Greuter, M., Oosting, M., Jungerkes, F., Tuting, T., Boon, L., O'Toole, T., Kraal, G. and Limmer, A., et al. (2010). Effective collaboration between marginal metallophilic macrophages and CD8+ dendritic cells in the generation of cytotoxic T cells. *Proc Natl Acad Sci U S A* **107**, 216–221.
- Balázs, M., Martin, F., Zhou, T. and Kearney, J. F. (2002). Blood dendritic cells interact with splenic marginal zone B cells to initiate T-independent immune responses. *Immunity* **17**, 341–352.
- Barreau, F., Meinzer, U., Chareyre, F., Berrebi, D., Niwa-Kawakita, M., Dussallant, M., Foligne, B., Ollendorff, V., Heyman, M., Bonacorsi, S., et al. (2007). CARD15/NOD2 is required for Peyer's patches homeostasis in mice. *PLoS ONE* **2**, e523.
- Barreto, V., Reina-San-Martin, B., Ramiro, A. R., McBride, K. M. and Nussenzweig, M. C. (2003). C-terminal deletion of AID uncouples class switch recombination from somatic hypermutation and gene conversion. *Mol Cell* **12**, 501–508.
- Batten, M., Groom, J., Cachero, T. G., Qian, F., Schneider, P., Tschopp, J., Browning, J. L. and Mackay, F. (2000). Baff mediates survival of peripheral immature B lymphocytes. *J Exp Med* **192**, 1453-1466.
- Baumgarth, N., Tung, J. W. and Herzenberg, L. A. (2005). Inherent specificities in natural antibodies: a key to immune defense against pathogen invasion. *Springer Semin Immun* **26**, 347–362.
- Bellacosa, A., Testa, J. R., Staal, S. P. and Tsichlis, P. N. (1991). A retroviral oncogene, akt, encoding a serine-threonine kinase containing an SH2-like region. *Science* **254**, 274-277.
- Benschop, R. J. and Cambier, J. C. (1999). B cell development: signal transduction by antigen receptors and their surrogates. *Curr Opin Immunol* **11**, 143–151.
- Berek, C., Berger, A. and Apel, M. (1991). Maturation of the immune response in germinal centers. *Cell* **67**, 1121-1229.
- Bernier, G. M. and Cebra, J. J. (1964). Polypeptide chains of human gamma-globulin: Cellular localization by fluorescent antibody. *Science* **3626**, 1590-1591.
- Biggs, W. H., Meisenhelder, J., Hunter, T., Cavenee, W. K. and Arden, K. C. (1999). Protein kinase B/Akt-mediated phosphorylation promotes nuclear exclusion of the winged helix transcription factor FKHR1. *Proc Natl Acad Sci U S A* **96**, 7421-7426.
- Bommhardt, U., Chang, K. C., Swanson, P. E., Wagner, T. H., Tinsley, K. W., Karl, I. E. and Hotchkiss, R. S. (2004). Akt decreases lymphocyte apoptosis and improves survival in sepsis. *J Immunol* **172**, 7583–7591.
- Bonnefoy, J.-Y., Aubry, J.-P., Peronne, C., Wijdenes, J., and Banchereau, J. (1987). Production and characterization of a monoclonal antibody specific for the human lymphocyte low affinity receptor for IgE: CD23 is a low affinity receptor for IgE. *J Immunol* **138**, 2970-2978.
- Boumsell, L., Bernard, A., Lepage, V., Degos, L., Lemerle, J. and Dausset, J. (1978). Some chronic lymphocytic leukemia cells bearing surface immunoglobulins share determinants with T cells. *Eur J Immunol* **12**, 900-904.

- Bransteitter, R., Pham, P., Scharff, M. D. and Goodman, M. F.** (2003). Activation-induced cytidine deaminase deaminates deoxycytidine on single-stranded DNA but requires the action of RNase. *Proc Natl Acad Sci U S A* **100**, 4102–4107.
- Broche, F and Tellado, J. M.** (2001). Defense mechanism of the peritoneal cavity. *Curr Opin Crit Care* **2**, 105–116.
- Brodbeck, D., Cron, P. and Hemmings, B. A.** (1999). A human protein kinase B with regulatory phosphorylation sites in the activation loop and in the C-terminal hydrophobic domain. *J Biol Chem* **274**, 9133–9136.
- Brown, E. J., Albers, M. W., Bum Shin, T., Ichikawa, K., Keith, C. T., Lane, W. S. and Schreiber, S. L.** (1994). A mammalian protein targeted by G1-arresting rapamycin–receptor complex. *Nature* **369**, 756–758.
- Brownawell, A. M., Kops, G. J. P. L., Macara, I. G. and Burgering, B. M. T.** (2001). Inhibition of nuclear import by protein kinase B (Akt) regulates the subcellular distribution and activity of the Forkhead transcription factor AFX. *Mol Cell Biol* **21**, 3534–3546.
- Brunet, A., Bonni, A., Zigmond, M. J., Lin, M. Z., Juo, P., Hu, L. S., Anderson, M. J., Arden, K. C., Blenis, J. and Greenberg, M. E.** (1999). Akt promotes cell survival by phosphorylating and inhibiting a Forkhead transcription factor. *Cell* **96**, 857–868.
- Burger, J. A., Ghia, P., Rosenwald, A. and Caligaris-Cappio, F.** (2009a). The microenvironment in mature B-cell malignancies: a target for new treatment strategies. *Blood* **114**, 3367–3375.
- Burger, J. A., Quiroga, M. P., Hartmann, E., Burkle, A., Wierda, W. G., Keating, M. J. and Rosenwald, A.** (2009b). High-level expression of the T-cell chemokines CCL3 and CCL4 by chronic lymphocytic leukemia B cells in nurselike cell cocultures and after BCR stimulation. *Blood* **113**, 3050–3058.
- Burger, J. A., Tsukada, N., Burger, M., Zvaifler, N. J., Dell'Aquila, M. and Kipps, T. J.** (2000). Blood-derived nurse-like cells protect chronic lymphocytic leukemia B cells from spontaneous apoptosis through stromal cell–derived factor-1. *Blood* **96**, 2655–2663.
- Burgering, B. M. T. and Coffey, P. J.** (1995). Protein kinase B (c-Akt) in phosphatidylinositol-3-OH kinase signal transduction. *Nature* **376**, 599–602.
- Burgering, B. M. T., Kops, G. J. P. L., Ruiters, N. D. de, De Vries-Smits, A. M. M., Powell, D. R. and Bos, J. L.** (1999). Direct control of the Forkhead transcription factor AFX by protein kinase B. *Nature* **398**, 630–634.
- Cafferkey, R., Young, P. R., McLaughlin, M. M., Bergsma, D.J., Koltin, Y., Sathe, G.M., Faucette, L., Eng, W. K., Johnson, R. K. and Livi, G. P.** (1993). Dominant missense mutations in a novel yeast protein related to mammalian phosphatidylinositol 3-kinase and VPS34 abrogate rapamycin cytotoxicity. *Mol Cell Biol* **13**, 6012–6023.
- Calame, K. L., Lin, K.-I. and Tunyaplin, C.** (2003). Regulatory mechanisms that determine the development and function of plasma cells. *Annu Rev Immunol* **21**, 205–230.
- Calamito, M., Juntilla, M. M., Thomas, M., Northrup, D. L., Rathmell, J., Birnbaum, M. J., Koretzky, G. and Allman, D.** (2010). Akt1 and Akt2 promote peripheral B-cell maturation and survival. *Blood* **115**, 4043–4050.
- Caligaris-Cappio, F.** (1996). B-chronic lymphocytic leukemia: a malignancy of anti-self B cells. *Blood* **87**, 2615–2620.
- Caligaris-Cappio, F., Gobbi, M., Bofill, M. and Janossy, G.** (1982). Infrequent normal B lymphocytes express features of B-chronic lymphocytic leukemia. *J Exp Med* **155**, 623–628.

- Caligaris-Cappio, F. and Janossy, G.** (1985). Surface markers in chronic lymphoid leukemias of B cell type. *Semin Hematol* **22**, 1-12.
- Cambier, J. C., Gauld, S. B., Merrell, K. T. and Vilen, B. J.** (2007). B-cell anergy: from transgenic models to naturally occurring anergic B cells? *Nat Rev Immunol* **7**, 633-643.
- Cambier, J. C., Pleiman, C. M. and Clark, M. R.** (1994). Signal transduction by the B cell antigen receptor and its coreceptors. *Annu Rev Immunol* **12**, 457-486.
- Campbell, K. S.** (1999). Signal transduction from the B cell antigen-receptor. *Curr Opin Immunol* **3**, 256-64.
- Campbell, M. A. and Sefton, B. M.** (1992). Association between B-lymphocyte membrane immunoglobulin and multiple members of the Src family of protein tyrosine kinases. *Mol Cell Biol* **12**, 2315-2321.
- Cariappa, A. and Pillai, S.** (2002). Antigen-dependent B-cell development. *Curr Opin Immunol* **14**, 241-249.
- Cariappa, A., Liou, H. C., Horwitz, B. H. and Pillai, S.** (2000). Nuclear factor kappa B is required for the development of marginal zone B lymphocytes. *J Exp Med* **192**, 1175-1182.
- Cariappa, A., Tang, M., Parng, C., Nebelitskiy, E., Carroll, M., Georgopoulos, K. and Pillai, S.** (2001). The Follicular versus Marginal Zone B Lymphocyte Cell Fate Decision Is Regulated by Aiolos, Btk, and CD21. *Immunity* **14**, 603-615.
- Cardone, M. H., Roy, N., Stennicke, H. R., Salvesen, G. S., Franke, T. F., Stanbridge, E., Frisch, S. and Reed, J. C.** (1998). Regulation of cell death protease caspase-9 by phosphorylation. *Science* **282**, 1318-1321.
- Carter, R. H. and Fearon, D. T.** (1992). CD19: lowering the threshold for antigen receptor stimulation of B lymphocytes. *Science* **256**, 105-107.
- Casola, S., Otipoby, K. L., Alimzhanov, M., Humme, S., Uyttersprot, N., Kutok, J. L., Carroll, M. C. and Rajewsky, K.** (2004). B cell receptor signal strength determines B cell fate. *Nat Immunol* **5**, 317-327.
- Cebra, J. J., Logan, A. C. and Weinstein, P. D.** (1991). The preference for switching to expression of the IgA isotype of antibody exhibited by B lymphocytes in Peyer's patches is likely due to intrinsic properties of their microenvironment. *Immunol Res* **10**, 393-395.
- Chacko, G. W., Tridandapani, S., Damen, J. E., Liu, L., Krystal, G. and Coggeshall, K. M.** (1996). Negative signaling in B lymphocytes induces tyrosine phosphorylation of the 145-kDa inositol polyphosphate 5-phosphatase, SHIP. *J Immunol* **157**, 2234-2238.
- Chan, V. W., Lowell, C. A. and DeFranco, A. L.** (1998). Defective negative regulation of antigen receptor signaling in Lyn-deficient B lymphocytes. *Curr Biol* **10**, 545-553.
- Chaudhuri, J. and Alt, F. W.** (2004). Class-switch recombination: interplay of transcription, DNA deamination and DNA repair. *Nat Immunol* **4**, 541-552.
- Chaudhuri, J., Tian, M., Khuong, C., Chua, K., Pinaud, E. and Alt, F. W.** (2003). Transcription-targeted DNA deamination by the AID antibody diversification enzyme. *Nature* **422**, 726-730.
- Chen, J., Limon, J. J., Blanc, C., Peng, S. L. and Fruman, D. A.** (2010). Foxo1 regulates marginal zone B-cell development. *Eur J Immunol* **40**, 1890-1896.
- Chen, X., Wang, X., Keaton, J. M., Reddington, F., Illarionov, P. A., Besra, G. S. and Gumperz, J. E.** (2007). Distinct endosomal trafficking requirements for presentation of autoantigens exogenous lipids by human CD1d molecules. *J Immunol* **10**, 6181-6190.

- Cheng, J. Q., Godwin, A. K., Bellacosa, A., Taguchi, T., Franke, T. F., Hamilton, T. C., Tsichlis, P. N. and Testa, J. R.** (1992). AKT2, a putative oncogene encoding a member of a subfamily of protein-serine/threonine kinases, is amplified in human ovarian carcinomas. *Proc Natl Acad Sci U S A* **89**, 9267-9271.
- Cheng, J. Q., Ruggeri, B., Klein, W. M., Sonoda, G., Altomare, D. A., Watson, D. K. and Testa, J. R.** (1996). Amplification of AKT2 in human pancreatic cells and inhibition of AKT2 expression and tumorigenicity by antisense RNA. *Proc Natl Acad Sci U S A* **93**, 3636-4641.
- Chiang, G. G. and Abraham, R. T.** (2005). Phosphorylation of Mammalian Target of Rapamycin (mTOR) at Ser-2448 Is Mediated by p70S6 Kinase. *J Biol Chem* **27**, 25485-25490
- Chiorazzi, N. and Ferrarini, M.** (2003). B Cell chronic lymphocytic leukemia: Lessons Learned from Studies of the B Cell Antigen Receptor. *Annu Rev Immunol* **21**, 841-894.
- Chiorazzi, N. and Ferrarini, M.** (2011). Cellular origin(s) of chronic lymphocytic leukemia: cautionary notes and additional considerations and possibilities. *Blood* **117**, 1781-1791.
- Chiorazzi, N., Rai, K. R. and Ferrarini, M.** (2005). Chronic Lymphocytic Leukemia. *N Engl J Med* **352**, 804-815.
- Cho, H.** (2001). Insulin Resistance and a Diabetes Mellitus-Like Syndrome in Mice Lacking the Protein Kinase Akt2 (PKBbeta). *Science* **292**, 1728-1731.
- Cho, H., Thorvaldsen, J. L., Chu, Q., Feng, F. and Birnbaum, M. J.** (2001). Akt1/PKBa is required for normal growth but dispensable for maintenance of glucose homeostasis in mice. *J Biol Chem* **276**, 3849-3852.
- Clayton, E., Bardi, G., Bell, S. E., Chantry, D., Downes, C. P., Gray, A., Humphries, L. A., Rawlings, D., Reynolds, H., Vigorito, E. and Turner, M.** (2002). A crucial role for the p110delta subunit of phosphatidylinositol 3-kinase in B cell development and activation. *J Exp Med* **196**, 753-763.
- Coffer, P. J. and Woodgett, J. R.** (1991). Molecular cloning and characterisation of a novel putative protein-serine kinase related to the cAMP-dependent and protein kinase C families. *Eur J Biochem* **201**, 475-481.
- Cohen, M. M.** (2013). The AKT Genes and Their Roles in Various Disorders. *Am J Med Genet A* **161A**, 2931-2937.
- Cohen, P., Alessi, D. R. and Cross, D. A. E.** (1997). PDK1, one of the missing links in insulin signal transduction? *FEBS Lett* **410**, 3-10.
- Coico, R. F., Bhogal, B. S. and Thorbecke, G. J.** (1983). Relationship of germinal centers in lymphoid tissue to immunologic memory. VI. Transfer of B cell memory with lymph node cells fractionated according to their receptors for peanut agglutinin. *J Immunol* **131**, 2254-2257.
- Cooke, M. P., Heath, A. W., Shokat, K. M., Zeng, Y., Finkelman, F. D., Linsley, P. S., Howard, M. and Goodnow, C. C.** (1994). Immunoglobulin signal transduction guides the specificity of B cell-T cell interactions and is blocked in tolerant self-reactive B cells. *J Exp Med* **179**, 425-438.
- Cornall, R. J., Cyster, J.G., Hibbs, M. L., Dunn, A. R., Otipoby, K. L., Clark, E. A. and Goodnow CC.** (1998). Polygenic autoimmune traits: Lyn, CD22, and SHP-1 are limiting elements of a biochemical pathway regulating BCR signaling and selection. *Immunity* **4**, 497-508.
- Cross, D. A. E., Alessi, D. R., Cohen, P., Andjelkovich, M. and Hemmings, B. A.** (1995). Inhibition of glycogen synthase kinase-3 by insulin mediated by protein kinase B. *Nature* **378**, 785-789.
- Cumano, A. and Rajewsky, K.** (1985). Structure of primary anti-(4-hydroxy-3-nitrophenyl)acetyl (NP) antibodies in normal and idiotypically suppressed C57BL/6 mice. *Eur J Immunol* **15**, 512-520.

- Currie, R. A., Walker, K.S., Gray, A., Deak, M., Casamayor, A., Downes, C. P., Cohen, P., Alessi, D. R. and Lucocq, J. (1999). Role of phosphatidylinositol 3,4,5-trisphosphate in regulating the activity and localization of 3-phosphoinositide-dependent protein kinase-1. *Biochem J* **337**, 575-583.
- Dan, H. C., Cooper, M. J., Cogswell, P. C., Duncan, J. A., Ting, J. P. and Baldwin, A. S. (2008). Akt-dependent regulation of NF-kappaB is controlled by mTOR and Raptor in association with IKK. *Genes Dev* **22**, 1490-1500.
- Datta, S. R., Brunet, A. and Greenberg, M. E. (1999). Cellular survival: a play in three Akts. *Genes Dev* **13**, 2905-2927.
- Datta, S. R., Dudek, H., Tao, X., Masters, S., Fu, H., Gotoh, Y. and Greenberg, M. E. (1997). Akt phosphorylation of BAD couples survival signals to the cell-intrinsic death machinery. *Cell* **91**, 231-241.
- Datta, K., Franke, T. F., Chan, T. O., Makris, A., Yang, S. I., Kaplan, D. R., Morrison, D. K., Golemis, E. A. and Tsichlis, P. N. (1995). AH/PH domain-mediated interaction between Akt molecules and its potential role in Akt regulation. *Mol Cell Biol* **15**, 2304-2310.
- Dengler, H. S., Baracho, G. V., Omori, S. A., Bruckner, S., Arden, K. C., Castrillon, D. H., DePinho, R. A. and Rickert, R. C. (2008). Distinct functions for the transcription factor Foxo1 at various stages of B cell differentiation. *Nat Immunol* **9**, 1388-1398.
- Dickerson, S. K., Market, E., Besmer, E. and Papavasiliou, F. N. (2003). AID Mediates Hypermutation by Deaminating Single Stranded DNA. *J Exp Med* **197**, 1291-1296.
- Doi, T., Kato, L., Ito, S., Shinkura, R., Wei, M., Nagaoka, H., Wang, J. and Honjo, T. (2009). The C-terminal region of activation-induced cytidine deaminase is responsible for a recombination function other than DNA cleavage in class switch recombination. *Proc Natl Acad Sci U S A* **106**, 2758-2763.
- Doi, T., Kinoshita, K., Ikegawa, M., Muramatsu, M. and Honjo, T. (2003). De novo protein synthesis is required for the activation-induced cytidine deaminase function in class-switch recombination. *Proc Natl Acad Sci U S A* **100**, 2634-2638.
- Engel, P., Zhou, L.-J., Ord, D. C., Sato, S., Koller, B. and Tedder, T. F. (1995). Abnormal B lymphocyte development, activation, and differentiation in mice that lack or overexpress the CD19 signal transduction molecule. *Immunity* **3**, 39-50.
- Esser, C., Radbruch, A. (1990). Immunoglobulin class switching - molecular and cellular analysis. *Annu Rev Immunol* **8**, 717-735.
- Essers, M. A., de Vries-Smits, L. M., Barker, N., Polderman, P. E., Burgering, B. M. and Korswagen, H. C. (2005). Functional interaction between beta-catenin and FOXO in oxidative stress signaling. *Science* **308**, 1181-1184.
- Fearon, D. T., Carroll, M. C. and Carroll, M. C. (2000). Regulation of B Lymphocyte Responses to Foreign and Self-Antigens by the CD19/CD21 Complex. *Annu Rev Immunol* **18**, 393-422.
- Fluckiger, A.-C., Li, Z., Kato, R. M., Wahl, M. I., Ochs, H. D., Longnecker, R., Kinet, J.-P., Witte, O. N., Scharenberg, A. M. and Rawlings, D. J. (1998). Btk/Tec kinases regulate sustained increases in intracellular Ca²⁺ following B-cell receptor activation. *EMBO J* **17**, 1973-1985.
- Franke, T. F. (1997). Direct Regulation of the Akt Proto-Oncogene Product by Phosphatidylinositol-3,4-bisphosphate. *Science* **275**, 665-668.
- Franke, T. F., Yang, S. I., Chan, T. O., Datta, K., Kazlauskas, A., Morrison, D. K., Kaplan, D. R. and Tsichlis, P. N. (1995). The protein kinase encoded by the Akt proto-oncogene is a target of the PDGF-activated phosphatidylinositol 3-kinase. *Cell* **81**, 727-736.

- Frech, M., Andjelkovic, M., Ingle, E., Reddy, K. K., Falck, J. R. and Hemmings, B. A.** (1997). High affinity binding of inositol phosphates and phosphoinositides to the pleckstrin homology domain of RAC/Protein kinase B and their influence on kinase activity. *J Biol Chem* **272**, 8474–8481.
- Frias, M. A., Thoreen, C. C., Jaffe, J. D., Schroder, W., Sculley, T., Carr, S. A. and Sabatini D. M.** (2006). mSin1 is necessary for Akt/PKB phosphorylation, and its isoforms define three distinct mTORC2s. *Curr Biol* **16**, 1865–1870.
- Fruman, D. A., Satterthwaite, A. B. and Witte, O. N.** (2000). Xid-like Phenotypes. *Immunity* **13**, 1–3.
- Fruman D. A., Snapper, S. B., Yballe, C. M., Davidson, L., Yu, J. Y., Alt, F. W., Cantley, L. C.** (1999). Impaired B cell development and proliferation in absence of phosphoinositide 3-kinase p85 α . *Science* **283**, 393–397.
- Fütterer, K., Wong, J., Grucza, R. A., Chan, A.C. and Waksman. G.** (1998). Structural basis for Syk tyrosine kinase ubiquity in signal transduction pathways revealed by the crystal structure of its regulatory SH2 domains bound to a dually phosphorylated ITAM peptide. *J Mol Biol* **281**, 523–537.
- Fu, C., Turck, C. W., Kurosaki, T. and Chan, A. C.** (1998). BLNK: a central linker protein in B cell activation. *Immunity* **1**, 93–103.
- Fujiwara, H., Kikutani, H., Suematsu, S., Naka, T., Yoshida, K., Yoshida, K., Tanaka, T., Suemura, M., Matsumoto, N., Kojima, S., et al.** (1994). The absence of IgE antibody-mediated augmentation of immune responses in CD23-deficient mice. *Proc Natl Acad Sci U S A* **91**, 6835–6839.
- Gagnerault, M. C., Luan, J. J., Lotton, C. and Lepault, F.** (2002). Pancreatic lymph nodes are required for priming of beta cell reactive T cells in NOD mice. *J Exp Med* **196**, 369–377.
- Genestier, L., Taillardet, M., Mondiere, P., Gheit, H., Bella, C. and Defrance, T.** (2007). TLR agonists selectively promote terminal plasma cell differentiation of B cell subsets specialized in thymus-independent responses. *J Immunol* **178**, 7779–7786.
- George, S.** (2004). A Family with severe insulin resistance and diabetes due to a mutation in AKT2. *Science* **304**, 1325–1328.
- Gergely, J., Pecht, I. and Sármay, G.** (1999). Immunoreceptor tyrosine-based inhibition motif-bearing receptors regulate the immunoreceptor tyrosine-based activation motif-induced activation of immune competent cells. *Immunol Lett* **68**, 3–15.
- Gibb, D. R., El Shikh, M., Kang, D. J., Rowe, W. J., El Sayed, R., Cichy, J., Yagita, H., Tew, J. G., Dempsey, P. J. and Crawford, H. C.** (2010). ADAM10 is essential for Notch2-dependent marginal zone B cell development and CD23 cleavage in vivo. *J Exp Med* **207**, 623–635.
- Gold, M. R., Ingham, R. J., McLeod, S. J., Christian, S. L., Scheid, M. P., Duronio, V., Santos, L. and Matsuuchi, L.** (2000). Targets of B-cell antigen receptor signaling: the phosphatidylinositol 3-kinase/Akt/glycogen synthase kinase-3 signaling pathway and the Rap1 GTPase. *Immunol Rev* **176**, 47–68.
- Goodnow, C. C.** (1997). Balancing Immunity, Autoimmunity, and self-tolerance. *Ann N Y Acad Sci* **815**, 55–60.
- Goodnow, C. C., Sprent, J., de St Groth, B. F. and Vinuesa, C. G.** (2005). Cellular and genetic mechanisms of self tolerance and autoimmunity. *Nature* **435**, 590–597.
- Gould, H. J. and Sutton, B. J.** (2008). IgE in allergy and asthma today. *Nat Rev Immunol* **8**, 205–217.
- Grande, S. M., Bannish, G., Fuentes-Panana, E. M., Katz, E. and Monroe, J. G.** (2007). Tonic B-cell and viral ITAM signaling: context is everything. *Immunol Rev* **218**, 214–234.

- Gray, D., MacLennan, I. C. M., Bazin, H. and Khan, M. (1982). Migrant $\mu+\delta+$ and static $\mu+\delta-$ B lymphocyte subsets. *Eur J Immunol* **12**, 564–569.
- Gray, D., McConnell, I., Kumararatne, D. S., MacLennan, I. C. M., Humphrey, J. H. and Bazin, H. (1984). Marginal zone B cells express CR1 and CR2 receptors. *Eur J Immunol* **14**, 47–52.
- Groom, J., Kalled, S. L., Cutler, A. H., Olson, C., Woodcock, S. A., Schneider, P., Tschoopp, J., Cachero, T. G., Batten, M., Wheway, J., Mauri, D., Cavill, D., Gordon, T. P., Mackay, C. R. and Mackay, F. (2002). Association of BAFF/BLyS overexpression and altered B cell differentiation with Sjögren's syndrome. *J Clin Invest* **109**, 59–68.
- Grouard, G., Durand, I., Filgueira, L., Banchereau, J. and Liu, Y.-J. (1996). Dendritic cells capable of stimulating T cells in germinal centres. *Nature* **384**, 364–367.
- Grucza, R. A., Fütterer, K., Chan, A. C. and Waksman, A. G. (1999). Thermodynamic Study of the Binding of the Tandem-SH2 Domain of the Syk Kinase to a Dually Phosphorylated ITAM Peptide: Evidence for Two Conformers. *Biochemistry* **38**, 5024–5033.
- Gu, H., Zou, R. Z. and Rajewsky, K. (1993). Independent control of immunoglobulin switch recombination at individual switch regions evidenced through Cre-loxP-mediated gene targeting. *Cell* **73**, 1155–1164.
- Haar, E. V., Lee, S.-I., Bandhakavi, S., Griffin, T. J. and Kim, D.-H. (2007). Insulin signalling to mTOR mediated by the Akt/PKB substrate PRAS40. *Nat Cell Biol* **9**, 316–323.
- Hampel, F., Ehrenberg, S., Hojer, C., Draeseke, A., Marschall-Schröter, G., Kühn, R., Mack, B., Gires, O., Vahl, C. J. and Schmidt-Suppran, M. (2011). CD19-independent instruction of murine marginal zone B-cell development by constitutive Notch2 signaling. *Blood* **118**, 6321–6331.
- Hanada, M., Feng, J. and Hemmings, B. A. (2004). Structure, regulation and function of PKB/AKT—a major therapeutic target. *BBA Prot Proteom* **1697**, 3–16.
- Hao, Z. and Rajewsky, K. (2001). Homeostasis of peripheral B cells in the absence of B cell influx from the bone marrow. *J Exp Med* **194**, 1151–1164.
- Hara, K., Maruki, Y., Long, X., Yoshino, K.-I., Oshiro, N., Hidayat, S., Tokunaga, C., Avruch, J. and Yonezawa, K. (2002). Raptor, a binding partner of target of rapamycin (TOR), mediates TOR action. *Cell* **110**, 177–189.
- Hardy, R. R., Carmack, C. E., Shinton, S. A., Kemp, J. D. and Hayakawa, K. (1991). Resolution and characterization of pro-B and pre-pro-B cell stages in normal mouse bone marrow. *J Exp Med* **173**, 1213–1225.
- Hardy, R. R. and Hayakawa, K. (2001). B cell development pathways. *Annu Rev Immunol* **19**, 595–621.
- Harris, R. S., Petersen-Mahrt S. K. and Neuberger, M.S. (2002). RNA editing enzyme APOBEC1 and some of its homologs can act as DNA mutators. *Mol Cell* **10**, 1247–1253.
- Hasler, J., Rada, C. and Neuberger, M. S. (2011). Cytoplasmic activation-induced cytidine deaminase (AID) exists in stoichiometric complex with translation elongation factor 1 (eEF1A). *Proc Natl Acad Sci U S A* **108**, 18366–18371.
- Havran, W. L., DiGiusto, D. L. and Cambier, J. C. (1984). mIgM:mIgD ratios on B cells: mean mIgD expression exceeds mIgM by 10-fold on most splenic B cells. *J Immunol* **132**, 1712–1716.
- Healy, J. I., Dolmetsch, R. E., Timmerman, L. A., Cyster, J. G., Thomas, M. L., Crabtree, G. R., Lewis, R. S. and Goodnow, C. C. (1997). Different nuclear signals are activated by the B cell receptor during positive versus negative signaling. *Immunity* **6**, 419–428.

- Herling, M., Patel, K. A., Khalili, J., Schlette, E., Kobayashi, R., Medeiros, L. J. and Jones, D.** (2006). TCL1 shows a regulated expression pattern in chronic lymphocytic leukemia that correlates with molecular subtypes and proliferative state. *Leukemia* **20**, 280–285.
- Hermiston, M. L., Xu, Z. and Weiss, A.** (2003). CD45: A critical regulator of signaling thresholds in immune cells. *Annu Rev Immunol* **21**, 107–137.
- Herzenberg, L. A., Black, S. J., Tokuhi, T., Herzenberg, L. A.** (1980). Memory B cells at successive stages of differentiation. Affinity maturation and the role of IgD receptors. *J Exp Med* **5**, 1071–1087.
- Hinman, R. M., Nichols, W. A., Diaz, T. M., Gallardo, T. D., Castrillon, D. H. and Satterthwaite, A. B.** (2009). Foxo3^{-/-} mice demonstrate reduced numbers of pre-B and recirculating B cells but normal splenic B cell sub-population distribution. *Int Immunol* **21**, 831–842.
- Höglund, P., Mintern, J., Waltzinger, C., Heath, W., Benoist, C and Mathis, D.** (1999). Initiation of autoimmune diabetes by developmentally regulated presentation of islet cell antigens in the pancreatic lymph nodes. *J Exp Med* **2**, 331–339.
- Hofbauer, S. W., Pinon, J. D., Bracht, G., Haginger, L., Wang, W., Johrer, K., Tinhofer, I., Hartmann, T. N. and Greil, R.** (2010). Modifying akt signaling in B-cell chronic lymphocytic leukemia cells. *Cancer Research* **70**, 7336–7344.
- Hogan, B., Constantini, F. and Lacy, I.** (1987). Manipulating the mouse embryo. Second Edition. Cold Spring Harbor Laboratory Press.
- Honjo, T. T. K.** (1978). Organization of immunoglobulin heavy chain genes and allelic deletion model. *Proc Natl Acad Sci U S A* **75**, 2140–2144.
- Honjo, T., Kinoshita, K. and Muramatsu, M.** (2002). Molecular mechanism of class switch recombination: linkage with somatic hypermutation. *Annu Rev Immunol* **20**, 165–196.
- Hsu, S. M.** (1985). Phenotypic expression of B lymphocytes. III. Marginal zone B cells in the spleen are characterized by the expression of Tac and alkaline phosphatase. *J Immunol* **135**, 123–130.
- Inoki, K., Li, Y., Zhu, T., Wu, J. and Guan, K.-L.** (2002). TSC2 is phosphorylated and inhibited by Akt and suppresses mTOR signalling. *Nat Cell Biol* **4**, 648–657.
- Ito, S., Nagaoka, H., Shinkura, R., Begum, N., Muramatsu, M., Nakata, M. and Honjo, T.** (2004). Activation-induced cytidine deaminase shuttles between nucleus and cytoplasm like apolipoprotein B mRNA editing catalytic polypeptide 1. *Proc Natl Acad Sci U S A* **101**, 1975–1980.
- Iwasato, T., Shimizu, A., Honjo, T. and Yamagishi, H.** (1990). Circular DNA is excised by immunoglobulin class switch recombination. *Cell* **62**, 143–149.
- Jaakkola, I., Jalkanen, S. and Hänninen, A.** (2003). Diabetogenic T cells are primed both in pancreatic and gut-associated lymph nodes in NOD mice. *Eur J Immunol* **33**, 3255–3264.
- Jacinto, E., Facchinetti, V., Liu, D., Soto, N., Wei, S., Jung, S. Y., Huang, Q., Qin, J. and Su, B.** (2006). SIN1/MIP1 Maintains rictor-mTOR complex integrity and regulates Akt phosphorylation and substrate specificity. *Cell* **127**, 125–137.
- Jacinto, E., Loewith, R., Schmidt, A., Lin, S., Ruegg, M. A., Hall, A. and Hall, M. N.** (2004). Mammalian TOR complex 2 controls the actin cytoskeleton and is rapamycin insensitive. *Nat Cell Biol* **6**, 1122–1128.
- Jacob, J., Kelsoe, G., Rajewsky, K. and Weiss, U.** (1991). Intraclonal generation of antibody mutants in germinal centres. *Nature* **354**, 389–392.

- James, S. R., Downes, C. P., Gigg, R., Grove, S. J., Holmes, A. B. and Alessi, D. R.** (1996). Specific binding of the Akt-1 protein kinase to phosphatidylinositol 3,4,5-trisphosphate without subsequent activation. *Biochem J* **315**, 709-713.
- Jenner, E.** (2014). Serum free light chains in clinical laboratory diagnostics. *Clin Chim Acta* **427**; 15-20.
- Jeong, S. J., Dasgupta, A., Jung, K. J., Um, J. H., Burke, A., Park, H. U. and Brady, J. N.** (2008). PI3K/AKT inhibition induces caspase-dependent apoptosis in HTLV-1-transformed cells. *Virology* **370**, 264-272.
- Jiang, A., Craxton, A., Kurosaki, T. and Clark, E. A.** (1998). Different protein tyrosine kinases are required for B cell antigen receptor-mediated activation of extracellular signal-regulated kinase, c-Jun NH2-terminal kinase 1, and p38 mitogen-activated protein kinase. *J Exp Med* **188**, 1297-1306.
- Jones, P.F., Jakubowicz, T. and Hemmings, B. A.** (1991b). Molecular cloning of a second form of rac protein kinase. *Cell Regul* **2**, 1001-1009.
- Jones, P. F., Jakubowicsi, Pitossi, F. J., Maurer, F. and Hemmings, B. A.** (1991a). Molecular cloning and identification of a serine/threonine protein kinase of the second-messenger subfamily. *Proc Natl Acad Sci U S A* **88**, 4171-4175.
- Jung, D., Giallourakis, C., Mostoslavsky, R. and Alt, F. W.** (2006). Mechanism and control of V(D)J recombination at the immunoglobulin heavy chain locus. *Annu Rev Immunol* **24**, 541-570.
- Jung, C., Hugot, J.-P. and Barreau, F.** (2010). Peyer's Patches: The Immune Sensors of the Intestine. *Int J Inflam* **2010**, 1-12.
- Kahl, B. and Yang, D.** (2008). Marginal zone lymphomas: Management of nodal, splenic, and MALT NHL. *Hematology Am Soc Hematol Educ Program* **2008**, 359-364.
- Kang, J. A., Kim, S. and Park, S. G.** (2014). Notch1 is an important mediator for enhancing of B-cell activation and antibody secretion by Notch ligand. *Immunology* **143(4)**:550-559.
- Kantor, A. B. and Herzenberg, L. A.** (1993). Origin of murine B cell lineages. *Annu Rev Immunol* **11**, 501-538.
- Kantor, A. B., Merrill, C. E., Herzenberg, L. A. and Hillson, J. L.** (1997). An unbiased analysis of V(H)-D-J(H) sequences from B-1a, B-1b, and conventional B cells. *J Immunol* **158**, 1175-1186.
- Kantor, A. B., Stall, A. M., Adams, S., Herzenberg, L. A. and Herzenberg, L. A.** (1992). Differential development of progenitor activity for three B-cell lineages. *Proc Natl Acad Sci U S A* **89**, 3320-3324.
- Karasuyama, H., Kudo, A. and Melchers, F.** (1990). The proteins encoded by the VpreB and lambda 5 pre-B cell-specific genes can associate with each other and with mu heavy chain. *J Exp Med* **172**, 969-972.
- Kataoka, T., Kawakami, T., Takahashi, N. and Honjo, T.** (1980). Rearrangement of immunoglobulin gamma 1-chain gene and mechanism for heavy-chain class switch. *Proc Natl Acad Sci U S A* **77**, 919-923.
- Kawamata, S., Du, C., Li, K. and Lavau, C.** (2002). Overexpression of the Notch target genes Hes in vivo induces lymphoid and myeloid alterations. *Oncogene* **24**, 3855-3863.
- Kerdiles, Y. M., Beisner, D. R., Tinoco, R., Dejean, A. S., Castrillon, D. H., DePinho, R. A. and Hedrick, S. M.** (2009). Foxo1 links homing and survival of naive T cells by regulating L-selectin, CCR7 and interleukin 7 receptor. *Nat Immunol* **10**, 176-184.

- Kerfoot, S. M., Yaari, G., Patel, J. R., Johnson, K. L., Gonzalez, D. G., Kleinstein, S. H. and Haberman, A. M.** (2011). Germinal center B cell and T follicular helper cell development initiates in the interfollicular zone. *Immunity* **34**, 947–960.
- Kim, D.-H., Sarbassov, D. D., Ali, S. M., King, J. E., Latek, R. R., Erdjument-Bromage, H., Tempst, P. and Sabatini, D. M.** (2002). mTOR interacts with raptor to form a nutrient-sensitive complex that signals to the cell growth machinery. *Cell* **110**, 163–175.
- Kim, D.-H., Sarbassov, D. D., Ali, S. M., Latek, R. R., Guntur, K. V. P., Erdjument-Bromage, H., Tempst, P. and Sabatini, D. M.** (2003). GβL, a Positive Regulator of the Rapamycin-Sensitive Pathway Required for the Nutrient-Sensitive Interaction between Raptor and mTOR. *Mol Cell* **11**, 895–904.
- Kinoshita, K., Harigai, M., Fagarasan, S., Muramatsu, M. and Honjo, T.** (2001). A hallmark of active class switch recombination: transcripts directed by I promoters on looped-out circular DNAs. *Proc Natl Acad Sci U S A* **98**, 12620–12623.
- Kohn, A. D., Summers, S. A., Birnbaum, M. J. and Roth, R. A.** (1996). Expression of a constitutively active Akt Ser/Thr Kinase in 3T3-L1 adipocytes stimulates glucose uptake and glucose transporter 4 translocation. *J Biol Chem* **271**, 31372–31378.
- Komono, Y., Kitaura, J., Watanabe-Okochi, N., Kato, N., Oki, T., Nakahara, F., Harada, Y., Harada, H., Shinkura, R., Nagaoka, H., et al.** (2010). AID T-lymphoma B-lymphoma. *Leukemia* **24**, 1018–1024.
- Konishi, H., Kuroda, S., Tanaka, M., Matsuzaki, H., Ono, Y., Kameyama, K., Haga, T. and Kikkawa, U.** (1995). Molecular cloning and characterization of a new member of the RAC protein kinase family: association of the pleckstrin homology domain of three types of RAC protein kinase with protein kinase C subspecies and beta gamma subunits of G proteins. *Biochem Biophys Res Commun* **216**, 526–534.
- Kovalchuk, A. L., Dubois, W., Mushinski, E., McNeil, N. E., Hirt, C., Qi, C. F., Li, Z., Janz, S., Honjo, T., Muramatsu, M., et al.** (2007). AID-deficient Bcl-xL transgenic mice develop delayed atypical plasma cell tumors with unusual Ig/Myc chromosomal rearrangements. *J Exp Med* **204**, 2989–3001.
- Kozak, M.** (2005). A second look at cellular mRNA sequences said to function as internal ribosome entry sites. *Nucleic Acids Res* **33**, 6593–6602.
- Kraal, G. and Janse, M.** (1986). Marginal metallophilic cells of the mouse spleen identified by a monoclonal antibody. *Immunology* **58**, 665–669.
- Kraus, M., Alimzhanov, M. B., Rajewsky, N. and Rajewsky, K.** (2004). Survival of resting mature B lymphocytes depends on BCR signaling via the Igα/β heterodimer. *Cell* **117**, 787–800.
- Kumararatne, D. S., Gagnon, R.F. and Smart, Y.** (1980). Selective loss of large lymphocytes from the marginal zone of the white pulp in rat spleens following a single dose of cyclophosphamide. A study using quantitative histological methods. *Immunology* **40**, 123–131.
- Kumararatne, D. S. and MacLennan, I. C. M.** (1981). Cells of the marginal zone of the spleen are lymphocytes derived from recirculating precursors. *Eur J Immunol* **11**, 865–869.
- Kunz, J., Henriquez, R., Schneider, U., Deuter-Reinhard, M., Movva, N. R. and Hall, M. N.** (1993). Target of rapamycin in yeast, TOR2, is an essential phosphatidylinositol kinase homolog required for G1 progression. *Cell* **73**, 585–596.
- Kurosaki, T.** (1999). Genetic analysis of B cell antigen receptor signaling. *Annu Rev Immunol* **17**, 555–592.

- Kwon, K., Hutter, C., Sun, Q., Bilic, I., Cobaleda, C., Malin, S. and Busslinger, M.** (2008). Instructive Role of the Transcription Factor E2A in Early B Lymphopoiesis and Germinal Center B Cell Development. *Immunity* **28**, 751–762.
- Laine, J., Künstle, G., Obata, T., Sha, M. and Noguchi, M.** (2000). The protooncogene TCL1 is an Akt kinase coactivator. *Mol Cell* **2**, 395–407.
- Lam, K. P., Kühn, R. and Rajewsky, K.** (1997). In vivo ablation of surface immunoglobulin on mature B cells by inducible gene targeting results in rapid cell death. *Cell* **90**, 1073–1083.
- Langman, R. E. and Cohn, M.** (1995). The proportion of B-cell subsets expressing κ and λ light chains changes following antigenic selection. *Immunol Today* **16**, 141–144.
- Lankester, A. C., van Schijndel, G. M., van der Schoot, C. E., van Oers, M. H., van Noesel, C. J. and van Lier, R. A.** (1995). Antigen receptor nonresponsiveness in chronic lymphocytic leukemia B cells. *Blood* **86**, 1090–1071.
- LeBien, T. W. and Tedder, T. F.** (2008). B lymphocytes: how they develop and function. *Blood* **112**, 1570–1580.
- Li, H. L., Davis, W. W., Whiteman, E. L., Birnbaum, M. J. and Pure, E.** (1999). The tyrosine kinases Syk and Lyn exert opposing effects on the activation of protein kinase Akt/PKB in B lymphocytes. *Proc Natl Acad Sci U S A* **96**, 6890–6895.
- Li, B., Thrasher, J. B. and Terranova, P.** (2015). Glycogen synthase kinase-3: A potential preventive target for prostate cancer management. *Urol Oncol* **11**, 456–463.
- Li, Y. S., Wasserman, R., Hayakawa, K. and Hardy, R. R.** (1996). Identification of the earliest B lineage stage in mouse bone marrow. *Immunity* **5**, 527–535.
- Limon, J. J. and Fruman, D. A.** (2012). Akt and mTOR in B cell activation and differentiation. *Front Immunol* **3**, 228.
- Lin, Y. C., Jhunjhunwala, S., Benner, C., Heinz, S., Welinder, E., Mansson, R., Sigvardsson, M., Hagman, J., Espinoza, C. A., Dutkowski, J., et al.** (2010). A global network of transcription factors, involving E2A, EBF1 and Foxo1, that orchestrates B cell fate. *Nat Immunol* **11**, 635–643.
- Liu, Y.-J., Cairns, J. A., Holder, M. J., Abbot, S. D., Jansen, K. U., Bonnefoy, K. U., Gordon, J. and MacLennan, I. C. M.** (1991). Recombinant 25-kDa CD23 and interleukin 1 alpha promote the survival of germinal center B cells: evidence for bifurcation in the development of centrocytes rescued from apoptosis. *Eur J Immunol* **21**, 1107–1114.
- Liu, P., Cheng, H., Roberts, T. M. and Zhao, J. J.** (2009). Targeting the phosphoinositide 3-kinase pathway in cancer. *Nat Rev Drug Discov* **8**, 627–644.
- Liu, Y. J., Joshua, D. E., Williams, G. T., Smith, C. A., Gordon, J. and MacLennan, I. C.** (1989). Mechanism of antigen-driven selection in germinal centres. *Nature* **342**, 929–931.
- Loder, B. F., Mutschler, B., Ray, R. J., Paige, C. J., Sideras, P., Torres, R., Lamers, M. C. and Carsetti, R.** (1999). B cell development in the spleen takes place in discrete steps and is determined by the quality of B cell receptor-derived signals. *J Exp Med* **190**, 75–90.
- Lu, T. T. and Cyster J. G.** (2002). Integrin-mediated long-term B cell retention in the splenic marginal zone. *Science* **297**, 409–412.
- MacLennan, I. C. M.** (1994). Germinal Centers. *Annu Rev Immunol* **12**, 117–139.
- MacNeal, WJ.** (1929). The circulation of blood through the spleen pulp. *Arch Pathol* **1**, 215–227.

- Mariño, E., Batten, M., Groom, J., Walters, S., Liuwantara, D., Mackay, F. and Grey, S. T.** (2008). Marginal-zone B-cells of nonobese diabetic mice expand with diabetes onset, invade the pancreatic lymph nodes, and present autoantigen to diabetogenic T-cells. *Diabetes* **57**, 395-404.
- Martin, F., Oliver, A. M. and Kearney, J. F.** (2001). Marginal zone and B1 B cells unite in the early response against T-independent blood-borne particulate antigens. *Immunity* **14**, 617-629.
- Matsumoto, Y., Marusawa, H., Kinoshita, K., Endo, Y., Kou, T., Morisawa, T., Azuma, T., Okazaki, I.-M., Honjo, T. and Chiba, T.** (2007). Helicobacter pylori infection triggers aberrant expression of activation-induced cytidine deaminase in gastric epithelium. *Nat Med* **13**, 470-476.
- Mattila, P. K., Feest, C., Depoil, D., Treanor, B., Montaner, B., Otipoby, K. L., Carter, R., Justement, L. B., Bruckbauer, A. and Batista, F. D.** (2013). The actin and tetraspanin networks organize receptor nanoclusters to regulate B cell receptor-mediated signaling. *Immunity* **38**, 461-474.
- McBride, K. M., Barreto, V., Ramiro, A. R., Stavropoulos, P. and Nussenzweig, M. C.** (2004). Somatic hypermutation is limited by CRM1-dependent nuclear export of activation-induced deaminase. *J Exp Med* **9**, 1235-1244.
- Mebius, R. E. and Kraal, G.** (2005). Structure and function of the spleen. *Nat Immunol* **5**, 606-616.
- Meffre, E., Casellas, R. and Nussenzweig, M. C.** (2000). Antibody regulation of B cell development. *Nat Immunol* **1**, 379-385.
- Meier, R., Alessi, D. R., Cron, P., Andjelkovic, M. and Hemmings, B. A.** (1997). Mitogenic activation, phosphorylation, and nuclear translocation of protein kinase B. *J Biol Chem* **272**, 30491-30497.
- Melchers, F., Karasuyama, H., Haasner, D., Bauer, S., Kudo, A., Sakaguchi, N., Jameson, B. and Rolink, A.** (1993). The surrogate light chain in B-cell development. *Immunol Today* **14**, 60-68.
- Merrell, K. T., Benschop, R. J., Gauld, S. B., Aviszus, K., Decote-Ricardo, D., Wysocki, L. J. and Cambier, J. C.** (2006). Identification of anergic B cells within a wild-type repertoire. *Immunity* **25**, 953-962.
- Michel, F., Merle-Béral, H., Legac, E., Michel, A., Debré, P. and Bismuth, G.** (1993). Defective calcium response in B-chronic lymphocytic leukemia cells. Alteration of early protein tyrosine phosphorylation and of the mechanism responsible for cell calcium influx. *J Immunol* **150**, 3624-3633.
- Mockridge, I. C., Potter, K. N., Wheatley, I., Neville, L. A., Packham, G. and Stevenson, F. K.** (2007). Reversible anergy of sIgM-mediated signaling in the two subsets of CLL defined by VH-gene mutational status. *Blood* **109**, 4424-4431.
- Monroe, J. G.** (2006). ITAM-mediated tonic signalling through pre-BCR and BCR complexes. *Nat Immunol* **6**, 283-294.
- Morgan, H. D., Dean, W., Coker, H. A., Reik, W. and Petersen-Mahrt, S. K.** (2004). Activation-induced cytidine deaminase deaminates 5-methylcytosine in DNA and is expressed in pluripotent tissues. *J Biol Chem* **279**, 52353-52360.
- Morisawa, T., Marusawa, H., Ueda, Y., Iwai, A., Okazaki, I.-M., Honjo, T. and Chiba, T.** (2008). Organ-specific profiles of genetic changes in cancers caused by activation-induced cytidine deaminase expression. *Int J Cancer* **123**, 2735-2740.
- Mullis, K. B. and Faloona, F. A.** (1987). Specific synthesis of DNA in vitro via a polymerase-catalyzed chain reaction. *Methods Enzymol* **155**, 335-350.
- Muramatsu, M., Kinoshita, K., Fagarasan, S., Yamada, S., Shinkai, Y. and Honjo, T.** (2000). Class switch recombination and hypermutation require activation-induced cytidine deaminase (AID), a potential RNA editing enzyme. *Cell* **102**, 553-563.

- Nagaoka, H.** (2002). Activation-induced deaminase (AID)-directed hypermutation in the immunoglobulin smicro region: Implication of AID involvement in a common step of class switch recombination and somatic hypermutation. *J Exp Med* **195**, 529–534.
- Nagasawa, T.** (2006). Microenvironmental niches in the bone marrow required for B-cell development. *Nat Rev Immunol* **6**, 107–116.
- Nakatani, K., Sakaue, H., Thompson, D. A., Weigel, R. J. and Roth, R. A.** (1999). Identification of a human Akt3 (protein kinase B gamma) which contains the regulatory serine phosphorylation site. *Biochem Biophys Res Commun* **257**, 906–910.
- Narducci, M. G., Virgilio, L., Isobe, M., Stoppacciaro, A., Elli, R., Fiorilli, M., Carbonari, M., Antonelli, A., Chessa, L., Croce, C. M. and Russo, G.** (1995). TCL1 oncogene activation in preleukemic T cells from a case of ataxia-telangiectasia. *Blood* **86**, 2358–2364.
- Navé, B. T., Ouwers, D. M., Withers, D. J., Alessi, D. R. and Shepherd, P. R.** (1999). Mammalian target of rapamycin is a direct target for protein kinase B: identification of a convergence point for opposing effects of insulin and amino-acid deficiency on protein translation. *Biochem. J.* **344**, 427–431.
- Nieuwenhuis, P. and Opstelten, D.** (1984). Functional anatomy of germinal centers. *Am J Anat.* **170**, 421–435.
- Niewmierzycka, A., Kurman, M., Leśniak, M., Winiarska, A., Pawłowska, A.** (2015). Prevalence and clinical significance of abnormal serum kappa/lambda light chain ratio in patients with chronic kidney disease. *Pol Arch Med Wewn* **125**, 532–537.
- Nishizumi, H., Horikawa, K., Mlinaric-Rascan, I. and Yamamoto, T.** (1998). A double-edged kinase Lyn: A positive and negative regulator for antigen receptor-mediated signals. *J Exp Med* **187**, 1343–1348.
- Nitschke, L.** (2005). The role of CD22 and other inhibitory co-receptors in B-cell activation. *Curr Opin Immunol* **17**, 290–297.
- Niwa, H., Yamamura, K. and Miyazaki, J.** (1991). Efficient selection for high-expression transfectants with a novel eukaryotic vector. *Gene* **108**, 193–199.
- Nolte, M. A., Arens, R., Kraus, M., van Oers, M. H. J., Kraal, G., van Lier, R. A. W. and Mebius, R. E.** (2004). B cells are crucial for both development and maintenance of the splenic marginal zone. *J Immunol* **172**, 3620–3627.
- Odermatt, B., Eppler, M., Leist, T. P., Hengartner, H. and Zinkernagel, R. M.** (1991). Virus-triggered acquired immunodeficiency by cytotoxic T-cell-dependent destruction of antigen-presenting cells and lymph follicle structure. *Proc Natl Acad Sci U S A* **88**, 8252–8256.
- Okazaki, I. M., Hiai, H., Kakazu, N., Yamada, S., Muramatsu, M., Kinoshita, K. and Honjo, T.** (2003). Constitutive expression of AID leads to tumorigenesis. *J Exp Med* **197**, 1173–1181.
- Oliver, A. M., Martin, F., Gartland, G. L., Carter, R. H. and Kearney, J. F.** (1997). Marginal zone B cells exhibit unique activation, proliferative and immunoglobulin secretory responses. *Eur J Immunol* **27**, 2366–2374.
- Oliver, A. M., Martin, F. and Kearney, J. F.** (1999). IgM^{high}CD21^{high} lymphocytes enriched in the splenic marginal zone generate effector cells more rapidly than the bulk of follicular B cells. *J Immunol* **162**, 7198–7207.
- Omori, S. A., Cato, M. H., Anzelon-Mills, A., Puri, K. D., Shapiro-Shelef, M., Calame, K. and Rickert, R. C.** (2006). Regulation of class-switch recombination and plasma cell differentiation by phosphatidylinositol 3-kinase signaling. *Immunity* **25**, 545–557.

- Otero, D. C., Omori, S. A. and Rickert, R. C. (2001). CD19-dependent activation of Akt kinase in B-lymphocytes. *J Biol Chem* **276**, 1474–1478.
- Papavasiliou, F., Jankovic, M., Suh, H. and Nussenzweig, M. C. (1995). The cytoplasmic domains of immunoglobulin (Ig) alpha and Ig beta can independently induce the precursor B cell transition and allelic exclusion. *J Exp Med* **182**, 1389–1394.
- Parker, P. J., Caudwell, F. B. and Cohen, P. (1983). Glycogen synthase from rabbit skeletal muscle; effect of insulin on the state of phosphorylation of the seven phosphoserine residues in vivo. *Eur J Biochem* **130**, 227–234.
- Pasqualucci, L., Bhagat, G., Jankovic, M., Compagno, M., Smith, P., Muramatsu, M., Honjo, T., Morse, H. C., Nussenzweig, M. C. and Dalla-Favera, R. (2007). AID is required for germinal center-derived lymphomagenesis. *Nat Genet* **40**, 108–112.
- Patenaude, A. M., Orthwein, A., Hu, Y., Campo, V. A., Kavli, B., Buschiazzo, A. and Di Noia, J. M. (2009). Active nuclear import and cytoplasmic retention of activation-induced deaminase. *Nat Struct Mol Biol* **16**, 517–527.
- Pedersen, I. M., Kitada, S., Leoni, L. M., Zapata, J. M., Karras, J. G., Tsukada, N., Kipps, T. J., Choi, Y. S., Bennett, F. and Reed, J. C. (2002). Protection of CLL B cells by a follicular dendritic cell line is dependent on induction of Mcl-1. *Blood* **100**, 1795–1801.
- Pearce, L. R., Huang, X., Boudeau, J., Pawlowski, R., Wullschleger, S., Deak, M., Ibrahim, A. F. M., Gourlay, R., Magnuson, M. A. and Alessi, D. R. (2007). Identification of Protor as a novel Rictor-binding component of mTOR complex-2. *Biochem J* **405**, 513–522.
- Peng, S. L. (2008). Foxo in the immune system. *Oncogene* **27**, 2337–2344.
- Peng, X.-D., Xu, P.-Z., Chen, M.-L., Hahn-Windgassen, A., Skeen, J., Jacobs, J., Sundararajan, D., Chen, W. S., Crawford, S. E., Coleman, K. G. and Hay N. (2003). Dwarfism, impaired skin development, skeletal muscle atrophy, delayed bone development, and impeded adipogenesis in mice lacking Akt1 and Akt2. *Genes Dev* **17**, 1352–1365.
- Pernis, B., Chiappino, G., Kelus, A. S. and Gell, P. G. H. (1965). Cellular localization of immunoglobulins with different allotypic specificities in rabbit lymphoid tissues. *J Exp Med* **122**(5):853–876.
- Petersen, S., Casellas, R., Reina-San-Martin, B., Chen, H. T., Difilippantonio, M. J., Wilson, P. C., Hanitsch, L., Celeste, A., Muramatsu, M., Pilch, D. R., Redon, C., Ried, T., Bonner, W. M., Honjo, T., Nussenzweig, M. C., Nussenzweig, A. (2001). AID is required to initiate Nbs1/gamma-H2AX focus formation and mutations at sites of class switching. *Nature* **6864**, 660–665.
- Petersen-Mahrt, S. K., Harris, R. S. and Neuberger, M. S. (2002). AID mutates E. coli suggesting a DNA deamination mechanism for antibody diversification. *Nature* **418**, 99–104.
- Peterson, T. R., Laplante, M., Thoreen, C. C., Sancak, Y., Kang, S. A., Kuehl, W. M., Gray, N. S. and Sabatini, D. M. (2009). DEPTOR Is an mTOR Inhibitor Frequently Overexpressed in Multiple Myeloma Cells and Required for Their Survival. *Cell* **137**, 873–886.
- Pierau, M., Na, S.-Y., Simma, N., Lowinus, T., Marx, A., Schraven, B. and Bommhardt, U. H. (2012). Constitutive Akt1 signals attenuate B-cell receptor signaling and proliferation, but enhance B-cell migration and effector function. *Eur J Immunol* **42**, 3381–3393.
- Pillai, S. and Cariappa, A. (2009). The follicular versus marginal zone B lymphocyte cell fate decision. *Nat Rev Immunol* **9**, 767–777.
- Pillai, S., Cariappa, A. and Moran, S. T. (2004). Positive selection and lineage commitment during peripheral B-lymphocyte development. *Immunol Rev* **197**, 206–218.

- Pillai, S., Cariappa, A. and Moran, S. T. (2005). Marginal Zone B Cells. *Annu Rev Immunol* **23**, 161-96.
- Pogue, S. L., Kurosaki, T., Bolen, J. and Herbst, R. (2000). B Cell antigen receptor-induced activation of Akt promotes B cell survival and is dependent on Syk kinase. *J Immunol* **165**, 1300-1306.
- Pone, E. J., Zhang, J., Mai, T., White, C. A., Li, G., Sakakura, J. K., Patel, P. J., Al-Qahtani, A., Zan, H., Xu, Z. and Casali, P. (2012). BCR-signalling synergizes with TLR-signalling for induction of AID and immunoglobulin class-switching through the non-canonical NF- κ B pathway. *Nat Commun* 2012 Apr 3;3:767.
- Porto, J. M. D., Haberman, A. M., Shlomchik, M. J. and Kelsoe, G. (1998). Antigen drives very low Affinity B cells to become plasmacytes and enter germinal centers. *J Immunol* **161**, 5373-5381.
- Qin, H., Suzuki, K., Nakata, M., Chikuma, S., Izumi, N., Thi Huong, L., Maruya, M., Fagarasan, S., Busslinger, M., Honjo, T. and Nagaoka, T. (2011). Activation-induced cytidine deaminase expression in CD4⁺ T cells is associated with a unique IL-10-producing subset that increases with age. *PLoS One* **6**, e29141.
- Radbruch, A., Muehlinghaus, G., Luger, E. O., Inamine, A., Smith, K. G. C., Dörner, T. and Hiepe, F. (2006). Competence and competition: the challenge of becoming a long-lived plasma cell. *Nat Immunol* **6**, 741-750.
- Ravetch, J. V., Guinamard, R., Okigaki, M. and Schlessinger, J. (2000). Absence of marginal zone B cells in Pyk-2-deficient mice defines their role in the humoral response. *Nat Immunol* **1**, 31-36.
- Rawstron, A. C., Yuille, M. R., Fuller, J., Cullen, M., Kennedy, B., Richards, S. J., Jack, A. S., Matutes, E., Catovsky, D., Hillmen, P., Houlston, R. S. (2002). Inherited predisposition to CLL is detectable as subclinical monoclonal B-lymphocyte expansion. *Blood* **7**, 2289-2290.
- Rena, G., Guo, S., Cichy, S. C., Unterman, T. G. and Cohen, P. (1999). Phosphorylation of the transcription factor Forkhead family member FKHR by protein kinase B. *J Biol Chem* **274**, 17179-17183.
- Revy, P., Muto, T., Levy, Y., Geissmann, F., Plebani, A., Sanal, O., Catalan, N., Forveille, M., Dufourcq-Labeuze, R., Gennery, A., Tezcan, I., Ersoy, F., Kayserili, H., Ugazio, A. G., Brousse, N., Muramatsu, M., Notarangelo, L. D., Kinoshita, K., Honjo, T., Fischer, A. and Durandy, A. (2000). Activation-induced cytidine deaminase (AID) deficiency causes the autosomal recessive form of the Hyper-IgM syndrome (HIGM2). *Cell* **102**, 565-575.
- Rickert, R. C., Rajewsky, K. and Roes, J. (1995). Impairment of T-cell-dependent B-cell responses and B-1 cell development in CD19-deficient mice. *Nature* **376**, 352-355.
- Rickert, R., Roes, J. and Rajewsky, K. (1997). B lymphocyte-specific, Cre-mediated mutagenesis in mice. *Nucleic Acids Res* **25**, 1317-1318.
- Roark, J. H., Park, S.-H., Jayawardena, J., Kavita, U., Shannon, M. and Bendelac, A. (1998). CD1.1 expression by mouse antigen-presenting cells and marginal zone B cells. *J Immunol* **160**, 3121-3127.
- Roes, J. and Rajewsky, K. (1993). Immunoglobulin D (IgD)-deficient mice reveal an auxiliary receptor function for IgD in antigen-mediated recruitment of B cells. *J Exp Med* **177**, 45-55.
- Roundy, K. M., Jacobson, A. C., Weis, J. J. and Weis, J. H. (2010). The in vitro derivation of phenotypically mature and diverse B cells from immature spleen and bone marrow precursors. *Eur J Immunol* **40**, 1139-1149.
- Rowley, R. B., Burkhardt, A. L., Chao, H. G., Matsueda, G. R. and Bolen, J. B. (1995). Syk protein-tyrosine kinase is regulated by tyrosine-phosphorylated Ig α /Ig β immunoreceptor tyrosine activation motif binding and autophosphorylation. *J Immunol* **160**, 3121-3127.

- Roy, H. K. (2002). AKT proto-oncogene overexpression is an early event during sporadic colon carcinogenesis. *Carcinogenesis* **23**, 201–205.
- Rubtsov, A. V., Swanson, C. L., Troy, S., Strauch, P., Pelanda, R. and Torres, R. M. (2008). TLR agonists promote marginal zone B cell activation and facilitate T-dependent IgM responses. *J Immunol* **180**, 3882–3888.
- Rucci, F., Cattaneo, L., Marrella, V., Sacco, M. G., Sobacchi, C., Lucchini, F., Nicola, S., Della Bella, S., Villa, M. L., Imberti, L., Gentili, F., Montagna, C., Tiveron, C., Tatangelo, L., Facchetti, F., Vezzoni, P. and Villa, A. (2006). Tissue-specific sensitivity to AID expression in transgenic mouse models. *Gene* **377**, 150–158.
- Sabatini, D.M., Erdjument-Bromage, H., Lui, M., Tempst, P. and Snyder, S. H. (1994). RAFT1: a mammalian protein that binds to FKBP12 in a rapamycin-dependent fashion and is homologous to yeast TORs. *Cell* **78**, 35–43.
- Sabers, C. J., Martin, M. M., Brunn, G. J., Williams, J. M., Dumont, F. J., Wiederrecht, G. and Abraham, R. T. (1995). Isolation of a protein target of the FKBP12-rapamycin complex in mammalian cells. *J Biol Chem* **270**, 815–822.
- Sable, C. L., Filippa, N., Filloux, C., Hemmings, B. A. and van Obberghen, E. (1998). Involvement of the pleckstrin homology domain in the insulin-stimulated activation of protein kinase B. *J Biol Chem* **273**, 29600–29606.
- Said, J. W., Hoyer, K. K., French, S. W., Rosenfelt, L., Garcia-Lloret, M., Koh, P. J., Cheng, T. C., Sulur, G. G., Pinkus, G. S., Kuehl, W. M., Rawlings, D. J., Wall, R. and Teitell, M. A. (2001). TCL1 oncogene expression in B cell subsets from lymphoid hyperplasia and distinct classes of B cell lymphoma. *Lab Invest* **4**, 555–564.
- Saiki, R. K., Gelfand, D. H., Stoffel, S., Scharf, S. J., Higuchi, R., Horn, G. T., Mullis, K. B., Erlich, H. A. (1988). Primer-directed enzymatic amplification of DNA with a thermostable DNA polymerase. *Science* **239**, 487–491.
- Saito, T., Chiba, S., Ichikawa, M., Kunisato, A., Asai, T., Shimizu, K., Yamaguchi, T., Yamamoto, G., Seo, S., Kumano, K., Nakagami-Yamaguchi, E., Hamada, Y., Aizawa, S. and Hirai, H. (2003). Notch2 is preferentially expressed in mature B cells and indispensable for marginal zone B lineage development. *Immunity* **18**, 675–685.
- Sakaguchi, N. and Melchers, F. (1986). $\lambda 5$, a new light-chain-related locus selectively expressed in pre-B lymphocytes. *Nature* **324**, 579–582.
- Sambrook, J. (1989). Molecular cloning. A laboratory manual, (2nd edition).
- Sancak, Y., Thoreen, C. C., Peterson, T. R., Lindquist, R. A., Kang, S. A., Spooner, E., Carr, S. A. and Sabatini, D. M. (2007). PRAS40 Is an insulin-regulated inhibitor of the mTORC1 protein kinase. *Mol Cell* **25**, 903–915.
- Sarbassov, D. D., Guertin, D. A., Ali, S. M. and Sabatini, D. M. (2005). Phosphorylation and regulation of Akt/PKB by the Rictor-mTOR complex. *Science* **307**, 1098–1101.
- Sarbassov, D. D., Ali, S. M., Kim, D.-H., Guertin, D. A., Latek, R. R., Erdjument-Bromage, H., Tempst, P. and Sabatini, D. M. (2004). Rictor, a novel binding partner of mTOR, defines a rapamycin-insensitive and Raptor-independent pathway that regulates the cytoskeleton. *Curr Biol* **14**, 1296–1302.
- Schamel, W. W. and Reth, M. (2000). Monomeric and oligomeric complexes of the B cell antigen receptor. *Immunity* **13**, 5–14.

- Scharenberg, A. M., Humphries, L. A. and Rawlings, D. J.** (2007). Calcium signalling and cell-fate choice in B cells. *Nat Immunol* **7**, 778–789.
- Scher, I., Sharrow, S. O., Wistar, R., Asofsky, R. and Paul, W. E.** (1976). B-lymphocyte heterogeneity: ontogenetic development and organ distribution of B-lymphocyte populations defined by their density of surface immunoglobulin. *J Exp Med* **144**, 494–506.
- Schmelzle, T., Hall, M. N.** (2000). TOR, a central controller of cell growth. *Cell* **103**, 253–262.
- Schmitz, R., Baumann, G. and Gram, H.** (1996). Catalytic specificity of phosphotyrosine kinases Blk, Lyn, c-Src and Syk as assessed by phage display. *J Mol Biol* **260**, 664–677.
- Schreck, S., Buettner, M., Kremmer, E., Bogdan, M., Herbst, H. and Niedobitek, G.** (2006). Activation-induced cytidine deaminase (AID) is expressed in normal spermatogenesis but only infrequently in testicular germ cell tumours. *J Pathol* **210**, 26–31.
- Schwickert, T. A., Alabyev, B., Manser, T. and Nussenzweig, M. C.** (2009). Germinal center reutilization by newly activated B cells. *J Exp Med* **206**, 2907–2914.
- Schwickert, T. A., Lindquist, R. L., Shakhar, G., Livshits, G., Skokos, D., Kosco-Vilbois, M. H., Dustin, M. L. and Nussenzweig, M. C.** (2007). In vivo imaging of germinal centres reveals a dynamic open structure. *Nature* **446**, 83–87.
- Shimizu, K., Chiba, S., Hosoya, N., Kumano, K., Saito, T., Kurokawa, M., Kanda, Y., Hamada, Y. and Hirai, H.** (2000). Binding of Delta1, Jagged1, and Jagged2 to Notch2 rapidly induces cleavage, nuclear translocation, and hyperphosphorylation of Notch2. *Mol Cell Biol* **20**, 6913–6922.
- Shinkura, R., Ito, S., Begum, N. A., Nagaoka, H., Muramatsu, M., Kinoshita, K., Sakakibara, Y., Hijikata, H. and Honjo, T.** (2004). Separate domains of AID are required for somatic hypermutation and class-switch recombination. *Nat Immunol* **5**, 707–712.
- Shiojima, I., Sato, K., Izumiya, Y., Schiekofer, S., Ito, M., Liao, R., Colucci, W. S. and Walsh, K.** (2005). Disruption of coordinated cardiac hypertrophy and angiogenesis contributes to the transition to heart failure. *J Clin Invest* **115**, 2108–2118.
- Shivarov, V., Shinkura, R. and Honjo, T.** (2008). Dissociation of in vitro DNA deamination activity and physiological functions of AID mutants. *Proc Nat Acad Sci* **105**, 15866–15871.
- Shlomchik, M. J. and Weisel, F.** (2012). Germinal center selection and the development of memory B and plasma cells. *Immunol Rev* **247**, 52–63.
- Silver, L. M.** (1995). Mouse genetics: Concepts and applications. *Oxford University Press*, New York.
- Smith, K. G. C., Tarlinton, D. M., Doody, G. M., Hibbs, M. L. and Fearon, D. T.** (1998). Inhibition of the B Cell by CD22: A Requirement for Lyn. *J Exp Med* **187**, 807–811.
- Snapper, C. M., Rosas, F. R., Jin, L., Wortham, C., Kehry, M. R. and Mond, J. J.** (1995). Bacterial lipoproteins may substitute for cytokines in the humoral immune response to T cell-independent type II antigens. *J Immunol* **155**, 5582–5589.
- Snapper, C. M., Yamada, H., Smoot, D., Sneed, R., Lees, A. and Mond, J. J.** (1993). Comparative in vitro analysis of proliferation, Ig secretion, and Ig class switching by murine marginal zone and follicular B cells. *J Immunol* **150**, 2737–2745.
- So, L. and Fruman, D. A.** (2012). PI3K signalling in B- and T-lymphocytes: new developments and therapeutic advances. *Biochem J* **3**, 465–481.
- Sohail, A., Klapacz, J., Samaranayake, M., Ullah, A. and Bhagwat, A. S.** (2003). Human activation-induced cytidine deaminase causes transcription-dependent, strand-biased C to U deaminations. *Nucleic Acids Res* **31**, 2990–2994.

- Soskic, V., Görlach, M., Poznanovic, S., Boehmer, F. D. and Godovac-Zimmermann, J. (1999). Functional proteomics analysis of signal transduction pathways of the platelet-derived growth factor beta receptor. *Biochemistry* **38**, 1757-1764.
- Srinivasan, L., Sasaki, Y., Calado, D. P., Zhang, B., Paik, J. H., DePinho, R. A., Kutok, J. L., Kearney, J. F., Otipoby, K. L. and Rajewsky K. (2009). PI3 kinase signals BCR-dependent mature B cell survival. *Cell* **139**: 573-586.
- Staal, S.P. (1987). Molecular cloning of the akt oncogene and its human homologues AKT1 and AKT2: amplification of AKT1 in a primary human gastric adenocarcinoma. *Proc Natl Acad Sci U S A* **84**, 5034-5037.
- Stadanlick, J. E., Kaileh, M., Karnell, F. G., Scholz, J. L., Miller, J. P., Quinn, W. J., Brezski, R. J., Treml, L. S., Jordan, K. A., Monroe, J. G., Sen, R. and Cancro, M. P. (2008). Tonic B cell antigen receptor signals supply an NF-kappaB substrate for prosurvival BLyS signaling. *Nat Immunol* **12**, 1379-1387.
- Steidl, C., Lee, T., Shah, S. P., Farinha, P., Han, G., Nayar, T., Delaney, A., Jones, S. J., Iqbal, J., Weisenburger, D. D., et al. (2010). Tumor-associated macrophages and survival in classic hodgkin's Lymphoma. *N Engl J Med* **362**, 875-885.
- Stephens, L. (1998). Protein kinase B kinases that mediate phosphatidylinositol 3,4,5-trisphosphate-dependent activation of protein kinase B. *Science* **279**, 710-714.
- Stokoe, D. (1997). Dual Role of phosphatidylinositol-3,4,5-trisphosphate in the activation of protein kinase B. *Science* **277**, 567-570.
- Sun, T., Clark, M. R. and Storb, U. (2002). A point mutation in the constant region of Ig lambda1 prevents normal B cell development due to defective BCR signaling. *Immunity* **16**, 245-255.
- Sutherland, C. and Cohen, P. (1994). The alpha-isoform of glycogen synthase kinase-3 from rabbit skeletal muscle is inactivated by p70 S6 kinase or MAP kinase-activated protein kinase-1 in vitro. *FEBS Lett* **338**, 37-42.
- Sutherland, C., Leighton, I. A. and Cohen, P. (1993). Inactivation of glycogen synthase kinase-3 beta by phosphorylation: new kinase connections in insulin and growth-factor signalling. *Biochem J* **296**, 15-19.
- Suzuki, A., Kaisho, T., Ohishi, M., Tsukio-Yamaguchi, M., Tsubata, T., Koni, P. A., Sasaki, T., Mak, T. W. and Nakano, T. (2003). Critical roles of Pten in B cell homeostasis and immunoglobulin class switch recombination. *J Exp Med* **197**, 657-667.
- Suzuki, K., Grigorova, I., Phan, T. G., Kelly, L. M. and Cyster, J. G. (2009). Visualizing B cell capture of cognate antigen from follicular dendritic cells. *J Exp Med* **206**, 1485-1493.
- Ta, V.-T., Nagaoka, H., Catalan, N., Durandy, A., Fischer, A., Imai, K., Nonoyama, S., Tashiro, J., Ikegawa, M., Ito, S., et al. (2003). AID mutant analyses indicate requirement for class-switch-specific cofactors. *Nat Immunol* **4**, 843-848.
- Takaishi, H., Konishi, H., Matsuzaki, H., Ono, Y., Shirai, Y., Saito, N., Kitamura, T., Ogawa, W., Kasuga, M., Kikkawa, U. and Nishizuka, Y. (1999). Regulation of nuclear translocation of Forkhead transcription factor AFX by protein kinase B. *Proc Natl Acad Sci U S A* **96**, 11836-11841.
- Takata, M. and Kurosaki, T. (1996). A role for Bruton's tyrosine kinase in B cell antigen receptor-mediated activation of phospholipase C-gamma 2. *J Exp Med* **184**(1):31-40.
- Takata, M., Sabe, H., Hata, A., Inazu, T., Homma, Y., Nukada, T., Yamamura, H. and Kurosaki, T. (1994). Tyrosine kinases Lyn and Syk regulate B cell receptor-coupled Ca²⁺ mobilization through distinct pathways. *EMBO J* **13**, 1341-1349.

- Takeda, S., Sonada, E. and Arakawa, H.** (1996). The $\kappa:\lambda$ ratio of immature B cells. *Immunol Today* **17**, 200-201.
- Takeuchi, F.** (1996). Akt, a pleckstrin homology domain containing kinase, is activated primarily by phosphorylation. *J Biol Chem* **271**, 21920–21926.
- Takizawa, M., Tolarova, H., Li, Z., Dubois, W., Lim, S., Callen, E., Franco, S., Mosaico, M., Feigenbaum, L., Alt, F. W., et al.** (2008). AID expression levels determine the extent of cMyc oncogenic translocations and the incidence of B cell tumor development. *J Exp Med* **205**, 1949–1957.
- Tang, E. D., Nunez, G., Barr, F. G. and Guan, K. L.** (1999). Negative regulation of the Forkhead transcription factor FKHR by Akt. *J Biol Chem* **274**, 16741–16746.
- Tanigaki, K., Han, H., Yamamoto, N., Tashiro, K., Ikegawa, M., Kuroda, K., Suzuki, A., Nakano, T. and Honjo, T.** (2002). Notch–RBP-J signaling is involved in cell fate determination of marginal zone B cells. *Nat Immunol* **3**, 443–450.
- Tan-Pertel, H. T., Walker, L., Browning, D., Miyamoto, A., Weinmaster, G. and Gasson, J. C.** (2000). Notch Signaling Enhances Survival and Alters Differentiation of 32D Myeloblasts. *J Immunol* **165**, 4428–4436.
- Teh, Y. M.** (1997). The immunoglobulin (Ig)alpha and Igbeta cytoplasmic domains are independently sufficient to signal B cell maturation and activation in transgenic mice. *J Exp Med* **185**, 1753–1758.
- Tedder, T. F., Inaoki, M. and Sato, S.** (1997). The CD19-CD21 complex regulates signal transduction thresholds governing humoral immunity and autoimmunity. *Immunity* **6**, 107-118.
- Thedieck, K., Polak, P., Kim, M. L., Molle, K. D., Cohen, A., Jenö, P., Arrieumerlou, C. and Hall, M. N.** (2007). PRAS40 and PRR5-Like protein are new mTOR interactors that regulate apoptosis. *PLoS ONE* **2**, e1217.
- Thien, M., Phan, T. G., Gardam, S., Amesbury, M., Basten, A., Mackay, F. and Brink, R.** (2004). Excess BAFF rescues self-reactive B cells from peripheral deletion and allows them to enter forbidden follicular and marginal zone niches. *Immunity* **20**, 785-798.
- Thomas, M. L. and Brown, E. J.** (1999). Positive and negative regulation of Src-family membrane kinases by CD45. *Immunol Today* **20**, 406-411.
- Thompson, E. C.** (2012). Focus issue: Structure and function of lymphoid tissues. *Trends Immunol* **33**, 255.
- Treml, L. S., Carlesso, G., Hoek, K. L., Stadanlick, J. E., Kambayashi, T., Bram, R. J., Cancro, M. P. and Khan, W. N.** (2007). TLR stimulation modifies BLyS receptor expression in follicular and marginal zone B cells. *J Immunol* **178**, 7531–7539.
- Tsukada, N.** (2002). Distinctive features of “nurselike” cells that differentiate in the context of chronic lymphocytic leukemia. *Blood* **99**, 1030–1037.
- Tung, J. W., Herzenberg, L. A** (2007). Unraveling B-1 progenitors. *Curr Opin Immunol* **19**, 150-155.
- Turner, M., Joseph Mee, P., Costello, P. S., Williams, O., Price, A. A., Duddy, L. P., Furlong, M. T., Geahlen, R. L. and Tybulewicz, V. L. J.** (1995). Perinatal lethality and blocked B-cell development in mice lacking the tyrosine kinase Syk. *Nature* **378**, 298–302.
- Tuveson, D. A., Carter, R. H., Soltoff, S.P. and Fearon, D. T.** (1993). CD19 of B cells as a surrogate kinase insert region to bind phosphatidylinositol 3-kinase. *Science* **5110**, 986-989.
- Vander-Mallie, R., Ishizaka, T. and Ishizaka, K.** (1982). Lymphocytes bearing receptors for 19B. VIII. Affinity of mouse IgE for Fc_ε receptor on mouse B lymphocytes. *J Immunol* **128**, 2306-2312.

- Victora, G. D. and Nussenzweig, M. C.** (2012). Germinal centers. *Annu Rev Immunol* **30**, 429-457.
- Wang, L., Harris, T. E., Roth, R. A. and Lawrence, J. C.** (2007). PRAS40 Regulates mTORC1 Kinase Activity by Functioning as a Direct Inhibitor of Substrate Binding. *J Biol Chem* **282**, 20036–20044.
- Wei, M., Shinkura, R., Doi, Y., Maruya, M., Fagarasan, S. and Honjo, T.** (2011). Mice carrying a knock-in mutation of Aicda resulting in a defect in somatic hypermutation have impaired gut homeostasis and compromised mucosal defense. *Nat Immunol* **12**, 264–270.
- Weidenreich, F.** (1901). Das Gefäßsystem der menschlichen Milz. *Arch Mikros Anat* **58**, 247-376.
- Weiss, U. and Rajewsky, K.** (1990). The repertoire of somatic antibody mutants accumulating in the memory compartment after primary immunization is restricted through affinity maturation and mirrors that expressed in the secondary response. *J Exp Med* **172**: 1681-1689.
- Welsh, G. I. and Proud, C. G.** (1993). Glycogen synthase kinase-3 is rapidly inactivated in response to insulin and phosphorylates eukaryotic initiation factor eIF-2B. *Biochem J* **15**;294 (Pt 3):625-629.
- Welsh, G. I., Wilson C. and Proug C.G.** (1996). A shaggy frog story. *Trends Cell Biol* **6**, 274–279.
- Weng, J., Rawal, S., Chu, F. Park, H. J., Sharma, R., Delgado, D. A., Fayad, L., Fanale, M., Romaguera, J., Luong, A., Kwak, L. W. and Neelapu, S. S.** (2012). TCL1: a shared tumor-associated antigen for immunotherapy against B-cell lymphomas. *Blood* **120**, 1613-1623.
- Wienands, J., Schweikert, J., Wollscheid, B., Jumaa, H., Nielsen, P. J. and Reth, M.** (1998). SLP-65: A new signaling component in B lymphocytes which requires expression of the antigen receptor for phosphorylation. *J Exp Med* **4**, 791-795.
- Wijkander, J., Holst, L. S., Rahn, T., Resjo, S., Castan, I., Manganiello, V., Belfrage, P. and Degerman, E.** (1997). Regulation of protein kinase B in rat adipocytes by insulin, vanadate, and peroxovanadate: MEMBRANE TRANSLOCATION IN RESPONSE TO PEROXOVANADATE. *J Biol Chem* **272**, 21520–21526.
- Won, W.-J. and Kearney, J. F.** (2002). CD9 Is a unique marker for marginal zone B cells, B1 cells, and plasma cells in mice. *J Immunol.* **168**, 5605-5611.
- Wullschleger, S., Loewith, R. and Hall, M. N.** (2006). TOR signaling in growth and metabolism. *Cell* **124**, 471-484.
- Xiong, H., Dolpady, J., Wabl, M., de Lafaille, M. A. C. and Lafaille, J. J.** (2012). Sequential class switching is required for the generation of high affinity IgE antibodies. *J Exp Med* **209**, 353-364.
- Yamanashi, Y., Kakiuchi, T., Mizuguchi, J., Yamamoto, T. and Toyoshima, K.** (1991). Association of B cell antigen receptor with protein tyrosine kinase Lyn. *Science* **251**, 192–194.
- Yang, L., Dan, H. C., Sun, M., Liu, Q., Sun, X. M., Feldman, R. I., Hamilton, A. D., Polokoff, M., Nicosia, S. V., Herlyn, M., Sebt, S. M. and Cheng, J. Q.** (2004a). Akt/protein kinase B signaling inhibitor-2, a selective small molecule inhibitor of Akt signaling with antitumor activity in cancer cells overexpressing Akt. *Cancer Res* **13**, 4394-4399.
- Yang, Y., Tung, J. W., Ghosn, E. E., Herzenberg, L. A., Herzenberg, L. A.** (2007). Division and differentiation of natural antibody-producing cells in mouse spleen. *Proc Natl Acad Sci* **104**, 4542-4546.
- Yang, J. and Reth, M.** (2010). Oligomeric organization of the B-cell antigen receptor on resting cells. *Nature* **467**, 465–469.
- Yang, Z. Z., Tschopp, O., Baudry, A., Dümmler, B., Hynx, D. and Hemmings, B. A.** (2004b). Physiological functions of protein kinase B/Akt. *Biochem Soc Trans* **32**, 350-354.

Zhang, X. and Vik, T. A. (1997). Growth factor stimulation of hematopoietic cells leads to membrane translocation of AKT1 protein kinase. *Leuk Res* **21**, 849–856.

Zhang, X., Tang, N., Hadden, T. J. and Rishi, A. K. (2011). Akt, FoxO and regulation of apoptosis. *Biochim Biophys Acta* **11**, 1978-1986.

Zucchetto, A., Tripodo, C., Benedetti, D., Deaglio, S., Gaidano, G., Del Poeta, G. and Gattei, V. (2010). Monocytes/macrophages but not T lymphocytes are the major targets of the CCL3/CCL4 chemokines produced by CD38 +CD49d +chronic lymphocytic leukaemia cells. *Br J Haematol* **150**, 111-113.

8 Acknowledgments

9 Versicherung

Ich versichere, dass ich die von mir vorgelegte Dissertation selbständig angefertigt, die benutzten Quellen und Hilfsmittel vollständig angegeben und die Stellen der Arbeit - einschließlich Tabellen, Karten und Abbildungen -, die anderen Werken im Wortlaut oder dem Sinn nach entnommen sind, in jedem Einzelfall als Entlehnung kenntlich gemacht habe; dass diese Dissertation noch keiner anderen Fakultät oder Universität zur Prüfung vorgelegen hat; dass sie noch nicht veröffentlicht worden ist sowie, dass ich eine solche Veröffentlichung vor Abschluss des Promotionsverfahrens nicht vornehmen werde. Die Bestimmungen dieser Promotionsordnung sind mir bekannt. Die von mir angefertigte Dissertation ist von [REDACTED] und [REDACTED] betreut worden.

Mainz, 18. November 2015

Eva-Maria Cox

10 Lebenslauf